

Lecture Notes in Physics

Alto Osada
Rekishu Yamazaki
Atsushi Noguchi

Introduction to Quantum Technologies

MOREMEDIA 

 Springer

Lecture Notes in Physics

Founding Editors

Wolf Beiglböck

Jürgen Ehlers

Klaus Hepp

Hans-Arwed Weidenmüller

Volume 1004

Series Editors

Roberta Citro, Salerno, Italy

Peter Hänggi, Augsburg, Germany

Morten Hjorth-Jensen, Oslo, Norway

Maciej Lewenstein, Barcelona, Spain

Angel Rubio, Hamburg, Germany

Wolfgang Schleich, Ulm, Germany

Stefan Theisen, Potsdam, Germany

James D. Wells, Ann Arbor, MI, USA

Gary P. Zank, Huntsville, AL, USA

The series Lecture Notes in Physics (LNP), founded in 1969, reports new developments in physics research and teaching - quickly and informally, but with a high quality and the explicit aim to summarize and communicate current knowledge in an accessible way. Books published in this series are conceived as bridging material between advanced graduate textbooks and the forefront of research and to serve three purposes:

- to be a compact and modern up-to-date source of reference on a well-defined topic;
- to serve as an accessible introduction to the field to postgraduate students and non-specialist researchers from related areas;
- to be a source of advanced teaching material for specialized seminars, courses and schools.

Both monographs and multi-author volumes will be considered for publication. Edited volumes should however consist of a very limited number of contributions only. Proceedings will not be considered for LNP.

Volumes published in LNP are disseminated both in print and in electronic formats, the electronic archive being available at springerlink.com. The series content is indexed, abstracted and referenced by many abstracting and information services, bibliographic networks, subscription agencies, library networks, and consortia.

Proposals should be sent to a member of the Editorial Board, or directly to the responsible editor at Springer:

Dr Lisa Scalzone
Springer Nature
Physics
Tiergartenstrasse 17
69121 Heidelberg, Germany
lisa.scalone@springernature.com

Alto Osada · Rekishu Yamazaki ·
Atsushi Noguchi

Introduction to Quantum Technologies

Alto Osada
Komaba Institute for Science
The University of Tokyo
Meguro-ku, Tokyo, Japan

Rekishi Yamazaki
College of Liberal Arts
International Christian University
Mitaka-shi, Tokyo, Japan

Atsushi Noguchi
Komaba Institute for Science
The University of Tokyo
Meguro-ku, Tokyo, Japan

ISSN 0075-8450
Lecture Notes in Physics
ISBN 978-981-19-4643-1
<https://doi.org/10.1007/978-981-19-4641-7>

ISSN 1616-6361 (electronic)
ISBN 978-981-19-4641-7 (eBook)

© The Editor(s) (if applicable) and The Author(s), under exclusive license to Springer Nature Singapore Pte Ltd. 2022

This work is subject to copyright. All rights are solely and exclusively licensed by the Publisher, whether the whole or part of the material is concerned, specifically the rights of translation, reprinting, reuse of illustrations, recitation, broadcasting, reproduction on microfilms or in any other physical way, and transmission or information storage and retrieval, electronic adaptation, computer software, or by similar or dissimilar methodology now known or hereafter developed.

The use of general descriptive names, registered names, trademarks, service marks, etc. in this publication does not imply, even in the absence of a specific statement, that such names are exempt from the relevant protective laws and regulations and therefore free for general use.

The publisher, the authors, and the editors are safe to assume that the advice and information in this book are believed to be true and accurate at the date of publication. Neither the publisher nor the authors or the editors give a warranty, expressed or implied, with respect to the material contained herein or for any errors or omissions that may have been made. The publisher remains neutral with regard to jurisdictional claims in published maps and institutional affiliations.

This Springer imprint is published by the registered company Springer Nature Singapore Pte Ltd.
The registered company address is: 152 Beach Road, #21-01/04 Gateway East, Singapore 189721,
Singapore

For Yuki and Ray

Preface

What is quantum technology? Is it a fancy bandwagon fresh from the academics? Definitely, this is not the case. Let us trace the history in reverse order from 2022. Now the quantum technology is known to everybody, thanks to the many-qubit quantum “computers” developed by several companies and laboratories. Some of them are available on the cloud platform and are used for the educational and business use, while quantum communication and quantum sensing/metrology are also under intense investigation. Why does quantum computer gather such an attention? An answer is that such a novel computer based on the unconventional working principle—quantum mechanics—is expected to outperform conventional computers, or classical computers as a counterpart of the quantum computer, when a certain computational task is given. A celebrated quantum algorithm of prime factorization was invented by Peter Shor in 1994 [1]. In 1995, he invented another landmark of the first proposal of a quantum error correction code [2]. We would like to stress that this very work ignited the experimental exploration of quantum computer which had been distinguished from a mere analog computer intolerable to errors occurring in an analog manner as well. To date, a number of breathtaking progress have been made in various quantum systems, especially in ion-trap and superconducting-circuit systems.

Readers might have heard of another fancy word of quantum teleportation in which a quantum state is transferred between remote parties by a bit tricky use of the “spooky interaction” of quantum particles, or the quantum entanglement, a concept coined back in 1935 by Einstein, Podolsky, and Rosen [3]. Quantum teleportation was proposed in 1993 by Bennet *et al.* [4], which was then followed by its realizations in 1997–1998 [5, 6] using optical photons. These studies lay the basis of quantum communication. Optical photons are indispensable for the quantum technologies that demand the transfer of quantum states from one place to a distant place, which is indeed made possible by the invention of optical fibers with excellent property of extremely low-loss propagation at room temperature. This nature can also be utilized for another quantum technology of quantum cryptography, pioneered by Bennett and Brassard in 1984 [7].

Quantum technologies, or even quantum mechanics, have established their relevance in the development of Atomic, Molecular, and Optical (AMO) physics during the twentieth century. Furthermore, the spectroscopic and control techniques frequently used in AMO physics originate in the Nuclear Magnetic

Resonance (NMR) experiments since the late 1930s with celebrated pioneers such as Rabi, Ramsey, Bloch, and Purcell. NMR technique is widely applied in our daily life, for instance to Magnetic Resonance Induction (MRI) tomography and to identification of materials using chemical shifts of NMR spectra, both of which can be regarded as early forms of quantum sensing.

What we want to say is that quantum technology is not (or should not be) just a short-lived trend, a scam business, nor a mathematical game in the Hilbert space, but a technology that has been pursued substantially with physics and devices in the history of understanding and controlling matters in real life, at least at the current technological levels. Therefore, the name of the game is to know what physical objects we want to address in quantum technologies and how to do that. Abstracted, perfect (error-corrected) logical qubits are not at our hand—even for a single logical qubit. Realization of them is a “holy grail,” at the time in 2022.

Various physical systems are used to aim it, and numerous experimental techniques are developed for them. Readers might be overwhelmed when they think about which quantum system to learn, since different quantum systems can have different theoretical backgrounds and experimental techniques. However, we, the researcher in this field, know that there are many theories and concepts in common among the various quantum systems, such as quantum optics, quantum electronics, and so on.

The purpose of this book is to summarize such common basics of quantum technologies as a foundation for cultivating a comprehensive view of the state-of-the-art quantum systems. The book is roughly divided into three parts.

- In Part I, we describe how the quantum states are represented based on linear algebra, which is frequently used in quantum technology. We also cover the fundamentals of quantum mechanics necessary for understanding the basic quantum manipulations. It is an excerpt of what is to be collected and summarized in a concise form.
- Part II starts with a description of two-level systems and electromagnetic waves, and how they interact. We describe the interaction between the fundamental quantum systems, two-level systems, electromagnetic waves, and harmonic oscillators. We also describe the theory relating it to the actual quantum experiments and how they are realized. In particular, we cover details of the “resonator”, which is an almost indispensable tool in the current quantum technology.
- In Part III, we describe an overview of the quantum operations, quantum measurements, quantum error corrections, and an introduction to the state-of-the-art quantum technologies.

Readers who are familiar with analytical mechanics, statistical mechanics, quantum mechanics, and electromagnetism should be able to read this book by using those textbooks as references. In particular, Part I is a review of quantum mechanics, so readers who are quite familiar with quantum mechanics may start reading

from Part II and continue reading while returning to Part I as necessary. However, Part I also includes some details of the methods and concepts that are often seen in quantum technology, so it is recommended that you read them at some point. In this sense, the subject of this book is suited for the third- and fourth-year undergraduate students who have been studying physics. We also hope that some ambitious first- and second-year students try reading. It may be a review for many graduate students and researchers, but comprehensive coverage of the quantum technologies compiled here may provide a new insight. In addition, this book may be used by the researchers who wish to study quantum technologies, but currently working outside the field. We also warn readers to be aware that there may be some parts that lack theoretical rigor because we prioritize the description of the quantum processes as a whole, instead of focusing on the details of the quantum theories, which you may find in other literature. Lastly, problems are provided in the last part of each chapter, except for Chaps. 1 and 11. The authors strongly recommend the readers to tackle with them and check the solutions which are electronically distributed on the Springer website.

One important topic that we are omitting in this book is the advancement of the control and fabrication systems, forming a fundamental basis of the state-of-the-art experimental quantum technologies. Digital controlling systems including Direct-Digital-Synthesis (DDS) and Field-Programmable Gate Array (FPGA), low-noise amplifier technologies, and single-photon detectors are only a few of the examples that have been made in the lab by the researchers, but these high-end products are now readily available commercially. Ultra-high vacuum systems and dilution refrigerators to provide an environment with extremely low background noise are also available. Furthermore, the advancement in the field of material sciences and micro/nano fabrication technologies have allowed researchers to develop a “Designer’s Quantum”, such as Quantum dots, NV-center, and superconducting qubits, with various novel materials and fabrication techniques. These fundamental bases for the experiment might differ depending on the quantum system of the choice, and we encourage the reader to refer to these details in the future.

Lastly, we would like to show our greatest appreciation to people who have helped us preparing these materials. In writing this book, Masato Shigefuji, Yuki Nakajima, and Genya Watanabe, members of Noguchi Laboratory in The University of Tokyo, Yoshimi Rokugawa, Sorato Nakano, Yutaro Nakai, and Tsubasa Karino, members of Shu Lab in International Christian University, cooperated in calculation check and proofreading of the text. Yuta Masuyama from National Institute of Quantum Science and Technology gave us very useful advice on the content. We would love to mention that Akiyuki Tokuno, Sridevi Purushothaman, and Satish Ambikanithi from Springer worked really hard for the publication of this book and Akiyuki in particular has made invaluable advice and comments. We would like to express our gratitude here.

Meguro-ku, Japan
Mitaka-shi, Japan
Meguro-ku, Japan

Alto Osada
Rekishu Yamazaki
Atsushi Noguchi

Contents

Part I Quantum States and Quantum Mechanics

1	Introduction	3
1.1	Common Language in Quantum Information	3
1.2	Various Quantum Systems	5
1.3	Electromagnetic Waves for Quantum Operations	5
1.3.1	Development of Electromagnetic Wave Source	6
1.4	Concept of Temperature	8
2	Linear Algebra	13
2.1	Vector Space	13
2.1.1	Vectors in Three-Dimensional Vector Space	13
2.1.2	Inner Product	14
2.1.3	Orthonormal Basis	14
2.1.4	Vector Components	15
2.1.5	Norm of a Vector	15
2.1.6	Outer Product	16
2.1.7	Expansion for Multidimensional System	16
2.2	Matrix and Operator	17
2.2.1	Matrix Element	17
2.2.2	Transpose Matrix	17
2.2.3	Matrix Multiplication	18
2.2.4	Square Matrix	18
2.3	Eigenvectors and Eigenvalues	20
2.4	Summary of Vector Characteristics in Index Notation	21
3	Wavefunction and Notations in Quantum Mechanics	25
3.1	Equation of Motion in Classical and Quantum Mechanics	25
3.2	Wavefunction	27
3.2.1	Inner Product of Wavefunction	27
3.2.2	Continuous and Discretized Wavefunction	28
3.3	Operator	30
3.4	Dirac Notation	30
3.5	Matrix Representation	32

3.6	Properties of Wavefunction	35
3.7	Composite System	36
3.7.1	Operator in Composite System	39
3.8	Examples of Notation for Frequently Used Quantum State	40
3.9	Quantum State Representation: Qubit	42
3.9.1	One-Qubit state	42
3.9.2	Bloch Sphere	43
3.9.3	Two-Qubit State	45
3.10	Eigenvalue Equation in Quantum Mechanics	50
3.10.1	Example: Atom	52
3.11	Operator Classification	53
3.11.1	Operator Functions	53
3.11.2	Hermitian Operator	54
3.11.3	Projection Operator	56
3.11.4	Unitary Operator	58
3.11.5	Pauli Operators	59
3.12	Density Operator	61
3.12.1	Example of a Mixed State	63
3.12.2	General Properties of Density Operator	63
3.12.3	Density Operator of Composite System and its Reduction	64
3.13	Commutator and Anti-Commutator	66
3.13.1	Heisenberg's Uncertainty Principle	67
4	Time Evolution in Quantum System	73
4.1	Time-Independent Schrödinger Equation	73
4.2	Time Evolution in Terms of Unitary Operator	76
4.3	Three Pictures in Quantum Mechanics	78
4.3.1	General Overview	79
4.3.2	Schrödinger Picture	81
4.3.3	Heisenberg Picture	81
4.3.4	Example: Harmonic Oscillator in Schrödinger and Heisenberg Picture	83
4.3.5	Dirac Picture	86
4.4	Heisenberg Equation of Motion	88
4.5	von Neumann Equation	89
4.6	Unitary Transformation to a Rotating Frame	91
4.7	Driven Two-Level System	94
5	Perturbation Theory	101
5.1	Time Independent Perturbation Theory	101
5.1.1	Zeeman Effect	104
5.2	Treatment of Time-Dependent Perturbation	107
5.2.1	Time-Dependent Perturbation Expansion	114

Part II Harmonic Oscillator, Qubit and Coupled Quantum Systems

6	Harmonic Oscillator	123
6.1	Harmonic Oscillator and Its Hamiltonian	123
6.2	Electromagnetic Waves and Ladder Operators	124
6.2.1	Quantization of Electromagnetic Waves	124
6.2.2	Ladder Operators of a Harmonic Oscillator	125
6.3	Quantum States of a Harmonic Oscillator	126
6.3.1	Coherent State	126
6.3.2	Schrödinger's Cat State	129
6.3.3	Squeezed State	130
6.3.4	Thermal State	132
6.4	Photon Correlations	133
6.4.1	Amplitude Correlation/First-Order Coherence	133
6.4.2	Intensity Correlation/Second-Order Coherence	134
6.5	Wigner Function	134
6.5.1	General Remarks	134
6.5.2	Examples	136
7	Two-level System and Interaction with Electromagnetic Waves	141
7.1	Two-level System, Spin, and Bloch Sphere	141
7.2	Interaction Between Two-level System and Electromagnetic Field	143
7.2.1	Spontaneous and Stimulated Emission	145
7.3	Two-level Systems and Electromagnetic Waves in Practice	146
7.3.1	Two-level Systems in Nuclear Magnetic Resonance	146
7.3.2	Two-level Systems in Atomic Gases	147
7.3.3	Two-level Systems in Solid-state Quantum Defects	148
7.3.4	Two-level System in an Optically Controlled Semiconductor Quantum Dot	148
7.3.5	Two-level System in Superconducting Circuit	149
7.4	Dynamics and Relaxations of Two-level Systems	149
7.4.1	Bloch Equations and Relaxations	149
7.4.2	Rabi Oscillation	153
7.4.3	Ramsey Interference	155
7.4.4	Spin Echo	155
8	Electromagnetic Cavities and Cavity Quantum Electrodynamics	159
8.1	Properties of Cavities	159
8.1.1	Q Factor	161
8.1.2	Finesse	161

8.2	Measurement of a Cavity	162
8.2.1	Reflection and Transmission Measurements	163
8.2.2	Actual Measurement Systems	164
8.3	Input-Output Theory	166
8.3.1	Propagating Mode and Input-Output Theory	166
8.3.2	Single-Port Measurement	168
8.3.3	Dual-Port Measurement	171
8.4	Cavity Quantum Electrodynamics	172
8.4.1	Jaynes–Cummings Model	172
8.4.2	Tavis–Cummings Model	173
8.4.3	Weak and Strong Coupling Regimes	175
8.4.4	Dispersive Regime	178
8.4.5	Waveguide-Coupled Cavity QED System	179
9	Various Couplings in Quantum Systems	185
9.1	Interaction Hamiltonians	185
9.1.1	Jaynes–Cummings and Anti-Jaynes–Cummings Interactions	186
9.1.2	Beam-Splitter and Two-Mode-Squeezing Interactions	186
9.1.3	Interaction Between Qubits	188
9.1.4	Nonlinear Interactions	188
9.2	Atomic Ions	189
9.2.1	Atom-Light Interaction	189
9.2.2	Sideband Transitions: Optomechanics with an Ion	192
9.2.3	Phonon–Phonon Interaction	193
9.3	Superconducting Circuits	195
9.3.1	Quantum-Mechanical Treatment of an LC Resonator	196
9.3.2	Superconducting Quantum Bit	197
9.3.3	Coupling Between a Transmon and an LC Resonator	199
9.4	Optomechanical Interaction	201
9.4.1	Brief Introduction	201
9.4.2	Optomechanical Interaction	202
9.4.3	Linearized Optomechanical Interaction	203
9.5	Hybrid Quantum Systems and Cooperativity	204
Part III Quantum Information Processing and Quantum Technologies		
10	Basics of Quantum Information Processing	211
10.1	Quantum Gates	211
10.1.1	Single-Qubit Gates	212
10.1.2	Two-Qubit Gates	213
10.1.3	Clifford and Non-Clifford Gates	218

10.2	Quantum Circuit Model	219
10.3	Measurement and Imperfections of Quantum States	220
10.3.1	Projective and Generalized Measurement	220
10.3.2	State Tomography	221
10.3.3	Fidelity	222
10.3.4	Estimation of Gate Errors	223
10.4	Essential Idea of Quantum Error Correction	227
10.4.1	Stabilizer Formalism	228
10.4.2	Three-Qubit Repetition Code	229
10.4.3	Nine-Qubit Shor Code	230
10.4.4	Advanced Quantum Error Correction Codes	231
10.5	DiVincenzo Criteria	232
11	Quantum Technologies	235
11.1	Quantum Computer	235
11.1.1	Grover's Algorithm	236
11.1.2	Phase Estimation Algorithm	237
11.1.3	Shor's Algorithm	238
11.2	Quantum Key Distribution	239
11.2.1	BB84	239
11.3	Quantum Sensing	240
11.3.1	Ramsey Interference	240
11.3.2	Quantum Sensing with Entanglement	241
11.4	Quantum Simulation	242
11.5	Quantum Internet	242
Appendix A: Position and Momentum Representations		245
Appendix B: Unitary Transformation to a Rotating Frame		247
Appendix C: Extraction of a Two-Level System from a Three-Level System		251
Appendix D: Quantum Theory of Hydrogen Atom		253
Appendix E: Master Equation		257
Appendix F: Schrieffer–Wolff Transformation		269
Appendix G: Derivation of the SWAP Gate from the Heisenberg Hamiltonian		273
Appendix H: Cavity Cooling of a Mechanical Mode		275
Appendix I: Entangled States and Quantum Teleportation		281
Appendix J: Quantum No-Cloning Theorem		289
References		291
Index		295

Part I

Quantum States and Quantum Mechanics



Introduction

1

1.1 Common Language in Quantum Information

Since the early 1900s, quantum mechanics has been constructed through numerous discussions by renowned physicists such as Einstein, Dirac, Heisenberg, and Schrödinger and has made significant progress. The seemingly non-trivial physical phenomena predicted by the theory have plagued many physicists (and students), but no observations contradicting quantum mechanics have yet to be found in this long history.

The recent development of quantum mechanics over the past 50 years has been greatly influenced by the maturity of experimental methods and new measurements. Observation and manipulation of nuclear spin states by developing nuclear magnetic resonance (NMR), spectroscopic experiments of atoms and ions in an ultra-high vacuum, and verification of quantum properties of light through the development of high-performance lasers and nonlinear optics have all contributed to form firm foundations of quantum manipulation and technologies. Various quantum operations have also been confirmed even in solid-state devices, which have been said to be difficult to guarantee their quantum properties. These experiments have made it possible to verify quantum mechanics from various angles. Through these developments, the quantum object, long been considered as a target of “observation” has been transformed into that of “manipulation”. In other words, human beings have acquired a way to freely *manipulate* the quanta, the smallest entity possible in this world, which was previously only intended to be *seen*.

Meanwhile, the field of quantum information science has made great progress in the last 20 years or so. With the development of experimental methods, the operation of each physical system has improved, and the unique characteristics of these physical systems have become more and more apparent. Information technology that makes use of quantum properties, has been greatly developed. In quantum information, the object holding the bit of information is the quantum entity called quantum bit

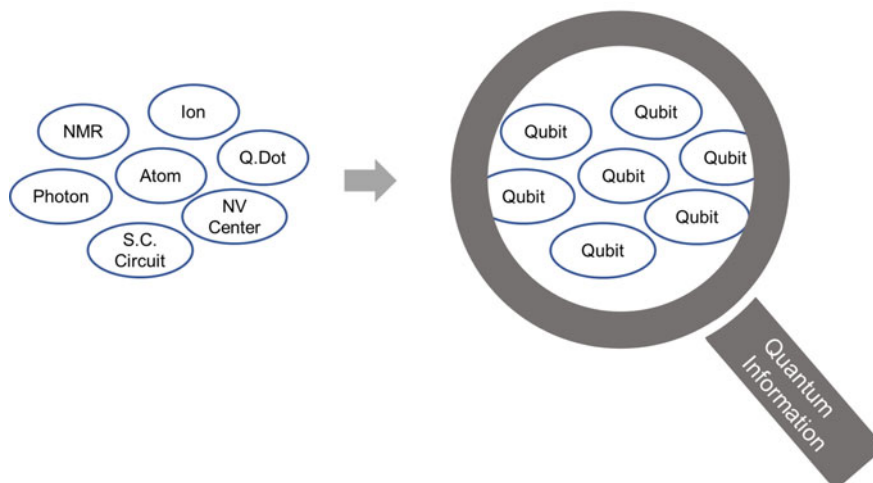


Fig. 1.1 Seemingly different physical systems can all be seen as qubits (quantum bits) from the perspective of the quantum information

or qubit for short. The qubit allows the expansion of the computational capability by incorporating the quantum features, such as superposition and entanglement. This research on quantum information has given rise to some new findings. It has become clear that even seemingly completely different physical systems have many similarities by regarding quantum as the origin of information (Fig. 1.1). So far, each quantum system has progressed independently. However, by taking a bird's-eye view of these various quantum systems in the framework of quantum information, it has become possible to comprehensively understand different physical systems under a unified common language.

This book provides an attempt to capture the characteristics of various quantum physical systems within the framework of quantum information and to promote the development of quantum systems by providing a bird's-eye view to young researchers. It may still take some time before quantum information technology advances into society. However, there are many proposals for the development of quantum devices that greatly exceed existing technologies such as quantum computers, quantum communications/internet, quantum simulations, and quantum sensors. Many scientists believe that these novel technologies will significantly change even the way society should be. We believe that new ideas from young people will be the key to the breakthrough of these quantum technologies, along with existing quantum technologies. We would like to welcome all young students, demonstrating your strength for the future development of the quantum technology.

1.2 Various Quantum Systems

There are many quantum systems, such as ion traps, cold atoms, quantum dots, and superconducting circuits, but of course, the strengths and weaknesses of the system depends on the characteristics of each quantum system. For example, just as an existing computer is composed of individual parts, CPU, memory, hard drive, and Internet adapter, each quantum system could have a different “utility” suited to its characteristics.

There are also many quantum systems that have some common elements. For example, similarity in the manufacturing method (fabrication), the equipment used for control/operation, and the environment (temperature, etc.) in which the device is placed. In those similar systems, learning operations and techniques is often easier than a completely new system. In addition, even quantum systems that look very different at first glance are often said to be similar when the core elements are considered. Also, as mentioned previously, in the framework of quantum information, it is often easier to capture the characteristics and similarities of various quantum systems by considering all the systems as different qubits. For these reasons, it is expected that comprehensive understanding will be promoted by learning various quantum systems.

With the maturation of quantum operations, the development of quantum systems called “hybrid quantum systems” is being promoted worldwide. In hybrid quantum systems, several quantum systems are combined in order to extend the strengths of each quantum system and suppress its weaknesses. For example, photons in optical fibers allow long-range quantum state transmission, but instead, it is very difficult to keep photons (i.e., quantum states) in one place. By coupling an optical fiber with an atom or ion trap, the quantum state is retained in the atom or trapped-ion, and when necessary, it is taken out as a photon and sent to the fiber, thereby providing memory and transmission functions. Understanding the pros and cons of each quantum system to come up with complementary combination is a key for the development of a novel hybrid quantum system.

1.3 Electromagnetic Waves for Quantum Operations

First of all, a physical phenomenon is the movement or influence of an object through some kind of **force**, and we all learned that there are four forces in the world, weak nuclear, strong nuclear, electromagnetic, and gravitational force, with corresponding elementary particles called weak bosons, gluons, photons, and gravitons that are responsible for the propagation of each force. Of these, the electromagnetic force is the closest to our everyday life. Of course, without the nuclear force, the atoms that make up the basic structure of the world would be disjointed and everything falls apart, but everyday phenomena such as friction, sound propagation, and phase transitions between gases, liquids, and solids, as well as the functions in the electrical circuits, are all results of the electromagnetic interaction. Furthermore, nearly all

physiological processes in the living body are phenomena that are manifested by electromagnetic force. In other words, photons intervene in all these phenomena.

The quantum systems that we are manipulating are no exception. Quantum operations are performed using electric and magnetic fields and various types of electromagnetic waves. Therefore, “quantum optics”, which treats electromagnetic waves themselves as a quantum object can be considered as the basis of quantum operations. Important concepts in the quantum optics appear in various forms of the quantum research. There are many wonderful literature on quantum optics, so this book will only introduce the basics, but we encourage students to explore these literature yourself. In addition, quantum optics has been studied mainly for “light” among electromagnetic waves as its origin, but due to the maturation of dilution refrigerators and the remarkable development of superconducting quantum circuits in recent years, electromagnetic waves in the microwave region have become another focus. These are called “microwave quantum optics” and have grown as a discipline with features different from those in the optical domain. In addition, research and development of electromagnetic waves in the THz region, which was difficult to generate and measure, has been steadily progressing in recent years. There is still little research in the context of quantum operations, but we look forward to future developments.

1.3.1 Development of Electromagnetic Wave Source

The role of electromagnetic waves in quantum operations is described, and one can see that the quality of quantum operations using electromagnetic waves is directly related to the issue of “how to manipulate the electromagnetic waves precisely”. The history of the quantum operation has always progressed with the development of microwave oscillators and lasers as the electromagnetic wave source, so let’s touch on the development of the electromagnetic wave source, although it is a bit technical subject.

The state basis used for the qubit is often the energy states as shown in Fig. 1.2, and the transition between the states is manipulated by electromagnetic waves. Common electromagnetic waves used are the RF (MHz range), microwave (GHz range), and the optical region (on the order of 100 THz). The frequency of the electromagnetic wave corresponds to the energy difference of the transition as $\omega_0 = \frac{E_e - E_g}{\hbar}$. To be more specific with the physical system, NMR is mainly operated by RF, microwaves are mainly used in superconducting circuits and spin systems, and optical light is used in atoms and ions, for example.

One of the characteristics of electromagnetic waves, which is important experimentally but hardly ever talked about in a textbook, is the “Linewidth” of electromagnetic waves. Considering an electromagnetic wave oscillator that radiates an electromagnetic wave ω_0 which is in resonance with an atomic transition in Fig. 1.2, the output frequency of the ideal oscillator is a single frequency as shown on the left side of Fig. 1.3. However, in an actual oscillator, there is a certain amount of frequency or phase fluctuation, and the frequency staggers around ω_0 . In the same

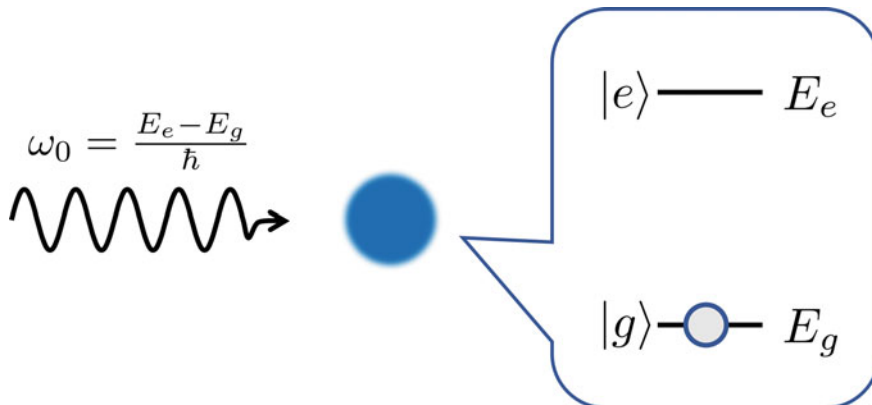


Fig. 1.2 Electromagnetic waves are used for transitions between energy eigenstates

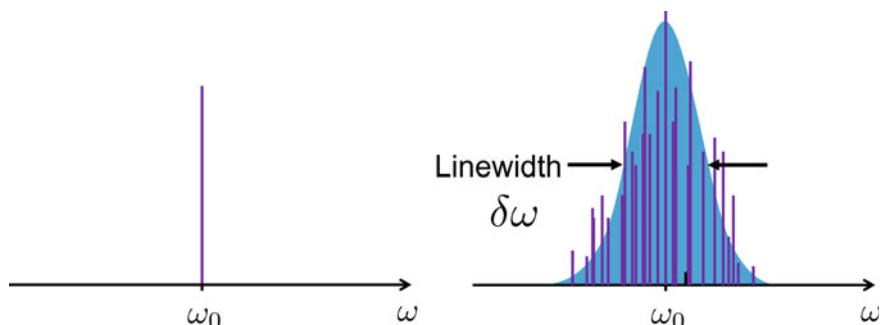


Fig. 1.3 (Left) Ideal single frequency oscillator output, (Right) Fluctuating oscillator output

figure on the right, the fluctuation is drawn as a histogram. The frequency spread $\delta\omega$ of the oscillator measured within a specific time is called the “Linewidth” of the electromagnetic wave, and it is an index of how stable the electromagnetic wave is. Of course, a stable electromagnetic wave oscillator can perform stable quantum operations. In other words, narrowing the linewidth of the electromagnetic wave source can be a cornerstone of the higher operability and refined control of the quantum systems.

The origin of the linewidth broadening of electromagnetic waves may be from a variety of reasons, such as oscillator performance, the vibration of the experiment table, and the Fourier limit (which spreads in frequency due to the short pulse time of electromagnetic waves). In addition, the performance required for electromagnetic waves varies greatly depending on the linewidth of the target energy level and the operation time, so it is necessary to always consider what kind of oscillator performance is required for each experiment.

RF and microwaves have long been used commercially for communications and sensors, and various oscillators, filters, and related parts are well-developed. For the electromagnetic wave generation, ultra-stabilized oscillators, arbitrary

waveform generators, pulse generators, and various mixers and filters are used. Many high-performance peripheral products such as high-speed oscilloscopes, spectrum analyzers, and network analyzers are readily available in the market. In that sense, it is probably safe to say that the RF and microwave oscillators have already accumulated extremely high technological capabilities. In addition, with the recent evolution of microwave quantum optics and the maturation of superconducting circuits with quantum computers in mind, novel RF/microwave devices are rapidly developed. These developments include ultra-low temperature circulators without magnetic field, arbitrary waveform generators making full use of FPGAs (Field Programmable Gate Arrays) and DDSs (Direct Digital Synthesizers), noiseless quantum amplifiers using parametric oscillations, and traveling wave parametric amplifiers that have a wider bandwidth. Many of these novel devices are developed for quantum operations, particularly the large-scale quantum information processing being one of the strong drives.

The linewidth of electromagnetic waves is very low, easily less than 1 Hz, in commercialized RF/microwave oscillators, whereas it can be of several GHz in commonly available lasers, such as semiconductor lasers. Since the frequency of light itself is much higher than that of RF/microwave, one may think it is unfair to compare them directly and better to compare the relative fluctuation. However, the relative fluctuation $\delta\omega/\omega_0$, normalized with the carrier frequency ω_0 , is also overwhelmingly better for common microwave oscillators than the lasers. The narrow linewidth and high performance of RF/microwave oscillators are understandable because of the long history of RF/microwave oscillators for their active commercial use.

Under such circumstances, it was necessary to make a home-made high-performance laser suited for the precise control of the quantum states. Thus, the evolution of high-performance lasers has always been cultivated with the development of quantum technologies. Many laser developments such as ultra-stable laser with a linewidth less than 1 Hz, ultra-wideband optical combs, and integrated laser circuits on chip have emerged as the foundation of quantum operations. The ultimate electromagnetic wave operation is indispensable for the future of quantum technology, and these research and development will continue to be a part of the adventure in the development of quantum technologies.

1.4 Concept of Temperature

We have mentioned that different quantum systems may have various similarities. One of the important experimental parameters is the energy of the quantum systems and the electromagnetic waves used to manipulate them. It is described below that the importance comes from the temperature of the environment in which the quantum system is installed at the time of the experiment.

Many quantum operations require a single quantum operation, where a single quantum of energy is exchanged in various forms. The system can be easily explained by using the energy levels of an atom. For example, as shown in Fig. 1.4, there is an atom with two different energy levels, the ground state $|g\rangle$ and

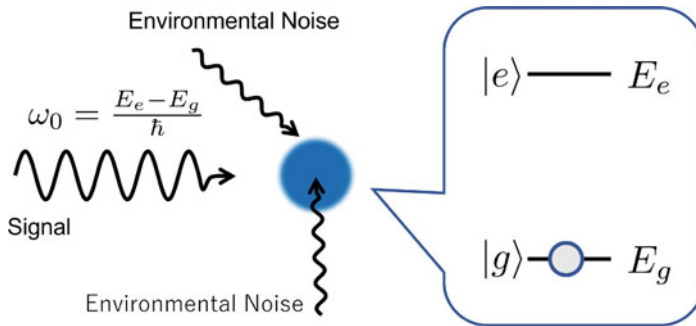


Fig. 1.4 Transition between the energy states. The origin of the energy state transition is not limited to the signal light intended in the experiment, but also includes noise from the surrounding environment such as phonons and spins in thermally excited solids

the excited state $|e\rangle$, with corresponding energy E_g and E_e , respectively. Normally, the electron is in the ground state, but when the electromagnetic wave with energy $E_0 = E_e - E_g$ is absorbed, the electron makes a transition to the excited state (Fig. 1.4). The electromagnetic wave here may be the electromagnetic wave intended to use in the experiment, but if it is not, the atom may be mistakenly excited.

Let's consider where this “unintended electromagnetic wave” possibly comes from. We consider the temperature T of the environment surrounding the atoms and bosonic particles (e.g., photons) that are in thermal equilibrium with the environment. Using the frequency ω of the bosonic particle, the energy of the particle is written as $E_{\text{Boson}} = \hbar\omega$, and the average number of particles $\langle n \rangle$ is given following the Bose–Einstein distribution as

$$\langle n \rangle = \frac{1}{e^{\frac{\hbar\omega}{k_B T}} - 1}, \quad (1.4.1)$$

where $\hbar = h/2\pi$ and k_B are the Dirac constant and the Boltzmann constant, respectively. The Dirac constant is a variation of the Planck constant, and it is customary to use the Dirac constant rather than the Planck constant in many quantum research areas, including quantum optics and quantum information sciences.

When the effective energy of the thermal environment $E_{\text{env}} = k_B T$ is sufficiently higher than the boson particle energy $E_{\text{particle}} = \hbar\omega$, this equation is approximated as

$$\langle n \rangle \simeq \frac{k_B T}{\hbar\omega}. \quad (1.4.2)$$

As can be seen from this equation, the average number of bosonic particles $\langle n \rangle$, proportional to T , is swelling in the environment surrounding the quantum system. Elementary excited particles such as phonons in a solid, and even in a vacuum



Fig. 1.5 Temperature of the environment and number of microwave photons inside a cavity. (Left) At $T = 300$ K, average number of microwave photons is $\langle n \rangle \simeq 600$, which intervene with the signal microwave photon. (Right) At $T = 10$ mK, $\langle n \rangle \simeq 0.02$ and hardly any microwave photons are present except the signal microwave

Table 1.1 Relationship between the electromagnetic wave frequency and experimental environment temperature

EM wave	Frequency ($\omega_0/2\pi$)	Effective Temp. (T_{eff})	Environment Temp. (T)
Microwave	10 GHz	500 mK	10 mK
Optical light	200 THz	10,000 K	300 K

chamber, bosonic particles such as photons are zipping around with an average number of $\langle n \rangle$. The thermal bosonic particles that roar in these environments with a temperature of T become “unintended electromagnetic wave”, an obstacle for the quantum operation. To eliminate the bosonic particles from the environment at the electromagnetic wave frequency $\omega_0 = E_0/\hbar$, the environment temperature T needs to be sufficiently low to satisfy $\langle n \rangle \ll 1$.

An example of the effect of the environment temperature is shown in Fig. 1.5. On the left, there is a microwave cavity at temperature $T = 300$ K with a quantum sample inside. In this cavity, the average number of microwave photons with frequency $\omega_0/2\pi = 10$ GHz is about $\langle n_{\text{MW}} \rangle \simeq 600$, and the signal microwave photon intended to control the sample is buried under these background photons. On the other hand, when the sample is installed in a dilution refrigerator where $T = 10$ mK, the number of background microwave photons drops to $\langle n_{\text{MW}} \rangle \simeq 0.02$, enabling a quantum control of the sample with the signal microwave.

From above, the requirement of the environmental temperature reads

$$T \ll T_{\text{eff}} = \frac{\hbar\omega_0}{k_B}. \quad (1.4.3)$$

This equation tells us that the effect of the thermal bosonic particles is mitigated when the environmental temperature is sufficiently lower than the effective temperature of electromagnetic waves ($T_{\text{eff}} = \frac{\hbar\omega_0}{k_B}$). In many of the quantum control experiments, electromagnetic waves such as microwaves and optical light are often used. In Table 1.1, we summarize the frequency, effective temperature, and common environmental temperature for the microwave and optical light.

As can be seen from this table, the effective temperature of a microwave is about 500 mK, requiring an extremely low-temperature environment often achieved using a dilution refrigerator. For the optical light, in contrast, the effective temperature is about 10,000 K, and many experiments can be performed at room temperature 300 K. One can intuitively understand that $\langle n \rangle \ll 1$ is fulfilled for optical light in a room temperature from the fact that all the walls in our rooms are not “glowing” (with optical light) from the heat.

As described above, the suited environmental temperature of the quantum device greatly differs depending on the frequency of the electromagnetic wave used. Also, it should be remembered that due to this stringent environmental condition for the microwave experiment, the techniques and technologies related to experiments differ greatly between microwaves and light despite the fact that both are electromagnetic waves.



Linear Algebra

2

In the introductory quantum mechanics course, we all learn the behavior of wavefunction $\psi(x)$ satisfying the Schrödinger equation. The wavefunction can actually be represented as a vector in a vector space, the so-called Hilbert space. In the quantum technology, we focus on the manipulation of the quantum state, where the vector in the Hilbert space is transformed, measured, and manipulated through various physical interactions. These dynamics can be represented simply by using the terminologies and techniques of the vector space, using the language of linear algebra. Here, we review the basics of the vector space by introducing frequently used terminologies.

2.1 Vector Space

2.1.1 Vectors in Three-Dimensional Vector Space

\vec{V} and \vec{W} are vectors in a three-dimensional vector space, represented as

$$\vec{V} = V_x \hat{x} + V_y \hat{y} + V_z \hat{z} \quad (2.1.1)$$

$$\vec{W} = W_x \hat{x} + W_y \hat{y} + W_z \hat{z}. \quad (2.1.2)$$

A vector is formed with unit vectors \hat{x} , \hat{y} , \hat{z} , called *basis* and its components (scalar amplitudes) V_x , V_y , V_z and W_x , W_y , W_z , respectively. In an actual calculation, it is convenient to use a matrix representation of a vector, column matrix, to represent the vector.

Supplementary Information The online version contains supplementary material available at https://doi.org/10.1007/978-981-19-4641-7_2.

Unit vectors can be represented using the column matrix as

$$\hat{x} \equiv \begin{pmatrix} 1 \\ 0 \\ 0 \end{pmatrix}, \quad \hat{y} \equiv \begin{pmatrix} 0 \\ 1 \\ 0 \end{pmatrix}, \quad \hat{z} \equiv \begin{pmatrix} 0 \\ 0 \\ 1 \end{pmatrix} \quad (2.1.3)$$

and the vectors can be represented as

$$\vec{V} = V_x \begin{pmatrix} 1 \\ 0 \\ 0 \end{pmatrix} + V_y \begin{pmatrix} 0 \\ 1 \\ 0 \end{pmatrix} + V_z \begin{pmatrix} 0 \\ 0 \\ 1 \end{pmatrix} = \begin{pmatrix} V_x \\ V_y \\ V_z \end{pmatrix} \quad (2.1.4)$$

$$\vec{W} = W_x \begin{pmatrix} 1 \\ 0 \\ 0 \end{pmatrix} + W_y \begin{pmatrix} 0 \\ 1 \\ 0 \end{pmatrix} + W_z \begin{pmatrix} 0 \\ 0 \\ 1 \end{pmatrix} = \begin{pmatrix} W_x \\ W_y \\ W_z \end{pmatrix}. \quad (2.1.5)$$

2.1.2 Inner Product

Inner product of two vectors is defined as

$$\vec{V} \cdot \vec{W} \equiv V_x W_x + V_y W_y + V_z W_z. \quad (2.1.6)$$

A scalar value is calculated from the inner product of two vectors. Using the matrix representation, the inner product can be defined as a vector multiplication of the transpose of the first vector

$$\vec{V}^T \equiv (V_x \ V_y \ V_z), \quad (2.1.7)$$

and the second vector as

$$\vec{V} \cdot \vec{W} = \vec{V}^T \vec{W} = (V_x \ V_y \ V_z) \begin{pmatrix} W_x \\ W_y \\ W_z \end{pmatrix} = V_x W_x + V_y W_y + V_z W_z. \quad (2.1.8)$$

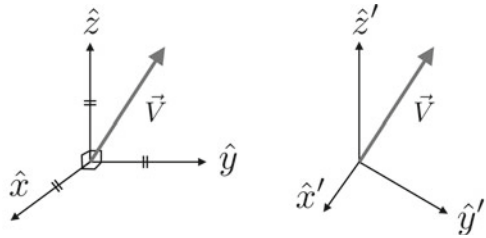
It is clear from the matrix representation that the two vectors, \vec{V} and \vec{W} , need to have the same dimension to form an inner product.

2.1.3 Orthonormal Basis

When the inner product of two vectors is zero, $\vec{V}_1 \cdot \vec{V}_2 = 0$. \vec{V}_1 and \vec{V}_2 are said to be *orthogonal*. Also, a vector whose length is of unity is said to be *normalized*. In many cases, the basis vectors such as \hat{x} , \hat{y} , and \hat{z} in Fig. 2.1 (left) are chosen to be orthogonal and normalized, referred to as *orthonormal set of basis*. Representing the basis \hat{x} , \hat{y} , and \hat{z} with \hat{x}_i , $i = 1, 2, 3$, the orthonormal set of basis follows the condition

$$\hat{x}_i \cdot \hat{x}_j = \delta_{ij}, \quad (2.1.9)$$

Fig. 2.1 (Left) Orthonormal set of basis \hat{x} , \hat{y} , and \hat{z} .
 (Right) Non-orthonormal set of basis \hat{x}' , \hat{y}' , and \hat{z}' . One can choose any basis to represent \vec{V} ; however, it is more convenient and intuitive to use the orthonormal set of basis in most cases



where δ_{ij} is called the Kronecker delta and has the property

$$\delta_{ij} = \begin{cases} 0, & \text{if } i \neq j \\ 1, & \text{if } i = j. \end{cases} \quad (2.1.10)$$

Generally speaking, the basis does not require to be normalized or orthogonal as shown in Fig. 2.1 (right). One can use a non-orthonormal set of basis \hat{x}' , \hat{y}' , and \hat{z}' to represent \vec{V} ; however, it is much more intuitive to use the orthonormal set of basis, and also it makes many of the calculations much simpler.

2.1.4 Vector Components

Given a vector \vec{V} , one can obtain the amplitude of each component using the inner product with the normalized basis. For example, the x-component of V , V_x , can be calculated as

$$V_x = \hat{x} \cdot \vec{V}. \quad (2.1.11)$$

Using the matrix representation, V_x is calculated as

$$V_x = (1 \ 0 \ 0) \begin{pmatrix} V_x \\ V_y \\ V_z \end{pmatrix}. \quad (2.1.12)$$

2.1.5 Norm of a Vector

From each vector component V_i , one can calculate the “length” of the vector, called *Norm* of the vector. Norm can be defined using the inner product as

$$\text{norm}(\vec{V}) \equiv \sqrt{\vec{V} \cdot \vec{V}} = \sqrt{V_x^2 + V_y^2 + V_z^2}. \quad (2.1.13)$$

Using this norm, one can calculate a unit vector \hat{v} , which is pointing in the direction of an arbitrary vector \vec{V} as

$$\hat{v} = \frac{\vec{V}}{\text{norm}(\vec{V})}. \quad (2.1.14)$$

Using this unit vector, the original vector \vec{V} can easily be represented as

$$\vec{V} = \text{norm}(\vec{V})\hat{v}. \quad (2.1.15)$$

2.1.6 Outer Product

For the case of inner product, a scalar is calculated from two vectors. Outer product of vectors, on the other hand, calculates a matrix from two vectors. Using the same \vec{V} and \vec{W} defined earlier, the matrix representation of the outer product of two vectors is written as

$$\vec{V} \otimes \vec{W} \equiv \vec{V}\vec{W}^T = \begin{pmatrix} V_x \\ V_y \\ V_z \end{pmatrix} (W_x \ W_y \ W_z) \quad (2.1.16)$$

$$= \begin{pmatrix} V_x W_x & V_x W_y & V_x W_z \\ V_y W_x & V_y W_y & V_y W_z \\ V_z W_x & V_z W_y & V_z W_z \end{pmatrix}. \quad (2.1.17)$$

In this example, a matrix with a size 3×3 is calculated from two three-dimensional vectors; however, in general, the vector dimensions do not have to be the same. The outer product of m - and n -dimensional vectors results in a matrix of dimension $m \times n$.

2.1.7 Expansion for Multidimensional System

All the examples so far are shown with three-dimensional vectors, familiar to many of us. In the Hilbert space, where a quantum state is represented, the space dimension can be much larger than three, requiring systematic expansion methods that are simple and easy to calculate.

By introducing the subscript index to expand the basis as $(\hat{x}, \hat{y}, \hat{z}) \rightarrow (\hat{x}_i, i = 1, 2, 3, 4, \dots)$, a vector in a multidimensional space can be represented as

$$\vec{V} = \sum_i V_i \hat{x}_i = V_1 \hat{x}_1 + V_2 \hat{x}_2 + \dots \quad (2.1.18)$$

$$\vec{W} = \sum_i W_i \hat{x}_i = W_1 \hat{x}_1 + W_2 \hat{x}_2 + \dots, \quad (2.1.19)$$

where V_i and W_i are the components of the vector in the basis x_i .

2.2 Matrix and Operator

As shown earlier, the outer product of two vectors forms a matrix. $m \times n$ -dimensional matrix \hat{A} is represented as

$$\hat{A} \equiv \begin{pmatrix} A_{11} & A_{12} & \dots & A_{1n} \\ A_{21} & A_{22} & \dots & A_{2n} \\ \vdots & \vdots & \ddots & \vdots \\ A_{m1} & A_{m2} & \dots & A_{mn} \end{pmatrix}, \quad (2.2.1)$$

where A_{ij} is the matrix element for the corresponding row i and column j .

2.2.1 Matrix Element

A matrix element, for example, A_{21} , can be calculated from matrix \hat{A} with unit vectors,

$$\hat{x}_1 = \begin{pmatrix} 1 \\ 0 \\ 0 \\ \vdots \\ 0 \end{pmatrix}, \quad \hat{x}_2 = \begin{pmatrix} 0 \\ 1 \\ 0 \\ \vdots \\ 0 \end{pmatrix} \quad (2.2.2)$$

as

$$A_{21} = (0 \ 1 \ 0 \ \dots \ 0) \begin{pmatrix} A_{11} & A_{12} & \dots & A_{1n} \\ A_{21} & A_{22} & \dots & A_{2n} \\ \vdots & \vdots & \ddots & \vdots \\ A_{m1} & A_{m2} & \dots & A_{mn} \end{pmatrix} \begin{pmatrix} 1 \\ 0 \\ 0 \\ \vdots \\ 0 \end{pmatrix}. \quad (2.2.3)$$

Following the recipe above, matrix element A_{ij} can be obtained as a matrix product of (row vector)·(matrix)·(column vector) as

$$A_{ij} = \hat{x}_i^T \hat{A} \hat{x}_j. \quad (2.2.4)$$

2.2.2 Transpose Matrix

Transpose matrix \hat{A}^T of $m \times n$ -dimensional matrix \hat{A} is

$$\hat{A}^T \equiv \begin{pmatrix} A_{11} & A_{21} & \dots & A_{m1} \\ A_{12} & A_{22} & \dots & A_{m2} \\ \vdots & \vdots & \ddots & \vdots \\ A_{1n} & A_{2n} & \dots & A_{mn} \end{pmatrix}. \quad (2.2.5)$$

\hat{A}^T is $n \times m$ -dimensional and the matrix element A_{ij}^T satisfies

$$A_{ij}^T = A_{ji}. \quad (2.2.6)$$

2.2.3 Matrix Multiplication

Matrix multiplication results in a new matrix, for example, $\hat{C} = \hat{A}\hat{B}$. Matrix element C_{ij} of this new matrix \hat{C} satisfies

$$C_{ij} = \sum_k A_{ik} B_{kj}. \quad (2.2.7)$$

As can be seen in this equation, when the product \hat{C} is $l \times n$ -dimensional and \hat{A} is $l \times m$ -dimensional, the other matrix \hat{B} has to be $m \times n$ -dimension to fulfill the dimensional requirement of the product.

Matrix element of the transpose of \hat{C} , \hat{C}^T , can be found by simply swapping the indices as

$$C_{ij}^T = C_{ji} = \sum_k A_{jk} B_{ki}. \quad (2.2.8)$$

2.2.4 Square Matrix

A matrix with the same number of rows and columns, $m \times m$ matrix, is called a square matrix. Most of the matrices used in the quantum technologies are square matrices. Here, we review some characteristics and special types of square matrices often used.

Trace of a Matrix

Trace of a square matrix \hat{A} is defined as

$$\text{Tr } \hat{A} \equiv \sum_i A_{ii} = A_{11} + A_{22} + \dots \quad (2.2.9)$$

and is a sum of the diagonal matrix elements A_{ii} . When the product of matrices, $\hat{C} = \hat{A}\hat{B}$, is a square matrix, the trace of \hat{C} is given as

$$\text{Tr } \hat{C} = \sum_i C_{ii} = \sum_{i,j} A_{ij} B_{ji}. \quad (2.2.10)$$

Unit Matrix

One of the special square matrices is the unit matrix \hat{I} , where all the matrix elements in the diagonal are 1 with the rest of the elements being 0s. Three-dimensional unit matrix is

$$\hat{I} \equiv \begin{bmatrix} 1 & 0 & 0 \\ 0 & 1 & 0 \\ 0 & 0 & 1 \end{bmatrix}. \quad (2.2.11)$$

The matrix element I_{ij} of unit matrix follows

$$I_{ij} = \delta_{ij}. \quad (2.2.12)$$

Given a set of orthonormal basis \hat{x}_i , the unit matrix can be obtained from outer products of basis as

$$\hat{I} = \sum_i \hat{x}_i \hat{x}_i^T \quad (2.2.13)$$

$$= \begin{bmatrix} 1 & 0 & \dots & 0 \\ 0 & 0 & \dots & 0 \\ \vdots & \vdots & \ddots & \vdots \\ 0 & 0 & \dots & 0 \end{bmatrix} + \begin{bmatrix} 0 & 0 & \dots & 0 \\ 0 & 1 & \dots & 0 \\ \vdots & \vdots & \ddots & \vdots \\ 0 & 0 & \dots & 0 \end{bmatrix} + \dots + \begin{bmatrix} 0 & 0 & \dots & 0 \\ 0 & 0 & \dots & 0 \\ \vdots & \vdots & \ddots & \vdots \\ 0 & 0 & \dots & 1 \end{bmatrix} \quad (2.2.14)$$

$$= \begin{bmatrix} 1 & 0 & \dots & 0 \\ 0 & 1 & \dots & 0 \\ \vdots & \vdots & \ddots & \vdots \\ 0 & 0 & \dots & 1 \end{bmatrix}. \quad (2.2.15)$$

Matrix as an Operator

An operator acting on a vector maps the vector to another vector in the same vector space. The operator can be represented with a matrix, with the operation given as a matrix multiplication with a vector.

For example, when a operator \hat{A} maps vector \vec{V} to another vector \vec{W} , the operation can be written as

$$\vec{W} = \hat{A} \vec{V}. \quad (2.2.16)$$

Let us take a look at the operation focusing on the vector and matrix element. The operator \hat{A} and vector \vec{V} are given as

$$\hat{A} = \begin{pmatrix} A_{11} & A_{12} & A_{13} \\ A_{21} & A_{22} & A_{23} \\ A_{31} & A_{32} & A_{33} \end{pmatrix} \quad (2.2.17)$$

$$\vec{V} = \begin{pmatrix} V_1 \\ V_2 \\ V_3 \end{pmatrix}. \quad (2.2.18)$$

Resulting vector \vec{W} is calculated as a product

$$\vec{W} = \hat{A}\vec{V} = \begin{pmatrix} A_{11} & A_{12} & A_{13} \\ A_{21} & A_{22} & A_{23} \\ A_{31} & A_{32} & A_{33} \end{pmatrix} \begin{pmatrix} V_1 \\ V_2 \\ V_3 \end{pmatrix} = \begin{pmatrix} A_{11}V_1 + A_{12}V_2 + A_{13}V_3 \\ A_{21}V_1 + A_{22}V_2 + A_{23}V_3 \\ A_{31}V_1 + A_{32}V_2 + A_{33}V_3 \end{pmatrix}. \quad (2.2.19)$$

Using an index notation, the operation above can be given as

$$W_i = \sum_j A_{ij} V_j. \quad (2.2.20)$$

2.3 Eigenvectors and Eigenvalues

There is an important set of vectors for an operator, called eigenvectors. When an operator acts on a vector to create a new vector, where the new vector is a non-zero scalar multiple of the original vector, it is called an *eigenvector* of the operator. It is much simpler to see it in an equation form. Vector \vec{V} is an eigenvector of an operator \hat{A} when the following equation is satisfied:

$$\hat{A}\vec{V} = a\vec{V}, \quad (2.3.1)$$

where a is a scalar factor. This scalar factor is called an *eigenvalue* of the operator \hat{A} , corresponding to the eigenvector \vec{V} . From the form of Eq. 2.3.1, where the resulting vector has the same dimension as the original vector, we identify that the operator \hat{A} needs to be a square matrix.

The eigenvalues of an arbitrary operator \hat{A} can be found as a solution of a characteristic function

$$c(\lambda) \equiv \det(\hat{A} - \lambda\hat{I}) = 0, \quad (2.3.2)$$

where \hat{I} is a unit matrix and $\det(\hat{O})$ represents determinant of matrix \hat{O} . From the expression of the characteristic function, there can be multiple eigenvalues λ , and it is known that any operator has at least one eigenvalue and its corresponding eigenvector as a consequence of the formal algebra. There is also a case, where one might find multiple eigenvalues λ having the same value. For example, for a matrix

$$\hat{A} = \begin{pmatrix} 1 & 0 & 2 \\ 0 & -1 & 0 \\ 2 & 0 & 1 \end{pmatrix}, \quad (2.3.3)$$

the characteristic equation is

$$c(\lambda) = \det \begin{pmatrix} 1 - \lambda & 0 & 2 \\ 0 & -1 - \lambda & 0 \\ 2 & 0 & 1 - \lambda \end{pmatrix} = 0, \quad (2.3.4)$$

from which we can find the eigen values $\lambda = 3, -1, -1$ with corresponding eigenvectors

$$\vec{V}_1 = \begin{pmatrix} 1 \\ 0 \\ 1 \end{pmatrix}, \quad \vec{V}_2 = \begin{pmatrix} 1 \\ 0 \\ -1 \end{pmatrix}, \quad \vec{V}_3 = \begin{pmatrix} 0 \\ 1 \\ 0 \end{pmatrix}. \quad (2.3.5)$$

The multiplets of the eigenvalues (here, $\lambda = -1$) are called *degenerate* eigenvalues. It is important to notice that even if the eigenvalues are degenerate, the eigenvectors can be orthogonal, which is easily checked as

$$\vec{V}_2 \cdot \vec{V}_3 = (1 \ 0 \ -1) \begin{pmatrix} 0 \\ 1 \\ 0 \end{pmatrix} = 0. \quad (2.3.6)$$

2.4 Summary of Vector Characteristics in Index Notation

Throughout the text, certain vector characteristics are used frequently. It is convenient to use an index notation, which provides a compact representation, instead of the bulky matrix representation. Following is the summary of the important and frequently used vector characteristics using index notation.

Vectors in Multidimensional Space

$$\text{Orthonormality} \quad \hat{x}_i \hat{x}_j = \delta_{ij} \quad (2.4.1)$$

$$\text{Vector component} \quad V_i = \hat{x}_i \cdot \vec{V} \quad (2.4.2)$$

$$\text{Norm of a vector} \quad \text{norm}(\vec{V}) = \sqrt{\sum_i V_i^2} \quad (2.4.3)$$

$$\text{Normalized vector} \quad \sum_i V_i^2 = 1 \quad (2.4.4)$$

$$\text{Inner product} \quad \vec{V} \cdot \vec{W} = \sum_i V_i W_i \quad (2.4.5)$$

$$\text{Outer product} \quad (\vec{V} \otimes \vec{W})_{ij} = V_i W_j. \quad (2.4.6)$$

For the outer product, matrix element of the product $\vec{V} \otimes \vec{W}$ is given. When vectors \vec{V} and \vec{W} are of dimension m and n , indices are given as $i = 1 \dots m$, $j = 1 \dots n$, respectively.

Matrix element

For vectors and matrices satisfying $\vec{W} = \hat{A}\vec{V}$ and $\hat{C} = \hat{A}\hat{B}$,

$$\text{Matrix element and basis} \quad A_{ij} = \hat{x}_i^T \hat{A} \hat{x}_j \quad (2.4.7)$$

$$\text{Matrix element of products of matrices} \quad C_{ij} = \sum_k A_{ik} B_{kj} \quad (2.4.8)$$

$$\text{Transpose matrix} \quad C_{ij}^T = C_{ji} = \sum_k A_{jk} B_{ki} \quad (2.4.9)$$

$$\text{Trace} \quad \text{Tr } C = \sum_i C_{ii} = \sum_{i,j} A_{ij} B_{ji} \quad (2.4.10)$$

$$\text{Unit matrix} \quad \hat{I} = \sum_i \hat{x}_i \hat{x}_i^T \quad (2.4.11)$$

$$\text{Matrix-Vector multiplication} \quad W_i = \sum_j A_{ij} V_j. \quad (2.4.12)$$

Problems

Problem 2-1 Normalize the following vector \vec{V} to find the normalized vector \vec{V}' .

- (i) $\vec{V} = \hat{x} + \hat{y}$.
- (ii) $\vec{V} = 2\hat{x} + 3\hat{y} - 4\hat{z}$.

Problem 2-2

- (i) Show $\vec{V}_1 = \frac{1}{\sqrt{2}}\hat{x} + \frac{1}{\sqrt{2}}\hat{y}$ and $\vec{V}_2 = \frac{1}{\sqrt{2}}\hat{x} - \frac{1}{\sqrt{2}}\hat{y}$ are orthogonal.
- (ii) Find a vector $\hat{V}_2 = V_{2x}\hat{x} + V_{2y}\hat{y}$ which is orthogonal to $\vec{V}_1 = 3\hat{x} - 2\hat{y}$ and normalized.

Problem 2-3 Prove that a vector $\vec{V} = \begin{pmatrix} \sin \theta \cos \phi \\ \sin \theta \sin \phi \\ \cos \theta \end{pmatrix}$ is a normalized vector for arbitrary chosen θ and ϕ .

Problem 2-4 Prove that three vectors

$$\vec{a} = \frac{1}{3} \begin{pmatrix} 1 \\ 2 \\ 2 \end{pmatrix}, \vec{b} = \frac{1}{3} \begin{pmatrix} -2 \\ -1 \\ 2 \end{pmatrix}, \text{ and } \vec{c} = \frac{1}{3} \begin{pmatrix} 2 \\ -2 \\ 1 \end{pmatrix}$$

form a orthonormal set of basis.

Problem 2-5 Find an outer product $\vec{V}_1 \otimes \vec{V}_2$ of two vectors,

$$\vec{V}_1 = \begin{pmatrix} 1 \\ 0 \\ 2 \end{pmatrix} \text{ and } \vec{V}_2 = \begin{pmatrix} 3 \\ 1 \\ 4 \\ 2 \end{pmatrix}.$$

Problem 2-6 There is a “ sibling” of outer product, called the Kronecker product. For matrices \hat{A} of $m \times n$ -dimension and \hat{B} , the Kronecker product is defined as

$$\hat{A} \otimes \hat{B} = \begin{pmatrix} A_{11}\hat{B} & \cdots & A_{1n}\hat{B} \\ \vdots & \ddots & \vdots \\ A_{m1}\hat{B} & \cdots & A_{mn}\hat{B} \end{pmatrix}. \quad (2.4.13)$$

Find the Kronecker product, $\hat{A} \otimes \hat{B}$ for $\hat{A} = \begin{pmatrix} 0 & 1 \\ 1 & 0 \end{pmatrix}$ and $\hat{B} = \begin{pmatrix} 1 & 0 \\ 0 & -1 \end{pmatrix}$.

Problem 2-7 For square matrices \hat{A} , \hat{B} , and \hat{C} , prove the following properties of matrix trace using the index notation, e.g., $\text{Tr } A = \sum_i A_{ii}$

- (i) $\text{Tr}(\hat{A} + \hat{B}) = \text{Tr } \hat{A} + \text{Tr } \hat{B}$.
- (ii) $\text{Tr}(c\hat{A}) = c \text{Tr } \hat{A}$.
- (iii) $\text{Tr}(\hat{A}\hat{B}) = \text{Tr}(\hat{B}\hat{A})$.
- (iv) $\text{Tr}(\hat{A}\hat{B}\hat{C}) = \text{Tr}(\hat{B}\hat{C}\hat{A}) \neq \text{Tr}(\hat{B}\hat{A}\hat{C})$ (Cyclic rule).

Problem 2-8 Use the property $I_{ij} = \delta_{ij}$ to prove $\hat{I}\hat{A} = \hat{A}\hat{I} = \hat{A}$.

Problem 2-9 Find the eigenvalues λ_i and corresponding eigenvectors \vec{V}_i of following matrices:

$$(i) \hat{A} = \begin{pmatrix} 2 & 2 \\ 1 & 3 \end{pmatrix}.$$

$$(ii) \hat{B} = \begin{pmatrix} 4 & 2 \\ 1 & 3 \end{pmatrix}.$$

(iii) For a matrix \hat{A} , its eigenvalues λ_i and the trace of the matrix has the following relations,

$$(a) \text{Tr}(\hat{C}) = \sum_i \lambda_i$$

$$(b) \det(\hat{C}) = \prod_i \lambda_i = i.$$

Show these relations are satisfied for matrix \hat{A} and \hat{B} .

Problem 2-10 As we shall see in details later, for a two-level system with a drive, the Hamiltonian of the system can be written as

$$\hat{\mathcal{H}} = \begin{pmatrix} \frac{\Delta}{2} & \frac{\Omega}{2} \\ \frac{\Omega}{2} & -\frac{\Delta}{2} \end{pmatrix}. \quad (2.4.14)$$

Find the energy eigenvalues λ_i of this Hamiltonian.



Wavefunction and Notations in Quantum Mechanics

3

In this chapter, we review the properties of wavefunction and different representations. The introductory quantum mechanics courses usually start out with the wave-mechanics based on wavefunction representation, while it is often more convenient to use the matrix representation in the context of quantum information sciences. However, there are always some exceptions, and we often switch back and forth between two representations; thus, it is important for readers to be familiar with both representations.

It is also important to be able to represent the composite system. For example, for the case of *two – qubit gate* in a quantum computer, one wavefunction consisting of two quantum bits of information is input to perform the gate. To do this, we need a representation of a wavefunction, composed of several individual quantum states. We also cover the representation for *operator*, as self-evident, which performs the operation to a quantum state wavefunction for various tasks. Finally, we cover the commutation relation, which is one of the unique and important properties of the operators in quantum mechanics. We also relate the commutation relation to the celebrated Heisenberg uncertainty principle.

3.1 Equation of Motion in Classical and Quantum Mechanics

In both classical and quantum mechanics, we are considering the motion of some “object”; however, it is always the quantum mechanics which we stumble on. In

Supplementary Information The online version contains supplementary material available at https://doi.org/10.1007/978-981-19-4641-7_3.

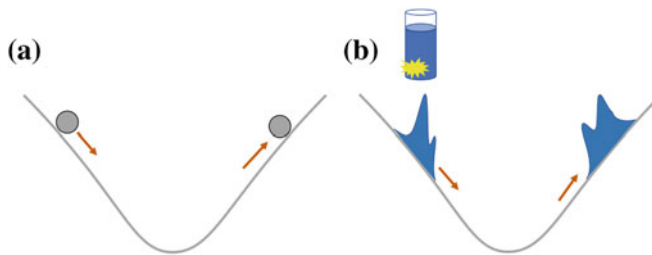


Fig. 3.1 Classical motion (left) and Quantum motion (right)

classical mechanics, as shown in Fig. 3.1 (left), we often consider the motion of a particle with mass m in a potential $V(x)$. Applying Newton's law, we can describe the motion as

$$m\ddot{x} = -\frac{\partial V(x)}{\partial x}, \quad (3.1.1)$$

where $\ddot{x} = \frac{d\dot{x}}{dt} = \frac{d^2x}{dt^2}$.

On the other hand, in quantum mechanics, we are forced to deal with some liquidy object so-called “wavefunction” as if it is spilled out of a cup as shown in Fig. 3.1 (right). The motion of this wavefunction is governed by the celebrated Schrödinger equation as

$$i\hbar\frac{\partial\Psi(x, t)}{\partial t} = -\frac{\hbar^2}{2m}\frac{\partial^2\Psi(x, t)}{\partial x^2} + V(x)\Psi(x, t). \quad (3.1.2)$$

Form of the wavefunction $\Psi(x, t)$ can be determined by solving this equation of motion.

There is a vast difference between these two mechanics. In classical mechanics, the position of the object $x(t)$ can be directly obtained from the equation of motion. Once $x(t)$ is found, other physical observables such as velocity $v(t) = \frac{dx}{dt}$, momentum $p = mv$, and kinetic energy $KE = \frac{1}{2}mv^2 = \frac{p^2}{2m}$ are readily available from simple calculation. In quantum mechanics, however, we learn that the wavefunction is analytically solvable in only a few special cases, and even when we are super-lucky to be able to solve the actual wavefunction $\Psi(x)$, we are still told that “the particle is *somewhere* under the curve”. What a nightmare...

In order to extract useful information or some physical observables of interest, one would have to use the “operators” on the wavefunction. For many students, this quantum-mechanics-specific procedure and mysterious overall composition seem to be an obstacle. The founders of the quantum mechanics were not ignorant about these difficulties. They came up with numerous tools to make the quantum mechanics simpler and easy to handle. One of the tools adopted is linear algebra. All the quantum states are described as a vector in a quantum vector space, called the Hilbert space. The operations such as time evolution and extraction of physical observables are performed with linear algebraic operations on the state vector. In other words, seemingly peculiar wavefunction can be systematically handled by using the framework

of linear algebra. In this chapter, we apply the basics of the linear algebra covered in the previous chapter and review the fundamentals of quantum mechanics.

3.2 Wavefunction

3.2.1 Inner Product of Wavefunction

An arbitrary one-dimensional wavefunction $\Psi(x)$ can be considered as a vector in a functional space. When states are described as vectors, first step is to define an inner product of vectors within the vector space. With two wavefunctions Ψ and Φ , inner product of two wavefunctions is defined as

$$\int_{-\infty}^{\infty} \Psi^*(x)\Phi(x)dx, \quad (3.2.1)$$

where Ψ^* is a complex conjugate of Ψ .

Wavenfunction $\Psi(x)$ can be written in terms of linearly independent basis $\psi_i(x)$ as

$$\begin{aligned} \Psi(x) &= c_1\psi_1(x) + c_2\psi_2(x) + \cdots + c_n\psi_n(x) \\ &= \sum_{i=1}^n c_i\psi_i(x), \end{aligned} \quad (3.2.2)$$

where c_i is complex coefficient and basis ψ_i satisfies the orthonormal condition,

$$\int_{-\infty}^{\infty} \psi_i^*(x)\psi_j(x)dx = \delta_{ij}. \quad (3.2.3)$$

Using the relation above, the inner product of Ψ with itself reads

$$\begin{aligned} \int_{-\infty}^{\infty} \Psi^*(x)\Psi(x)dx &= \int_{-\infty}^{\infty} \sum_{i,j=1}^n c_i^*c_j\psi_i^*(x)\psi_j(x)dx \\ &= \sum_{i,j=1}^n c_i^*c_j\delta_{ij} = \sum_{i=1}^n |c_i|^2, \end{aligned}$$

and the normalization condition of the wavefunction $\Psi(x)$ now reads,

$$\sum_{i=1}^n |c_i|^2 = 1. \quad (3.2.4)$$

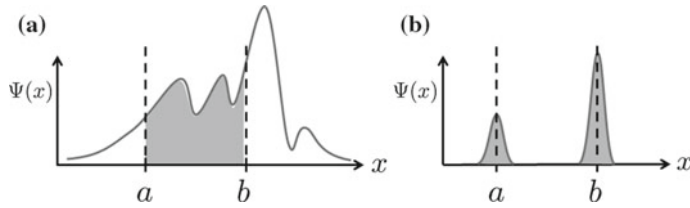


Fig. 3.2 **a** Continuous wavefunction; **b** discretized wavefunction

3.2.2 Continuous and Discretized Wavefunction

Since the definition of the inner product and normalization is set, let's take a look at an example of wavefunction. In an introductory quantum mechanics course, a particle wavefunction $\Psi(x)$ in one-dimensional space is often described as in Fig. 3.2a. Probability density of the particle is described as absolute square of the wavefunction ($|\Psi|^2 = \Psi^*\Psi$), and probability of finding a particle in $a \leq x \leq b$, $P(a \leq x \leq b)$ can be calculated as

$$P(a \leq x \leq b) = \int_a^b dx |\Psi(x)|^2. \quad (3.2.5)$$

In the context of quantum information, the continuous wavefunction as shown above may be used, but we often deal with discretized wavefunctions as in Fig. 3.2b. In this example, we have Ψ_a in the vicinity of $x = a$ and another hump Ψ_b around $x = b$. We often describe these wavefunctions as separate states.

$$\Psi_a = \Psi(x) \quad \text{for } x_a - \delta x < x < x_a + \delta x \quad (3.2.6)$$

$$\Psi_b = \Psi(x) \quad \text{for } x_b - \delta x < x < x_b + \delta x, \quad (3.2.7)$$

where δx is a large enough distance to cover each wavefunction near $x = a, b$.

Each wavefunction can be normalized to define

$$\psi_a = \frac{\Psi_a(x)}{\sqrt{\int_{a-\delta x}^{a+\delta x} dx |\Psi_a|^2}} \quad (3.2.8)$$

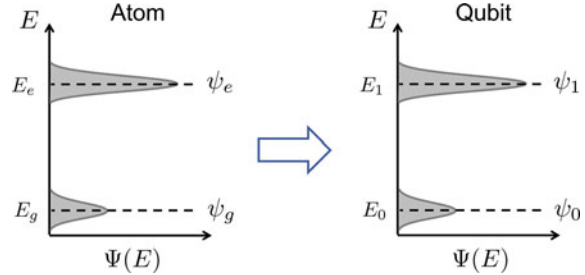
$$\psi_b = \frac{\Psi_b(x)}{\sqrt{\int_{b-\delta x}^{b+\delta x} dx |\Psi_b|^2}}. \quad (3.2.9)$$

Since there is no spatial overlap between ψ_a and ψ_b ,

$$\int_{-\infty}^{\infty} dx \psi_i^* \psi_j = \delta_{ij} \quad (3.2.10)$$

is satisfied, allowing these states to form a orthonormal basis.

Fig. 3.3 Discretized wavefunction in energy spectrum



Using these wavefunctions as basis, the original wavefunction Ψ can be written as

$$\Psi(x) = c_a \psi_a(x) + c_b \psi_b(x), \quad (3.2.11)$$

where

$$c_a = \int_{-\infty}^{\infty} dx \psi_a^*(x) \Psi(x)$$

$$c_b = \int_{-\infty}^{\infty} dx \psi_b^*(x) \Psi(x)$$

and satisfies $|c_a|^2 + |c_b|^2 = 1$. If a continuous wavefunction can be segmented with respect to some parameter (in this example, ψ_a and ψ_b were segmented in position x), one could make them into a discrete set of wavefunctions.

In many of the quantum bits or quantum states shown later, wavefunctions are not described as a spatial function, but of energy function as shown in Fig. 3.3 for the case of an atom. In these cases, one could use a similar step to define the wavefunction Ψ in terms of its basis ψ_i as

$$\Psi = c_g \psi_g + c_e \psi_e, \quad (3.2.12)$$

where subscripts g and e refer to the ground and excited states. From the normalization condition

$$|\Psi|^2 = |c_g|^2 + |c_e|^2 = 1, \quad (3.2.13)$$

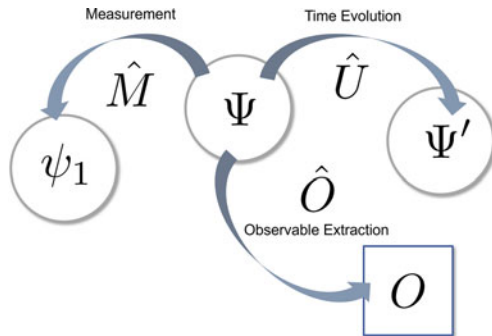
we see the state is in the ground and excited state with probability $|c_g|^2$ and $|c_e|^2$, respectively. We can describe the state as if the particle is located in discrete states.

As shown above, many quantum systems have continuous energy structures often separated into segments. If the segments are far enough that they do not have overlap, one can easily describe these “bands” as discrete states by integrating each segment. Discretized states are often defined as 0-state, $\psi_0 \equiv \psi_g$, and 1-state $\psi_1 \equiv \psi_e$ to use them as a basis for a quantum bit

$$\Psi = c_0 \psi_0 + c_1 \psi_1. \quad (3.2.14)$$

Fig. 3.4 Operators in action.

Various operations can be performed on the quantum state Ψ for different tasks



3.3 Operator

Operators act on wavefunctions to perform linear mapping of wavefunctions. They may perform different tasks, such as time evolution, measurement, and finding expectation values of physical observables (Fig. 3.4). In the early part of this text, we use the accent symbol \hat{A} to write the operators. In the later part of the text, we often dismiss the accent symbol to avoid the clumsiness of the equations. We expect readers to be familiarized enough with different operators, so you can identify the operators without the accent symbol.

When an operator \hat{A} is acted on a wavefunction Ψ , the new wavefunction Ψ' emerged as a result of the operation can be written as

$$\Psi' = \hat{A}\Psi. \quad (3.3.1)$$

The operator for a physical observable O is often denoted as \hat{O} . The expectation value of O for a state Ψ is calculated as

$$\langle O \rangle = \int_{-\infty}^{\infty} \Psi^*(x) \hat{O} \Psi(x) dx. \quad (3.3.2)$$

As mentioned above, since the operator changes the state, one can see that the state can be manipulated by selecting an appropriate operator. Also, using the same effect, it can be seen that the operator is also used to extract a physical quantity from a wavefunction.

3.4 Dirac Notation

In this section, we introduce an alternative representation for the wavefunctions, known as the Dirac notation, used in the quantum information. The Dirac notation often simplifies the equations and is also quite intuitive once you get a hang of it. We only cover the notation briefly and skip some of the details and formal descriptions.

A quantum state described by a wavefunction Ψ can be written as

$$\Psi \rightarrow |\Psi\rangle. \quad (3.4.1)$$

Since the state is using the later part of the “braket” symbol $\langle \quad \rangle$, it is called a ket-vector. There exist a dual space vector for the ket-vector, called bra-vector denoted as

$$\Psi^* \rightarrow \langle \Psi |. \quad (3.4.2)$$

When the wavefunction depends on specific parameters, such as quantum numbers (n, l, m, \dots) , it is customary to include them in the notation as

$$\Psi_{nlm\dots} \rightarrow |nlm\dots\rangle. \quad (3.4.3)$$

Using this Dirac notation, the inner product of two quantum states $|\Psi\rangle$ and $|\Phi\rangle$ is denoted as

$$\int_{-\infty}^{\infty} \Psi^*(x)\Phi(x)dx \rightarrow \langle \Psi | \Phi \rangle. \quad (3.4.4)$$

Some careful readers may notice that the open-braket $|\Psi\rangle$ and $\langle \Psi |$ are vectors, and ones with closed-braket $\langle \Psi | \Phi \rangle$ are a scalar. We review common quantum concepts using this convenient notation.

Wavefunction $|\Psi\rangle$ can be written in terms of linearly independent basis $|\psi_i\rangle$ as

$$\begin{aligned} |\Psi\rangle &= c_1|\psi_1\rangle + c_2|\psi_2\rangle + \cdots + c_n|\psi_n\rangle \\ &= \sum_{i=1}^n c_i|\psi_i\rangle. \end{aligned} \quad (3.4.5)$$

Also, a corresponding bra-vector can be written as

$$\begin{aligned} \langle \Psi | &= c_1^* \langle \psi_1 | + c_2^* \langle \psi_2 | + \cdots + c_n^* \langle \psi_n | \\ &= \sum_{i=1}^n c_i^* \langle \psi_i |. \end{aligned} \quad (3.4.6)$$

Orthonormality condition of the basis, the component or the probability amplitude of a wavefunction, and the wavefunction normalization can be written in a simple form as

$$\langle \psi_i | \psi_j \rangle = \delta_{ij} \quad (3.4.7)$$

$$\begin{aligned} \langle \psi_i | \Psi \rangle &= \langle \psi_i | \sum_{j=1}^n c_j |\psi_j\rangle = \sum_{j=1}^n c_j \langle \psi_i | \psi_j \rangle \\ &= \sum_{j=1}^n c_j \delta_{ij} = c_i \end{aligned} \quad (3.4.8)$$

$$\begin{aligned}\langle \Psi | \Psi \rangle &= \sum_{i,j=1}^n c_i c_j^* \langle \psi_j | \psi_i \rangle = \sum_{i,j=1}^n c_i c_j^* \delta_{ji} \\ &= \sum_{i=1}^n |c_i|^2 = 1,\end{aligned}\tag{3.4.9}$$

respectively. Norm of the wavefunction is also given as

$$\text{norm}(\Psi) = \sqrt{\sum_i \langle \Psi | \Psi \rangle} = \sqrt{\sum_i |c_i|^2}.\tag{3.4.10}$$

Similarly, the action of operator can also be written using the Dirac notation. Upon operation of \hat{A} on a state $|\Psi\rangle$, new state is given as

$$|\Psi'\rangle = \hat{A}|\Psi\rangle.\tag{3.4.11}$$

Expectation value of an observable O of wavefunction Ψ is

$$\langle O \rangle = \langle \Psi | \hat{O} \Psi \rangle = \langle \Psi | \hat{O} | \Psi \rangle.\tag{3.4.12}$$

The expectation value is (of course) a scalar and it can be confirmed with the closed-braket as described previously. The last equality may seem obvious, but in $|\hat{O}\Psi\rangle$, it explicitly shows that the state is the resulting state of the operation \hat{O} on $|\Psi\rangle$. Further details are shown in Appendix A.

3.5 Matrix Representation

Following the Dirac notation, let us introduce the matrix representation of the quantum state here. In the wavefunction representation, the function is regarded as a state “vector”, which might not be intuitive at first. The quantum state can also be described in the form of a matrix, which is much familiar to us as a “vector”.

The ket-vector $|\Psi\rangle$ is usually represented as a vertical vector. Using the orthonormal basis set $|\psi_i\rangle$, the wavefunction can be written as

$$\begin{aligned}|\Psi\rangle &= c_1 |\psi_1\rangle + c_2 |\psi_2\rangle + \cdots + c_n |\psi_n\rangle \\ &= c_1 \begin{pmatrix} 1 \\ 0 \\ \vdots \\ 0 \end{pmatrix} + c_2 \begin{pmatrix} 0 \\ 1 \\ \vdots \\ 0 \end{pmatrix} + \cdots + c_n \begin{pmatrix} 0 \\ 0 \\ \vdots \\ 1 \end{pmatrix} \\ &= \begin{pmatrix} c_1 \\ c_2 \\ \vdots \\ c_n \end{pmatrix}.\end{aligned}\tag{3.5.1}$$

On the other hand, $\langle \Psi |$ is written as a horizontal vector with the vector elements taking the complex conjugate, written as

$$\langle \Psi | = (c_1^* \ c_2^* \ \cdots \ c_n^*). \quad (3.5.2)$$

The inner product can be calculated by arranging bra and ket-vectors as a standard matrix multiplication as

$$\begin{aligned} \langle \Psi | \Psi \rangle &= (c_1^* \ c_2^* \ \cdots \ c_n^*) \begin{pmatrix} c_1 \\ c_2 \\ \vdots \\ c_n \end{pmatrix} \\ &= \sum_{i=1}^n |c_i|^2 = 1. \end{aligned} \quad (3.5.3)$$

The last line shows the normalization condition of the wavefunction. We can also write the general inner product as

$$\begin{aligned} \langle \Psi | \Psi' \rangle &= (c_1^* \ c_2^* \ \cdots \ c_n^*) \begin{pmatrix} c'_1 \\ c'_2 \\ \vdots \\ c'_n \end{pmatrix} \\ &= \sum_{i=1}^n c_i^* c'_i = \sum_{i=1}^n (c_i c'^*_i)^* \\ &= \langle \Psi' | \Psi \rangle^*, \end{aligned} \quad (3.5.4)$$

where $\langle \Psi | \Psi' \rangle = \langle \Psi' | \Psi \rangle^*$ is shown in the last line. The outer product of wavefunctions is

$$|\Psi'\rangle \langle \Psi'| = \begin{pmatrix} c'_1 \\ c'_2 \\ \vdots \\ c'_n \end{pmatrix} (c_1^* \ c_2^* \ \cdots \ c_n^*) \quad (3.5.5)$$

$$= \begin{pmatrix} c'_1 c_1^* & c'_1 c_2^* & \cdots & c'_1 c_n^* \\ c'_2 c_1^* & c'_2 c_2^* & \cdots & c'_2 c_n^* \\ \vdots & \vdots & \ddots & \vdots \\ c'_n c_1^* & c'_n c_2^* & \cdots & c'_n c_n^* \end{pmatrix}, \quad (3.5.6)$$

whose matrix element $(|\Psi'\rangle\langle\Psi'|)_{ij}$ is also calculated as

$$\begin{aligned} (|\Psi'\rangle\langle\Psi'|)_{ij} &= \langle\psi_i|\Psi'\rangle\langle\Psi|\psi_j\rangle \\ &= (0 \cdots 1 \cdots \cdots 0) \begin{pmatrix} c'_1 c_1^* & c'_1 c_2^* & \cdots & c'_1 c_n^* \\ c'_2 c_1^* & c'_2 c_2^* & \cdots & c'_2 c_n^* \\ \vdots & \vdots & \ddots & \vdots \\ c'_n c_1^* & c'_n c_2^* & \cdots & c'_n c_n^* \end{pmatrix} \begin{pmatrix} 0 \\ \vdots \\ 1 \\ \vdots \\ 0 \end{pmatrix} \\ &= c'_i c_j^*, \end{aligned} \quad (3.5.7)$$

where $|\psi_{i,j}\rangle$ are basis vectors. Operators are represented as matrices; for example, an operator \hat{A} acting on a three-basis space is written as

$$\hat{A} = \begin{pmatrix} A_{11} & A_{12} & A_{13} \\ A_{21} & A_{22} & A_{23} \\ A_{31} & A_{32} & A_{33} \end{pmatrix}. \quad (3.5.8)$$

The operation on a state is simply written as a matrix operating on a vector as

$$\begin{aligned} |\Psi'\rangle &= \hat{A}|\Psi\rangle \\ &= \begin{pmatrix} A_{11} & A_{12} & A_{13} \\ A_{21} & A_{22} & A_{23} \\ A_{31} & A_{32} & A_{33} \end{pmatrix} \begin{pmatrix} c_1 \\ c_2 \\ c_3 \end{pmatrix} \\ &= \begin{pmatrix} c_1 A_{11} + c_2 A_{12} + c_3 A_{13} \\ c_1 A_{21} + c_2 A_{22} + c_3 A_{23} \\ c_1 A_{31} + c_2 A_{32} + c_3 A_{33} \end{pmatrix}. \end{aligned} \quad (3.5.9)$$

Also, from Eq. (3.5.2),

$$\begin{aligned} \langle\Psi'| &\quad (3.5.10) \\ &= ((c_1^* A_{11}^* + c_2^* A_{12}^* + c_3^* A_{13}^*) (c_1^* A_{21}^* + c_2^* A_{22}^* + c_3^* A_{23}^*) (c_1^* A_{31}^* + c_2^* A_{32}^* + c_3^* A_{33}^*)) \\ &= (c_1^* \ c_2^* \ c_3^*) \begin{pmatrix} A_{11}^* & A_{21}^* & A_{31}^* \\ A_{12}^* & A_{22}^* & A_{32}^* \\ A_{13}^* & A_{23}^* & A_{33}^* \end{pmatrix} \\ &= \langle\Psi|\hat{A}^\dagger. \end{aligned} \quad (3.5.11)$$

In the last line, $\hat{A}^\dagger \equiv (\hat{A}^T)^*$ is a Hermite conjugate, equivalent to the complex conjugate of transpose of \hat{A} . Here, bra-vector of $|\Psi'\rangle$ is obtained as

$$|\Psi'\rangle = \hat{A}|\Psi\rangle \rightarrow \langle\Psi'| = \langle\Psi|\hat{A}^\dagger. \quad (3.5.12)$$

Using $\langle \Psi | \Psi' \rangle = \langle \Psi' | \Psi \rangle^*$ described previously, it is quite simple to obtain other useful relations,

$$\langle \Phi | \Psi \rangle = \langle \Psi | \Phi \rangle^* \quad (3.5.13)$$

$$\langle \Phi | \hat{A} | \Psi \rangle = \langle \Psi | \hat{A}^\dagger | \Phi \rangle^*. \quad (3.5.14)$$

Since many operators are square matrices in quantum system analysis, it is important to define the trace of operators. It is simply the same as a matrix trace,

$$\text{Tr } \hat{A} = \sum_i \langle \psi_i | \hat{A} | \psi_i \rangle = \sum_i A_{ii}. \quad (3.5.15)$$

3.6 Properties of Wavefunction

Below is a summary of the main properties of the wavefunction. We did not derive all of them due to the limited space, but should be easy to derive. There is a one-to-one correspondence with “Vectors in Multidimensional Space” in Sect. 2.4. If you are new to the material below, it is quite helpful to see the parallel between the two.

In the summary below, $|\Psi' \rangle = \hat{A} |\Psi \rangle$, $|\Psi \rangle = \sum_i c_i |\psi_i \rangle$, $|\Psi_a \rangle = \sum_i a_i |\psi_i \rangle$, $|\Psi_b \rangle = \sum_i b_i |\psi_i \rangle$, $|\Psi' \rangle = \sum_i c'_i |\psi_i \rangle$, $\hat{C} = \hat{A} \hat{B}$ are used.

$$\text{Orthonormal basis} \quad \langle \psi_i | \psi_j \rangle = \delta_{ij} \quad (3.6.1)$$

$$\text{Component of wavefunction} \quad c_i = \langle \psi_i | \Psi \rangle \quad (3.6.2)$$

$$\text{Norm} \quad \text{norm}(\Psi) = \sqrt{\sum_i |c_i|^2} \quad (3.6.3)$$

$$\text{Wavefunction normalization} \quad \sum_i |c_i|^2 = 1 \quad (3.6.4)$$

$$\text{Inner product of wavefunctions} \quad \langle \Psi_a | \Psi_b \rangle = \langle \Psi_b | \Psi_a \rangle^* = \sum_i a_i^* b_i \quad (3.6.5)$$

$$\text{Outer product of wavefunctions} \quad (\langle \Psi_a | \Psi_b \rangle)_{ij} = \langle \psi_i | \Psi_a \rangle \langle \Psi_b | \psi_j \rangle = a_i^* b_j \quad (3.6.6)$$

$$\text{Operator matrix element} \quad A_{ij} = \langle \psi_i | \hat{A} | \psi_j \rangle \quad (3.6.7)$$

$$\begin{aligned} \text{Operator given by the product} \quad C_{ij} &= \langle \psi_i | \hat{C} | \psi_j \rangle \\ &= \sum_k \langle \psi_i | \hat{A} | \psi_k \rangle \langle \psi_k | \hat{B} | \psi_j \rangle \\ &= \sum_k A_{ik} B_{kj} \end{aligned} \quad (3.6.8)$$

$$\text{Hermitian conjugate of operator} \quad C_{ij}^\dagger = \langle \psi_i | \hat{C}^\dagger | \psi_j \rangle = \langle \psi_j | \hat{C} | \psi_i \rangle^*$$

$$= \sum_k \left(\langle \psi_j | \hat{A} | \psi_k \rangle \langle \psi_k | \hat{B} | \psi_i \rangle \right)^* = \sum_k A_{jk}^* B_{ki}^* \quad (3.6.9)$$

Trace $\text{Tr } \hat{A} = \sum_i \langle \psi_i | \hat{A} | \psi_i \rangle = \sum_i A_{ii} \quad (3.6.10)$

Completeness $\hat{I} = \sum_i |\psi_i\rangle\langle\psi_i| \quad (3.6.11)$

Operation $c'_i = \langle \psi_i | \Psi' \rangle = \sum_j \langle \psi_i | \hat{A} | \psi_j \rangle \langle \psi_j | \Psi \rangle$
 $= \sum_j A_{ij} c_j. \quad (3.6.12)$

3.7 Composite System

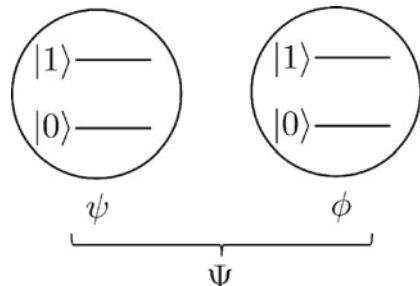
We have considered the state of a single particle so far, but when considering different particles at the same time or how the particles interact with each other, it is necessary to describe multiple quantum states as one wavefunction in a concise form. For example, if there are two qubits as shown in Fig. 3.5, we can consider them as one composite system by using the direct product symbol \otimes as

Composite system $|\Psi\rangle$ of ψ and ϕ : $|\Psi\rangle = |\psi\rangle \otimes |\phi\rangle$.

It is customary to use simplified notations, such as

$$|\Psi\rangle = |\psi\rangle \otimes |\phi\rangle = |\psi\rangle |\phi\rangle = |\psi\phi\rangle.$$

Fig. 3.5 A composite system Ψ consists of two qubits, ψ and ϕ



The composite system can be expanded to many particles; for example, a system containing $\psi_1, \psi_2, \dots, \psi_n$ can also be represented as any of the following notations

$$\begin{aligned} |\Psi\rangle &= |\psi_1\rangle \otimes |\psi_2\rangle \otimes \cdots \otimes |\psi_n\rangle \\ &= |\psi_1\rangle|\psi_2\rangle \cdots |\psi_n\rangle \\ &= |\psi\rangle_1|\psi\rangle_2 \cdots |\psi\rangle_n \\ &= |\psi_1\psi_2 \cdots \psi_n\rangle. \end{aligned}$$

The notation could be cumbersome and care needs to be taken to keep it simple.

The composite system has the following linear characteristics:

$$\alpha(|\psi\phi\rangle) = (\alpha|\psi\rangle)|\phi\rangle = |\psi\rangle(\alpha|\phi\rangle) \quad (3.7.1)$$

$$(|\psi\rangle + |\psi'\rangle)|\phi\rangle = |\psi\phi\rangle + |\psi'\phi\rangle \quad (3.7.2)$$

$$|\psi\rangle(|\phi\rangle + |\phi'\rangle) = |\psi\phi\rangle + |\psi\phi'\rangle. \quad (3.7.3)$$

Two-Qubit State Examples

Let us show two simple examples.

Two-qubit state

$$|\Psi\rangle = |\psi\phi\rangle = |01\rangle \quad (3.7.4)$$

is a state in which the first qubit $|\psi\rangle$ is in 0-state ($|\psi\rangle = |0\rangle$) and the second qubit $|\phi\rangle$ is in 1-state ($|\phi\rangle = |1\rangle$).

Next example is for two-qubit states,

$$\begin{aligned} |\psi\rangle &= \frac{1}{2}|0\rangle + \frac{\sqrt{3}}{2}|1\rangle \\ |\phi\rangle &= \frac{1}{\sqrt{2}}|0\rangle - \frac{1}{\sqrt{2}}|1\rangle, \end{aligned}$$

and then the composite state $|\Psi\rangle = |\psi\phi\rangle$ is

$$\begin{aligned} |\Psi\rangle &= \left(\frac{1}{2}|0\rangle + \frac{\sqrt{3}}{2}|1\rangle \right) \otimes \left(\frac{1}{\sqrt{2}}|0\rangle - \frac{1}{\sqrt{2}}|1\rangle \right) \\ &= \frac{1}{2\sqrt{2}}|0\rangle|0\rangle + \frac{1}{2\sqrt{2}}|0\rangle|1\rangle + \frac{\sqrt{3}}{2\sqrt{2}}|1\rangle|0\rangle - \frac{\sqrt{3}}{2\sqrt{2}}|1\rangle|1\rangle \\ &= \frac{1}{2\sqrt{2}} \left(|00\rangle + |01\rangle + \sqrt{3}|10\rangle - \sqrt{3}|11\rangle \right), \end{aligned}$$

where we used different notations for each line. The last line is probably the most frequently used notation, due to its simplicity. When the notation without indices is used, ordering obviously matters and care needs to be taken.

In general, two-particle state basis can be written, using orthonormal basis of each state ψ_i and ϕ_j , as

$$\begin{aligned} |\Psi_{ij}\rangle &= |\psi_i\rangle|\phi_j\rangle \\ |\Psi_{kl}\rangle &= |\psi_k\rangle|\phi_l\rangle. \end{aligned}$$

The inner product of these states can be written as

$$\begin{aligned} \langle\Psi_{ij}|\Psi_{kl}\rangle &= (\langle\psi_i|\langle\phi_j|)(\langle\psi_k|\phi_l\rangle) \\ &= \langle\psi_i\phi_j|\psi_k\phi_l\rangle \\ &= \langle\psi_i|\psi_k\rangle\langle\phi_j|\phi_l\rangle \\ &= \delta_{ik}\delta_{jl}. \end{aligned} \tag{3.7.5}$$

It is important to note here that the inner product is only taken with the same physical system (e.g., qubit 1 to qubit 1). In other words, if even one of the individual systems is orthogonal, the composite system is also orthogonal. For example, two-qubit system $|\Psi_a\rangle = |01\rangle$ and $|\Psi_b\rangle = |11\rangle$ is orthogonal since,

$$\langle\Psi_a|\Psi_b\rangle = \langle01|11\rangle = \langle0|1\rangle\langle1|1\rangle \tag{3.7.6}$$

$$= \delta_{01}\delta_{11} = 0 \cdot 1 = 0, \tag{3.7.7}$$

even when the two qubits are both 1.

One can expand this idea to describe an arbitrary state as

$$|\Psi_a\rangle = \sum_{i,j} a_{ij} |\psi_i\rangle|\phi_j\rangle \tag{3.7.8}$$

$$|\Psi_b\rangle = \sum_{k,l} b_{kl} |\psi_k\rangle|\phi_l\rangle. \tag{3.7.9}$$

Then the inner product is written as

$$\begin{aligned} \langle\Psi_a|\Psi_b\rangle &= \sum_{i,j,k,l} a_{ij}^* b_{kl} \langle\psi_i|\psi_k\rangle\langle\phi_j|\phi_l\rangle \\ &= \sum_{i,j,k,l} a_{ij}^* b_{kl} \delta_{ik}\delta_{jl} \\ &= \sum_{i,j} a_{ij}^* b_{ij}. \end{aligned} \tag{3.7.10}$$

Now, let us introduce an example using the system in Fig. 3.6. When two qubits are given as

$$|\psi\rangle = a_0|0\rangle + a_1|1\rangle \tag{3.7.11}$$

$$|\phi\rangle = b_0|0\rangle + b_1|1\rangle, \tag{3.7.12}$$

then from normalization,

$$\sum_{i=0}^1 |a_i|^2 = |a_0|^2 + |a_1|^2 = 1 \quad (3.7.13)$$

$$\sum_{j=0}^1 |b_j|^2 = |b_0|^2 + |b_1|^2 = 1. \quad (3.7.14)$$

For the composite system of two qubits, the wavefunction can be expanded as

$$\begin{aligned} |\Psi\rangle &= |\psi\rangle|\phi\rangle \\ &= (a_0|0\rangle + a_1|1\rangle) \otimes (b_0|0\rangle + b_1|1\rangle) \\ &= a_0b_0|00\rangle + a_0b_1|01\rangle + a_1b_0|10\rangle + a_1b_1|11\rangle. \end{aligned} \quad (3.7.15)$$

As mentioned above, $|00\rangle$, $|01\rangle$, $|10\rangle$, and $|11\rangle$ are orthogonal to each other.

The inner product of this composite system wavefunction by itself is

$$\begin{aligned} \langle \Psi | \Psi \rangle &= (a_0^*b_0^*\langle 00| + a_0^*b_1^*\langle 01| + a_1^*b_0^*\langle 10| + a_1^*b_1^*\langle 11|) \\ &\quad \cdot (a_0b_0|00\rangle + a_0b_1|01\rangle + a_1b_0|10\rangle + a_1b_1|11\rangle) \\ &= |a_0|^2|b_0|^2 + |a_0|^2|b_1|^2 + |a_1|^2|b_0|^2 + |a_1|^2|b_1|^2 \\ &= (|a_0|^2 + |a_1|^2)(|b_0|^2 + |b_1|^2) \\ &= \sum_i |a_i|^2 \sum_j |b_j|^2 = 1. \end{aligned} \quad (3.7.16)$$

As one can see that if each state ($|\psi\rangle$ and $|\phi\rangle$) is normalized, it assures the normalization condition for the composite state $|\Psi\rangle$.

3.7.1 Operator in Composite System

If two qubits are far enough apart and can be manipulated independently, as shown in Fig. 3.6, then of course one operation has no effect on the other. That is, when the quantum state of two qubits $|\psi_a\rangle$ and $|\psi_b\rangle$ is written as $|\psi\rangle = |\psi_a\rangle \otimes |\psi_b\rangle$, with corresponding operator acting on each qubit \hat{A} and \hat{B} , respectively, the operators that act on the composite system is written as

$$\hat{A} \otimes \hat{B}, \quad (3.7.17)$$

and it operate on the state as

$$\begin{aligned} (\hat{A} \otimes \hat{B})|\psi\rangle &= (\hat{A} \otimes \hat{B})|\psi_a\rangle \otimes |\psi_b\rangle \\ &= \hat{A}|\psi_a\rangle \otimes \hat{B}|\psi_b\rangle. \end{aligned} \quad (3.7.18)$$

Fig. 3.6 A composite system Ψ consists of two qubits, ψ_a and ψ_b

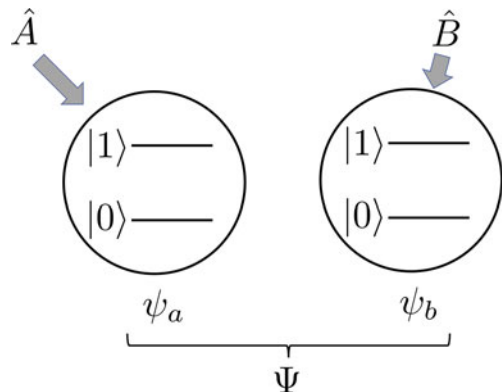
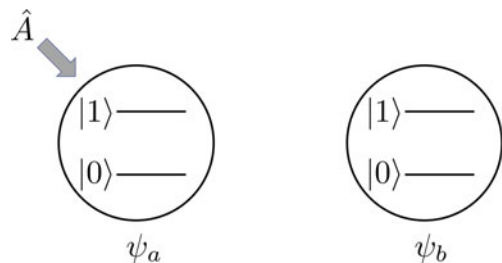


Fig. 3.7 A composite system of two qubits, where only one of the qubits is under an operation



When \hat{A} is applied only to $|\psi_a\rangle$ in the composite system, with $|\psi_b\rangle$ untouched as Fig. 3.7, the operator acting on the system is $\hat{A} \otimes \hat{I}$.

It is often required to use a Hermite conjugate of the composite operator $\hat{A} \otimes \hat{B}$, which takes a form

$$(\hat{A} \otimes \hat{B})^\dagger = \hat{A}^\dagger \otimes \hat{B}^\dagger. \quad (3.7.19)$$

Again, one can see that each system is treated independently.

3.8 Examples of Notation for Frequently Used Quantum State

In this book, the discussions cover various concepts in quantum technologies; however, the descriptions are given mainly with the two-level system and harmonic oscillator. There is a qubit as a representative of the two-level system, and its states are expressed as $|0\rangle$ and $|1\rangle$. In addition, the harmonic oscillator can be described with the state $|n\rangle$, where n represents the number of particles or excitations.

As one starts reading journal papers, readers may encounter various kinds of quantum states and notations introduced depending on the quantum system of interest. Examples of various notations for quantum states in different physical systems are shown in Fig. 3.8. For example, in atoms, the ground and excited state is often referred to as $|g\rangle$ and $|e\rangle$, respectively. In some experiments, higher states are denoted as $|f\rangle$, $|h\rangle$, ... Also, $|a\rangle$ may be used to represent an “A”uxiliary state (or Ancillary

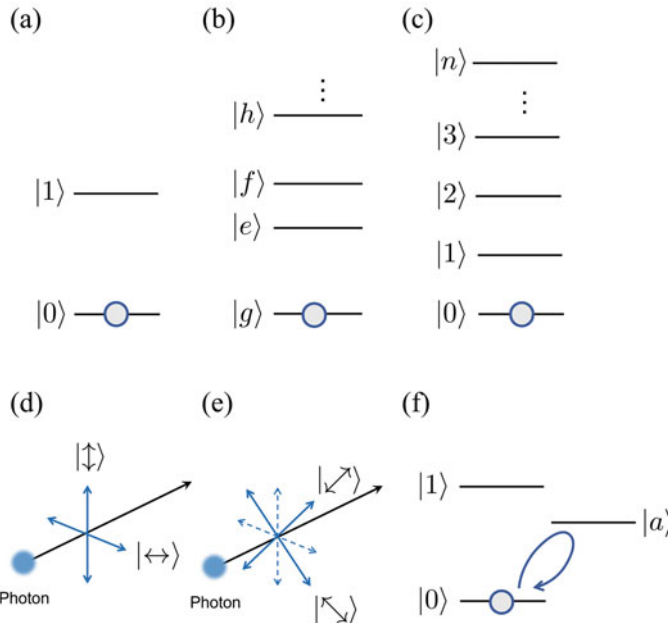


Fig. 3.8 Example of notations used to describe different quantum states. **a** Qubit, **b** atom, **c** harmonic oscillator, **d** photon (vertical and horizontal), **e** photon (diagonal), and **f** auxiliary or ancillary state

states) in various quantum systems. Further, for photon states, the state basis may be given in the polarization state of light, such as vertical, horizontal,

Notation and the choice of physical states to be used may vary depending on the actual system. Typical state notations used in this book or in other literature are summarized in Table 3.1.

Table 3.1 Notation for frequently used quantum states

Physical System	State	Notation
Atom	Ground State	$ g\rangle$
	Excited State	$ e\rangle$
	Higher States	$ f\rangle, h\rangle, \dots$
Qubit	0-state	$ 0\rangle$
	1-state	$ 1\rangle$
Harmonic Oscillator	n-particle state ($0, 1, 2, \dots, n$)	$ 0\rangle, 1\rangle, 2\rangle, \dots, n\rangle$
Photon	Vertical Polarization State	$ \uparrow\rangle$
	Horizontal Polarization State	$ \downarrow\rangle$
	Right-diagonal Polarization State	$ \nearrow\rangle$
	Left-diagonal Polarization State	$ \nwarrow\rangle$
	Auxiliary State	$ a\rangle$
Other State		

3.9 Quantum State Representation: Qubit

Now we have the Dirac notation and matrix representation down. Let us take a look at the representation of the qubit, the main workhorse for the quantum information and quantum technology.

3.9.1 One-Qubit state

A qubit state $|\psi\rangle$ consists of two physical states denoted as $|0\rangle$ and $|1\rangle$, and an arbitrary qubit state with corresponding complex amplitudes c_0 and c_1 , respectively, can be written as

$$\begin{aligned} |\psi\rangle &= c_0|0\rangle + c_1|1\rangle \\ &\equiv c_0 \begin{pmatrix} 1 \\ 0 \end{pmatrix} + c_1 \begin{pmatrix} 0 \\ 1 \end{pmatrix} = \begin{pmatrix} c_0 \\ c_1 \end{pmatrix}, \end{aligned} \quad (3.9.1)$$

where the matrix representations $|0\rangle \equiv \begin{pmatrix} 1 \\ 0 \end{pmatrix}$ and $|1\rangle \equiv \begin{pmatrix} 0 \\ 1 \end{pmatrix}$ are used in the second line. Throughout this book, we may use either representations suited for the context.

Taking an inner product of the state itself, the normalization condition is given as

$$\langle\psi|\psi\rangle = (c_0^* \ c_1^*) \begin{pmatrix} c_0 \\ c_1 \end{pmatrix} = |c_0|^2 + |c_1|^2 = 1. \quad (3.9.2)$$

It is often more intuitive to separate the complex probability amplitudes c_0 and c_1 in terms of its amplitude and phase as $c_0 = |c_0|e^{i\phi_0}$ and $c_1 = |c_1|e^{i\phi_1}$. The qubit state now reads

$$\begin{aligned} |\psi\rangle &= |c_0|e^{i\phi_0}|0\rangle + |c_1|e^{i\phi_1}|1\rangle \\ &= e^{i\phi_0} \left(|c_0||0\rangle + |c_1|e^{-i\phi}|1\rangle \right), \end{aligned} \quad (3.9.3)$$

where $\phi = \phi_0 - \phi_1$. Recall that the probability density $|\psi|^2$ allows an arbitrary phase factor for the wavefunction, meaning that the results will not change if we use $|\psi\rangle$ or $e^{i\theta}|\psi\rangle$. The phase factor $e^{i\theta}$ is called *Global Phase* and can be ignored without a loss of generality.

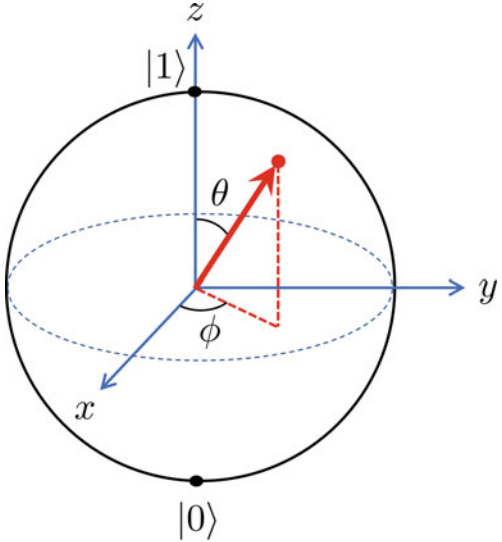
Ignoring the global phase ϕ_0 , the qubit state is finally represented as

$|\psi\rangle = c_0|0\rangle + c_1e^{-i\phi}|1\rangle,$

(3.9.4)

where $|c_0| \rightarrow c_0$ and $|c_1| \rightarrow c_1$ is used since the phase factor is explicitly written and the amplitudes can be understood as real positive values.

Note here that the important phase factor is the difference of the state phase ϕ , and, as we have seen, the global phase is ignored.

Fig. 3.9 Bloch sphere

3.9.2 Bloch Sphere

There is a geographical representation for a qubit, called the *Bloch sphere* representation, which is quite convenient and intuitive. We discuss the physics of the two-level system in detail later, where the dynamics of the qubit are discussed using the Bloch sphere. Here, we introduce the general concept of the Bloch sphere and show some fundamental properties of the qubit state on the Bloch sphere.

The qubit state discussed above has three parameters, c_0 , c_1 , and ϕ , with one constraint, the normalization condition, which means two parameters are enough to define the state of the qubit.

The normalization condition can be conveniently rewritten as

$$c_0^2 + c_1^2 = \sin^2 \frac{\theta}{2} + \cos^2 \frac{\theta}{2} = 1, \quad (3.9.5)$$

which makes the qubit state,

$$|\psi\rangle = \sin \frac{\theta}{2} |0\rangle + \cos \frac{\theta}{2} e^{-i\phi} |1\rangle. \quad (3.9.6)$$

An arbitrary qubit state can be specified using two parameters, θ and ϕ . Using a geometrical representation, Bloch sphere, the quantum state can be represented as an arrow pointing at anywhere on the spherical surface of radius 1 as shown in Fig. 3.9.

Using this representation, the qubit state assignments for $\pm x$, $\pm y$, and $\pm z$ -direction are as follows:

$$|+z\rangle = |1\rangle$$

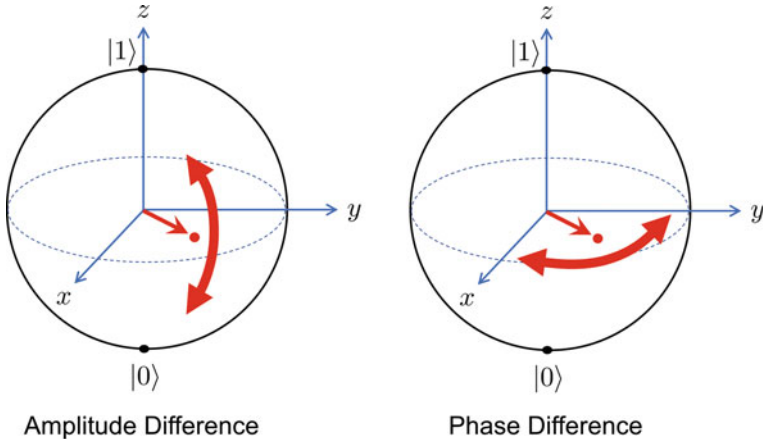


Fig. 3.10 Motion of the qubit state on the Bloch sphere for amplitude difference variation (left), and phase difference variation (right) between $|0\rangle$ and $|1\rangle$ state

$$\begin{aligned}
 |-z\rangle &= |0\rangle \\
 |+x\rangle &= \frac{1}{\sqrt{2}} (|0\rangle + |1\rangle) \\
 |-x\rangle &= \frac{1}{\sqrt{2}} (|0\rangle - |1\rangle) \\
 |+y\rangle &= \frac{1}{\sqrt{2}} (|0\rangle - i|1\rangle) \\
 |-y\rangle &= \frac{1}{\sqrt{2}} (|0\rangle + i|1\rangle).
 \end{aligned}$$

As one can see, the poles of the sphere represent $|0\rangle$ and $|1\rangle$ state, while the equator of the sphere represents the superposition of $|0\rangle$ and $|1\rangle$ with equal amplitude and varying phase difference. The reader may check these state assignments using Eq. 3.9.6.

The role of two parameters representing the qubit can be understood as

- θ : Amplitude difference between $|0\rangle$ and $|1\rangle$.
- ϕ : Phase difference between $|0\rangle$ and $|1\rangle$.

If the relative occupancy between $|0\rangle$ and $|1\rangle$ changes, the qubit state will move up and down in the polar direction (latitudinal direction), while the variation of the phase difference between $|0\rangle$ and $|1\rangle$ moves the state in azimuthal direction (longitudinal direction) as shown in Fig. 3.10.

Starting from Eq. 3.9.6, one may think it is possible to move an arbitrary qubit state toward $+z$ -direction (north pole) to make a quantum state,

$$|\psi\rangle = \sin \frac{\theta}{2} |0\rangle + \cos \frac{\theta}{2} e^{-i\phi} |1\rangle \rightarrow |\psi\rangle = e^{-i\phi} |1\rangle. \quad (3.9.7)$$

At a first glance, this state is different from $|1\rangle$ ($e^{-i\phi}|1\rangle \neq |1\rangle$); however, the phase factor $e^{-i\phi}$ here is considered as a global phase, which can be ignored. It is also easy to see from the Bloch sphere representation that there is no phase angle (azimuthal angle) that can be defined at the north pole, which makes $e^{-i\phi}|1\rangle \equiv |1\rangle$.

Similarly, $|+y\rangle$ -state can also be written as

$$|+y\rangle = \frac{1}{\sqrt{2}} (i|0\rangle + |1\rangle), \quad (3.9.8)$$

which is equivalent as the $|y\rangle$ -state shown previously since it is different just by the global phase factor i .

The Bloch sphere representation provides a pictorial and intuitive understanding of the qubit. Unfortunately, there is no two-qubit or many-qubit equivalent of the Bloch sphere, and its use is limited only for one-qubit state.

3.9.3 Two-Qubit State

Composite qubit state consisting of two qubits,

$$|\psi_a\rangle = a_0|0\rangle + a_1|1\rangle \equiv \begin{pmatrix} a_0 \\ a_1 \end{pmatrix} \quad (3.9.9)$$

$$|\psi_b\rangle = b_0|0\rangle + b_1|1\rangle \equiv \begin{pmatrix} b_0 \\ b_1 \end{pmatrix}, \quad (3.9.10)$$

$|\psi\rangle = |\psi_a\rangle|\psi_b\rangle$ can be written using a matrix representation as

$$\begin{aligned} |\psi\rangle &= |\psi_a\rangle|\psi_b\rangle \\ &= \begin{pmatrix} a_0 \\ a_1 \end{pmatrix} \otimes \begin{pmatrix} b_0 \\ b_1 \end{pmatrix} \\ &= \begin{pmatrix} a_0 & \begin{pmatrix} b_0 \\ b_1 \end{pmatrix} \\ a_1 & \begin{pmatrix} b_0 \\ b_1 \end{pmatrix} \end{pmatrix} \\ &= \begin{pmatrix} a_0b_0 \\ a_0b_1 \\ a_1b_0 \\ a_1b_1 \end{pmatrix}. \end{aligned} \quad (3.9.11)$$

The following are the examples of two qubit state basis using the matrix notation

$$|00\rangle = \begin{pmatrix} 1 \\ 0 \\ 0 \\ 0 \end{pmatrix},$$

$$|01\rangle = \begin{pmatrix} 0 \\ 1 \\ 0 \\ 0 \end{pmatrix},$$

$$|10\rangle = \begin{pmatrix} 0 \\ 0 \\ 1 \\ 0 \end{pmatrix},$$

$$|11\rangle = \begin{pmatrix} 0 \\ 0 \\ 0 \\ 1 \end{pmatrix}.$$

Similarly, when \hat{X}_a acting on $|\psi_a\rangle$ and \hat{Z}_b acting on ψ_b are written as

$$\hat{X}_a = \begin{pmatrix} 0 & 1 \\ 1 & 0 \end{pmatrix} \quad (3.9.12)$$

$$\hat{Z}_b = \begin{pmatrix} 1 & 0 \\ 0 & -1 \end{pmatrix}, \quad (3.9.13)$$

THE MATRIX REPRESENTATION OF THE composite operator reads

$$X_a \otimes Z_b = \begin{pmatrix} 0 \cdot \begin{pmatrix} 1 & 0 \\ 0 & -1 \end{pmatrix} & 1 \cdot \begin{pmatrix} 1 & 0 \\ 0 & -1 \end{pmatrix} \\ 1 \cdot \begin{pmatrix} 1 & 0 \\ 0 & -1 \end{pmatrix} & 0 \cdot \begin{pmatrix} 1 & 0 \\ 0 & -1 \end{pmatrix} \end{pmatrix} = \begin{pmatrix} 0 & 0 & 1 & 0 \\ 0 & 0 & 0 & -1 \\ 1 & 0 & 0 & 0 \\ 0 & -1 & 0 & 0 \end{pmatrix}. \quad (3.9.14)$$

The reader should be careful with the nesting order of both states and operators when dealing with the composite system.

Quantum Entangled State

Previously, the quantum states of two individual particles are represented in the form of a direct product, but there are quantum states that cannot be described by a direct product. For example,

$$|\Psi\rangle = \frac{1}{\sqrt{2}}(|00\rangle + |11\rangle), \quad (3.9.15)$$

this state cannot be represented as a direct product in a form $|\psi_a\rangle \otimes |\psi_b\rangle$. Contrarily, an example of a quantum state which can be decomposed as a direct product is

$$|\Psi\rangle = \frac{1}{\sqrt{2}}(|00\rangle + |01\rangle) = |0\rangle \otimes \frac{1}{\sqrt{2}}(|0\rangle + |1\rangle). \quad (3.9.16)$$

A state that cannot be expressed by a direct product like Eq. 3.9.15 is called a quantum entangled state (or quantum entanglement state) and is an important state in quantum information. These following four states, called Bell states, are frequently used to describe entangled two-qubit states.

$$|\Phi_+\rangle = \frac{1}{\sqrt{2}}(|00\rangle + |11\rangle) \quad (3.9.17)$$

$$|\Phi_-\rangle = \frac{1}{\sqrt{2}}(|00\rangle - |11\rangle) \quad (3.9.18)$$

$$|\Psi_+\rangle = \frac{1}{\sqrt{2}}(|01\rangle + |10\rangle) \quad (3.9.19)$$

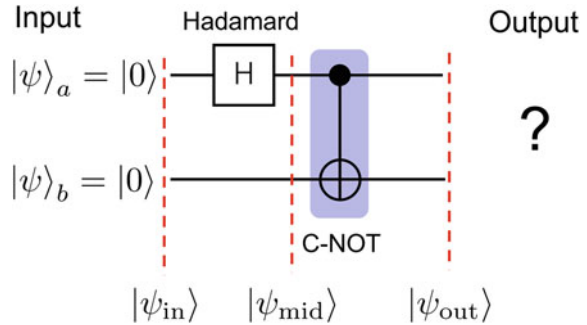
$$|\Psi_-\rangle = \frac{1}{\sqrt{2}}(|01\rangle - |10\rangle). \quad (3.9.20)$$

For those who have never studied the entanglement state before, it may sound mysterious and possibly very difficult to make. It actually is not. We show an example of a quantum logic circuit that creates an entanglement state. We will discuss more about the quantum logic circuit later, and this will be a preparatory example. (You might not understand what the circuit is doing, but it is OK, details are covered later in Sect. 9.2.)

The quantum logic circuit in Fig. 3.11 has two-qubit input and two-qubit output with two quantum logic gates inside. The first gate is a one-qubit Hadamard gate (H) only applied to the top qubit $|\psi_a\rangle$, followed by a two-qubit C-NOT gate. Initially, two inputs are both 0-state, making the initial state

$$|\psi_{\text{in}}\rangle = |00\rangle \equiv \begin{pmatrix} 1 \\ 0 \\ 0 \\ 0 \end{pmatrix}.$$

Fig. 3.11 Quantum logic circuit to make an entanglement state. The circuit consists of a one-qubit Hadamard gate on the first qubit, followed by a two-qubit C-NOT gate



The input for the Hadamard gate is $|\psi_a\rangle = |0\rangle \equiv \begin{pmatrix} 1 \\ 0 \end{pmatrix}$, and the Hadamard gate in a matrix representation is

$$\hat{H} = \frac{1}{\sqrt{2}} \begin{bmatrix} 1 & 1 \\ 1 & -1 \end{bmatrix}. \quad (3.9.21)$$

The output

$$\begin{aligned} |\psi'_a\rangle &= \hat{H}|\psi_a\rangle \equiv \frac{1}{\sqrt{2}} \cdot \begin{bmatrix} 1 & 1 \\ 1 & -1 \end{bmatrix} \begin{pmatrix} 1 \\ 0 \end{pmatrix} = \frac{1}{\sqrt{2}} \begin{pmatrix} 1 \\ 1 \end{pmatrix} \\ &= \frac{1}{\sqrt{2}} (|0\rangle + |1\rangle) \end{aligned}$$

is a superposition of $|0\rangle$ and $|1\rangle$ with equal weight. Now the state in the middle of two gates is

$$|\psi_{\text{mid}}\rangle = \frac{1}{\sqrt{2}} (|0\rangle + |1\rangle) \otimes |0\rangle = \frac{1}{\sqrt{2}} (|00\rangle + |10\rangle) \equiv \frac{1}{\sqrt{2}} \begin{pmatrix} 1 \\ 0 \\ 1 \\ 0 \end{pmatrix}. \quad (3.9.22)$$

Next, C-NOT is applied to $|\psi_{\text{mid}}\rangle$, generating the output state,

$$\begin{aligned} |\psi_{\text{out}}\rangle &= \hat{U}_{\text{CNOT}}|\psi_{\text{mid}}\rangle \equiv \begin{pmatrix} 1 & 0 & 0 & 0 \\ 0 & 1 & 0 & 0 \\ 0 & 0 & 0 & 1 \\ 0 & 0 & 1 & 0 \end{pmatrix} \cdot \frac{1}{\sqrt{2}} \begin{pmatrix} 1 \\ 0 \\ 1 \\ 0 \end{pmatrix} = \frac{1}{\sqrt{2}} \begin{pmatrix} 1 \\ 0 \\ 0 \\ 1 \end{pmatrix} \\ &= \frac{1}{\sqrt{2}} (|00\rangle + |11\rangle), \end{aligned} \quad (3.9.23)$$

which is one of the Bell states discussed earlier. As shown above, it is quite simple to generate an entangled state using two-qubit gate.

The entangled state, for example, $|\Phi_+\rangle = \frac{1}{\sqrt{2}}(|00\rangle + |11\rangle)$, has a 50% probability of measuring either $|00\rangle$ or $|11\rangle$. This is very strange when you think about it. As

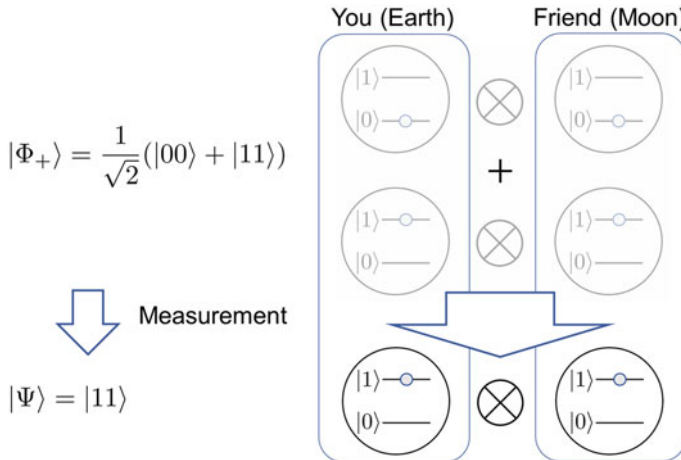


Fig. 3.12 Measurement of Bell state $|\Phi_+\rangle$

shown in Fig. 3.12, suppose that you give the first of the two qubits in $|\Phi_+\rangle$ to a friend, and then that friend goes to the moon. One day, you came up with the idea of measuring your qubit and $|1\rangle$ was observed. Since it is confirmed that the state is collapsed to $|11\rangle$ from your qubit, you know the qubit that your friend has is $|1\rangle$ with 100 % certainty. It is as if the information about the state of your friend's qubit, which is up in the moon, flew all the way to the earth instantaneously. Contrary, if the two shared a state mentioned previously $|\psi_a\rangle|\psi_b\rangle = (a_0|0\rangle + a_1|1\rangle) \otimes (b_0|0\rangle + b_1|1\rangle)$, which is in a form of a direct product. Even if you find out the state of your qubit $|1\rangle$, the qubit state of friend on the moon $|0\rangle$ cannot be determined.

This mysterious correlation (relationship between particles) that arises from an entangled state is called a quantum correlation, which is a non-classical correlation that occurs only in quantum states. This quantum correlation is considered as an important source of its power in the quantum information processing; however, how the entanglement is related to the computational power, nor in that matter, how to quantify the degree of entanglement is still a hot topic in current research.

Although, we do not have a precise measure for the entanglement yet, there are certain entanglement states that are believed to be more entangled than the others. For example, consider a three-qubit system, $|\psi\rangle = |\psi_1\psi_2\psi_3\rangle$. The Greenberger–Horne–Zeilinger state, also known as GHZ-state, and W-state, named after Wolfgang Dür, are defined as

$$|GHZ\rangle = \frac{1}{\sqrt{2}} (|000\rangle - |111\rangle) \quad (3.9.24)$$

$$|W\rangle = \frac{1}{\sqrt{3}} (|001\rangle + |010\rangle + |100\rangle), \quad (3.9.25)$$

respectively.

Suppose, you measure the first qubit of this GHZ-state and found $|\psi_1\rangle = |1\rangle$, then you would automatically know the rest of the qubits (2 and 3) being $|1\rangle$. The

same kind of result is obtained for the measurement result $|\psi_1\rangle = |0\rangle$, where you will know the rest of qubits are in $|0\rangle$. Now, try the same measurement on W-state. When the measurement is $|\psi_1\rangle = |1\rangle$, again, you will know the rest of the qubits (2 and 3) are $|0\rangle$, but if you measure $|\psi_1\rangle = |0\rangle$, the resulting state is

$$|W\rangle \rightarrow |\psi\rangle = |0\rangle \otimes \frac{1}{\sqrt{2}} (|01\rangle + |10\rangle), \quad (3.9.26)$$

where there are still some uncertainty in the state of qubit 2 and 3.

The strong entanglement seen in GHZ-state is sometimes referred to as a “fragile entanglement”. For example, if the measurement previously discussed is not the intended one, but done by some anonymous person, or mistakenly measured by the environmental noise, then the entanglement of the state, after the measurement, is completely gone. W-state, on the other hand, still maintains the entanglement (50% of time) between qubits 2 and 3 even after the measurement of qubit 1. Different entangled states have different reactions to the measurement and therefore different noise tolerance. Depending on the application, the use of entanglement and the choice of entangled state may vary.

It is also important to note that, when two particles interact, in general, they will make an entanglement. The degree of entanglement may be small, but this process could be a serious obstacle for the quantum operations in some cases.

For example, let us consider a qubit $|\psi_{\text{qubit}}\rangle = |0\rangle$ which we are interested in performing quantum operations. Suppose, an extraneous two-level system $|\psi_{\text{env}}\rangle = |1\rangle$ from environment is present in the vicinity of the qubit (such as background gas and impurities in solids). As long as there is no interaction between the two, the system stays as $|\Psi\rangle = |\psi_{\text{qubit}}\rangle \otimes |\psi_{\text{env}}\rangle = |0\rangle \otimes |1\rangle$. However, even with a small interaction, the system could evolve to a new state, for example,

$$|\Psi\rangle = |01\rangle \rightarrow |\Psi'\rangle = \sqrt{\frac{999}{1000}}|01\rangle + \sqrt{\frac{1}{1000}}|10\rangle. \quad (3.9.27)$$

The equation tells us that *practically nothing happened* as you can see the state is nearly $|01\rangle$, but this state cannot be decomposed to a direct product, thus an entangled state. Why is this entanglement a problem? If the two-level system $|\psi_{\text{env}}\rangle$ is measured by any means, we measure $|01\rangle$ most of the time, but there is a small chance of measuring $|10\rangle$, changing our qubit state to $|\psi_{\text{qubit}}\rangle = |1\rangle$! Many of the decoherence mechanisms (deterioration of “quantumness” in the state) for the quantum system are believed to be originated from this sort of “micro-entanglement” with a large number of unintended particles in the environment.

3.10 Eigenvalue Equation in Quantum Mechanics

Previously, the eigenvalue equation in linear algebra was reviewed. The formulation of the quantum mechanics is built upon these tools of linear algebra. In quantum

mechanics, all physical observable A can be described as an operator \hat{A} with corresponding observable value a in a form,

$$\hat{A}|\psi\rangle = a|\psi\rangle, \quad (3.10.1)$$

represented as an eigenvalue equation. In that matter, the time-independent Schrödinger equation described later,

$$-\frac{\hbar^2}{2m}\frac{\partial^2|\psi\rangle}{\partial x^2} + \hat{V}(x)|\psi\rangle = E|\psi\rangle, \quad (3.10.2)$$

can also be seen as an eigenvalue equation, by recognizing the Hamiltonian operator

$$\hat{\mathcal{H}} = -\frac{\hbar^2}{2m}\frac{\partial^2}{\partial x^2} + \hat{V}(x), \quad (3.10.3)$$

which makes

$$\hat{\mathcal{H}}|\psi\rangle = E|\psi\rangle. \quad (3.10.4)$$

Here, we can see the energy E is an eigenvalue of the system Hamiltonian $\hat{\mathcal{H}}$, and Schrödinger equation is just an eigenvalue equation of the system Hamiltonian. Similarly, if the momentum operator \hat{p} is applied to the wavefunction $|\Psi_p\rangle$, which is the eigenstate of momentum, the momentum value p of the state can be retrieved from the operation

$$\hat{p}|\Psi_p\rangle = p|\Psi_p\rangle, \quad (3.10.5)$$

as an eigenvalue.

If an operator has multiple eigenvalues λ_i and the corresponding eigenvectors $|\psi_i\rangle$ that can be orthonormalized, the operator can be represented as

$$\begin{aligned} \hat{A} &= \sum_i^n \lambda_i |\psi_i\rangle\langle\psi_i| \\ &= \begin{pmatrix} \lambda_1 & & & \\ & \lambda_2 & & \\ & & \ddots & \\ & & & \lambda_n \end{pmatrix}, \end{aligned} \quad (3.10.6)$$

where off-diagonal elements of the matrix are all zeros. This representation of the operator is called the diagonal representation, and the operator which can be represented in this form is called the diagonalizable operator. There are number of useful characteristics in the diagonalized operator. It is simply easy for calculations and have straight-forward correspondence between the eigenvalues and eigenvectors. It is also useful for some contexts such as quantum measurement as discussed later.

Fig. 3.13 Atomic states

$$|2\rangle \text{ --- } E_2$$

$$|1\rangle \text{ --- } E_1$$

$$|0\rangle \text{ --- } E_0$$

3.10.1 Example: Atom

Let us consider a short example, where the Hamiltonian of an atomic system is expressed as a diagonal matrix. Consider a three-level atomic system shown in Fig. 3.13. Let us use a simple state basis,

$$|\psi_0\rangle = \begin{pmatrix} 1 \\ 0 \\ 0 \end{pmatrix}, \quad |\psi_1\rangle = \begin{pmatrix} 0 \\ 1 \\ 0 \end{pmatrix}, \quad |\psi_2\rangle = \begin{pmatrix} 0 \\ 0 \\ 1 \end{pmatrix}, \quad (3.10.7)$$

and we would like to derive the system Hamiltonian $\hat{\mathcal{H}}$. Solving the Schrödinger equation with $\hat{\mathcal{H}} = \begin{pmatrix} a & b & c \\ d & e & f \\ g & h & i \end{pmatrix}$ for state $|\psi_0\rangle$,

$$\begin{aligned} \hat{\mathcal{H}}|\psi_0\rangle &= \begin{pmatrix} a & b & c \\ d & e & f \\ g & h & i \end{pmatrix} \begin{pmatrix} 1 \\ 0 \\ 0 \end{pmatrix} = \begin{pmatrix} a \\ d \\ g \end{pmatrix} = E_0 \begin{pmatrix} 1 \\ 0 \\ 0 \end{pmatrix} \\ \rightarrow \quad a &= E_0, \quad d = 0, \quad g = 0. \end{aligned} \quad (3.10.8)$$

The Hamiltonian can be found by repeating the procedure for $|\psi_1\rangle$ and $|\psi_2\rangle$ as

$$\hat{\mathcal{H}}|\psi_0\rangle = \begin{pmatrix} E_0 & 0 & 0 \\ 0 & E_1 & 0 \\ 0 & 0 & E_2 \end{pmatrix}. \quad (3.10.9)$$

The Hamiltonian is also expressed as

$$\hat{\mathcal{H}} = \sum_i E_i |\psi_i\rangle \langle \psi_i|. \quad (3.10.10)$$

In many cases in quantum technology, the system Hamiltonian describing the energy eigenstates used for the manipulation is expressed as a simple diagonal matrix with the energy eigenvalues E_i .

3.11 Operator Classification

There are various operators that act on the Hilbert space in which the quantum state is manipulated. They can be classified according to the characteristics of the operators. Here, we describe the definitions of Hermitian, unitary, and positive operators, which will be important later, and their properties in quantum mechanics.

3.11.1 Operator Functions

Before going into details of the operator classification, here is a short review on the operator functions. One may occasionally encounter a function of operator \hat{A} , such as $f(\hat{A})$. As any of the arbitrary function $f(x)$ can be expanded using the Taylor series as

$$f(x) = f(0) + f'(0)x + \cdots \frac{1}{n!} f^{(n)}(0)x^n + \cdots, \quad (3.11.1)$$

the function of operators can also be expanded as

$$f(\hat{A}) = f(0)\hat{I} + f'(0)\hat{A} + \cdots \frac{1}{n!} f^{(n)}(0)\hat{A}^n + \cdots, \quad (3.11.2)$$

where $\hat{A}^n = \hat{A} \cdots \hat{A}$ denotes the product of n operators \hat{A} . Of particular importance is the exponential function of operators, which is represented as follows:

$$e^{\hat{A}} \equiv \sum_{n=0}^{\infty} \frac{\hat{A}^n}{n!} = I + \hat{A} + \frac{\hat{A}^2}{2!} + \frac{\hat{A}^3}{3!} \cdots. \quad (3.11.3)$$

It is also easy to derive from above

$$(e^{\hat{A}})^\dagger = e^{\hat{A}^\dagger}. \quad (3.11.4)$$

Both of the above calculations can be tedious, but some special operator functions are easily derived. For example, for a polynomial function $f(x) = \sum_{i=0}^{\infty} c_i x^i$, the operator function can be written as

$$f(\hat{A}) = \sum_{i=0}^{\infty} c_i \hat{A}^i. \quad (3.11.5)$$

When $|\psi_n\rangle$ is one of the eigenvectors of operator \hat{A} with an eigenvalue a_n , then the operator function satisfies

$$\hat{A}^i |\psi_n\rangle = (a_n)^i |\psi_n\rangle \quad (3.11.6)$$

$$\Rightarrow f(\hat{A}) |\psi_n\rangle = f(a_n) |\psi_n\rangle, \quad (3.11.7)$$

for polynomial functions.

Another example similar to above is when the operator \hat{A} is diagonal. For example, when an operator has a form

$$\hat{A} = \begin{pmatrix} A_1 & & \\ & A_2 & \\ & & A_3 \end{pmatrix}, \quad (3.11.8)$$

where blank matrix elements are all zeros, the matrix satisfies

$$\hat{A}^n = \begin{pmatrix} A_1^n & & \\ & A_2^n & \\ & & A_3^n \end{pmatrix}, \quad (3.11.9)$$

and polynomial functions are simply

$$f(\hat{A}) = \begin{pmatrix} f(A_1) & & \\ & f(A_2) & \\ & & f(A_3) \end{pmatrix}. \quad (3.11.10)$$

In unitary operators, exponential functions of operators such as $e^{\hat{A}}$ frequently appear. Below are some useful formulas for the exponential operator. They become particularly useful for changing the pictures (Schrödinger, Heisenberg, and Dirac picture) or the frame rotation as discussed later.

The Baker–Campbell–Hausdorff identity

$$e^{\alpha \hat{A}} \hat{B} e^{-\alpha \hat{A}} = \hat{B} + \alpha [\hat{A}, \hat{B}] + \frac{\alpha^2}{2!} [\hat{A}, [\hat{A}, \hat{B}]] + \dots. \quad (3.11.11)$$

Glauber's formula

$$e^{\hat{A}} e^{\hat{B}} = e^{\hat{A} + \hat{B}} e^{\frac{1}{2} [\hat{A}, \hat{B}]} \quad (3.11.12)$$

Here, we used the commutator symbol, $[\hat{A}, \hat{B}] = \hat{A}\hat{B} - \hat{B}\hat{A}$.

3.11.2 Hermitian Operator

For any operator \hat{H} , the Hermitian conjugate operator \hat{H}^\dagger can be defined as the operator, which satisfies the following inner product of the wavefunction.

$$\langle \phi | \hat{H} \psi \rangle = \int \psi^* \hat{H} \phi dx = \int \psi (\hat{H}^\dagger \phi)^* dx = \langle \hat{H}^\dagger \phi | \psi \rangle. \quad (3.11.13)$$

With a matrix representation, \hat{H}^\dagger can be found very easily as

$$\hat{H}^\dagger = (\hat{H}^T)^*, \quad (3.11.14)$$

where \hat{H}^T is a transpose of \hat{H} , thus the Hermitian conjugate of \hat{H} is derived from the transpose of the complex conjugate of \hat{H} . Also, the matrix representation eases the derivation of the following characteristics of Hermitian conjugate operators.

$$(\hat{H}^\dagger)^\dagger = \left\{ \left[(\hat{H}^T)^* \right]^T \right\}^* = (\hat{H}^T)^T = \hat{H} \quad (3.11.15)$$

$$(c\hat{H})^\dagger = c^* \hat{H}^\dagger \quad (3.11.16)$$

$$(\hat{H}_1 + \hat{H}_2)^\dagger = \hat{H}_1^\dagger + \hat{H}_2^\dagger \quad (3.11.17)$$

$$(\hat{H}_1 \hat{H}_2)^\dagger = \hat{H}_2^\dagger \hat{H}_1^\dagger. \quad (3.11.18)$$

If the Hermitian conjugate operator of an operator is the same as the original operator, that is,

$$\hat{H}^\dagger = \hat{H}, \quad (3.11.19)$$

then \hat{H} is called the Hermitian operator.

The Hermitian operator has the following characteristics regarding the inner product of wavefunctions.

$$\langle \psi | \hat{H} \phi \rangle = \langle \hat{H} \psi | \phi \rangle. \quad (3.11.20)$$

The Hermitian operator is closely related to the physical quantity, and all the operators corresponding to the physical quantity we measure are, in fact, the Hermitian operator.

By its nature, all measured physical observables must be real numbers, so of course the expectation value should also be real numbers. The following is a reverse proof but shows that the expectation values and eigenvalues of the Hermitian operators are real numbers.

Consider the conjugate complex of the expectation value of Hermitian operator \hat{H} ,

$$\langle H \rangle^* = \langle \Psi | \hat{H} \Psi \rangle^* = \langle \hat{H} \Psi | \Psi \rangle = \langle \Psi | \hat{H} \Psi \rangle = \langle H \rangle. \quad (3.11.21)$$

The expectation value is the same as that of \hat{H} , which implies the expectation value is a real number. Similarly, with the eigenvector $|\psi_i\rangle$ and its eigenvalue λ_i , $\langle H \rangle^*$ has two solutions as

$$\langle H \rangle^* = \left(\langle \psi_i | \hat{H} \psi_i \rangle \right)^* = (\lambda_i \langle \psi_i | \psi_i \rangle)^* = \lambda_i^* \quad (3.11.22)$$

$$\langle H \rangle^* = \left(\langle \psi_i | \hat{H} \psi_i \rangle \right)^* = \left(\langle \hat{H} \psi_i | \psi_i \rangle \right)^* \quad (3.11.23)$$

$$= (\lambda_i^* \langle \psi_i | \psi_i \rangle)^* = \lambda_i. \quad (3.11.24)$$

The eigenvalue λ_i satisfying the conditions above is a real number. Thus, as stated, the eigenvalue of Hermitian operators is real, and all the physical observables are expressed as Hermitian operators.

3.11.3 Projection Operator

One of the most important Hermitian operator is the projection operator. Suppose a state is written in a basis $|\psi_i\rangle \equiv |i\rangle$. Projection operator \hat{P}_m which projects the basis to $|\psi_m\rangle \equiv |m\rangle$ can be written as

$$\hat{P}_m = |m\rangle\langle m|. \quad (3.11.25)$$

The state $|i\rangle$ can be projected in basis $|m\rangle$ as

$$\hat{P}_m|i\rangle = |m\rangle\langle m|i\rangle = c_m|m\rangle, \quad (3.11.26)$$

where projected amplitude is $c_m = \langle m|i\rangle$.

The sum of the projection operator \hat{P}_m formed with orthonormal basis $|m\rangle$ that spans the vector space is

$$\sum_m \hat{P}_m = \sum_m |m\rangle\langle m| = \sum_m |\psi_m\rangle\langle\psi_m| = \hat{I}. \quad (3.11.27)$$

This is called *completeness relation* and is quite practical. The identity \hat{I} can be thrown in just about anywhere, and this relation conveniently allows a transformation of its basis.

For example, suppose a wavefunction $|\Phi\rangle$ is expressed in basis $|\phi_i\rangle$ that is different from the basis above as

$$|\Phi\rangle = \sum_i d_i |\phi_i\rangle. \quad (3.11.28)$$

This wavefunction can be transformed in terms of new basis using the completeness relation $\hat{I} = \sum_m |\psi_m\rangle\langle\psi_m|$ as

$$|\Phi\rangle = \sum_i d_i \hat{I} |\phi_i\rangle \quad (3.11.29)$$

$$= \sum_{i,m} d_i |\psi_m\rangle\langle\psi_m|\phi_i\rangle \quad (3.11.30)$$

$$= \sum_m c_m |\psi_m\rangle, \quad (3.11.31)$$

where $c_m = \sum_i d_i \langle\psi_m|\phi_i\rangle$. The projection operator allows to express or transform the wavefunction into any basis of choice.

Changing the Qubit basis

Let us try to change the basis of qubit from $|0\rangle$ and $|1\rangle$ to $|+x\rangle$ and $|-x\rangle$ using the projection operator \hat{P} . As derived previously,

$$\begin{aligned}|+x\rangle &= \frac{1}{\sqrt{2}} (|0\rangle + |1\rangle) \\ |-x\rangle &= \frac{1}{\sqrt{2}} (|0\rangle - |1\rangle),\end{aligned}$$

these states form a orthonormal set of basis, satisfying the condition $\langle\psi_i|\psi_j\rangle = \delta_{ij}$ as

$$\begin{aligned}\langle+x|+x\rangle &= \frac{1}{2} (\langle 0| + \langle 1|) (|0\rangle + |1\rangle) = 1 \\ \langle-x|-x\rangle &= \frac{1}{2} (\langle 0| - \langle 1|) (|0\rangle - |1\rangle) = 1 \\ \langle+x|-x\rangle &= \frac{1}{2} (\langle 0| + \langle 1|) (|0\rangle - |1\rangle) = 0.\end{aligned}$$

To write $|0\rangle(|1\rangle)$ in terms of $|+x\rangle$ and $|-x\rangle$, the completeness relation,

$$\hat{I} = \sum_i |\psi_i\rangle\langle\psi_i| = |+x\rangle\langle+x| + |-x\rangle\langle-x|, \quad (3.11.32)$$

is used as

$$\begin{aligned}|0\rangle &= \hat{I}|0\rangle = (|+x\rangle\langle+x| + |-x\rangle\langle-x|)|0\rangle \\ &= \frac{1}{\sqrt{2}} [|+x\rangle (\langle 0| + \langle 1|) + |-x\rangle (\langle 0| - \langle 1|)]|0\rangle \\ &= \frac{1}{\sqrt{2}} [|+x\rangle (\langle 0|0\rangle + \langle 1|0\rangle) + |-x\rangle (\langle 0|0\rangle - \langle 1|0\rangle)] \\ &= \frac{1}{\sqrt{2}} (|+x\rangle + |-x\rangle).\end{aligned}$$

Taking the same procedure for $|1\rangle$, we obtain

$$\begin{aligned}|0\rangle &= \frac{1}{\sqrt{2}} (|+x\rangle + |-x\rangle) \equiv \frac{1}{\sqrt{2}} (|0'\rangle + |1'\rangle) \\ |1\rangle &= \frac{1}{\sqrt{2}} (|+x\rangle - |-x\rangle) \equiv \frac{1}{\sqrt{2}} (|0'\rangle - |1'\rangle).\end{aligned}$$

Recognizing the new qubit basis $|0'\rangle \equiv |+x\rangle$ and $|1'\rangle \equiv |-x\rangle$, the original state $|0\rangle$ and $|1\rangle$ is now written as a superposition of the new qubit basis (Fig. 3.14).

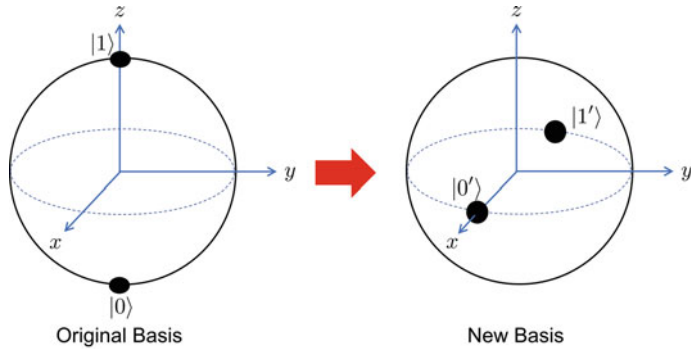


Fig. 3.14 Changing the basis of Qubit

Another example is shown for the calculation of expectation value $\langle A \rangle$, which is transformed in terms of density matrix using the projection operator. One can expand $\langle A \rangle = \langle \psi | \hat{A} | \psi \rangle$ using the projection operator as

$$\begin{aligned}
 \langle A \rangle &= \langle \psi | \hat{A} | \psi \rangle \\
 &= \sum_i \langle \psi | \hat{A} | i \rangle \langle i | \psi \rangle \\
 &= \sum_i \langle i | \psi \rangle \langle \psi | \hat{A} | i \rangle = \sum_i \left(|\psi\rangle\langle\psi|\hat{A}\right)_{ii} \\
 &= \text{Tr} \left(|\psi\rangle\langle\psi|\hat{A} \right) = \text{Tr} \left(\hat{\rho}\hat{A} \right). \tag{3.11.33}
 \end{aligned}$$

$\hat{\rho} \equiv |\psi\rangle\langle\psi|$ is called *Density matrix*, which will be described in detail later in Sect.3.12. Here, we only emphasize that it becomes quite simple to calculate the expectation value using the density matrix.

3.11.4 Unitary Operator

When an operator \hat{U} satisfies the condition,

$$\hat{U}^\dagger \hat{U} = I, \tag{3.11.34}$$

the operator \hat{U} is said to be unitary. For arbitrary vectors $|\psi\rangle$ and $|\phi\rangle$, transformed by \hat{U} as $(|\psi\rangle, |\phi\rangle \rightarrow \hat{U}|\psi\rangle \equiv |\alpha\rangle, \hat{U}|\phi\rangle \equiv |\beta\rangle)$, the inner product of the new vectors are the same as that of the original vectors as

$$\begin{aligned}
 \langle \alpha | \beta \rangle &= \langle \psi | \hat{U}^\dagger \hat{U} | \phi \rangle \\
 &= \langle \psi | \phi \rangle. \tag{3.11.35}
 \end{aligned}$$

The unitary transformation thus preserves the inner product of the vectors. In a close quantum system, the time evolution of the system can be described by the

unitary operator. Also, it is important to mention that Eq. (3.11.34) can be rewritten as $U^{-1} = U^\dagger$, which implies that all unitary operators have its inverse. In other words, all the manipulations using unitary operators are reversible. In the context of quantum information, it is ideal to manipulate the system without loss, meaning the system is closed and the operation is reversible. For this reason, the term “unitary manipulation” is often used to describe the ideal quantum manipulation without loss.

Let us show an important example that the exponential operator of a form $e^{i\hat{H}}$, where \hat{H} is a Hermitian operator, is a unitary operator. For a Hermitian operator \hat{H} , define an exponential operator $\hat{U} = e^{i\hat{H}}$. The Hermitian conjugate of this operator is

$$\begin{aligned}\hat{U}^\dagger &= \left(e^{i\hat{H}} \right)^\dagger \\ &= e^{-i\hat{H}},\end{aligned}$$

where the property of the Hermitian operator $\hat{H}^\dagger = \hat{H}$ is used. It is straight forward to see $\hat{U} \hat{U}^\dagger = e^{i\hat{H}} e^{-i\hat{H}} = \hat{I}$ (and $\hat{U}^{-1} = \hat{U}^\dagger$); therefore, \hat{U} is an unitary operator. To show above, two identities $e^{\hat{A}} e^{\hat{B}} = e^{\hat{A} + \hat{B}}$ for commuting operators \hat{A} and \hat{B} ($[\hat{A}, \hat{B}] = 0$) and $(e^{\hat{A}})^\dagger = e^{\hat{A}^\dagger}$ are used.

This exponential form is used quite often in the later section, where different pictures in quantum mechanics, as well as use of rotating frames, are discussed. Also, the exponential operator of a system Hamiltonian \mathcal{H} is later discussed as a time-evolution operator.

3.11.5 Pauli Operators

The Pauli operators are important operators, not just for the quantum information, but also for a wide range of physics. These operators, also known as the Pauli matrices, are used to describe the angular momentum of spin-1/2 particles. As later shown in detail, the qubit has the same structure as the spin-1/2 system, as they are called “pseudo-spins”. In other words, we can use the Pauli matrices that describe the spin-1/2 dynamics as the fundamental building blocks for the qubit operations.

They are simple but powerful tool in many areas and we recommend readers to make it stick as a second nature. Different literature have slightly different notations for the Pauli matrices, but usually one of the followings is used.

$$\hat{\sigma}_0 \equiv \hat{I} \equiv \begin{pmatrix} 1 & 0 \\ 0 & 1 \end{pmatrix} \quad (3.11.36)$$

$$\hat{\sigma}_1 \equiv \hat{\sigma}_x \equiv \hat{X} \equiv \begin{pmatrix} 0 & 1 \\ 1 & 0 \end{pmatrix} \quad (3.11.37)$$

$$\hat{\sigma}_2 \equiv \hat{\sigma}_y \equiv \hat{Y} \equiv \begin{pmatrix} 0 & -i \\ i & 0 \end{pmatrix} \quad (3.11.38)$$

$$\hat{\sigma}_3 \equiv \hat{\sigma}_z \equiv \hat{Z} \equiv \begin{pmatrix} 1 & 0 \\ 0 & -1 \end{pmatrix}. \quad (3.11.39)$$

All Pauli matrices satisfy

$$\sigma_i^\dagger = \sigma_i \quad (3.11.40)$$

$$\sigma_i^\dagger \sigma_i = I, \quad (3.11.41)$$

and they are Hermitian operators. Also, they have the following characteristics.

$$\sigma_1^2 = \sigma_2^2 = \sigma_3^2 = -i\sigma_1\sigma_2\sigma_3 = I. \quad (3.11.42)$$

In the description of the two-level system using the Bloch sphere, the rotation operator $\hat{R}_i(\theta)$, which is an exponential operator of Pauli matrices, becomes an important tool. The rotation matrix performs the rotation of the state vector on the Bloch sphere. Here, we briefly introduce the action of the rotation operator.

When an arbitrary operator \hat{A} satisfies $\hat{A}^2 = \hat{I}$, the following equation is satisfied:

$$e^{i\theta\hat{A}} = \cos\theta\hat{I} + i\sin\theta\hat{A}. \quad (3.11.43)$$

Using this relation, the rotation operators are given as

$$\hat{R}_x(\theta) \equiv e^{-i\frac{\theta}{2}\hat{X}} = \begin{pmatrix} \cos\frac{\theta}{2} & -i\sin\frac{\theta}{2} \\ -i\sin\frac{\theta}{2} & \cos\frac{\theta}{2} \end{pmatrix} \quad (3.11.44)$$

$$\hat{R}_y(\theta) \equiv e^{-i\frac{\theta}{2}\hat{Y}} = \begin{pmatrix} \cos\frac{\theta}{2} & -\sin\frac{\theta}{2} \\ \sin\frac{\theta}{2} & \cos\frac{\theta}{2} \end{pmatrix} \quad (3.11.45)$$

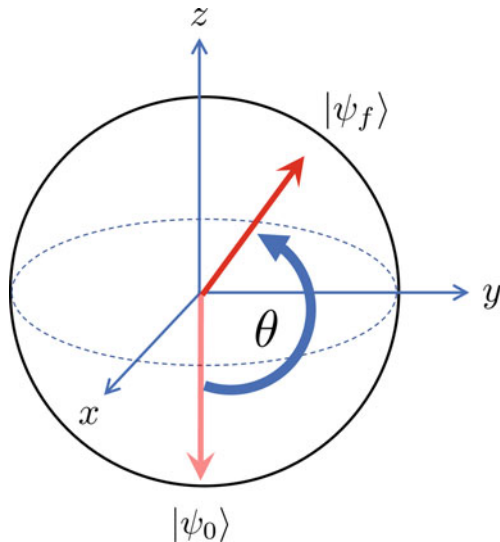
$$\hat{R}_z(\theta) \equiv e^{-i\frac{\theta}{2}\hat{Z}} = \begin{pmatrix} e^{-i\theta/2} & 0 \\ 0 & e^{i\theta/2} \end{pmatrix}. \quad (3.11.46)$$

The rotation operator $\hat{R}_i(\theta)$ is an operator that rotates the state vector by θ with respect to the i -axis. Figure 3.15 shows an example, where the initial state vector $|\psi_0\rangle$, which points at the south pole, is rotated at an angle θ by the x -axis.

The final state $|\psi_f\rangle$ is written in terms of the initial state and the rotation operator as

$$\begin{aligned} |\psi_f\rangle &= \hat{R}_x(\theta)|\psi_0\rangle \\ &= \begin{pmatrix} \cos\frac{\theta}{2} & -i\sin\frac{\theta}{2} \\ -i\sin\frac{\theta}{2} & \cos\frac{\theta}{2} \end{pmatrix} \begin{pmatrix} 1 \\ 0 \end{pmatrix} \\ &= \begin{pmatrix} \cos\frac{\theta}{2} \\ -i\sin\frac{\theta}{2} \end{pmatrix}. \end{aligned} \quad (3.11.47)$$

Fig. 3.15 Rotation of the state vector on the Bloch sphere



3.12 Density Operator

The quantum state has been represented by the ket-vector $|\psi\rangle$. According to this representation, it is possible to describe a superposition state as an element of the complex vector space, and even for the quantum state of the composite system, the tensor product of the basis stretches the vector space, enabling a new representation.

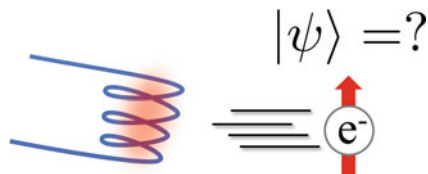
For example, in the Stern–Gerlach experiment, the time evolution of the quantum state of a single electron with an upward spin $|\uparrow\rangle$ incident on the apparatus can be analyzed precisely by solving the Schrödinger equation of motion. A quantum state that can be expressed by a ket-vector in this way is called a *pure state*.

In reality, when a single electron is emitted out of a hot tungsten wire (Fig. 3.16), for example, it is a 50-50 chance that the spin is upward or downward. What kind of quantum state is it in such a case? If we want to express it as a ket-vector, we may try to express it as a superposition state of upward spin and downward spin, for example,

$$|\psi\rangle = \frac{1}{\sqrt{2}} (|\uparrow\rangle + |\downarrow\rangle), \quad (3.12.1)$$

which we recognize as $|+x\rangle$ -state. However, if it can be written as a superposition state in this way, the direction of the spin should be fixed when looking at it from

Fig. 3.16 State of the thermally emitted electron



some other direction (e.g., x -direction). In reality, thermal electrons are statistically dispersed so that the spin direction is not fixed in any direction. So the pure state representation cannot correctly represent these hot electrons.

Consider a more general quantum state, where the state is found in one of the pure states with a certain probability, say 50% in $|\uparrow\rangle$ and 50% in $|\downarrow\rangle$. Also in a regular superposition state, the phase relationship between the spin up and down states are fixed. Let's discard this constraint too and not worry about the phase relation between different pure states. Such a quantum state is called a mixed state and is a good representation of the quantum state of hot electrons out of tungsten. Here, we introduce how these states can be represented.

First, we consider the statistical mixture of electrons with upward spin $|\uparrow\rangle = |\psi_1\rangle$ and downward spin $|\downarrow\rangle = |\psi_2\rangle$ with probabilities p_1 and p_2 , respectively, and focus on the expectation value of the observable O (for example, the z -component of spin) in the experiment. The expectation value for the pure state $|\psi\rangle$ is $\langle\psi|\hat{O}|\psi\rangle$, but for later convenience, we change the form with a trace, by using a completeness relation $\sum_m |m\rangle\langle m| = \hat{I}$ as

$$\begin{aligned}\langle\psi|\hat{O}|\psi\rangle &= \sum_{m,n} \langle\psi|m\rangle\langle m|\hat{O}|n\rangle\langle n|\psi\rangle \\ &= \sum_{m,n} \langle n|\psi\rangle\langle\psi|m\rangle\langle m|\hat{O}|n\rangle \\ &= \text{Tr} \left[|\psi\rangle\langle\psi|\hat{O} \right].\end{aligned}\quad (3.12.2)$$

Now, the expectation value for the mixed state can be written in terms of the expectation value for each pure state that is statistically mixed as

$$\langle O \rangle = p_1\langle\psi_1|\hat{O}|\psi_1\rangle + p_2\langle\psi_2|\hat{O}|\psi_2\rangle = \sum_i p_i \langle\psi_i|\hat{O}|\psi_i\rangle.\quad (3.12.3)$$

As in the pure state, transforming into a form with a trace shows

$$\langle O \rangle = \sum_i p_i \langle\psi_i|\hat{O}|\psi_i\rangle\quad (3.12.4)$$

$$= \sum_{mn} \sum_i p_i \langle\psi_i|m\rangle\langle m|\hat{O}|n\rangle\langle n|\psi_i\rangle\quad (3.12.5)$$

$$= \sum_{mn} \sum_i p_i \langle n|\psi_i\rangle\langle\psi_i|m\rangle\langle m|\hat{O}|n\rangle\quad (3.12.6)$$

$$= \text{Tr} \left[\sum_i p_i |\psi_i\rangle\langle\psi_i|\hat{O} \right].\quad (3.12.7)$$

As shown above, $|\psi\rangle\langle\psi|$ appearing in the calculation for the pure state is replaced with $\sum_i p_i |\psi_i\rangle\langle\psi_i|$ in the mixed state. For that matter, if only one p_i is 1 and the

others are all 0, then the results for the mixed state include those in pure state. This quantity,

$$\hat{\rho} = \sum_i p_i |\psi_i\rangle\langle\psi_i|, \quad (3.12.8)$$

is a natural extension of the quantum state description in that sense and called *density matrix* or *density operator*. It should be noted that the statistical mixture weight $p_i \geq 0$ that appears here is fundamentally different from the quantum probability amplitudes used in the coefficients of the superposition state.

3.12.1 Example of a Mixed State

In the previous example of thermal electron spin states, the quantum states of the upward spin and the downward spin are statistically mixed with equal probability, and the density operator is given as

$$\hat{\rho} = \frac{1}{2}|\uparrow\rangle\langle\uparrow| + \frac{1}{2}|\downarrow\rangle\langle\downarrow|. \quad (3.12.9)$$

For electron spin with only possible states $|\uparrow\rangle$ and $|\downarrow\rangle$, this leads to

$$\hat{\rho} = \frac{1}{2}\hat{I}. \quad (3.12.10)$$

This is called a *completely mixed state* for a single spin-1/2 system.

Another example is the thermal state of the harmonic oscillator. As explained later, the state of the harmonic oscillator can be specified with “how many” quantized vibrations exist (number state); however, the thermal state has a statistical distribution of this number state $|n\rangle$ according to the Boltzmann distribution.

Specifically, the density operator $\hat{\rho}_{\text{th}}$ of the harmonic oscillator in the thermal state can be written as

$$\hat{\rho}_{\text{th}} = \sum_{n=0}^{\infty} e^{-n\hbar\omega/k_B T} (1 - e^{-\hbar\omega/k_B T}) |n\rangle\langle n|, \quad (3.12.11)$$

where \hbar , ω , k_B , and T shown in the above equation are the Dirac constant, the intrinsic angular frequency of the harmonic oscillator, the Boltzmann constant, and the temperature of the state, respectively.

3.12.2 General Properties of Density Operator

The density operator can describe any state, whether quantum or classical. It becomes especially important when the noise, which tends to diminish the “quantumness” of the states, is considered. Here, we list the general properties of the density operator $\hat{\rho}$, which may be useful in the later chapter.

- The trace of density operator is always 1,

$$\text{Tr} [\hat{\rho}] = 1. \quad (3.12.12)$$

This is immediately derived from the fact that $\sum_i p_i = 1$ holds for statistical mixing probabilities.

- The density operator is a Hermite operator.
- The density operator is positive-semidefinite, that is, $\langle \phi | \hat{\rho} | \phi \rangle \geq 0$ holds for any $|\phi\rangle$. This can be seen from $p_i \geq 0$, and it also implies that the eigenvalues of the density operator are non-negative.
- For a pure state, the diagonal elements of the matrix representation of the density operator correspond to the occupancy probabilities in the corresponding basis state.
- $\hat{\rho}^2 = \hat{\rho}$ holds for the pure state.
- For a general density operator $\text{Tr} [\rho^2] \leq 1$, but only in pure state $\text{Tr} [\hat{\rho}^2] = \text{Tr} [\hat{\rho}] = 1$.
- Since it can be used as a measure to distinguish between the pure and mixed state, $\text{Tr} [\hat{\rho}^2]$ is often called “purity” of the state.
- The expectation value of a physical observable O is given by $\text{Tr} [\hat{\rho} \hat{O}]$.

3.12.3 Density Operator of Composite System and its Reduction

For two independently prepared quantum systems, their density operators can be written as $\hat{\rho}_1$ and $\hat{\rho}_2$. The density operator $\hat{\rho}$ of the composite system of these two quantum systems could be defined by the tensor product of ket-vectors if it is a separable pure state. In general, even with the mixed state, if they are separable after all by adding statistical weights by considering both the ket and bra vectors, we may write

$$\hat{\rho} = \hat{\rho}_1 \otimes \hat{\rho}_2. \quad (3.12.13)$$

The composite system like above will evolve in time according to the system Hamiltonian and we would like to know the final state of each quantum system. We consider a case where $\hat{\rho}_2$ is a system with many degrees of freedom as shown in Fig. 3.17, that is, a density operator consisting of a large number of spins and a collection of harmonic oscillators, and it is extremely difficult to reconstruct the density operator from measurement. In such a case, we have no choice but to consider only the quantum system of interest $\hat{\rho}_1$. Then, what kind of operation would it take to obtain the information about the system of interest without the knowledge of $\hat{\rho}_2$?

Consider the density operators $\hat{\rho}_1$ and $\hat{\rho}_2$ and basis $\sum_{k_1} |k_1\rangle\langle k_1|$, $\sum_{k_2} |k_2\rangle\langle k_2|$. After the time evolution, the density operator has evolved to $\hat{\rho}'$ as

$$\hat{\rho} = \hat{\rho}_1 \otimes \hat{\rho}_2 \rightarrow \hat{\rho}'. \quad (3.12.14)$$

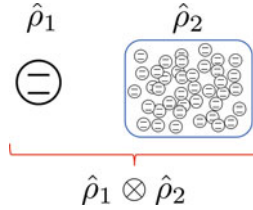


Fig. 3.17 Density operator for composite system. Where $\hat{\rho}_1$ is the system of interest and $\hat{\rho}_2$ is a collection of two-level systems or harmonic oscillators, that could be thought of as a noisy environment for $\hat{\rho}_1$

The expectation value of observable O on the system of interest (System 1) is written as

$$\begin{aligned}
 \langle O \rangle &= \text{Tr}_{12} \left[\hat{\rho}' \hat{O} \right] \\
 &= \sum_{k_1, k_2} \langle k_1 | \otimes \langle k_2 | \hat{\rho}' \hat{O} | k_1 \rangle \otimes | k_2 \rangle \\
 &= \sum_{k_1} \langle k_1 | \left(\sum_{k_2} \langle k_2 | \hat{\rho}' | k_2 \rangle \right) \hat{O} | k_1 \rangle \\
 &= \text{Tr}_1 \left[\left(\sum_{k_2} \langle k_2 | \hat{\rho}' | k_2 \rangle \right) \hat{O} \right] \\
 &= \text{Tr}_1 \left[(\text{Tr}_2 \hat{\rho}') \hat{O} \right] \\
 &= \text{Tr}_1 \left[\hat{\rho}'_1 \hat{O} \right]. \tag{3.12.15}
 \end{aligned}$$

Here, a trace operation with a subscript means to take a trace for either or both of system $\hat{\rho}_1$ and $\hat{\rho}_2$. A trace operation for only one system is also called a *partial trace*.

From the above derivation, the reduced density operator $\hat{\rho}'_1 = \text{Tr}_2 \hat{\rho}'$ can be thought of as the density operator of the system $\hat{\rho}_1$ after the time evolution. In the last expression, the expectation value of the operator \hat{O} is calculated from the density operator $\hat{\rho}'_1$. As shown above, the reduced density operator comes in handy when measuring the physical observable of only a partial system of the composite system.

One thing to note here is that the density operator after time evolution $\hat{\rho}'$ cannot be written as $\hat{\rho}' = \text{Tr}_2 \hat{\rho}' \otimes \text{Tr}_1 \hat{\rho}'$. This is only true when $\hat{\rho}'$ is separable. If there is entanglement between the two systems, a partial trace operation on one system leads to the loss of information on the other system.

For example, if the $\hat{\rho}_1$ and $\hat{\rho}_2$ system are a qubit and a collection of harmonic oscillators, respectively, and they interact. After sometime, the qubit obtains an extremely complex entanglement formed between the qubit and the group of harmonic oscillators, and then the state of the quantum bit loses coherence.

3.13 Commutator and Anti-Commutator

We have seen the matrix representation of the operators in the previous sections. As we know from linear algebra, the matrix multiplication $\hat{A}\hat{B}$ is not always the same as $\hat{B}\hat{A}$ and the ordering matters. In quantum mechanics, this plays an important role and we often check the *commutation relation* of the operators. Commutator and anti-commutator of operators are each defined as

$$[\hat{A}, \hat{B}] \equiv \hat{A}\hat{B} - \hat{B}\hat{A} \quad (3.13.1)$$

$$\{\hat{A}, \hat{B}\} \equiv \hat{A}\hat{B} + \hat{B}\hat{A}. \quad (3.13.2)$$

When operators \hat{A} and \hat{B} satisfy $[\hat{A}, \hat{B}] = 0$ ($\hat{A}\hat{B} = \hat{B}\hat{A}$), then they commute, while if $[\hat{A}, \hat{B}] \neq 0$ ($\hat{A}\hat{B} \neq \hat{B}\hat{A}$) is satisfied, the operators do not commute. One important consequence is when the operators of physical observables A and B commute, then those observables can be measured simultaneously. The two commuting observables are called Simultaneous *observables* and can also have the same set of eigenfunctions.

On the contrary, in a non-commutative case, the measurement of one observable changes the other observable. This is quite non-intuitive and arose as one of the upsetting consequences of the quantum mechanics in the early development. The commutator is strongly associated with measurement and sets a new type of measurement constraint. In the next section, we derive the celebrated Heisenberg uncertainty principle from the commutation relation.

Many readers have probably seen the canonical commutation relation $[\hat{x}, \hat{p}] = i\hbar$. In quantum technology, some important commutation relations include that of the ladder operators and Pauli operators, which are used repeatedly to describe the dynamics of harmonic oscillators and two-level systems, respectively.

Annihilation and creation operators, \hat{a} and \hat{a}^\dagger , respectively, has the following commutation relation:

$$[\hat{a}, \hat{a}^\dagger] = 1, \quad (3.13.3)$$

from which other commutation relations, such as $[\hat{a}^\dagger \hat{a}, \hat{a}]$ and $[\hat{a}^\dagger \hat{a}, \hat{a}^\dagger]$, are derived. We recommend readers to derive some of these commutation relations.

Pauli operators obey the following commutation relations:

$$[\hat{\sigma}_x, \hat{\sigma}_y] = 2i\hat{\sigma}_z, \quad [\hat{\sigma}_y, \hat{\sigma}_z] = 2i\hat{\sigma}_x, \quad [\hat{\sigma}_z, \hat{\sigma}_x] = 2i\hat{\sigma}_y,$$

which can be summarized in a simple form,

$$[\hat{\sigma}_i, \hat{\sigma}_j] = 2i\epsilon_{ijk}\hat{\sigma}_k, \quad (3.13.4)$$

where ϵ_{ijk} is the Levi–Civita symbol defined by

$$\epsilon_{ijk} = \begin{cases} 0 & \text{for } i = j, j = k, \text{ or } k = i \\ +1 & \text{for cyclic permutation, } (i, j, k) = (1, 2, 3), (2, 3, 1), (3, 1, 2) \\ -1 & \text{for non-cyclic permutation, } (i, j, k) = (1, 3, 2), (3, 2, 1), (2, 1, 3). \end{cases}$$

3.13.1 Heisenberg's Uncertainty Principle

The commutation relation can be used to derive a generalized uncertainty principle. When the result of repeated measurements of a physical observable A is A_1, A_2, A_3, \dots , the classical mean value $\langle A \rangle$, the deviation from the mean ΔA_i , and the variance σ_A are each defined as

$$\langle A \rangle = \frac{1}{n} \sum_i^n A_i \quad (3.13.5)$$

$$\Delta A_i = A_i - \langle A \rangle \quad (3.13.6)$$

$$\sigma_A^2 = \langle (\Delta A_i)^2 \rangle = \langle (A_i - \langle A \rangle)^2 \rangle. \quad (3.13.7)$$

Similarly, in the quantum system, the expectation value $\langle A \rangle$ for the wavefunction $|\psi\rangle$, the deviation from the expectation value ΔA , and the variance σ_A are defined, respectively, as

$$\langle A \rangle = \langle \Psi | \hat{A} | \Psi \rangle \quad (3.13.8)$$

$$\Delta A = \hat{A} - \langle A \rangle \quad (3.13.9)$$

$$\begin{aligned} \sigma_A^2 &= \langle \Psi | (\hat{A} - \langle A \rangle)^2 | \Psi \rangle \\ &= \langle (\hat{A} - \langle A \rangle) \Psi | (\hat{A} - \langle A \rangle) \Psi \rangle \end{aligned} \quad (3.13.10)$$

In the last line, we used that all physical observables are represented by the Hermitian operator.

For two observables A and B , we can define $|a\rangle$ and $|b\rangle$ as

$$|a\rangle \equiv (\hat{A} - \langle A \rangle) |\Psi\rangle \quad (3.13.11)$$

$$|b\rangle \equiv (\hat{B} - \langle B \rangle) |\Psi\rangle \quad (3.13.12)$$

and using above, we may rewrite variance as

$$\sigma_A^2 = \langle a | a \rangle \quad (3.13.13)$$

$$\sigma_B^2 = \langle b | b \rangle. \quad (3.13.14)$$

Using Schwarz's inequality, we may write

$$\sigma_A^2 \sigma_B^2 = \langle a | a \rangle \langle b | b \rangle \geq |\langle a | b \rangle|^2. \quad (3.13.15)$$

If we separate the real and imaginary part as $\langle a|b\rangle = \alpha + i\beta$, one can derive

$$|\langle a|b\rangle|^2 = \alpha^2 + \beta^2 \geq \beta^2 = \left(\frac{\langle a|b\rangle - \langle b|a\rangle}{2i} \right)^2. \quad (3.13.16)$$

Here,

$$\begin{aligned} \langle a|b\rangle &= \langle \Psi | (\hat{A} - \langle A \rangle)(\hat{B} - \langle B \rangle) | \Psi \rangle \\ &= \langle \Psi | (\hat{A}\hat{B} - \langle A \rangle\hat{B} - \langle B \rangle\hat{A} + \langle A \rangle\langle B \rangle) | \Psi \rangle \\ &= \langle AB \rangle - \langle A \rangle \langle B \rangle, \end{aligned} \quad (3.13.17)$$

and similarly

$$\langle b|a\rangle = \langle BA \rangle - \langle A \rangle \langle B \rangle, \quad (3.13.18)$$

and we get

$$\langle a|b\rangle - \langle b|a\rangle = \langle AB \rangle - \langle BA \rangle = \langle [\hat{A}, \hat{B}] \rangle. \quad (3.13.19)$$

Finally, when Eqs. (3.13.15–3.13.19) are combined, we obtain

$$\sigma_A^2 \sigma_B^2 \geq \left(\frac{1}{2i} \langle [\hat{A}, \hat{B}] \rangle \right)^2. \quad (3.13.20)$$

It describes the generalized Heisenberg uncertainty principle with the commutator of the physical observable operators \hat{A} and \hat{B} . That is, given the commutator, the Heisenberg uncertainty principle of those physical quantities can be derived.

Using the well-known commutation relation $[\hat{x}, \hat{p}] = i\hbar$, the famous position and momentum uncertainty principle can be derived as

$$\sigma_x^2 \sigma_p^2 \geq \left(\frac{\hbar}{2} \right)^2 \quad (3.13.21)$$

$$\boxed{\sigma_x \sigma_p \geq \frac{\hbar}{2}}. \quad (3.13.22)$$

As another example, we consider the spin commutation relation. For a spin-1/2 system, spin operators \hat{S}_i are represented using Pauli operators $\hat{\sigma}_i$ as

$$\hat{S}_i = \frac{\hbar}{2} \hat{\sigma}_i. \quad (3.13.23)$$

Commutation relation for spin operators \hat{S}_i are given as

$$[S_i, S_j] = i\hbar\epsilon_{ijk} S_k. \quad (3.13.24)$$

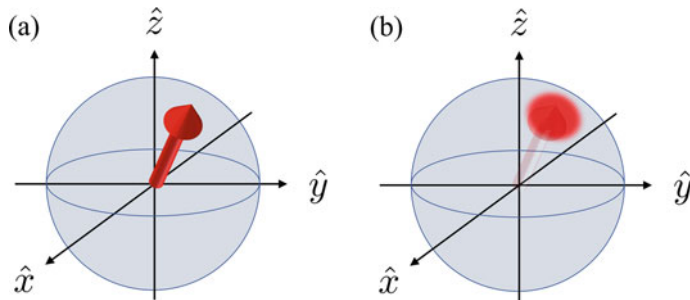


Fig. 3.18 State vector on a Bloch sphere

For $i = x$, $j = y$, and $k = z$, the spin commutator is given as

$$[\hat{S}_x, \hat{S}_y] = i\hbar\hat{S}_z \quad (3.13.25)$$

$$\sigma_{S_x}\sigma_{S_y} \geq \frac{\hbar}{2}\langle\hat{S}_z\rangle. \quad (3.13.26)$$

Let us consider for a moment what this commutation relations mean. If there is a spin pointing at $+z$ -direction, then $\langle\hat{S}_z\rangle = \hbar/2$, so the uncertainty relation becomes

$$\sigma_{S_x}\sigma_{S_y} \geq \frac{\hbar^2}{4}. \quad (3.13.27)$$

This means that spins pointing in the $+z$ -direction have uncertainty in x and y -directions. Since the spin equation permutes with respect to the subscript, the spin directed in the x -direction (y -direction) has an uncertainty in the y and z -directions (x - and z -directions). In other words, the uncertainty is spread in the direction orthogonal to the pointing direction of the spin state.

Using the Bloch sphere, the state of qubits can be described similarly as shown in Fig. 3.18a. The arrow pointing from the origin to the surface of the sphere represents the state of the qubit wavefunction. Keep in mind that the uncertainty of the state spreads in the direction perpendicular to the arrow (on the sphere) as shown in Fig. 3.18b. A detailed description is given in the chapter covering the physics of two-level systems.

Problems

Problem 3-1 Consider a wavefunction,

$$|\Psi\rangle = |\psi_1\rangle + \sqrt{2}|\psi_2\rangle - 2|\psi_3\rangle + i\sqrt{3}|\psi_4\rangle.$$

- (i) Normalize $|\Psi\rangle$.

(ii) Find the expectation value $\langle A \rangle$ for

$$\hat{A} = \begin{bmatrix} 1 & 0 & i & 0 \\ 0 & 1 & 0 & -i \\ i & 0 & 1 & 0 \\ 0 & i & 0 & 1 \end{bmatrix}. \quad (3.13.28)$$

(iii) Is operator \hat{A} a Hermitian? Show it from (a) the matrix property of Hermitian operator and (b) check with the expectation value $\langle A \rangle$ calculated.

Problem 3-2

- (i) Show $|+y\rangle$ and $|-y\rangle$ -state form a set of orthonormal basis for a two-level system.
- (ii) Use the completeness relation $\hat{I} = |+y\rangle\langle +y| + |-y\rangle\langle -y|$ to express $|0\rangle$ and $|1\rangle$ -state in terms of $|+y\rangle$ and $|-y\rangle$.

Problem 3-3 For an arbitrary state $|\Psi\rangle$, use the completeness relation, $\hat{I} = \sum_i |\psi_i\rangle\langle\psi_i|$ to show

$$\langle A \rangle = \text{Tr}(|\Psi\rangle\langle\Psi|\hat{A}). \quad (3.13.29)$$

(It is in the text, but don't look!)

Problem 3-4 Consider a three-level system with energy eigenvalues $E_i = \hbar\omega_i$ ($i = 1, 2, 3$) with corresponding eigenstates $|\psi_1\rangle = \begin{pmatrix} 1 \\ 0 \\ 0 \end{pmatrix}$, $|\psi_2\rangle = \begin{pmatrix} 0 \\ 1 \\ 0 \end{pmatrix}$, $|\psi_3\rangle = \begin{pmatrix} 0 \\ 0 \\ 1 \end{pmatrix}$.

- (i) Write the system Hamiltonian $\hat{\mathcal{H}}$ using *ket-bra* notation, e.g., $|\psi_1\rangle\langle\psi_1|$.
- (ii) Write the system Hamiltonian $\hat{\mathcal{H}}$ in a matrix representation.

Problem 3-5 Show that a general form of the eigenvalues of unitary operator \hat{U} is $\lambda = e^{i\theta}$. (Meaning that the absolute value of eigenvalue is always 1.)

Problem 3-6 Inverse of a 2×2 matrix $\hat{A} = \begin{pmatrix} a & b \\ c & d \end{pmatrix}$ is given by

$$\hat{A}^{-1} = \frac{1}{ad - bc} \begin{pmatrix} d & -b \\ -c & a \end{pmatrix}.$$

- (i) Show Pauli matrices $\hat{\sigma}_x = \begin{pmatrix} 0 & 1 \\ 1 & 0 \end{pmatrix}$, $\hat{\sigma}_y = \begin{pmatrix} 0 & -i \\ i & 0 \end{pmatrix}$, and $\hat{\sigma}_z = \begin{pmatrix} 1 & 0 \\ 0 & -1 \end{pmatrix}$ are unitary operators by showing $\hat{U}^\dagger = \hat{U}^{-1}$.
- (ii) Find the eigenvalues and eigenvectors for Pauli matrices.

Problem 3-7 Show Eq. 3.11.43,

$$e^{i\theta \hat{A}} = \cos \theta \hat{I} + i \sin \theta \hat{A}$$

when $\hat{A}^2 = \hat{I}$, using the definition of the exponential of a matrix,

$$e^{\hat{A}} \equiv \sum_{n=0}^{\infty} \frac{\hat{A}^n}{n!} = I + \hat{A} + \frac{\hat{A}^2}{2!} + \frac{\hat{A}^3}{3!} \dots . \quad (3.13.30)$$

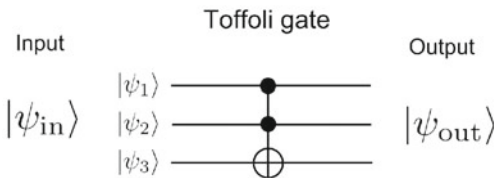
Problem 3-8 For a two-qubit system, where the wavefunction of each qubit is

$$\begin{aligned} |\psi_1\rangle &= \frac{1}{\sqrt{5}} (\sqrt{2}|0\rangle + \sqrt{3}|1\rangle) \\ |\psi_2\rangle &= \frac{1}{2} (\sqrt{3}|0\rangle - i|1\rangle), \end{aligned}$$

find $|\Psi\rangle = |\psi_1\rangle|\psi_2\rangle = |\psi_1\psi_2\rangle$ in

- (i) Braket notation;
- (ii) Matrix notation;
- (iii) Find density operator $\hat{\rho}$ for this two-qubit state in matrix notation.
- (iv) From above matrix, check $\text{Tr}[\hat{\rho}] = 1$.

Problem 3-9 In classical computation, (three-bit) Toffoli gate shown below in Fig. 3.19 is conceptually important, due to its (a) reversibility, and (b) functional completeness, meaning that a combination of Toffoli gates can be used to construct an arbitrary logic gate.

Fig. 3.19 Toffoli gate

Toffoli gate \hat{T} can be represented in a matrix form as

$$\hat{T} = \begin{bmatrix} 1 & 0 & 0 & 0 & 0 & 0 & 0 & 0 \\ 0 & 1 & 0 & 0 & 0 & 0 & 0 & 0 \\ 0 & 0 & 1 & 0 & 0 & 0 & 0 & 0 \\ 0 & 0 & 0 & 1 & 0 & 0 & 0 & 0 \\ 0 & 0 & 0 & 0 & 1 & 0 & 0 & 0 \\ 0 & 0 & 0 & 0 & 0 & 1 & 0 & 0 \\ 0 & 0 & 0 & 0 & 0 & 0 & 0 & 1 \\ 0 & 0 & 0 & 0 & 0 & 0 & 1 & 0 \end{bmatrix}. \quad (3.13.31)$$

- (i) Show Toffoli gate is unitary (thus reversible) and find the inverse of Toffoli gate \hat{T}^{-1} .
- (ii) Write the input state $|\psi_{in}\rangle = |\psi_1\rangle|\psi_2\rangle|\psi_3\rangle = (a_0|0\rangle + a_1|1\rangle) \otimes |1\rangle \otimes |0\rangle$ in matrix representation and calculate the output state $|\psi_{out}\rangle$. Also, write out a braket representation of the output state.
- (iii) When you measure the output state calculated in (ii), $|\psi_1\rangle$ and $|\psi_3\rangle$ should be identical (otherwise your answer in (ii) should be rechecked!). In quantum mechanics, there is “No-cloning theorem”, which prohibit the copying of a quantum state. Discuss if this gate violates the no-cloning theorem.”

Problem 3-10 In a quantum harmonic oscillator, the position and momentum operator can be expressed in terms of ladder operators (\hat{a} and \hat{a}^\dagger) as

$$\begin{aligned} \hat{x} &= x_{zp} (\hat{a}^\dagger + \hat{a}) \\ \hat{p} &= i p_{zp} (\hat{a}^\dagger - \hat{a}), \end{aligned}$$

where $x_{zp} = \sqrt{\frac{\hbar}{2m\omega}}$ and $p_{zp} = \sqrt{\frac{\hbar m \omega}{2}}$. \hat{a} and \hat{a}^\dagger are ladder operators satisfying the commutation relation $[\hat{a}, \hat{a}^\dagger] = 1$. Using these ladder-operator representation of position and momentum operators to derive the commutation relation for the position and momentum,

$$[\hat{x}, \hat{p}] = i\hbar.$$



Time Evolution in Quantum System

4

In quantum technology, the control of a quantum system is usually referred to as the control of *time-dependent dynamics of the system*. For example, in quantum computation, we apply sequences of quantum gates to qubits to perform calculations. It is important to be able to derive the time evolution of the system for a given system Hamiltonian and the external perturbations. In this chapter, we review the fundamentals of quantum mechanics focusing on the time evolution of the quantum system.

4.1 Time-Independent Schrödinger Equation

As shown in Fig. 4.1, in classical mechanics, we often consider a situation where a point-like object is moving in a potential $V(x)$. It is easy to see that when this potential changes over time, $V(x) \rightarrow V(x, t)$, the problem suddenly becomes difficult.

It is the same in quantum mechanics. Schrödinger equation is given as

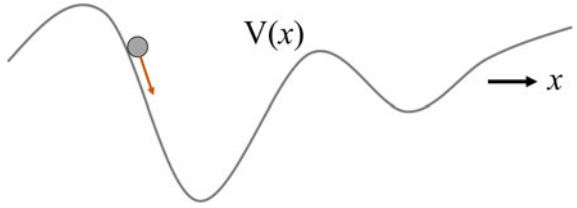
$$i\hbar \frac{\partial \Psi(x, t)}{\partial t} = -\frac{\hbar^2}{2m} \frac{\partial^2 \Psi(x, t)}{\partial x^2} + \hat{V}(x, t)\Psi(x, t), \quad (4.1.1)$$

but when the potential is time independent, $\hat{V}(x, t) \rightarrow \hat{V}(x)$, the solution for $\Psi(x, t)$ can be found relatively easy.

When the potential $\hat{V}(x)$ is time independent, the wavefunction can be divided into time and space functions using the method of separation of variables

Supplementary Information The online version contains supplementary material available at https://doi.org/10.1007/978-981-19-4641-7_4.

Fig. 4.1 Time-independent potential $V(x)$



$\Psi(x, t) = \psi(x)\varphi(t)$. The Schrödinger equation is then divided into two parts, spatial and time equation as

$$-\frac{\hbar^2}{2m} \frac{d^2\psi(x)}{dx^2} + \hat{V}(x)\psi(x) = E\psi \quad (4.1.2)$$

$$\frac{d\varphi(t)}{dt} = -\frac{iE}{\hbar}\varphi(t). \quad (4.1.3)$$

The solution for the time equation is easily found as

$$\varphi(t) = e^{-iEt/\hbar}, \quad (4.1.4)$$

and the wavefunction $\Psi(x, t)$ is expressed as

$$\Psi(x, t) = \psi(x)e^{-iEt/\hbar}, \quad (4.1.5)$$

where E is the energy eigenvalue and $\psi(x)$ is the eigenfunction associated with the energy. Equation (4.1.2) is called *Time-independent Schrödinger equation* and solving for a solution $\psi(x)$ becomes the goal to identify the wavefunction $\Psi(x, t)$ of the system.

The wavefunction in Eq. (4.1.5) is called *Stationary state*. It can easily be checked that when the probability distribution of this eigenstate is calculated

$$|\Psi^2(x, t)| = \psi^*(x)e^{iEt/\hbar}\psi(x)e^{-iEt/\hbar} \quad (4.1.6)$$

$$= |\psi(x)|^2, \quad (4.1.7)$$

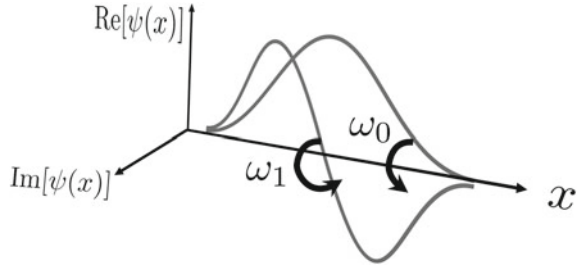
this wavefunction does not change in time, as it is called stationary. Also, the expectation value $\langle Q \rangle$ of the physical observable Q for this eigenstate is calculated as

$$\langle Q \rangle = \int_{-\infty}^{\infty} dx \psi^*(x)e^{iEt/\hbar} \hat{Q}\psi(x)e^{-iEt/\hbar} \quad (4.1.8)$$

$$= \int_{-\infty}^{\infty} dx \psi^*(x) \hat{Q}\psi(x), \quad (4.1.9)$$

and the time dependence cancels out, thus again, it is stationary in time.

Fig. 4.2 Rotation of the wavefunction from the time evolution in a phase space



There may be several energy eigenvalues E_n and associated eigenfunctions $\psi_n(x)$ depending on the shape of the potential and the boundary conditions. The general solution for the quantum state can be written as

$$\Psi(x, t) = \sum_n c_n \psi_n(x) e^{-i E_n t / \hbar}, \quad (4.1.10)$$

and one can see that the variation of the wavefunction in time is originated from the phase evolution of the wavefunction with the angular frequency $\omega_n = \frac{E_n}{\hbar}$ associated with each eigenfunction.

Figure 4.2 shows the idea of this phase evolution in a cartoon. Considering a phase space with the vertical axis as the real part of the wave function $\psi(x)$ and the horizontal axis as the imaginary part, the wave function rotates at an angular frequency ω_n along the x -axis. This is the time evolution of each eigenstate $\psi_n(x)$. Since it is rotating in the phase-space, $|\Psi(x, t)|^2 = |\psi_0(x, t)|^2$ or $|\psi_1(x, t)|^2$ is constant and stationary as derived previously. Here, the ground state and the first excited state of the harmonic oscillator, which may be familiar to many readers, are considered as examples.

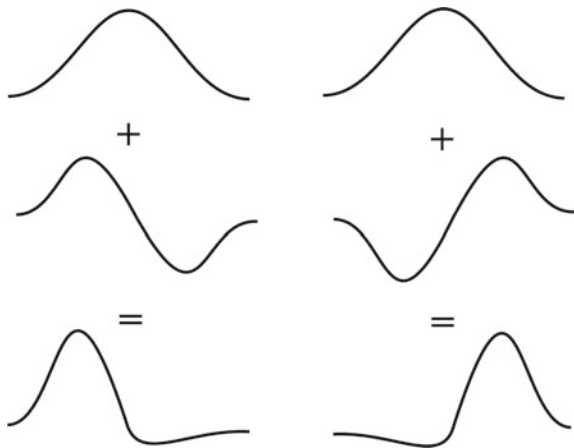
We mentioned that the probability distribution $|\Psi(x, t)|^2$ is time independent, when one of the eigenstate is the solution. However, the situation is quite different in a superposition state. Let us consider the superposition of two harmonic oscillator states used in Fig. 4.2

$$\Psi(x, t) = \frac{1}{\sqrt{2}} \psi_0(x) e^{-i \omega_0 t} + \frac{1}{\sqrt{2}} \psi_1(x) e^{-i \omega_1 t}, \quad (4.1.11)$$

where $\psi_0(x)$ and $\psi_1(x)$ are normalized spatial wavefunction for two harmonic oscillator states. In the example shown in Fig. 4.2, the rotation frequency ω_0 and ω_1 are different. At a certain moment as shown in Fig. 4.3, the wave function $\Psi(x, t)$ is shifted to the left, while at other time it is shifted to the right. In other words, in this superposition, the expectation value of the particle position is not $\langle x \rangle = 0$, but its center of mass oscillating at $\omega_1 - \omega_0$, thus not stationary. This vibration is manifested by the interference of multiple wavefunctions, while each wavefunction alone is stationary in time.

Qubits are no exception in this regard. In many experiments, the energy eigenstates discussed above are used in qubits. The ground state $|g\rangle \equiv |0\rangle$ and the excited state

Fig. 4.3 Oscillation of the probability distribution from the superposition of the wavefunctions



$|e\rangle \equiv |1\rangle$ forms the qubit state with the corresponding energies $E_0 = 0$ and $E_1 = \hbar\omega$, respectively. The time evolution of this qubit is written as

$$|\Psi(t)\rangle = c_0 |0\rangle + c_1 e^{-i\omega t} |1\rangle. \quad (4.1.12)$$

It should be remembered that the phase of the excited state rotates with the frequency $\omega = E_1/\hbar$ between the ground and the excited state. A careful reader might remember that the change in the phase difference between $|0\rangle$ and $|1\rangle$ represents the motion of the state vector in the azimuthal direction in the Bloch sphere. In the qubit, where energy states are used as the qubit states, there is a perpetual rotation of the state vector at frequency $\omega = E_1/\hbar$. In order to get rid of this “background rotation”, the qubit state is often written in the rotating frame of the qubit energy as discussed later.

4.2 Time Evolution in Terms of Unitary Operator

The time evolution of the quantum state $|\Psi\rangle$ is described by the Schrödinger equation as

$$\hat{\mathcal{H}} |\Psi\rangle = i\hbar \frac{\partial}{\partial t} |\Psi\rangle. \quad (4.2.1)$$

Here, we introduce a method, where the wave function at an arbitrary time t is obtained by describing the time evolution as a unitary operator, acting on the initial wavefunction at $t = 0$.

Describing the time evolution is closely related to the idea of quantum computation. In classical information processing, the computation is proceeded by sequentially executing discrete digital logic gates (AND, XOR, etc.). For example, the NOT gate in digital logic is $0 \rightarrow 1$, $1 \rightarrow 0$. While in quantum computation, quantum states such as spin states are used to describe the qubit. When the downward spin $|\downarrow\rangle \equiv |0\rangle$

is flipped to upward spin $|\uparrow\rangle \equiv |1\rangle$, the time evolution inverting the spin can be considered as a quantum equivalent gate of the classical NOT gate. In other words, the time evolution operator itself can be thought of as a quantum gate.

Suppose, the initial wavefunction $|\psi_0\rangle$ at time $t = 0$ is time-evolved to $|\psi(t)\rangle$ by the time evolution operator $\hat{U}(t)$ as

$$|\psi(t)\rangle = \hat{U}(t) |\psi_0\rangle. \quad (4.2.2)$$

Substituting into the Schrödinger equation, we obtain

$$\hat{\mathcal{H}}\hat{U}(t) |\psi_0\rangle = i\hbar \frac{\partial(\hat{U}(t) |\psi_0\rangle)}{\partial t} = i\hbar \frac{\partial \hat{U}(t)}{\partial t} |\psi_0\rangle \quad (4.2.3)$$

$$\rightarrow \hat{\mathcal{H}}\hat{U}(t) = i\hbar \frac{\partial \hat{U}(t)}{\partial t}, \quad (4.2.4)$$

and integrating the equation, the time evolution operator $\hat{U}(t)$ is derived as

$$\begin{aligned} \hat{U}(t) &= \hat{U}_0 e^{-i\hat{\mathcal{H}}t/\hbar} \\ &= e^{-i\hat{\mathcal{H}}t/\hbar}. \end{aligned} \quad (4.2.5)$$

Here, we consider that the Hamiltonian $\hat{\mathcal{H}}$ is time-independent. Also, in the last line, $\hat{U}_0 = \hat{I}$ is used since the time evolution starts at $t = 0$ (when nothing has happened yet). In principle, one could start from a time-dependent Hamiltonian $\hat{\mathcal{H}} = \hat{\mathcal{H}}(t)$, and solve them slightly differently. Here, we chose a time-independent Hamiltonian for simplicity.

The time evolution of the wave function $|\psi(t)\rangle$ for arbitrary time t_1 to t_2 using this time evolution operator $\hat{U}(t)$ is written as

$$|\psi(t_2)\rangle = \hat{U}(t_2 - t_1) |\psi(t_1)\rangle = e^{-i\hat{\mathcal{H}}(t_2-t_1)/\hbar} |\psi(t_1)\rangle. \quad (4.2.6)$$

Previously, we mentioned that the rotation of the state vector in the Bloch sphere can be performed by using a rotation matrix such as $\hat{R}_x(\theta) = e^{-i\frac{\theta}{2}\hat{X}}$, where in this operator, the quantum state is rotated by θ with respect to the x -axis of the Bloch sphere. Now, the question is how could we get the time evolution operator $\hat{U}(t)$ act as an $\hat{R}_i(\theta)$, or in other words, what is necessary for $\hat{U}(t)$ to have a form of $\hat{R}_i(\theta)$?

If the system Hamiltonian $\hat{\mathcal{H}}$ contains operators, such as $\hat{X}, \hat{Y}, \hat{Z}$, it creates a rotation matrix. For example, if the system Hamiltonian is

$$\hat{\mathcal{H}} = \hbar\alpha\hat{X}, \quad (4.2.7)$$

the time evolution operator reads

$$\begin{aligned} \hat{U}(t) &= e^{-i\hat{\mathcal{H}}t/\hbar} = e^{-i\alpha\hat{X}t} \\ &= \hat{R}_x(2\alpha t), \end{aligned} \quad (4.2.8)$$

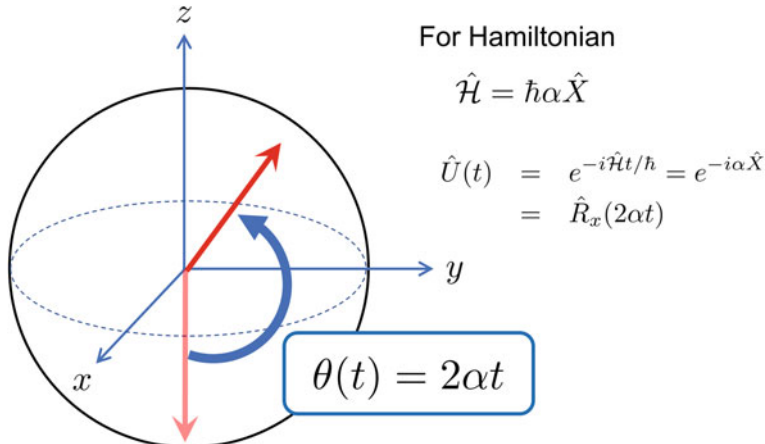


Fig. 4.4 Rotation operator as an time-evolution operator

which rotates the qubit around \$x\$-axis by an arbitrary angle \$\theta = 2\alpha t\$ as shown in Fig. 4.4. Note here that, as long as the Hamiltonian has a form \$\hat{\mathcal{H}} = \hbar\alpha\hat{X}\$, the state vector will keep rotating. What we need to do is to turn on the Hamiltonian just momentary, like a pulse, so when the state vector reaches the target position, the rotation will stop. For an arbitrary qubit rotation on the Bloch sphere, it is necessary to be able to rotate the state vector by at least 2-axis. We later describe these controls on the Bloch sphere.

4.3 Three Pictures in Quantum Mechanics

In the previous section, the time evolution of quantum state is described by the unitary operator \$\hat{U}(t) = e^{-i\hat{\mathcal{H}}t/\hbar}\$. However, what we can usually measure experimentally is not the wavefunction itself, but some physical observable \$A\$. As the wave function changes in time, the expectation value \$\langle A \rangle\$ also varies as

$$\begin{aligned}\langle A(t) \rangle &= \langle \psi(t) | \hat{A} | \psi(t) \rangle \\ &= \langle \psi_0 | e^{i\hat{\mathcal{H}}t/\hbar} \hat{A} e^{-i\hat{\mathcal{H}}t/\hbar} | \psi_0 \rangle.\end{aligned}\quad (4.3.1)$$

Here, we consider the time variation of the physical observable \$A\$, relating it to the variation of the states and operators. In quantum mechanics, there are so-called “three pictures”, in which each picture has a different treatment of the time evolution of state and operators to describe the system dynamics. There are pros and cons for each picture, and we often select a picture that is suitable or easy to calculate depending on the problem. Three pictures are Schrödinger, Heisenberg, and Dirac picture. Here we describe the overview and distinctions between these pictures.

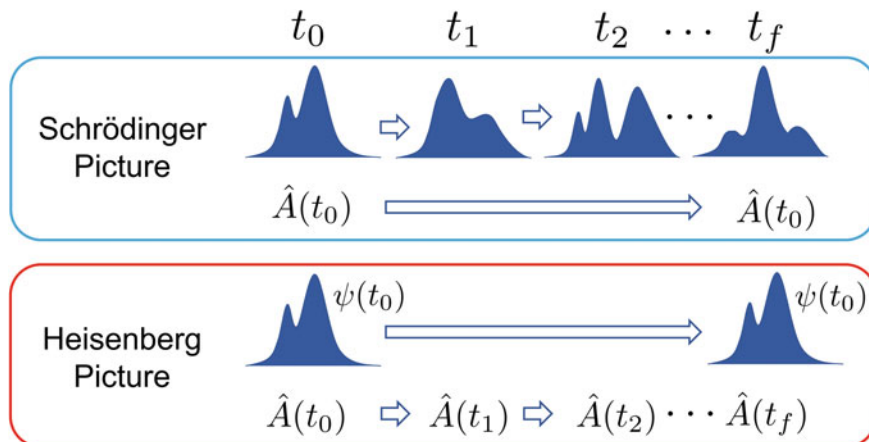


Fig. 4.5 Difference between the Schrödinger and Heisenberg picture

4.3.1 General Overview

There are no definitive rules to pick which picture to be used for a particular situation, but generally, these rules might be a good starting point.

Schrödinger picture

If the time evolution of the wavefunction $\psi(t)$ is of interest, e.g., calculating the electronic wavefunction in a quantum well and observing its spatial dynamics.

Heisenberg picture

If the time evolution of the observable $A(t)$ is of interest, e.g., calculating the dynamics of electric field strength $E(t)$ in and out of an optical cavity for a laser spectroscopy.

Dirac picture

If you start out with one system and turn on an extra perturbation. For example, a Hydrogen atom itself is a quantum system consisting of an electron under the potential created by the nucleus. External magnetic field (perturbation) is then introduced to the system to investigate the dynamics under the influence.

First, the difference between the Schrödinger and Heisenberg picture is the difference in the focus between the quantum state and its observable. In most of the introductory quantum mechanics courses, we start out with the Schrödinger picture. In this picture, the system dynamics are explained in terms of the state evolution as shown in Fig. 4.5, in other words, we focus on how the wavefunction evolves in time $\psi(t)$, while the operator \hat{A} is treated as time independent.

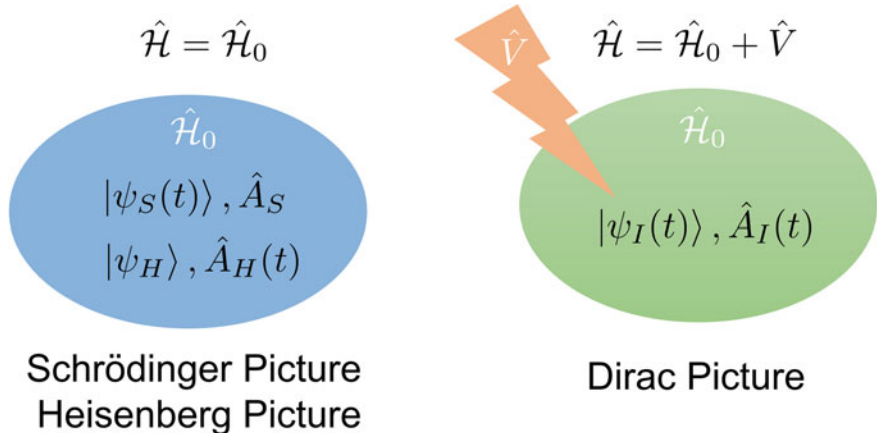


Fig. 4.6 Dirac picture is useful for addition of perturbation \hat{V}

Contrary, the Heisenberg picture focus on the time evolution of the physical observable $A(t)$. As discussed earlier, the observable A is represented as an operator \hat{A} , and the time evolution of this operator $\hat{A}(t)$ is the main focus, while the state ψ is considered time independent. We later show that the time evolution of operator $\hat{A}(t)$ can be prescribed in a simple manner using *Heisenberg equation of motion*.

As discussed earlier, in classical mechanics, observable such as position $x(t)$ is calculated from Newton's equation of motion. In this sense, the Heisenberg picture resembles more of the classical picture, while Schrödinger picture focuses on the wavefunction, which has no classical counterpart.

Dirac picture has slightly different benefits compared to Schrödinger and Heisenberg picture, however, the approach can be considered as an intermediate picture of two pictures as shown later in detail. As mentioned above, the Dirac picture becomes particularly useful when the external perturbation \hat{V} is applied to an existing quantum system with Hamiltonian \hat{H}_0 as shown in Fig. 4.6. The intermediacy of the picture can be seen from the fact that both state $\psi_I(t)$ and operator $\hat{A}_I(t)$ are time dependent in this picture.

While describing the differences, it is easy to mix up different pictures unless the notation is clearly defined. We use following notation for state and operators:

$$\begin{aligned} |\psi_0\rangle &\text{ Time-independent initial state} \\ \hat{A}_0 &\text{ Time-independent initial operator} \end{aligned}$$

- $\hat{A}_S, |\psi_S\rangle$ Operator and state in Schrödinger picture
- $\hat{A}_H, |\psi_H\rangle$ Operator and state in Heisenberg picture
- $\hat{A}_I, |\psi_I\rangle$ Operator and state in Dirac picture

To have a consistent result for all pictures, the expected value of the physical observable $\langle A(t) \rangle$ must be the same. We come back to this value $\langle A(t) \rangle$ time to time

while introducing how different pictures separate the time evolution of wavefunctions and operators.

4.3.2 Schrödinger Picture

Up to this point in the book, the dynamics of the quantum system are described with the initial wave function ψ_0 changes with time as $\psi(t)$, and the physical observable operator \hat{A} remains constant in time as $\hat{A} = \hat{A}_0$. Presumably, this is the way many readers first learn quantum mechanics and this picture is called Schrödinger Picture.

In this picture, the wavefunction evolves in time as

$$\boxed{\frac{d |\psi(t)\rangle}{dt} = -\frac{i}{\hbar} \hat{\mathcal{H}} |\psi(t)\rangle.} \quad (4.3.2)$$

The quantum state and operators are described as

$$|\psi_S(t)\rangle \equiv e^{-i\hat{\mathcal{H}}t/\hbar} |\psi_0\rangle \quad (4.3.3)$$

$$\hat{A}_S \equiv \hat{A}_0, \quad (4.3.4)$$

and only the wavefunction evolves in time. The expectation value $\langle A \rangle$ evolves in time as

$$\langle A(t) \rangle = \langle \psi_0 | e^{i\hat{\mathcal{H}}t/\hbar} \hat{A}_0 e^{-i\hat{\mathcal{H}}t/\hbar} | \psi_0 \rangle \quad (4.3.5)$$

$$= \langle \psi_S(t) | \hat{A}_S | \psi_S(t) \rangle, \quad (4.3.6)$$

along with the time evolution of the wavefunction.

4.3.3 Heisenberg Picture

In the Heisenberg picture, we take a position where the state ψ_0 remains constant while the operators are evolving in time.

In this picture, the time varying operator $\hat{A}(t)$ is described as

$$\hat{A}(t) = e^{i\hat{\mathcal{H}}t/\hbar} \hat{A}_0 e^{-i\hat{\mathcal{H}}t/\hbar}. \quad (4.3.7)$$

Summarizing the time evolution of state and operator in Heisenberg picture, we have

$$|\psi_H\rangle \equiv |\psi_0\rangle \quad (4.3.8)$$

$$\hat{A}_H(t) \equiv e^{i\hat{\mathcal{H}}t/\hbar} \hat{A}_0 e^{-i\hat{\mathcal{H}}t/\hbar}. \quad (4.3.9)$$

Since the state is stationary in the Heisenberg picture, there is no Schrödinger equation, which describes the time evolution of the state $i\hbar \frac{d|\psi_H\rangle}{dt} = \dots$. Instead, we will derive the equation of motion for the operator, called the Heisenberg equation of motion, later.

The expectation value $\langle A \rangle$ evolves in time as

$$\langle A(t) \rangle = \langle \psi_0 | e^{i\hat{\mathcal{H}}t/\hbar} \hat{A}_0 e^{-i\hat{\mathcal{H}}t/\hbar} | \psi_0 \rangle \quad (4.3.10)$$

$$= \langle \psi_H | \hat{A}_H(t) | \psi_H \rangle, \quad (4.3.11)$$

along with the variation of the operator.

A careful reader may point out that “if the operator changes over time, the Hamiltonian itself also changes over time, so the expression containing the Hamiltonian (4.3.9) should be more complicated.” One might think, the time evolution of the Hamiltonian is as follows:

$$\hat{\mathcal{H}}_H = e^{i\hat{\mathcal{H}}t/\hbar} \hat{\mathcal{H}} e^{-i\hat{\mathcal{H}}t/\hbar}, \quad (4.3.12)$$

with explicit time dependence. However, using Eq. (3.11.3)

$$e^{\hat{A}} \equiv \sum_{n=0}^{\infty} \frac{\hat{A}^n}{n!} = I + \hat{A} + \frac{\hat{A}^2}{2!} + \frac{\hat{A}^3}{3!} \dots,$$

$e^{i\hat{\mathcal{H}}t/\hbar}$ can be expressed as a polynomial function of $\hat{\mathcal{H}}$, which commute with $\hat{\mathcal{H}}$, resulting in

$$\hat{\mathcal{H}}_H = e^{i\hat{\mathcal{H}}t/\hbar} \hat{\mathcal{H}} e^{-i\hat{\mathcal{H}}t/\hbar} = \hat{\mathcal{H}}. \quad (4.3.13)$$

The Hamiltonian above is actually time-independent and we do not need to worry about the further complication.

Also, it is important to know how the commutation relation changes in the Heisenberg picture. For example, if the commutation relation in Schrödinger picture is given as $[\hat{A}, \hat{B}] = \hat{C}$, how would it change in the Heisenberg picture? Would the operators commuting in Schrödinger picture also commute in Heisenberg picture?

Consider a commutation relation in Schrödinger picture, $[\hat{A}_S, \hat{B}_S] = \hat{C}_S$, and define $\hat{U} = e^{-i\hat{\mathcal{H}}t/\hbar}$ and $\hat{U}^\dagger = e^{i\hat{\mathcal{H}}t/\hbar}$ to simplify the notation. The commutation relation in Heisenberg picture is given as

$$\begin{aligned} [\hat{A}_H, \hat{B}_H] &= \hat{A}_H \hat{B}_H - \hat{B}_H \hat{A}_H \\ &= \hat{U}^\dagger \hat{A}_S \hat{U} \hat{U}^\dagger \hat{B}_S \hat{U} - \hat{U}^\dagger \hat{B}_S \hat{U} \hat{U}^\dagger \hat{A}_S \hat{U} \\ &= \hat{U}^\dagger \hat{A}_S \hat{B}_S \hat{U} - \hat{U}^\dagger \hat{B}_S \hat{A}_S \hat{U} \\ &= \hat{U}^\dagger (\hat{A}_S \hat{B}_S - \hat{B}_S \hat{A}_S) \hat{U} \\ &= \hat{U}^\dagger \hat{C}_S \hat{U} = \hat{C}_H \end{aligned}$$

$$\boxed{[\hat{A}_H, \hat{B}_H] = \hat{C}_H}, \quad (4.3.14)$$

where $\hat{O}_H = \hat{U}^\dagger \hat{O}_S \hat{U} = e^{i\hat{\mathcal{H}}_H t/\hbar} \hat{O}_S e^{-i\hat{\mathcal{H}}_H t/\hbar}$.

As shown above, the form of the commutation relation stays the same as the Schrödinger picture, with a simple replacement of the operators to the ones in the Heisenberg picture.

4.3.4 Example: Harmonic Oscillator in Schrödinger and Heisenberg Picture

Let us try to derive and see the difference between the Schrödinger and Heisenberg picture using a familiar and one of the most important systems in quantum technology, the harmonic oscillator. It is cumbersome to write $\hat{A}_{S,H}$ for each operator and here we use the convention often used in much of the literature; the operators in Schrödinger picture is denoted as \hat{A} , while the operators in the Heisenberg picture is written $\hat{A}(t)$, with the explicit time dependence.

Schrödinger picture: In the Schrödinger picture, the system Hamiltonian, position \hat{x} , and momentum \hat{p} operators are given in terms of creation and annihilation operator, also known as ladder operators, \hat{a}^\dagger and \hat{a} as,

$$\begin{aligned}\hat{\mathcal{H}} &= \hbar\omega\hat{a}^\dagger\hat{a} \\ \hat{x} &= x_{zp}(\hat{a}^\dagger + \hat{a}) \\ \hat{p} &= i p_{zp}(\hat{a}^\dagger - \hat{a}),\end{aligned}$$

where $x_{zp} = \sqrt{\frac{\hbar}{2m\omega}}$ and $p_{zp} = \sqrt{\frac{\hbar m \omega}{2}}$. Also, the zero-point energy $E_0 = \frac{\hbar\omega}{2}$, which is just an offset energy, is ignored from the Hamiltonian for simplicity. Let us calculate the canonical commutation relation for \hat{x} and \hat{p}

$$\begin{aligned}[\hat{x}, \hat{p}] &= \hat{x}\hat{p} - \hat{p}\hat{x} \\ &= ix_{zp}p_{zp}[(\hat{a}^\dagger + \hat{a})(\hat{a}^\dagger - \hat{a}) - (\hat{a}^\dagger - \hat{a})(\hat{a}^\dagger + \hat{a})] \\ &= i\frac{\hbar}{2} \cdot 2(\hat{a}\hat{a}^\dagger - \hat{a}^\dagger\hat{a}) = i\hbar,\end{aligned} \quad (4.3.15)$$

where we used the commutation relation for the ladder operator $[\hat{a}, \hat{a}^\dagger] = 1$.

A general state in this picture is written in terms of number state $|n\rangle$ as

$$\begin{aligned}
|\psi(t)\rangle &= \sum_{n=0}^{\infty} c_n(t) |n\rangle \\
&= \sum_{n=0}^{\infty} c_n(0) e^{-i\omega_n t} |n\rangle,
\end{aligned} \tag{4.3.16}$$

where $\omega_n = E_n/\hbar = n\omega$ and the solution for the time-independent potential discussed earlier is used in the last line.

The expectation value of position $\langle x \rangle$ is calculated as

$$\begin{aligned}
\langle x(t) \rangle &\equiv \langle \psi(t) | \hat{x} | \psi(t) \rangle \\
&= \sum_{n,m=0}^{\infty} c_m^*(0) c_n(0) e^{-i(\omega_n - \omega_m)} \langle m | x_{\text{zp}} (\hat{a}^\dagger + \hat{a}) | n \rangle \\
&= x_{\text{zp}} \sum_{n,m=0}^{\infty} c_m^*(0) c_n(0) e^{-i(\omega_n - \omega_m)} \langle m | (\sqrt{n+1} |n+1\rangle + \sqrt{n} |n-1\rangle) \\
&= x_{\text{zp}} \sum_{n,m=0}^{\infty} c_m^*(0) c_n(0) e^{-i(\omega_n - \omega_m)} (\sqrt{n+1} \delta_{m,n+1} + \sqrt{n} \delta_{m,n-1}) \\
&= x_{\text{zp}} \sum_{n=0}^{\infty} (\sqrt{n+1} c_{n+1}^*(0) c_n(0) e^{i\omega t} + \sqrt{n} c_{n-1}^*(0) c_n(0) e^{-i\omega t}). \tag{4.3.17}
\end{aligned}$$

Previously, we discussed the qualitative understanding of the motion of the harmonic oscillator state, given in a superposition state using Fig. 4.3. The calculation above shows the analytical result, confirming the origin of motion as the interference between different states. Furthermore, the motion is provided *only* by the interference of neighboring states, n and $n+1$ (or $n-1$).

Heisenberg picture: For the Heisenberg picture, let us start with the annihilation and creation operator (\hat{a} , \hat{a}^\dagger). The system Hamiltonian in Schrödinger picture is $\hat{\mathcal{H}} = \hbar\omega \hat{a}^\dagger \hat{a}$ and which makes

$$\begin{aligned}
\hat{a}(t) &= e^{i\hat{\mathcal{H}}_t/\hbar} \hat{a} e^{-i\hat{\mathcal{H}}_t/\hbar} \\
&= e^{i\omega \hat{a}^\dagger \hat{a} t} \hat{a} e^{-i\omega \hat{a}^\dagger \hat{a} t} \\
&= \hat{a} e^{-i\omega t} = \hat{a}(0) e^{-i\omega t} \tag{4.3.18}
\end{aligned}$$

$$\hat{a}^\dagger(t) = \hat{a}^\dagger(0) e^{i\omega t}, \tag{4.3.19}$$

where Baker–Campbell–Hausdorff formula is used in the first derivation. Also, we use the fact that the operator in Schrödinger picture is the initial state of the operator in Heisenberg picture as $\hat{a} \rightarrow \hat{a}(0)$, $\hat{a}^\dagger \rightarrow \hat{a}^\dagger(0)$.

From the above results, the Hamiltonian has the same form as the Schrödinger picture as described previously,

$$\hat{\mathcal{H}}_H = \hbar\omega\hat{a}^\dagger(t)\hat{a}(t) = \hbar\omega\hat{a}^\dagger e^{i\omega t}\hat{a}e^{-i\omega t} = \hbar\omega\hat{a}^\dagger\hat{a} = \hat{\mathcal{H}}_S.$$

Using the results above, the position and momentum operators are derived as

$$\begin{aligned}\hat{x}(t) &= e^{i\omega\hat{a}^\dagger\hat{a}t}x_{zp}(\hat{a}^\dagger + \hat{a})e^{-i\omega\hat{a}^\dagger\hat{a}t} \\ &= x_{zp}[\hat{a}(0)^\dagger e^{i\omega t} + \hat{a}(0)e^{-i\omega t}]\end{aligned}\quad (4.3.20)$$

$$\hat{p}(t) = ip_{zp}[\hat{a}(0)^\dagger e^{i\omega t} - \hat{a}(0)e^{-i\omega t}]. \quad (4.3.21)$$

From above, we recognize $\hat{x}(0) = x_{zp}[\hat{a}(0)^\dagger + \hat{a}(0)]$ and $\hat{p}(0) = ip_{zp}[\hat{a}(0)^\dagger - \hat{a}(0)]$. Solving these for \hat{a} and \hat{a}^\dagger plug them back into Eqs. (4.3.20) and (4.3.21), the time evolution of position and momentum now reads

$$\hat{x}(t) = \hat{x}(0)\cos\omega t + \frac{\hat{p}(0)}{m\omega}\sin\omega t \quad (4.3.22)$$

$$\hat{p}(t) = \hat{p}(0)\cos\omega t + m\omega\hat{x}(0)\sin\omega t. \quad (4.3.23)$$

As discussed earlier, these operators certainly resemble the classical observable $x(t)$ and $p(t)$ of the harmonic oscillator.

We can also check the commutation relation for the ladder operators, and position and momentum operators in the Heisenberg picture as

$$\begin{aligned}[\hat{a}(t), \hat{a}^\dagger(t)] &= 1 \\ [\hat{x}(t), \hat{p}(t)] &= i\hbar.\end{aligned}$$

Both of them are consistent with our previous observation $[\hat{A}_S, \hat{B}_S] = \hat{C}_S \rightarrow [\hat{A}_H, \hat{B}_H] = \hat{C}_H$, where both 1 and $i\hbar$ are the same in the Heisenberg picture.

The state in the Heisenberg picture, which is intrinsically time-independent, is given simply as

$$|\psi\rangle_H = \sum_{n=0}^{\infty} c_n(0) |n\rangle, \quad (4.3.24)$$

from which the expectation value of position $\langle x \rangle$ is calculated as before

$$\begin{aligned}\langle x(t) \rangle &\equiv \langle \psi_H | \hat{x}(t) | \psi_H \rangle \\ &= \sum_{n,m=0}^{\infty} c_m^*(0)c_n(0) \langle m | x_{zp} (\hat{a}^\dagger e^{i\omega t} + \hat{a} e^{-i\omega t}) | n \rangle \\ &= x_{zp} \sum_{n=0}^{\infty} \left(\sqrt{n+1}c_{n+1}^*(0)c_n(0)e^{i\omega t} + \sqrt{n}c_{n-1}^*(0)c_n(0)e^{-i\omega t} \right),\end{aligned}\quad (4.3.25)$$

which is, of course, identical to the expectation value calculated in the Schrödinger picture.

4.3.5 Dirac Picture

Dirac picture has a characteristic that is half-way between the Schrödinger picture and the Heisenberg picture. In this picture, we consider a time-independent Hamiltonian $\hat{\mathcal{H}}_0$ and additional Hamiltonian \hat{V} in a form

$$\hat{\mathcal{H}} = \hat{\mathcal{H}}_0 + \hat{V}. \quad (4.3.26)$$

Since the Dirac picture focuses on this extra interaction \hat{V} , it is also called the interaction picture. We describe the state and operator in the Dirac picture with subscript I, referring to the “interaction”.

This picture becomes particularly important for controlling the quantum system. For example, let us consider controlling the electronic state of a Hydrogen atom with an external electric field. The electron is influenced by the Hydrogen nucleus regardless of the applied external field. In this example, $\hat{\mathcal{H}}_0$ becomes the Hamiltonian for the Hydrogen nucleus and the effect of the external field is given by \hat{V} . In other words, it is convenient because you can write the Hamiltonian that is always of influence in $\hat{\mathcal{H}}_0$, and our operation is solely described in \hat{V} .

In the Dirac picture, both the wave function and the operator evolves in time, but from different origin. The wavefunction time evolves from the influence of the added interaction \hat{V} , while the operator \hat{A} evolves from the influence of the stationary interaction $\hat{\mathcal{H}}_0$ expressed as

$$|\psi_I(t)\rangle \equiv e^{-i\hat{V}t/\hbar} |\psi_0\rangle \quad (4.3.27)$$

$$\hat{A}_I(t) \equiv e^{i\hat{\mathcal{H}}_0 t/\hbar} \hat{A}_0 e^{-i\hat{\mathcal{H}}_0 t/\hbar} \quad (4.3.28)$$

The expectation value $\langle A \rangle$ evolves in time as

$$\begin{aligned} \langle A(t) \rangle &= \langle \psi_0 | e^{i\hat{\mathcal{H}}_0 t/\hbar} \hat{A}_0 e^{-i\hat{\mathcal{H}}_0 t/\hbar} | \psi_0 \rangle \\ &= \langle \psi_0 | e^{i\hat{V}t/\hbar} \cdot e^{i\hat{\mathcal{H}}_0 t/\hbar} \hat{A}_0 e^{-i\hat{\mathcal{H}}_0 t/\hbar} \cdot e^{-i\hat{V}t/\hbar} | \psi_0 \rangle \\ &= \langle \psi_I(t) | \hat{A}_I(t) | \psi_I(t) \rangle, \end{aligned} \quad (4.3.29)$$

and the time evolution of the state in Dirac picture is described in terms of the state in Schrödinger picture as

$$\begin{aligned} |\psi(t)\rangle_I &= e^{-i\hat{V}t/\hbar} |\psi_0\rangle = e^{i\hat{\mathcal{H}}_0 t/\hbar} e^{-i(\hat{\mathcal{H}}_0 + \hat{V})t/\hbar} |\psi_0\rangle \\ &= e^{i\hat{\mathcal{H}}_0 t/\hbar} |\psi_S\rangle. \end{aligned} \quad (4.3.30)$$

In the Dirac picture, the operator also evolves in time, so let's check the time evolution of Hamiltonian $\hat{\mathcal{H}} = \hat{\mathcal{H}}_0 + \hat{V}$ as before.

$$\hat{\mathcal{H}}_{0I} = e^{i\hat{\mathcal{H}}_0 t/\hbar} \hat{\mathcal{H}}_0 e^{-i\hat{\mathcal{H}}_0 t/\hbar} = \hat{\mathcal{H}}_0 \quad (4.3.31)$$

$$\hat{V}_I = e^{i\hat{\mathcal{H}}_0 t/\hbar} \hat{V} e^{-i\hat{\mathcal{H}}_0 t/\hbar} \quad (4.3.32)$$

The above shows that the steady Hamiltonian $\hat{\mathcal{H}}_0$ does not evolve in time, however, the added Hamiltonian \hat{V}_I varies in time from the influence of $\hat{\mathcal{H}}_0$.

Now consider the time evolution of the state written in the Dirac picture. Using $|\psi\rangle_S = e^{-i\hat{\mathcal{H}}_0 t/\hbar} |\psi_0\rangle$ and $|\psi\rangle_I = e^{i\hat{\mathcal{H}}_0 t/\hbar} |\psi\rangle_S$, the state evolution can be written as

$$\begin{aligned} \frac{d|\psi\rangle_I}{dt} &= \frac{i}{\hbar} \hat{\mathcal{H}}_0 |\psi\rangle_I + e^{i\hat{\mathcal{H}}_0 t/\hbar} \frac{d|\psi\rangle_S}{dt} \\ &= \frac{i}{\hbar} e^{i\hat{\mathcal{H}}_0 t/\hbar} \hat{\mathcal{H}}_0 e^{-i\hat{\mathcal{H}}_0 t/\hbar} |\psi\rangle_I - \frac{i}{\hbar} e^{i\hat{\mathcal{H}}_0 t/\hbar} \hat{V} e^{-i\hat{\mathcal{H}}_0 t/\hbar} |\psi\rangle_I \\ &= -\frac{i}{\hbar} e^{i\hat{\mathcal{H}}_0 t/\hbar} \hat{V} e^{-i\hat{\mathcal{H}}_0 t/\hbar} |\psi\rangle_I = -\frac{i}{\hbar} \hat{V}_I |\psi\rangle_I, \end{aligned} \quad (4.3.33)$$

with final result

$$\frac{d|\psi\rangle_I}{dt} = -\frac{i}{\hbar} \hat{V}_I |\psi\rangle_I.$$

(4.3.34)

As we shall see later, the interaction picture becomes particularly useful in the time-dependent perturbation theory.

Summary Above is a quick overview of three pictures in quantum mechanics. As shown above, all pictures describe the same time evolution of the expectation value of a physical observable $\langle A(t) \rangle$, despite the difference in the time evolution of the state and operators.

There are pros and cons for all pictures. For example, finding the wavefunction for a potential well, as we all learn in the introductory quantum mechanics, is actually difficult in the Heisenberg picture. In the next section, we use the Heisenberg picture to derive the Heisenberg equation of motion, which describes the equation of motion for an operator and is a counterpart of the Schrödinger equation. In quantum technology, we often focus on the time evolution of the observables, such as resonator field mode and external electromagnetic noises that are described by operators. In such a case, the Heisenberg picture and the use of Heisenberg's equation of motion is an excellent alternative.

The Dirac picture is particularly useful when an additional perturbation is provided to a system with known eigenstates and corresponding eigenenergies. With the Dirac picture, as shown later, the time-dependent perturbation theory can be described in a much simpler form than the Schrödinger picture.

4.4 Heisenberg Equation of Motion

The time evolution of an arbitrary operator \hat{A} in the Heisenberg picture is given as

$$\hat{A}_H = \hat{A}_H(t) = e^{i\hat{\mathcal{H}}t/\hbar} \hat{A}_0 e^{-i\hat{\mathcal{H}}t/\hbar}. \quad (4.4.1)$$

In a form of time derivative, we can expand the above as

$$\begin{aligned} \frac{d\hat{A}_H(t)}{dt} &= \frac{i}{\hbar} \hat{\mathcal{H}} e^{i\hat{\mathcal{H}}t/\hbar} \hat{A}_0 e^{-i\hat{\mathcal{H}}t/\hbar} - e^{i\hat{\mathcal{H}}t/\hbar} \hat{A}_0 \frac{i\hat{\mathcal{H}}}{\hbar} e^{-i\hat{\mathcal{H}}t/\hbar} + e^{i\hat{\mathcal{H}}_0 t/\hbar} \frac{\partial \hat{A}_0}{\partial t} e^{-i\hat{\mathcal{H}}_0 t/\hbar} \\ &= \frac{i}{\hbar} \left[\hat{\mathcal{H}} e^{i\hat{\mathcal{H}}t/\hbar} \hat{A}_0 e^{-i\hat{\mathcal{H}}t/\hbar} - e^{i\hat{\mathcal{H}}t/\hbar} \hat{A}_0 e^{-i\hat{\mathcal{H}}t/\hbar} \hat{\mathcal{H}} \right] + e^{i\hat{\mathcal{H}}_0 t/\hbar} \frac{\partial \hat{A}_0}{\partial t} e^{-i\hat{\mathcal{H}}_0 t/\hbar} \\ &= \frac{i}{\hbar} [\hat{\mathcal{H}}, \hat{A}_H] + e^{i\hat{\mathcal{H}}_0 t/\hbar} \frac{\partial \hat{A}_0}{\partial t} e^{-i\hat{\mathcal{H}}_0 t/\hbar}, \end{aligned} \quad (4.4.2)$$

and we get

$$\boxed{\frac{d\hat{A}_H(t)}{dt} = \frac{i}{\hbar} [\hat{\mathcal{H}}, \hat{A}_H(t)] + \left(\frac{\partial \hat{A}(t)}{\partial t} \right)_H}, \quad (4.4.3)$$

where $\left(\frac{\partial \hat{A}(t)}{\partial t} \right)_H = e^{i\hat{\mathcal{H}}_0 t/\hbar} \frac{\partial \hat{A}_0}{\partial t} e^{-i\hat{\mathcal{H}}_0 t/\hbar}$. This equation is called the Heisenberg equation of motion. While Schrödinger equation describes the time evolution of the wavefunction, in the Heisenberg picture, the system evolution is described focusing on the evolution of the operators. The last term is included only when \hat{A}_0 is explicitly time-dependent, meaning the operator in Schrödinger picture have an explicit time dependence. Otherwise, the last term can be omitted, simplifying the equation as

$$\boxed{\frac{d\hat{A}_H(t)}{dt} = \frac{i}{\hbar} [\hat{\mathcal{H}}, \hat{A}_H(t)]}. \quad (4.4.4)$$

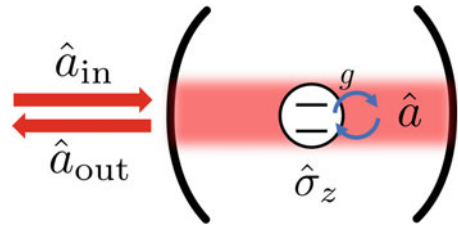
Let us take a look at the harmonic oscillator previously seen, as an explicit example. Here we omit the subscript ‘H’ to avoid clumsiness, but all the operators are understood to be in the Heisenberg picture. The annihilation and creation operators follow

$$\begin{aligned} \frac{d\hat{a}(t)}{dt} &= \frac{i}{\hbar} [\hbar\omega\hat{a}^\dagger\hat{a}, \hat{a}] \\ &= -i\omega\hat{a}(t), \end{aligned}$$

which can be integrated to obtain

$$\hat{a}(t) = \hat{a}(0)e^{-i\omega t}.$$

Fig. 4.7 Time evolution of operators, $\hat{\sigma}_z$ and \hat{a} in cavity QED system



The time evolution of the position operator \hat{x} is given by the Heisenberg equation of motion as

$$\begin{aligned}\frac{d\hat{x}(t)}{dt} &= \frac{i}{\hbar} [\hbar\omega\hat{a}^\dagger\hat{a}, x_{\text{zp}}(\hat{a}^\dagger + \hat{a})] \\ &= i\omega x_{\text{zp}}[\hat{a}^\dagger\hat{a}, \hat{a}^\dagger] + i\omega x_{\text{zp}}[\hat{a}^\dagger\hat{a}, \hat{a}] \\ &= i\omega x_{\text{zp}}\hat{a}^\dagger - i\omega x_{\text{zp}}\hat{a}.\end{aligned}$$

Integrating the above result, we obtain the position operator in Heisenberg picture as

$$\hat{x}(t) = x_{\text{zp}} \left(\hat{a}^\dagger e^{i\omega t} + \hat{a} e^{-i\omega t} \right),$$

which is identical to the previously obtained result.

In quantum technology, many signals including the incident electromagnetic waves to the resonator and the state in the resonator are mainly described as quantum modes using the ladder operators \hat{a} and \hat{b} .

By taking the spectroscopy of the resonator QED system as shown in Fig. 4.7 as an example, the resonator mode and the qubit state are described as operators \hat{a} and $\hat{\sigma}_z$, respectively. Also, the drive field \hat{a}_{in} from the outside and the reflected light \hat{a}_{out} are described by operators as well. In the actual experiment, we are often interested in the time evolution of the qubit $\hat{\sigma}_z(t)$ by the drive field, the time evolution of the resonator mode $\hat{a}(t)$, and the reflected light $\hat{a}_{\text{out}}(t)$. The time evolution of these operators can be calculated using Heisenberg's equation of motion, and it is easy to compare with the measured physical quantities that have a high affinity with the experiment.

4.5 von Neumann Equation

von Neumann equation is quite similar in appearance to Heisenberg's equation of motion and sometimes it is confusing.

von Neumann equation is give as

$$\frac{d\hat{\rho}(t)}{dt} = -\frac{i}{\hbar} [\hat{\mathcal{H}}, \hat{\rho}(t)]. \quad (4.5.1)$$

Note here that $\hat{\rho}(t) \equiv |\psi_S(t)\rangle\langle\psi_S(t)|$ is a density operator written in Schrödinger picture. At first glance, the von Neumann equation seems to be an adaptation of Heisenberg's equation of motion to the density operator $\rho(t)$, but the *sign is different*.

One can reach the von Neumann equation by describing the time evolution of the density operator in Schrödinger picture as follows,

$$\begin{aligned} i\hbar \frac{\partial \hat{\rho}(t)}{\partial t} &= i\hbar \frac{\partial (|\psi_S(t)\rangle\langle\psi_S(t)|)}{\partial t} \\ &= i\hbar \frac{\partial |\psi_S(t)\rangle}{\partial t} \langle\psi_S(t)| + i\hbar |\psi_S(t)\rangle \frac{\partial \langle\psi_S(t)|}{\partial t} \\ &= \hat{\mathcal{H}} |\psi_S(t)\rangle\langle\psi_S(t)| - |\psi_S(t)\rangle\langle\psi_S(t)| \hat{\mathcal{H}} \\ &= [\hat{\mathcal{H}}, \hat{\rho}(t)]. \end{aligned} \quad (4.5.2)$$

Keep in mind that the von Neumann equation is written in Schrödinger picture.

Similar confusion is likely to occur when finding the expectation value of operator \hat{A} . Earlier, we described $\langle A \rangle$ as

$$\langle A \rangle = \text{Tr}(\hat{\rho}\hat{A}). \quad (4.5.3)$$

In this equation, the density operator time evolves in Schrödinger picture, while the operator \hat{A} evolves in the Heisenberg picture and care needs to be taken. Form of ρ and \hat{A} for different picture is given as

$$\hat{\rho}_S(0) = \hat{\rho}_H \quad (4.5.4)$$

$$\hat{\rho}_S(t) = \hat{U}(t)\hat{\rho}_S(0)\hat{U}^\dagger(t) \quad (4.5.5)$$

$$\hat{A}_H(0) = \hat{A}_S \quad (4.5.6)$$

$$\hat{A}_H(t) = \hat{U}^\dagger(t)\hat{A}_H(0)\hat{U} \quad (4.5.7)$$

and the expectation value \hat{A} in each picture is

$$\langle A(t) \rangle_S = \text{Tr}(\hat{\rho}_S(t)\hat{A}_S) = \text{Tr}(\hat{U}(t)\hat{\rho}_S(0)\hat{U}^\dagger(t)\hat{A}_S) \quad (4.5.8)$$

$$\begin{aligned} \langle A(t) \rangle_H &= \text{Tr}(\hat{\rho}_H\hat{A}_H(t)) = \text{Tr}(\hat{\rho}_H\hat{U}^\dagger(t)\hat{A}_H(0)\hat{U}) \\ &= \text{Tr}(\hat{\rho}_S(0)\hat{U}^\dagger(t)\hat{A}_S\hat{U}) \\ &= \text{Tr}(\hat{U}(t)\hat{\rho}_S(0)\hat{U}^\dagger(t)\hat{A}_S) = \langle A(t) \rangle_S. \end{aligned} \quad (4.5.9)$$

In the last line, the permutation characteristic of the trace

$$\text{Tr}(ABC) = \text{Tr}(BCA) = \text{Tr}(CAB). \quad (4.5.10)$$

is used. As described above, the same expectation value $\langle A \rangle$ can be calculated for each picture. However, it is important to be consistent with the picture that you are using and should not mix the Schrödinger and Heisenberg picture. It might be a good idea to remember that only one of $\hat{\rho}$ or \hat{A} is time dependent in either picture.

4.6 Unitary Transformation to a Rotating Frame

Often it is desirable to analyze the dynamics of a quantum system from a frame that rotates at a certain frequency. In classical mechanics, say we are to analyze the trajectory of a baseball, we often ignore that the earth is rotating. We do that by looking at the baseball from the point of view of the person on the earth, who is also rotating with the earth. As we know, the dynamics can be much simpler that way and the same analogy applies to the dynamics in quantum systems.

As shown in Fig. 4.8, we often encounter a situation where a drive with frequency ω is introduced to a system with Hamiltonian $\hat{\mathcal{H}}$ and corresponding frequency (or energy) ω_{sys} . The unitary transformation which moves the system into the frame rotating at ω can be written in terms of the Hamiltonian \mathcal{H} as

$$\hat{U}(t) = \exp\left[i(\hat{\mathcal{H}}(\omega)/\hbar)t\right]. \quad (4.6.1)$$

The state vector $|\psi\rangle$ is now transformed to $|\phi\rangle = \hat{U}(t)|\psi\rangle$. Now the Schrödinger equation for this new state $|\phi\rangle$ is transformed as

$$\begin{aligned} i\hbar \frac{d|\phi\rangle}{dt} &= i\hbar \frac{d\hat{U}}{dt} |\psi\rangle + i\hbar \hat{U} \frac{d|\psi\rangle}{dt} \\ &= i\hbar \dot{\hat{U}} |\psi\rangle + \hat{U} \hat{\mathcal{H}} |\psi\rangle \\ &= i\hbar \dot{\hat{U}} \hat{U}^\dagger |\phi\rangle + \hat{U} \hat{\mathcal{H}} \hat{U}^\dagger |\phi\rangle \\ &= (\hat{U} \hat{\mathcal{H}} \hat{U}^\dagger - i\hbar \dot{\hat{U}} \hat{U}^\dagger) |\phi\rangle, \end{aligned} \quad (4.6.2)$$

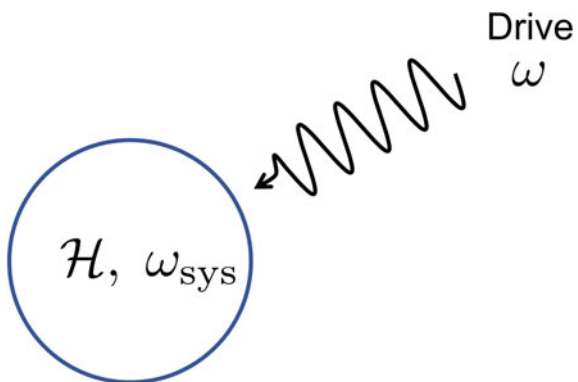
where we used $0 = d(\hat{U} \hat{U}^\dagger)/dt = \dot{\hat{U}} \hat{U}^\dagger + \hat{U} \dot{\hat{U}}^\dagger$ in the derivation.

$\hat{\mathcal{H}}$ is the Hamiltonian before the transformation and the new Hamiltonian is expressed as

$$\hat{\mathcal{H}}' = \hat{U} \hat{\mathcal{H}} \hat{U}^\dagger - i\hbar \dot{\hat{U}} \hat{U}^\dagger. \quad (4.6.3)$$

As in the baseball analysis on the earth, this unitary transformation let us see the quantum system from the frame rotating at ω , in which we often analyze the

Fig. 4.8 Driven system with an external drive with frequency ω



time evolution and/or the steady state of the system. Let's calculate an example of a harmonic oscillator and a qubit system below.

The first example is a single-mode harmonic oscillator with Hamiltonian $\hat{\mathcal{H}} = \hbar\omega_c \hat{a}^\dagger \hat{a}$. Let's use a unitary transformation $\hat{U}(t) = \exp[i\omega \hat{a}^\dagger \hat{a}t]$ to switch to a frame rotating at ω . $\hat{U}(t)$ can be Taylor-expanded, but we know that $\hat{a}^\dagger \hat{a}$ in the exponential commute with the Hamiltonian $\hat{\mathcal{H}} \propto \hat{a}^\dagger \hat{a}$, therefore, $\hat{U}(t)$ also commute with the Hamiltonian.

This simplifies the calculation of the unitary transformation (B.5). From $\hat{U}\hat{\mathcal{H}}\hat{U}^\dagger = \hat{U}\hat{U}^\dagger\hat{\mathcal{H}} = \hat{\mathcal{H}}$, we see

$$\begin{aligned}\hat{\mathcal{H}}' &= \hat{\mathcal{H}} - i\hbar\dot{\hat{U}}\hat{U}^\dagger = \hbar\omega_c \hat{a}^\dagger \hat{a} - i\hbar\hat{U}(-i\omega\hat{a}^\dagger \hat{a})\hat{U}^\dagger \\ &= \hbar(\omega_c - \omega)\hat{a}^\dagger \hat{a} \\ &= -\hbar\Delta_c \hat{a}^\dagger \hat{a}.\end{aligned}\quad (4.6.4)$$

As you can see, the difference between the frequency ω_c of the harmonic oscillator and the frequency ω of the rotating system, $\Delta_c = \omega - \omega_c$ appears in Hamiltonian after being on the rotating frame. Δ_c is called *detuning*, frequently used term in many of the spectroscopic studies of the quantum system.

We can perform a similar procedure for the unitary transformation of spin-1/2 system with Hamiltonian $\hat{\mathcal{H}} = \hbar\omega_a \hat{\sigma}_z/2$ with $\hat{U}(t) = \exp[i\omega(\hat{\sigma}_z/2)t]$. The new Hamiltonian in a rotating frame with frequency ω is calculated as $\hat{\mathcal{H}}' = -\hbar\Delta_a \hat{\sigma}_z/2$. We see the detuning $\Delta_a = \omega - \omega_a$ again here as well.

As an advanced example, let us consider the Jaynes–Cummings Hamiltonian

$$\hat{\mathcal{H}}_{\text{JC}} = \frac{\hbar\omega_a}{2} \hat{\sigma}_z + \hbar\omega_c \hat{a}^\dagger \hat{a} - i\hbar g(\hat{\sigma}_+ \hat{a} - \hat{a}^\dagger \hat{\sigma}_-).\quad (4.6.5)$$

The unitary operator is now $\hat{U}(t) = e^{i\omega\hat{\sigma}_z t/2 + i\omega\hat{a}^\dagger \hat{a}t} = \hat{U}_1(t)\hat{U}_2(t)$, combination of $\hat{U}_1(t) = \exp[i\omega\hat{\sigma}_z t/2]$ and $\hat{U}_2(t) = \exp[i\omega\hat{a}^\dagger \hat{a}t]$. This means that both the qubit and photon of the electromagnetic resonator are viewed from the frame rotating at the drive frequency ω . Since the harmonic oscillator creation/annihilation operator (\hat{a} , \hat{a}^\dagger) and the qubit Pauli operator ($\hat{\sigma}_i$) are commutative, the first two terms of Jaynes–Cummings Hamiltonian are $-\hbar\Delta_a \hat{\sigma}_z/2 - \hbar\Delta_c \hat{a}^\dagger \hat{a}$ as in the previous example. However, the interaction term (third term) does not commute with the unitary operator, and it is not that simple.

In order to pursue, the Baker–Campbell–Hausdorff formula

$$e^{-\hat{S}} \hat{H} e^{\hat{S}} = \hat{H} + [\hat{H}, \hat{S}] + \frac{1}{2!} [[\hat{H}, \hat{S}], \hat{S}] + \frac{1}{3!} [[[[\hat{H}, \hat{S}], \hat{S}], \hat{S}]] + \dots,\quad (4.6.6)$$

is quite useful. Additionally, we note a useful commutation relation $[\hat{a}^\dagger \hat{a}, \hat{a}] = -\hat{a}$, $[\hat{a}^\dagger \hat{a}, \hat{a}^\dagger] = \hat{a}^\dagger$, and $[\hat{\sigma}_z, \hat{\sigma}_\pm] = \pm 2\hat{\sigma}_\pm$.

Let us now pursue by first applying $U_2(t)$ to the interaction term

$$\begin{aligned}
& \hat{U}_2(t)(\hat{\sigma}_+ \hat{a} - \hat{a}^\dagger \hat{\sigma}_-) \hat{U}_2^\dagger(t) \\
&= e^{i\omega \hat{a}^\dagger \hat{a} t} (\hat{\sigma}_+ \hat{a} - \hat{a}^\dagger \hat{\sigma}_-) e^{-i\omega \hat{a}^\dagger \hat{a} t} \\
&= (\hat{\sigma}_+ \hat{a} - \hat{a}^\dagger \hat{\sigma}_-) + [(\hat{\sigma}_+ \hat{a} - \hat{a}^\dagger \hat{\sigma}_-), -i\omega \hat{a}^\dagger \hat{a} t] \\
&\quad + \frac{1}{2!} [[(\hat{\sigma}_+ \hat{a} - \hat{a}^\dagger \hat{\sigma}_-), -i\omega \hat{a}^\dagger \hat{a} t], -i\omega \hat{a}^\dagger \hat{a} t] + \dots \\
&= (\hat{\sigma}_+ \hat{a} - \hat{a}^\dagger \hat{\sigma}_-) + (-i\omega t)(\hat{\sigma}_+ \hat{a} + \hat{a}^\dagger \hat{\sigma}_-) \\
&\quad + \frac{(-i\omega t)^2}{2!} (\hat{\sigma}_+ \hat{a} - \hat{a}^\dagger \hat{\sigma}_-) + \frac{(-i\omega t)^3}{3!} (\hat{\sigma}_+ \hat{a} + \hat{a}^\dagger \hat{\sigma}_-) + \dots \\
&= \left[1 + (-i\omega t) + \frac{(-i\omega t)^2}{2!} + \frac{(-i\omega t)^3}{3!} + \dots \right] \hat{\sigma}_+ \hat{a} \\
&\quad - \left[1 - (-i\omega t) + \frac{(-i\omega t)^2}{2!} - \frac{(-i\omega t)^3}{3!} + \dots \right] \hat{a}^\dagger \hat{\sigma}_- \\
&= e^{-i\omega t} \hat{\sigma}_+ \hat{a} - e^{i\omega t} \hat{a}^\dagger \hat{\sigma}_-. \tag{4.6.7}
\end{aligned}$$

Now, applying $U_1(t)$ to the above Hamiltonian we get

$$\begin{aligned}
& \hat{U}_1(t)(e^{-i\omega t} \hat{\sigma}_+ \hat{a} - e^{i\omega t} \hat{a}^\dagger \hat{\sigma}_-) \hat{U}_1^\dagger(t) \\
&= e^{i\omega \hat{\sigma}_z t / 2} (e^{-i\omega t} \hat{\sigma}_+ \hat{a} - e^{i\omega t} \hat{a}^\dagger \hat{\sigma}_-) e^{-i\omega \hat{\sigma}_z t / 2} \\
&= e^{-i\omega t} \hat{a} \left(e^{i\omega \hat{\sigma}_z t / 2} \hat{\sigma}_+ e^{-i\omega \hat{\sigma}_z t / 2} \right) - e^{i\omega t} \hat{a}^\dagger \left(e^{i\omega \hat{\sigma}_z t / 2} \hat{\sigma}_- e^{-i\omega \hat{\sigma}_z t / 2} \right). \tag{4.6.8}
\end{aligned}$$

Using the following relation:

$$\begin{aligned}
e^{i\omega \hat{\sigma}_z t / 2} \hat{\sigma}_\pm e^{-i\omega \hat{\sigma}_z t / 2} &= \hat{\sigma}_\pm + \left[\hat{\sigma}_\pm, -i \frac{\omega \hat{\sigma}_z t}{2} \right] + \frac{1}{2!} \left[\left[\hat{\sigma}_\pm, -i \frac{\omega \hat{\sigma}_z t}{2} \right], -i \frac{\omega \hat{\sigma}_z t}{2} \right] \\
&\quad + \frac{1}{3!} \left[\left[\left[\hat{\sigma}_\pm, -i \frac{\omega \hat{\sigma}_z t}{2} \right], -i \frac{\omega \hat{\sigma}_z t}{2} \right], -i \frac{\omega \hat{\sigma}_z t}{2} \right] + \dots \\
&= \hat{\sigma}_\pm \mp (-i\omega t) \hat{\sigma}_\pm + \frac{1}{2!} (-i\omega t)^2 \hat{\sigma}_\pm \mp \frac{1}{3!} (-i\omega t)^3 \hat{\sigma}_\pm + \dots \\
&= e^{\pm i\omega t} \hat{\sigma}_\pm, \tag{4.6.9}
\end{aligned}$$

the Jaynes–Cummings interaction Hamiltonian in the rotating frame is derived as

$$\begin{aligned}
& \hat{U}_1(t) \hat{U}_2(t) (-i\hbar g) (\hat{\sigma}_+ \hat{a} - \hat{a}^\dagger \hat{\sigma}_-) \hat{U}_2^\dagger(t) \hat{U}_1^\dagger(t) \\
&= \hat{U}_1(t) (-i\hbar g) (e^{-i\omega t} \hat{\sigma}_+ \hat{a} - e^{i\omega t} \hat{a}^\dagger \hat{\sigma}_-) \hat{U}_1^\dagger(t) \\
&= -i\hbar g (\hat{\sigma}_+ \hat{a} - \hat{a}^\dagger \hat{\sigma}_-). \tag{4.6.10}
\end{aligned}$$

After all the calculations, the Jaynes–Cummings Hamiltonian in the rotating frame is actually the same as the original Hamiltonian. Writing all the terms together, the Jaynes–Cummings Hamiltonian in the rotating frame can be given as

$$\hat{\mathcal{H}}'_{\text{JC}} = -\frac{\hbar\Delta_a}{2}\hat{\sigma}_z - \hbar\Delta_c\hat{a}^\dagger\hat{a} - i\hbar g(\hat{\sigma}_+\hat{a} - \hat{a}^\dagger\hat{\sigma}_-). \quad (4.6.11)$$

4.7 Driven Two-Level System

Let us take a moment to see the effect of strong drive in a two-level system, using the formulation given above. This situation often arises when the drive field is introduced to control the two-level system, for example, laser spectroscopy of atoms or ions, Nuclear Magnetic Resonance (NMR), and Electron Spin Resonance (ESR), usually use a strong external drive field. Here, we omit the derivation of the interaction Hamiltonian and other details, and focus on the frame rotation, eigenenergies, and eigenstates of the driven two-level system.

Let us consider a situation where an atomic ground and excited state with corresponding energy $E_g = -\hbar\omega_a/2$ and $E_e = +\hbar\omega_a/2$ is driven by an external electric field $\mathbf{E}(t)$. For a strong drive $\mathbf{E} = \mathbf{E}_0 \cos\omega_d t$, where $E_0 \gg E_{\text{zpf}}$, the ladder operator can be approximated as a classical number ($\hat{a}^\dagger \rightarrow \alpha$, $\hat{a} \rightarrow \alpha$).¹ The interaction Hamiltonian can be given as

$$\hat{\mathcal{H}}_{\text{int}} = \hbar \left(\hat{\sigma}_+ \alpha e^{i\omega_d t} + \hat{\sigma}_- \alpha e^{-i\omega_d t} \right), \quad (4.7.1)$$

with a rotating wave approximation as discussed later. The Hamiltonian of entire system can be written as

$$\begin{aligned} \hat{\mathcal{H}} &= \frac{\hbar\omega_a}{2}\hat{\sigma}_z + \hbar \left(\hat{\sigma}_+ \alpha e^{i\omega_d t} + \hat{\sigma}_- \alpha e^{-i\omega_d t} \right) \\ &= \hbar \begin{pmatrix} \frac{\omega_a}{2} & \alpha e^{i\omega_d t} \\ \alpha e^{-i\omega_d t} & -\frac{\omega_a}{2} \end{pmatrix}. \end{aligned} \quad (4.7.2)$$

Moving into the rotating frame at drive frequency ω_d , the system Hamiltonian now reads

$$\begin{aligned} \hat{\mathcal{H}} &= -\frac{\hbar\Delta_a}{2}\hat{\sigma}_z + \frac{\hbar\Omega}{2}\hat{\sigma}_x \\ &= \frac{\hbar}{2} \begin{pmatrix} -\Delta_a & \Omega \\ \Omega & \Delta_a \end{pmatrix}, \end{aligned} \quad (4.7.3)$$

¹ Recall the effect of the ladder operator, e.g., $\hat{a}|n\rangle = \sqrt{n}|n-1\rangle$. For a large photon number (large n) $\hat{a}|n\rangle \simeq \sqrt{n}|n\rangle$ and $\hat{a} \rightarrow \alpha = \sqrt{n}$ is justified. Another words, with a strong drive annihilating or creating photons practically changes nothing to the photon number, and eigenvalue is approximated as a classical number.

where $\Delta_a = \omega_d - \omega_a$ is drive detuning and Rabi frequency $\Omega = 2\alpha$ is introduced. As described previously, the system has no time dependence in this rotating frame. The eigenenergies of this Hamiltonian is easily found as

$$E_+ = +\frac{\hbar\Delta_a}{2} \sqrt{1 + \frac{\Omega^2}{\Delta_a^2}}$$

$$E_- = -\frac{\hbar\Delta_a}{2} \sqrt{1 + \frac{\Omega^2}{\Delta_a^2}},$$

with corresponding eigenstates

$$|\psi_+\rangle = +\cos\theta |g\rangle - \sin\theta |e\rangle$$

$$|\psi_-\rangle = +\sin\theta |g\rangle + \cos\theta |e\rangle,$$

where

$$\sin\theta = \frac{-\Omega}{\sqrt{\Omega^2 + (\Delta_a + \Omega')^2}}$$

$$\cos\theta = \frac{\Delta_a + \Omega'}{\sqrt{\Omega^2 + (\Delta_a + \Omega')^2}}.$$

Here we introduced generalized Rabi frequency $\Omega' = \sqrt{\Delta_a^2 + \Omega^2}$.

The eigenenergies are altered by the laser detuning and the Rabi frequency. Also, the eigenstates with the drive is a superposition of the original states $|g\rangle$ and $|e\rangle$.

Without the Drive

Let us first take a look at the case where there is no drive ($\Omega = 0$). With $\sin\theta = 0$ and $\cos\theta = 1$, we recognize $|\psi_+\rangle = |g\rangle$, $|\psi_-\rangle = |e\rangle$ with corresponding eigenenergies and energy difference $E_+ = +\frac{\hbar}{2}\Delta_a$, $E_- = -\frac{\hbar}{2}\Delta_a$, and $\Delta E = E_+ - E_- = \hbar\Delta_a$.

Note here that these eigenenergies are in the rotating frame with respect to the drive frequency ω_d and the actual atomic energies remains E_g and E_e , since there is no drive. This is as if you are running the experiment, sweeping the laser frequency, but your mate is blocking the laser (don't do that). The eigenenergies with respect to the laser detuning Δ_a is shown in Fig. 4.9a. Without the drive, there is no coupling between $|g\rangle$ and $|e\rangle$, and the energy levels cross each other at detuning $\Delta_a = 0$.

With the Drive: Coherent Coupling and Dressed State

Now, with the drive, the states $|\psi_{\pm}\rangle$ are the superposition of the bare atomic states. These states are called *dressed states*. As opposed to the bare atomic states, these

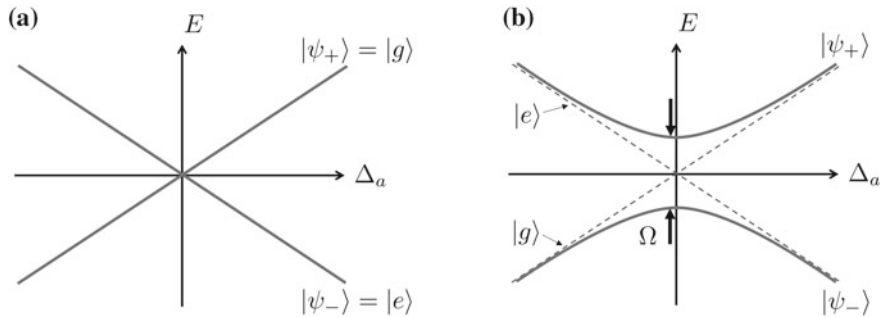


Fig. 4.9 Dressed states. **a** Without the drive. **b** With the drive

states are *dressed* by a sea of photons, creating new eigenstates. The energy eigenvalues vary with detuning Δ_a and Rabi frequency Ω with energy difference $\Delta E = \hbar\Omega'$. An example of the eigenenergies with a fixed Rabi frequency Ω is shown in Fig. 4.9b.

At zero detuning ($\Delta_a = 0$), the eigenstates have the equal participation from the ground and excited state as

$$\begin{aligned} |\psi_+\rangle &= \frac{1}{\sqrt{2}} (|g\rangle + |e\rangle) \\ |\psi_-\rangle &= \frac{1}{\sqrt{2}} (-|g\rangle + |e\rangle). \end{aligned}$$

The eigenenergies show the *anticrossing* (or avoided crossing) with the gap frequency of Ω (or energy of $\hbar\Omega$) at zero detuning. As we show later, this drive coherently transfers the population between the ground and the excited state of the atom. At zero detuning, the population oscillates between the ground and excited state, making half-and-half participation of two states. It is important to note that the oscillation frequency of the population is Ω , which is manifested as a gap between the eigenstates.

In far-detuned region ($|\Delta_a| \gg \Omega$), the eigenstates are nearly that of the bare atomic states, $|\psi_{\pm}\rangle \simeq |g\rangle, |e\rangle$. Also the eigenenergies can be approximated as

$$\begin{aligned} E_+ &\simeq \frac{\hbar\Delta_a}{2} \left(1 + \frac{\Omega^2}{2\Delta_a^2} \right) = \frac{\hbar\Delta_a}{2} + \frac{\hbar\Omega^2}{4\Delta_a} \\ E_- &\simeq -\frac{\hbar\Delta_a}{2} \left(1 + \frac{\Omega^2}{2\Delta_a^2} \right) = -\frac{\hbar\Delta_a}{2} - \frac{\hbar\Omega^2}{4\Delta_a}. \end{aligned}$$

The eigenenergies are also similar to that of the atomic states, but shifted slightly by $\frac{\hbar\Omega^2}{4\Delta_a}$. This shift is called AC Stark shift, or light shift, and originated from the strong far-detuned drive. The AC Stark shift could be actively used to control the state energies, or may happen as an artifact of the control. For example, if we have an additional state $|a\rangle$ to the two-level example shown above, creating a three-state

system. The drive may be on-resonant for $|g\rangle-|e\rangle$ transition, but very likely far-detuned for $|g\rangle-|a\rangle$ or $|e\rangle-|a\rangle$ transition, creating an AC Stark shift to the energy level of $|a\rangle$.

Let us wrap up this section by noting the importance of the anticrossing derived here. We mentioned that the anticrossing results from the coherent transfer of the population between $|g\rangle$ and $|e\rangle$ state. When we say “coherent”, we mean that the quantumness, such as superposition and entanglement, is preserved and the system follows the Schrödinger equation as we expect. In a real experiment, it is not that simple. Many disturbances and noises result in unwanted transitions and deterioration of the quantumness. In quantum technology, different quantum systems are coupled to enable various quantum state transfers and manipulations. Experimentally, anti-crossing of the energy levels is one of the first feature to look for, since it manifests the signature of the preservation of quantumness and clean coupling between states in the experimental setup.

Problems

These identities may be useful in the following problem set.

$$\begin{aligned} e^{i\theta(\hat{n}\cdot\vec{\sigma})} &= \hat{I}\cos\theta + i(\hat{n}\cdot\vec{\sigma})\sin\theta \\ e^{i\theta(\hat{n}\cdot\vec{\sigma})}\vec{\sigma}e^{-i\theta(\hat{n}\cdot\vec{\sigma})} &= \vec{\sigma}\cos2\theta + \hat{n}\times\vec{\sigma}\sin2\theta + \hat{n}\cdot\vec{\sigma}(1-\cos2\theta) \end{aligned}$$

Problem 4-1 Hamiltonian of a two-level system, such as qubit, without any interaction can be written as

$$\mathcal{H} = \frac{\hbar\omega_q}{2}\hat{\sigma}_z.$$

- (i) Calculate time-evolution unitary operator $\hat{U}(t)$ in a matrix representation.
- (ii) Apply this unitary operator to a qubit initial state $|\psi(0)\rangle = a_0|0\rangle + a_1|1\rangle$ to calculate the qubit state $|\psi(t)\rangle$ at arbitrary time t .
- (iii) Discuss the motion of the state vector on a Bloch sphere.

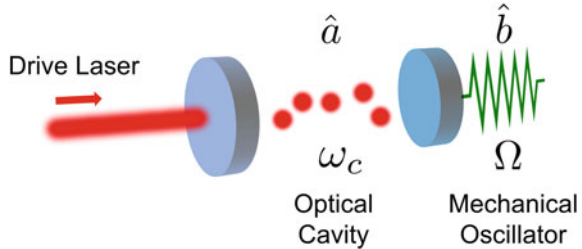
Problem 4-2 Consider a “bare” two-level system Hamiltonian,

$$\mathcal{H} = \frac{\hbar\omega_q}{2}\hat{\sigma}_z.$$

Calculate time-dependent operators in Heisenberg picture for the following operators:

- (i) $\hat{\sigma}_x, \hat{\sigma}_y, \hat{\sigma}_z$.
- (ii) $\hat{\sigma}_+ = (\hat{\sigma}_x + i\hat{\sigma}_y)/2, \hat{\sigma}_- = (\hat{\sigma}_x - i\hat{\sigma}_y)/2$.

Fig. 4.10 Optomechanical system



- (iii) Show that the commutation relation $[\hat{\sigma}_x(t), \hat{\sigma}_y(t)] = 2i\hat{\sigma}_z(t)$, holds for the operators in Heisenberg picture.

Problem 4-3 In cavity optomechanics, a system Hamiltonian is given as

$$\mathcal{H} = \hbar\omega_c \hat{a}^\dagger \hat{a} + \hbar\Omega \hat{b}^\dagger \hat{b} - \hbar g_0 \hat{a}^\dagger \hat{a} (\hat{b} + \hat{b}^\dagger), \quad (4.7.4)$$

where the first and second terms are the harmonic oscillator Hamiltonian of the optical cavity mode (\hat{a}) and mechanical mode (\hat{b}), respectively. The last term is the optomechanical interaction term. In many situation, the system is driven with an external drive. Experimentally, a laser beam is introduced to the optical cavity through the partial mirror of the optical cavity as shown in Fig. 4.10. With this drive, the system Hamiltonian is given as

$$\mathcal{H} = \hbar\omega_c \hat{a}^\dagger \hat{a} + \hbar\Omega \hat{b}^\dagger \hat{b} - \hbar g_0 \hat{a}^\dagger \hat{a} (\hat{b} + \hat{b}^\dagger) + i\hbar\alpha (\hat{a} e^{i\omega_d t} - \hat{a}^\dagger e^{-i\omega_d t}), \quad (4.7.5)$$

where α and ω_d are the drive amplitude (in frequency) and drive laser frequency, respectively.

Rewrite the system Hamiltonian above in a rotating frame defined by the cavity field photon number ($\hat{a}^\dagger \hat{a}$) rotating at the pump frequency drive frequency ω_d so that the time dependence of the drive can be eliminated (Fig. 4.10).

Problem 4-4 In a rotating frame, a system of harmonic oscillator with Hamiltonian $\mathcal{H} = \hbar\omega_c \hat{a}^\dagger \hat{a}$ can be transformed with a unitary operator $\hat{U} = e^{i\omega \hat{a}^\dagger \hat{a}t}$. Using the following relation for ladder operators and operator function (Baker–Campbell–Hausdorff identity)

$$\begin{aligned} [\hat{a}^\dagger \hat{a}, \hat{a}] &= -\hat{a} \\ [\hat{a}^\dagger \hat{a}, \hat{a}^\dagger] &= \hat{a}^\dagger \\ e^{\alpha \hat{A}} \hat{B} e^{-\alpha \hat{A}} &= \hat{B} + \alpha [\hat{A}, \hat{B}] + \frac{\alpha^2}{2!} [\hat{A}, [\hat{A}, \hat{B}]] + \dots, \end{aligned}$$

calculate

- (i) $\hat{U} \hat{a} \hat{U}^\dagger$
- (ii) $\hat{U} \hat{a}^\dagger \hat{U}^\dagger$
- (iii) $\hat{U} \hat{a}^\dagger \hat{a} \hat{U}^\dagger$

Problem 4-5 Consider two-level states. First state is a superposition state

$$|\psi_1\rangle = a_0 |0\rangle + a_1 |1\rangle, \quad (4.7.6)$$

and the second state is a mixed state described as

$$\hat{\rho}_2 = |a_0|^2 |0\rangle\langle 0| + |a_1|^2 |1\rangle\langle 1|. \quad (4.7.7)$$

- (i) Show density matrix for ψ_1 , $\hat{\rho}_1 = |\psi_1\rangle\langle\psi_1|$ and $\hat{\rho}_2$ in matrix representation.
- (ii) The density operator for an arbitrary state is known to be expressed in terms of Pauli operators as

$$\hat{\rho} = \frac{1}{2} \left(\hat{I} + \alpha \hat{\sigma}_x + \beta \hat{\sigma}_y + \gamma \hat{\sigma}_z \right), \quad (4.7.8)$$

where α , β , and γ are all real values, regardless of a pure or mixed state. Write $\hat{\rho}_1$ and $\hat{\rho}_2$ in this form to find appropriate coefficient α , β , and γ .

- (iii) Discuss the difference in a form of density matrix between two states in the matrix representation.

Problem 4-6 The density operator for an arbitrary two-level system can be expressed in terms of Pauli operators as,

$$\hat{\rho} = \frac{1}{2} \left(\hat{I} + \alpha \hat{\sigma}_x + \beta \hat{\sigma}_y + \gamma \hat{\sigma}_z \right), \quad (4.7.9)$$

where α , β , and γ are all real values.

For a system Hamiltonian,

$$\hat{\mathcal{H}} = \frac{\hbar\omega_q}{2} \hat{\sigma}_z + \frac{\hbar\Omega}{2} \hat{\sigma}_x.$$

- (i) Use von Neumann equation to derive the equations of motion (differential equations) for $\alpha(t)$, $\beta(t)$, and $\gamma(t)$.
- (ii) Consider the case where $\Omega = 0$ and calculate $\alpha(t)$, $\beta(t)$, and $\gamma(t)$ in terms of the initial value $\alpha(0)$, $\beta(0)$, and $\gamma(0)$.



Perturbation Theory

5

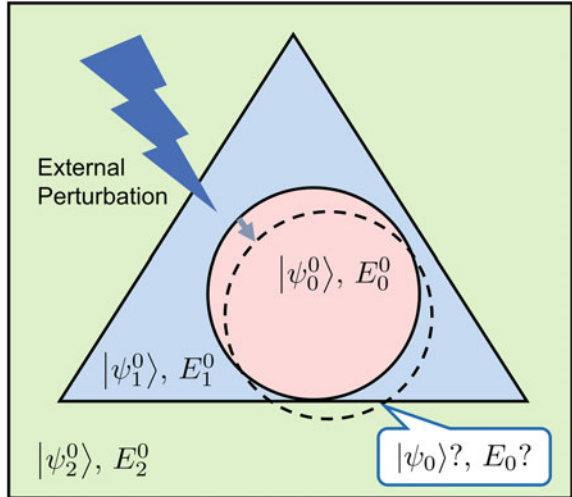
5.1 Time Independent Perturbation Theory

Perturbation theory is one of the important tools of quantum mechanics used to *quantitatively* determine deviation in the quantum system due to external influences. A cartoon to explain the concept of perturbation theory is shown in Fig. 5.1. A circle, triangle, and square drawn with solid lines can be considered as eigenstates $|\psi_n^0\rangle$ of the system with a corresponding eigenenergy E_n^0 , and here we focus on the state $|\psi_0^0\rangle$, the pink circle. When this quantum system is affected by an external influence (perturbation), the circle is pushed a little and moves to a different position from the original circle (dotted circle). This new circle $|\psi_0\rangle$ is almost the original circle, but a small portion of the triangular $|\psi_1^0\rangle$ and square $|\psi_2^0\rangle$ components outside the original circle are now added, causing the state to deviate slightly from the original state $|\psi_0^0\rangle$. Of course, as the state changes, the energy of the state also changes, $E_0^0 \rightarrow E_0$. In perturbation theory, we learn how this new state and energy ($|\psi_n\rangle, E_n$) are represented in terms of the original eigenstates and eigenenergies ($|\psi_n^0\rangle, E_n^0$). The perturbation theory also provides a way to calculate these changes quantitatively.

Experimentally, this “deviation” appears in various forms. It is possible that the system shifts due to the effects of electric and magnetic field noise that are not noticed, or Lasers that are used as a probe for the experiment. These unnoticed deviations can be a source of trouble, but conversely, this deviation can be used as a tool to cancel various shifts by actively introducing an external field. Here, we introduce perturbation theory and some of its applications.

Supplementary Information The online version contains supplementary material available at https://doi.org/10.1007/978-981-19-4641-7_5.

Fig. 5.1 A cartoon depicting the concept of perturbation theory



Consider the Hamiltonian of the system $\hat{\mathcal{H}}^0$ before the external influence is added, its energy eigenstates $|\psi_n^0\rangle$, and corresponding energies E_n^0 , satisfying

$$\hat{\mathcal{H}}^0 |\psi_n^0\rangle = E_n^0 |\psi_n^0\rangle, \quad (5.1.1)$$

where $n = 1, 2, \dots$. Now let us introduce an external influence (perturbation), so that the system Hamiltonian changes as

$$\hat{\mathcal{H}}^0 \rightarrow \hat{\mathcal{H}} = \hat{\mathcal{H}}^0 + \lambda \hat{V}, \quad (5.1.2)$$

where \hat{V} is the external perturbation and λ is the parameter which characterize the strength of the perturbation, which can be regarded as $\lambda \ll 1$. With this new Hamiltonian $\hat{\mathcal{H}}$, the eigenstate $|\psi_n\rangle$ and corresponding eigenenergy E_n fulfills

$$\hat{\mathcal{H}} |\psi_n\rangle = E_n |\psi_n\rangle. \quad (5.1.3)$$

The goal here is to describe this new eigenstate $|\psi_n\rangle$ and the eigenenergy E_n in terms of the original eigenstate $|\psi_n^0\rangle$ and energy E_n^0 .

From previous discussion, we know $|\psi_n\rangle \simeq |\psi_n^0\rangle$ but not quite equal. Using the parameter λ to expand the system state and energy into a power series of λ

$$|\psi_n\rangle = |\psi_n^0\rangle + \lambda |\psi_n^1\rangle + \lambda^2 |\psi_n^2\rangle + \dots \quad (5.1.4)$$

$$E_n = E_n^0 + \lambda E_n^1 + \lambda^2 E_n^2 + \dots, \quad (5.1.5)$$

where superscript on E^i and ψ^i describes the i th order correction, for example, $|\psi_n^1\rangle, E_n^1$ describes the first-order correction, and $|\psi_n^2\rangle$ and E_n^2 are the second-order correction.

We will derive the form of these corrections for state $|\psi_n^1\rangle$, $|\psi_n^2\rangle$, ..., and for energy E_n^1 , E_n^2 , ..., in terms of $|\psi_n^0\rangle$ and E_n^0 .

Substituting Eqs. (5.1.4, 5.1.5) to expand Eq. (5.1.3) as

$$(\hat{\mathcal{H}}^0 + \lambda \hat{V}) \{ |\psi_n^0\rangle + \lambda |\psi_n^1\rangle + \lambda^2 |\psi_n^2\rangle + \dots \} = (E_n^0 + \lambda E_n^1 + \lambda^2 E_n^2 + \dots) \{ |\psi_n^0\rangle + \lambda |\psi_n^1\rangle + \lambda^2 |\psi_n^2\rangle + \dots \}, \quad (5.1.6)$$

and now sort them by the order of λ , we get

$$\lambda^0 : \hat{\mathcal{H}}^0 |\psi_n^0\rangle = E_n^0 |\psi_n^0\rangle \quad (5.1.7)$$

$$\lambda^1 : \hat{\mathcal{H}}^0 |\psi_n^1\rangle + \hat{V} |\psi_n^0\rangle = E_n^0 |\psi_n^1\rangle + E_n^1 |\psi_n^0\rangle \quad (5.1.8)$$

$$\lambda^2 : \hat{\mathcal{H}}^0 |\psi_n^2\rangle + \hat{V} |\psi_n^1\rangle = E_n^1 |\psi_n^2\rangle + E_n^2 |\psi_n^0\rangle. \quad (5.1.9)$$

One can see that λ^0 term represents the state of the original system as we expect.

By taking an inner product of Eq. (5.1.8) with $\langle\psi_n^0|$

$$\langle\psi_n^0| \hat{\mathcal{H}}^0 |\psi_n^1\rangle + \langle\psi_n^0| \hat{V} |\psi_n^0\rangle = E_n^0 \langle\psi_n^0| \psi_n^1\rangle + E_n^1 \langle\psi_n^0| \psi_n^0\rangle. \quad (5.1.10)$$

Since $\hat{\mathcal{H}}^0$ is Hermitian, this equation is also

$$\langle\psi_n^0| \hat{\mathcal{H}}^0 |\psi_n^1\rangle = \langle\hat{\mathcal{H}}^0 \psi_n^0| \psi_n^1\rangle = E_n^0 \langle\psi_n^0| \psi_n^1\rangle, \quad (5.1.11)$$

which sets the first-order energy correction E_n^1 as

$$E_n^1 = \langle\psi_n^0| \hat{V} |\psi_n^0\rangle. \quad (5.1.12)$$

Next, consider the first-order correction $|\psi_n^1\rangle$ of the wavefunction. Expanding $|\psi_n^1\rangle$ in terms of the original wavefunction $|\psi_m^0\rangle$, we have

$$|\psi_n^1\rangle = \sum_{m \neq n} c_m |\psi_m^0\rangle \quad (5.1.13)$$

The case $m = n$ in the equation above is omitted since we are considering the first-order correction terms for $|\psi_n^1\rangle$ and $|\psi_n^0\rangle$ is already included in the 0th correction.

Now our goal is to find this c_m . Similar to the previous case, substituting $|\psi_n^1\rangle$ into Eq. (5.1.8) and taking an inner product with $\langle\psi_k^0|$ shows

$$\begin{aligned} \text{L.H.S. } \langle\psi_k^0| \hat{\mathcal{H}}^0 |\psi_n^1\rangle + \langle\psi_k^0| \hat{V} |\psi_n^0\rangle &= \sum_{m \neq n} c_m \langle\psi_k^0| \hat{\mathcal{H}}^0 |\psi_m^0\rangle + \langle\psi_k^0| \hat{V} |\psi_n^0\rangle \\ &= \sum_{m \neq n} c_m E_m^0 \langle\psi_k^0| \psi_m^0\rangle + \langle\psi_k^0| \hat{V} |\psi_n^0\rangle \\ &= c_k E_k^0 + \langle\psi_k^0| \hat{V} |\psi_n^0\rangle \end{aligned}$$

$$\text{R.H.S. } E_n^0 \langle \psi_k^0 | \psi_n^1 \rangle + E_n^1 \langle \psi_k^0 | \psi_n^0 \rangle = E_n^0 \sum_{m \neq n} c_m \langle \psi_k^0 | \psi_m^0 \rangle \\ = c_k E_n^0, \quad (5.1.14)$$

and setting them equal to each other and solving for c_k to derive

$$c_k = \frac{\langle \psi_k^0 | \hat{V} | \psi_n^0 \rangle}{E_n^0 - E_k^0}. \quad (5.1.15)$$

Finally, substituting this into Eq. (5.1.13), we obtain the first-order correction of the wavefunction

$$\boxed{\langle \psi_n^1 \rangle = \sum_{m \neq n} \frac{\langle \psi_m^0 | \hat{V} | \psi_n^0 \rangle}{E_n^0 - E_m^0} \langle \psi_m^0 \rangle}. \quad (5.1.16)$$

The same procedure can be taken to calculate the higher-order corrections. We only show the result of the second-order energy correction

$$\boxed{E_n^2 = \sum_{m \neq n} \frac{|\langle \psi_m^0 | \hat{V} | \psi_n^0 \rangle|^2}{E_n^0 - E_m^0}}. \quad (5.1.17)$$

The higher-order correction for the energy and wavefunction can be calculated, however, the accuracy of the correction would be diminished. In general, the correction up to the first or second order is routinely used.

In the above perturbation theory, the case with degeneracy was omitted. Looking at the first-order energy correction (5.1.12), there is an energy difference $E_n^0 - E_m^0$ for corresponding states in the denominator, but this term is 0 between the two degenerate states. It seems that the energy shift will blow up. Many quantum mechanics textbooks describe in detail that this problem can be avoided by using a basis in which $\hat{\mathcal{H}}_0$ and \hat{V} can be diagonalized at the same time. Please refer to other textbooks for more details on the perturbation theory with degeneracies.

5.1.1 Zeeman Effect

Let us look at an example of a time-independent perturbation. For electrons with orbital and spin angular momentum L and S , respectively, the Zeeman effect is described with a Hamiltonian

$$\hat{V} = \frac{e}{2m} (\hat{\mathbf{L}} + 2\hat{\mathbf{S}}) \cdot \mathbf{B}_{\text{ext}}, \quad (5.1.18)$$

where $\hat{\mathbf{L}}$ and $\hat{\mathbf{S}}$ are the operators for electron orbital angular momentum and spin angular momentum, respectively. e , m , and \mathbf{B}_{ext} are elementary charge, electron mass, and applied external magnetic field, respectively.

First of all, the quantum states of atom appears as a result of many kinds of perturbations. In the introductory quantum mechanics course, we all study the hydrogen atom where only the central potential from the nucleus is concerned. On top of that, a real atom has multiple electrons, causing Coulomb interaction between electrons, spin-orbit interaction, spin-spin interaction of nucleus and electron spin, and so on. Studying all of that is another subject and a crash course is given in Appendix D. Here we assume the electronic state is well defined in the basis $|LSJm_J\rangle$, where the total orbital angular momentum quantum number L , the total spin angular momentum quantum number S , the total electronic angular momentum quantum number J of operator defined by $\hat{\mathbf{J}} = \hat{\mathbf{L}} + \hat{\mathbf{S}}$, and the second electronic total angular momentum quantum number m_J are used.

In many experiments in atoms and ions, one may encounter the energy state assignments, such as ${}^3\text{P}_1$ and ${}^1\text{D}_2$. These are labeled conveniently, using the convention

$$^{2S+1}L_J \quad (5.1.19)$$

where $L = S, P, D, \dots$ are used instead of $L = 0, 1, 2, \dots$

The Zeeman effect arises from a simple interaction between electrons in atoms (and in solids) and an external magnetic field. From that aspect, it is quite important since the effect is quite general and can appear in various physical systems. Electrons with angular momentum and spin generate an effective magnetic field \mathbf{B}_{int} , the Zeeman effect can be considered as the interaction between the internal magnetic field ($\hat{\mathbf{L}}, \hat{\mathbf{S}} \propto \mathbf{B}_{\text{int}}$) and the external magnetic field \mathbf{B}_{ext} , or more simply, the “magnet” created by the electronic system reacting with the magnet creating the external field.

When $\mathbf{B}_{\text{ext}} \ll \mathbf{B}_{\text{int}}$ is satisfied, the effect can be considered as a small perturbation. The first-order energy correction can be derived using Eq. (5.1.12) as

$$\begin{aligned} E_{LSJm_J}^1 &= \langle LSJm_J | \hat{V} | LSJm_J \rangle \\ &= \left\langle LSJm_J \left| \frac{e}{2m} (\hat{\mathbf{L}} + 2\hat{\mathbf{S}}) \cdot \mathbf{B}_{\text{ext}} \right| LSJm_J \right\rangle \\ &= \frac{e}{2m} \left\langle LSJm_J \left| \hat{L}_z + 2\hat{S}_z \right| LSJm_J \right\rangle B_z \\ &= \frac{e}{2m} \langle L_z + 2S_z \rangle B_z \end{aligned}$$

where in the last line we defined z -direction along the applied magnetic field $\mathbf{B}_{\text{ext}} = B_z \hat{z}$.

The expectation value $\langle L_z + 2S_z \rangle$ is worked out as

$$\langle L_z + 2S_z \rangle = \hbar \left(\frac{3}{2} + \frac{S(S+1) - L(L+1)}{2J(J+1)} \right) m_J$$

where

$$g_J = \frac{3}{2} + \frac{S(S+1) - L(L+1)}{2J(J+1)} \quad (5.1.20)$$

is called Landé g -factor.

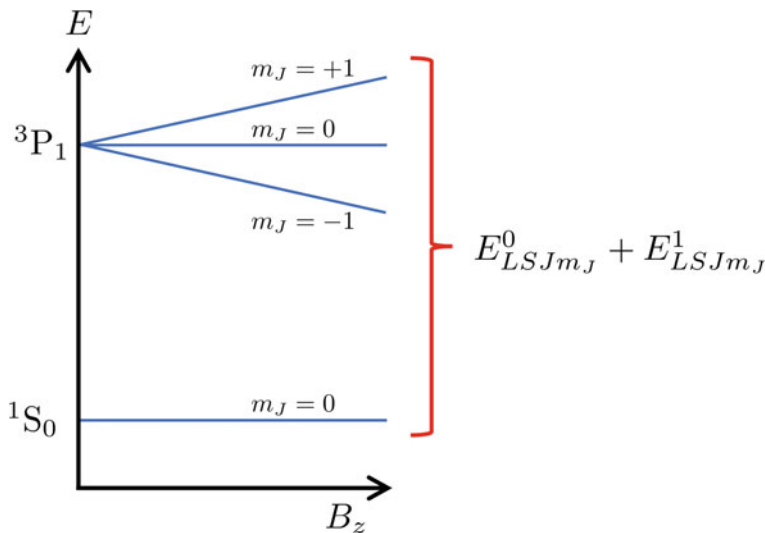


Fig. 5.2 Zeeman shift of energy levels

Finally, the first-order energy correction reads

$$E_{LSJm_J}^1 = \mu_B g_J m_J B_z, \quad (5.1.21)$$

where $\mu_B \equiv \frac{e\hbar}{2m} = 5.79 \times 10^{-5}$ eV/T is a constant called Bohr magneton.

An example of the Zeeman shift is shown in Fig. 5.2. At $B_z = 0$, magnetic sub-levels (states with different m_J) are degenerate. The degeneracy is broken with the applied magnetic field. The energy shift is linear in B_z and the slope depends on the g_J of state. Some state such as 1S_0 has $J = 0$ (and $m_J = 0$) and is not susceptible to the applied magnetic field.

In an actual experiment, the Zeeman effect allows one to adjust the energy of the atoms by the external applied magnetic field. In some experiments using trapped ions, a magnetic field gradient (the magnetic field with varying strength in space) is applied to an array of ions. Each ion in the array now feels a different magnetic field, thus the energies are different for each ion. The effect is used to individually address the ions, which now have different resonance frequencies due to the magnetic field gradient.

Another application is for the quantum sensing. Some system intrinsically has high magnetic field sensitivity (large energy shift from a small field) can be used as a magnetic field sensor that can indirectly measure the magnetic field by the energy shift of the states.

The Zeeman effect can sometimes be a double-edged sword. In experiments where you do not want the energy to change due to the external field, it is necessary to suppress the effect by introducing a magnetic shield or field compensating coils.

5.2 Treatment of Time-Dependent Perturbation

Fundamentals of quantum technology lies in the capability to perform quantum state manipulation. To assure that the quantum system complies, the first step is to isolate the system to retain the quantum coherence in the system. Secondly, we need to introduce some kind of external signal from the outside to control and operate the quantum system. It is important to prescribe a method which describes the time evolution of the quantum system, under the influence of time-varying perturbation applied as our control signal.

When a time-varying perturbation $\hat{V}(t)$ is introduced to the system, Hamiltonian is perturbed as

$$\hat{\mathcal{H}}^0 \rightarrow \hat{\mathcal{H}} = \hat{\mathcal{H}}^0 + \hat{V}(t), \quad (5.2.1)$$

from which we derive an equation of motion of the system.

Assume that the original Hamiltonian $\hat{\mathcal{H}}^0$ is time independent with eigenstate $|\psi_n^0\rangle$ and eigenvalue E_n^0 satisfying

$$\hat{\mathcal{H}}^0 |\psi_n^0\rangle = E_n^0 |\psi_n^0\rangle. \quad (5.2.2)$$

When incorporating time-dependent perturbation, the Dirac picture described previously is quite convenient. The time evolution of the wavefunction in Schrödinger picture is written as

$$i\hbar \frac{d|\psi(t)\rangle_S}{dt} = \hat{\mathcal{H}} |\psi(t)\rangle_S, \quad (5.2.3)$$

and in Dirac picture, the wavefunction $|\psi(t)\rangle_I$ can be written in terms of $|\psi\rangle_S$ as

$$|\psi(t)\rangle_I = e^{i\hat{\mathcal{H}}^0 t/\hbar} |\psi(t)\rangle_S. \quad (5.2.4)$$

Now the time evolution of $|\psi(t)\rangle_I$ is derived as

$$\begin{aligned} i\hbar \frac{d|\psi(t)\rangle_I}{dt} &= i\hbar \left(e^{i\hat{\mathcal{H}}^0 t/\hbar} \frac{d|\psi\rangle_S}{dt} + \frac{i\hat{\mathcal{H}}^0}{\hbar} e^{i\hat{\mathcal{H}}^0 t/\hbar} |\psi\rangle_S \right) \\ &= e^{i\hat{\mathcal{H}}^0 t/\hbar} (\hat{\mathcal{H}} - \hat{\mathcal{H}}^0) |\psi\rangle_S \\ &= e^{i\hat{\mathcal{H}}^0 t/\hbar} \hat{V}(t) e^{-i\hat{\mathcal{H}}^0 t/\hbar} e^{i\hat{\mathcal{H}}^0 t/\hbar} |\psi\rangle_S, \end{aligned}$$

$i\hbar \frac{d|\psi(t)\rangle_I}{dt} = \hat{V}_I(t) |\psi(t)\rangle_I$

$$(5.2.5)$$

In the last line, $\hat{V}_I(t) = e^{i\hat{\mathcal{H}}^0 t/\hbar} \hat{V}(t) e^{-i\hat{\mathcal{H}}^0 t/\hbar}$ is used. Expanding $|\psi(t)\rangle_I$ in terms of eigenstate $|\psi_n^0\rangle$ of unperturbed Hamiltonian $\hat{\mathcal{H}}^0$ as

$$|\psi(t)\rangle_I = \sum_n c_n(t) |\psi_n^0\rangle \quad (5.2.6)$$

and substituting this into Eq. (5.2.5), we derive

$$\begin{aligned} i\hbar \sum_n \dot{c}_n(t) |\psi_n^0\rangle &= \sum_n c_n(t) \lambda \hat{V}_I(t) |\psi_n^0\rangle \\ &= \sum_n c_n(t) \lambda e^{i\hat{\mathcal{H}}^0 t/\hbar} \hat{V}(t) e^{-i\hat{\mathcal{H}}^0 t/\hbar} |\psi_n^0\rangle \\ &= \sum_n c_n(t) \lambda e^{i\hat{\mathcal{H}}^0 t/\hbar} \hat{V}(t) e^{-iE_n^0 t/\hbar} |\psi_n^0\rangle. \end{aligned} \quad (5.2.7)$$

Taking an inner product of the equation above with $\langle \psi_m^0 |$

$$\begin{aligned} i\hbar \sum_n \dot{c}_n(t) \langle \psi_m^0 | \psi_n^0 \rangle &= \sum_n c_n(t) \langle \psi_m^0 | e^{i\hat{\mathcal{H}}^0 t/\hbar} \hat{V}(t) e^{-iE_n^0 t/\hbar} |\psi_n^0\rangle \\ &= \sum_n c_n(t) \langle \psi_m^0 | \hat{V}(t) |\psi_n^0\rangle e^{i(E_m^0 - E_n^0)t/\hbar} \end{aligned} \quad (5.2.8)$$

and using $\langle \psi_m^0 | \psi_n^0 \rangle = \delta_{mn}$

$i\hbar \dot{c}_m(t) = \sum_n c_n(t) \langle \psi_m^0 | V(t) |\psi_n^0\rangle e^{i(E_m^0 - E_n^0)t/\hbar}. \quad (5.2.9)$

This is the equation of motion for the state amplitude $c_m(t)$. Our goal is to solve this $c_m(t)$ to obtain the time-dependent wavefunction

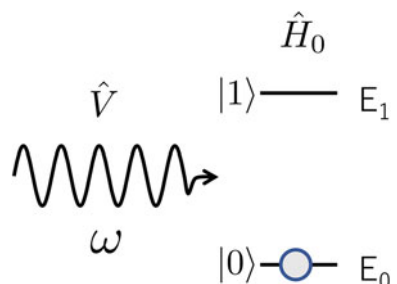
$|\psi(t)\rangle_I = \sum_m c_m(t) |\psi_m^0\rangle. \quad (5.2.10)$

Time Evolution of Two-Level System

Based on the previous results, let us look at an example of the time evolution of a quantum system with an added perturbation.

Consider a two-level system, such as the ground state and the first excited state of an atom. As shown in Fig. 5.3, the population of the ground and excited states

Fig. 5.3 Time evolution of two-level system



vary in time when an external field oscillating at frequency ω_d is applied to this two-level system. Unperturbed system Hamiltonian $\hat{\mathcal{H}}_0$ of the two-level system and the perturbation $\hat{V}(t)$ is given as

$$\hat{\mathcal{H}}^0 = \begin{bmatrix} E_1^0 & 0 \\ 0 & E_0^0 \end{bmatrix} = \hbar \begin{bmatrix} \omega_1 & 0 \\ 0 & \omega_0 \end{bmatrix} \quad (5.2.11)$$

$$\hat{V}(t) = \hbar \begin{bmatrix} 0 & \frac{\Omega}{2} e^{-i\omega_d t} \\ \frac{\Omega}{2} e^{i\omega_d t} & 0 \end{bmatrix}, \quad (5.2.12)$$

where Ω , called Rabi frequency, can be regarded as an effective amplitude of the perturbation.

The time evolution of the state amplitude, Eq. (5.2.9), can be written as

$$\begin{aligned} i\hbar\dot{c}_1(t) &= c_0(t) \langle \psi_1^0 | \hat{V}(t) | \psi_0^0 \rangle e^{i(\omega_1 - \omega_0)t} = c_0(t) \frac{\hbar\Omega}{2} e^{i(\omega_1 - \omega_0)t} e^{-i\omega_d t} \\ i\hbar\dot{c}_0(t) &= c_1(t) \langle \psi_0^0 | \hat{V}(t) | \psi_1^0 \rangle e^{i(\omega_0 - \omega_1)t} = c_1(t) \frac{\hbar\Omega}{2} e^{i(\omega_0 - \omega_1)t} e^{i\omega_d t} \end{aligned}$$

which can be conveniently expressed using the matrix representation $\vec{c}(t) = \begin{bmatrix} c_1(t) \\ c_0(t) \end{bmatrix}$ as,

$$\begin{aligned} i\hbar \begin{bmatrix} \dot{c}_1(t) \\ \dot{c}_0(t) \end{bmatrix} &= \hbar \begin{bmatrix} 0 & \frac{\Omega}{2} e^{i(\omega_1 - \omega_0)t} e^{-i\omega_d t} \\ \frac{\Omega}{2} e^{i(\omega_0 - \omega_1)t} e^{i\omega_d t} & 0 \end{bmatrix} \begin{bmatrix} c_1(t) \\ c_0(t) \end{bmatrix} \\ &= \frac{\hbar\Omega}{2} \begin{bmatrix} e^{-i(\omega_d - \omega_{10})t} c_0(t) \\ e^{i(\omega_d - \omega_{10})t} c_1(t) \end{bmatrix}, \end{aligned} \quad (5.2.13)$$

where $\omega_{10} = \omega_1 - \omega_0$. Eliminating one state amplitude and writing it in terms of $c_1(t)$, a differential equation

$$\ddot{c}_1(t) + i(\omega_d - \omega_{10})\dot{c}_1(t) + \frac{\Omega^2}{4}c_1(t) = 0, \quad (5.2.14)$$

is derived. Solving the differential equation and defining the detuning $\Delta = \omega_d - \omega_{10}$, the solution is

$$c_1(t) = A e^{-i\Delta t/2} \sin \frac{\Omega'}{2} t, \quad (5.2.15)$$

where $\Omega' = [\Delta^2 + \Omega^2]^{1/2}$ is called generalized Rabi frequency.

The coefficient A is calculated from the initial condition $c_0(t = 0) = 1$, $c_1(t = 0) = 0$ as

$$A = \left[\frac{\Omega^2}{\Omega^2 + \Delta^2} \right]^{1/2}. \quad (5.2.16)$$

Finally, the population of state $|0\rangle$ and $|1\rangle$ are derived as

$$|c_1(t)|^2 = \frac{\Omega^2}{\Omega^2 + \Delta^2} \sin^2 \frac{\Omega'}{2} t = \frac{\Omega^2}{\Omega^2 + \Delta^2} \frac{1}{2} (1 - \cos \Omega' t) \quad (5.2.17)$$

$$|c_0(t)|^2 = 1 - |c_1|^2. \quad (5.2.18)$$

A cartoon of the two-level system dynamics calculated above is shown in Fig. 5.4. Let us first assume that the driving field is *on resonance*, meaning the driving field frequency matches the frequency difference between the ground and excited state $\Delta = \omega_d - \omega_{10} = 0 \rightarrow \Omega' = \Omega$. Initial state at $t = 0$ is the ground state $|0\rangle$. The time variation of the population simplifies to

$$|c_1(t)|^2 = \frac{1}{2} (1 - \cos \Omega t) \quad (5.2.19)$$

$$|c_0(t)|^2 = \frac{1}{2} (1 + \cos \Omega t). \quad (5.2.20)$$

The external field drives the population from $|0\rangle$ to $|1\rangle$ and oscillates between the two states. This population oscillation is called Rabi oscillation, which is one of the most fundamental quantum state manipulation.

On resonance, the occupation probability in the ground and the excited state oscillates between 0 and 1. Conversely, if ω_d is *off resonant* ($\Delta = \omega_d - \omega_{10} \neq 0$), only a partial population is going to oscillate. Also, at off-resonant condition, the oscillation frequency Ω' will increase with the detuning Δ .

As long as the external field continues to perturb the system, the occupation probability oscillates, but when the external field is turned off, the oscillation stops and the population at that time is maintained (Fig. 5.4c). If the states $|0\rangle$ and $|1\rangle$ are regarded as a bit of information 0 and 1, the two-level system can be used as a qubit. The timing of the drive turn-off can be controlled to generate a superposition state $|\psi\rangle = c_0|0\rangle + c_1|1\rangle$ with an arbitrary population difference. Rabi oscillation is the most fundamental manipulation of a qubit. The detailed derivation of Rabi

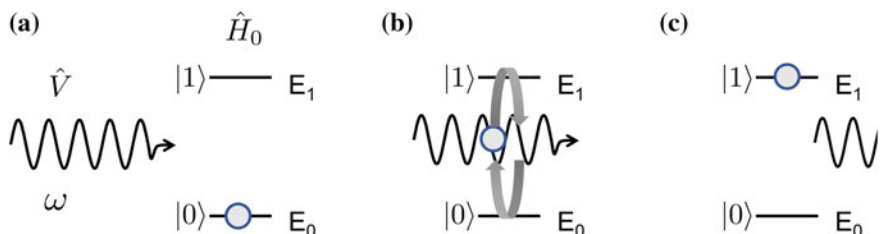


Fig. 5.4 Dynamics of two-level state system. **a** Two-level system with the state energy E_0 and E_1 . In addition to the unperturbed Hamiltonian \hat{H}_0 , which defines the two-level system and the perturbation \hat{V} , an external field with frequency ω is added. We assume the initial state of the system is in the ground state $|0\rangle$. **b** The occupancy probability of the two-level system affected by the external field Rabi-oscillates between the states $|0\rangle$ and $|1\rangle$. **c** When the external field is turned off, the occupation probability stops oscillating and stays at where it ended

oscillation using the Bloch equation and the visualization using the Bloch sphere will be described later in Sect. 6.4.

Fermi's Golden Rule

In the previous section, Rabi oscillation was considered in a two-level system, and found the occupation probability oscillates between states at Rabi frequency Ω . Often in experiments, it becomes necessary to calculate the transition probability per unit time from a certain initial state $|i\rangle$ to the final state $|f\rangle$, that is, the transition rate. Fermi's golden rule is a method for calculating this transition rate using the time-dependent perturbation theory.

From Eq. (5.2.9), the final state time evolution can be written as

$$\begin{aligned}\dot{c}_f(t) &= -\frac{i}{\hbar} \sum_n c_n(t) \langle \psi_f^0 | \hat{V}(t) | \psi_n^0 \rangle e^{i(E_f^0 - E_n^0)t/\hbar} \\ &= -\frac{i}{\hbar} \sum_n c_n(t) \langle \psi_f^0 | \hat{V}(t) | \psi_n^0 \rangle e^{i\omega_{fn}t},\end{aligned}$$

where in the last line, $\omega_{ij} = (E_i^0 - E_j^0)/\hbar$ is used. By integrating this equation, one obtains

$$c_f(t) - c_f(0) = -\frac{i}{\hbar} \sum_n \int_0^t dt' c_n(t') \langle \psi_f^0 | \hat{V}(t') | \psi_n^0 \rangle e^{i\omega_{fn}t'}. \quad (5.2.21)$$

For a weak perturbation, we can assume $c_n(t) \simeq c_n(0)$. Also, we assume that at $t = 0$, only the initial state is populated as $c_i(0) = 1$ ($c_n(0) = 0$ for $n \neq i$), then this equation is simplified as

$$c_f(t) \simeq -\frac{i}{\hbar} \sum_n c_n(0) \int_0^t dt' \langle \psi_f^0 | \hat{V}(t) | \psi_n^0 \rangle e^{i\omega_{fn}t'} \quad (5.2.22)$$

$$= -\frac{i}{\hbar} c_i(0) \int_0^t dt' \langle \psi_f^0 | \hat{V}(t) | \psi_i^0 \rangle e^{i\omega_{fi}t'} \quad (5.2.23)$$

$$= -\frac{i}{\hbar} \int_0^t dt' \langle \psi_f^0 | \hat{V}(t) | \psi_i^0 \rangle e^{i\omega_{fi}t'}. \quad (5.2.24)$$

Now consider two scenarios. The first case is when the perturbation \hat{V} does not change in time (though we are thinking of time-dependent perturbation theory). It sounds a bit confusing, but experimentally, for example, we can consider a situation in which a DC electric field is suddenly applied and then observe how the system develops.

The probability amplitude $c_f(t)$ in the final state is written as

$$c_f(t) = -\frac{i}{\hbar} \langle \psi_f^0 | \hat{V} | \psi_i^0 \rangle \int_0^t dt' e^{i\omega_{fi}t'} \quad (5.2.25)$$

$$= -\frac{1}{\hbar\omega_{fi}} \langle \psi_f^0 | \hat{V} | \psi_i^0 \rangle (e^{i\omega_{fi}t} - 1), \quad (5.2.26)$$

and the transition probability of the final state $P_{i \rightarrow f} = |c_f(t)|^2$ is derived as

$$P_{i \rightarrow f} = \frac{(e^{i\omega_{fi}t} - 1)(e^{-i\omega_{fi}t} - 1)}{\hbar^2 \omega_{fi}^2} \left| \langle \psi_f^0 | \hat{V} | \psi_i^0 \rangle \right|^2, \quad (5.2.27)$$

which simplifies to

$$P_{i \rightarrow f} = \frac{4 \sin^2 \left(\frac{\omega_{fi} t}{2} \right)}{\hbar^2 \omega_{fi}^2} \left| \langle \psi_f^0 | \hat{V} | \psi_i^0 \rangle \right|^2. \quad (5.2.28)$$

The denominator ω_{fi} can be very large value, such as in the case of optical transitions, and the transition probability decreases as the square of ω_{fi} .

For a short time interval or “right at the beginning”, the transition probability is

$$\begin{aligned} P_{i \rightarrow f} &\simeq \frac{4 \left(\frac{\omega_{fi} t}{2} \right)^2}{\hbar^2 \omega_{fi}^2} \left| \langle \psi_f^0 | \hat{V} | \psi_i^0 \rangle \right|^2 \\ &= \frac{t^2}{\hbar^2} \left| \langle \psi_f^0 | \hat{V} | \psi_i^0 \rangle \right|^2, \end{aligned}$$

from which the transition rate to the final state $\Gamma_f = \frac{dP_{i \rightarrow f}}{dt}$ is calculated as

$$\Gamma_f = \frac{t}{\hbar^2} \left| \langle \psi_f^0 | \hat{V} | \psi_i^0 \rangle \right|^2. \quad (5.2.29)$$

For the second case, we consider a sinusoidal perturbation $\hat{V}(t) = \hat{V}_0 e^{-i\omega t}$. Experimentally, this is quite common, since just about any spectroscopy using RF/microwave to optical electric field fits into this. Similar to the previous case, consider the probability amplitude of the final state $c_f(t)$, which is written as

$$c_f(t) = -\frac{i}{\hbar} \int_0^t dt' \langle \psi_f^0 | \hat{V}_0 | \psi_i^0 \rangle e^{-i(\omega - \omega_{fi})t'} \quad (5.2.30)$$

$$= \frac{1}{\hbar(\omega - \omega_{fi})} \langle \psi_f^0 | \hat{V}_0 | \psi_i^0 \rangle (e^{-i(\omega - \omega_{fi})t} - 1), \quad (5.2.31)$$

from which the transition probability of the final state $P_{i \rightarrow f}$ is calculated as

$$P_{i \rightarrow f} = \frac{4 \sin^2 \left(\frac{(\omega - \omega_{fi})t}{2} \right)}{\hbar^2 (\omega - \omega_{fi})^2} \left| \langle \psi_f^0 | \hat{V}_0 | \psi_i^0 \rangle \right|^2. \quad (5.2.32)$$

When the perturbation frequency ω is the same as the frequency difference of the states ω_{fi} , fulfilling the resonant condition ($\omega = \omega_{fi}$), and for a large t ($t \rightarrow \infty$), one can use the relation

$$\frac{\sin^2(\alpha t)}{\alpha^2 t} = \pi \delta(\alpha), \quad (5.2.33)$$

which simplifies the transition probability as

$$P_{i \rightarrow f} = \frac{\pi t \left| \langle \psi_f^0 | \hat{V}_0 | \psi_i^0 \rangle \right|^2}{\hbar^2}. \quad (5.2.34)$$

Transition rate to the final state $\Gamma_f = \frac{dP_{i \rightarrow f}}{dt}$ now takes a simple form

$$\boxed{\Gamma_f = \frac{\pi \left| \langle \psi_f^0 | \hat{V}_0 | \psi_i^0 \rangle \right|^2}{\hbar^2}}, \quad (5.2.35)$$

which is called a Fermi's golden rule which allows to calculate the transition rate from the perturbation.

So far, we have been focusing on the transition from the initial state $|i\rangle$ to a single final state $|f\rangle$ as shown in Fig. 5.5a.

As in Fig. 5.5, if there are multiple or continuum of final states, the total transition probability can be expanded as

Single final state

$$P_{\text{tot}} = P_{i \rightarrow f}$$

Multiple final states

$$P_{\text{tot}} = \sum_n P_{i \rightarrow f_n}$$

Continuum of final states

$$P_{\text{tot}} = \int P_{i \rightarrow f} \rho(E_f) dE,$$

where $\rho(E)$ is the density of states. It is probably straightforward in multiple final states, where the transition probability is a sum of all the different final states. For

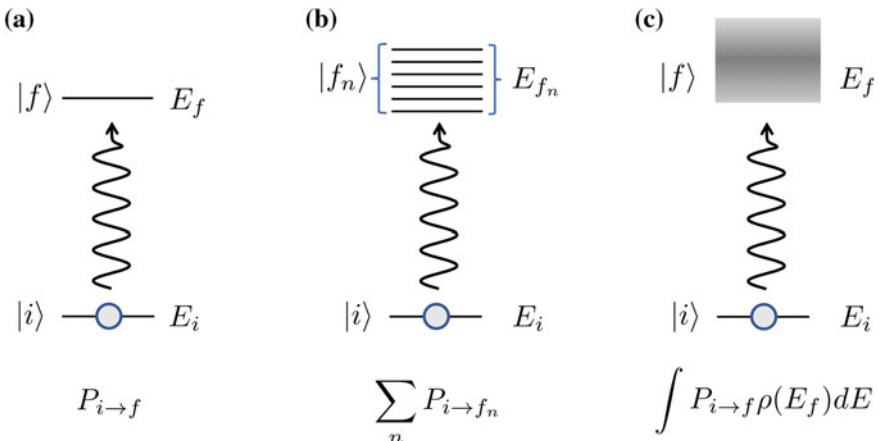


Fig. 5.5 Transition probability to various final state. **a** A single final state, **b** multiple final states, and **c** continuum of final states

in the case of a continuum, the density of states $\rho(E)$ is introduced. The density of state has a dimension

$$\rho(E) = \frac{\text{Number of states at } E}{\text{Unit energy}}, \quad (5.2.36)$$

which allows for the incorporation of all the final states within a continuum with a form $\int \rho(E_f) dE$.

5.2.1 Time-Dependent Perturbation Expansion

In the case of a two-level system with a sinusoidal drive, simple oscillatory dynamics in the occupation probability was observed. However, in general, the dynamics of time-dependent perturbation $\hat{V}(t)$ is difficult to calculate because there is no analytical solution for the perturbed Hamiltonian $\hat{\mathcal{H}} = \hat{\mathcal{H}}^0 + \hat{V}(t)$ for most cases. Here, we describe an approximation method that can be calculated by perturbation expansion of the time dependence of the external field.

As mentioned previously, the eigenstate $|\psi_n^0\rangle$ and the eigenenergy E_n^0 of the system before adding the perturbation satisfies

$$\hat{\mathcal{H}}^0 |\psi_n^0\rangle = E_n^0 |\psi_n^0\rangle. \quad (5.2.37)$$

The external perturbation alters the system Hamiltonian as

$$\hat{\mathcal{H}}^0 \rightarrow \hat{\mathcal{H}} = \hat{\mathcal{H}}^0 + \lambda \hat{V}. \quad (5.2.38)$$

The time evolution of the wavefunction using the Dirac picture is generally described as

$$|\psi(t)\rangle_I = \sum_n c_n(t) |\psi_n^0\rangle. \quad (5.2.39)$$

We can expand the state probability amplitude $c_n(t)$ in the power series of λ as

$$c_n(t) = c_n^0(t) + \lambda c_n^1(t) + \lambda^2 c_n^2(t) + \dots. \quad (5.2.40)$$

Now, the goal is to describe this coefficient c_n^i using $\hat{V}(t)$ and the unperturbed basis $|\psi_n^0\rangle$.

First, the time evolution from the initial state $|\psi(t_0)\rangle_I \equiv |i\rangle$ at $t = 0$ in the Dirac picture can be written using the time-evolution operator $\hat{U}_I(t, t_0)$ as

$$|\psi(t)\rangle_I = \hat{U}_I(t, t_0) |i\rangle. \quad (5.2.41)$$

Substituting the above to the Schrödinger equation in Dirac picture

$$i\hbar \frac{d|\psi(t)\rangle_I}{dt} = \lambda \hat{V}_I(t) |\psi(t)\rangle_I, \quad (5.2.42)$$

we obtain

$$i\hbar \frac{d\hat{U}_I(t, t_0)}{dt} |i\rangle = \lambda \hat{V}_I(t) \hat{U}_I(t, t_0) |i\rangle. \quad (5.2.43)$$

This equation is satisfied for an arbitrary initial state $|i\rangle$, and therefore, it can be rewritten as

$i\hbar \frac{d\hat{U}_I(t, t_0)}{dt} = \lambda \hat{V}_I(t) \hat{U}_I(t, t_0),$

(5.2.44)

which is the equation of motion for the unitary operator. Here, we used $\hat{V}_I = e^{i\hat{\mathcal{H}}^0 t/\hbar} \hat{V} e^{-i\hat{\mathcal{H}}^0 t/\hbar}$. $\hat{U}_I(t, t_0)$ represent the time-evolution operator from the initial time t_0 with a boundary condition $\hat{U}(t_0, t_0) = \hat{I}$.

Integrating this equation of motion, the left-hand-side of the equation is

$$\begin{aligned} i\hbar \int_{t_0}^t dt' \frac{d\hat{U}_I(t', t_0)}{dt'} &= i\hbar [\hat{U}_I(t, t_0) - \hat{U}_I(t_0, t_0)] \\ &= i\hbar [\hat{U}_I(t, t_0) - \hat{I}], \end{aligned} \quad (5.2.45)$$

and now the form of $\hat{U}_I(t, t_0)$ is written as

$$\hat{U}_I(t, t_0) = \hat{I} - \frac{i}{\hbar} \int_{t_0}^t dt' \lambda \hat{V}_I(t') \hat{U}_I(t', t_0). \quad (5.2.46)$$

The equation above is a nested equation in $\hat{U}_I(t, t_0)$ and it can be expanded as

$$\begin{aligned} \hat{U}_I(t, t_0) &= \hat{I} - \frac{i}{\hbar} \int_{t_0}^t dt' \lambda \hat{V}_I(t') \hat{U}_I(t', t_0) \\ &= \hat{I} - \frac{i}{\hbar} \int_{t_0}^t dt' \lambda \hat{V}_I(t') + \left(-\frac{i}{\hbar}\right)^2 \int_{t_0}^t dt' \int_{t_0}^{t'} dt'' \lambda^2 \hat{V}_I(t') \hat{V}_I(t'') \hat{U}_I(t'', t_0) \\ &= \hat{I} - \frac{i}{\hbar} \int_{t_0}^t dt' \lambda \hat{V}_I(t') + \left(-\frac{i}{\hbar}\right)^2 \int_{t_0}^t dt' \int_{t_0}^{t'} dt'' \lambda^2 \hat{V}_I(t') \hat{V}_I(t'') + \dots \end{aligned} \quad (5.2.47)$$

$$= \sum_{n=0}^{\infty} \left(-\frac{i}{\hbar}\right)^n \int_{t_0}^t dt_1 \dots \int_{t_0}^{t_{n-1}} dt_n \lambda^n \hat{V}_I(t_1) \hat{V}_I(t_2) \dots \hat{V}_I(t_n). \quad (5.2.48)$$

In the last line, the term $n = 0$ in the sum is \hat{I} and the time variable is rewritten as $t' \rightarrow t_1, t'' \rightarrow t_2, \dots \rightarrow t_n$ for a simplicity.

Since the form of the time evolution operator $\hat{U}_I(t, t_0)$ is obtained, now we consider the time evolution from the initial state $|i\rangle$ using Eq. (5.2.41).

$|\psi(t)\rangle_I$ is expanded using the unperturbed eigenstate $|n\rangle \equiv |\psi_n^0\rangle$ as

$$\begin{aligned} |\psi(t)\rangle_I &= \hat{U}_I(t, t_0) |i\rangle = \sum_n |n\rangle \langle n| \hat{U}_I(t, t_0) |i\rangle \\ &= \sum_n \langle n| \hat{U}_I(t, t_0) |i\rangle |n\rangle \end{aligned} \quad (5.2.49)$$

$$\begin{aligned} &= \sum_n \left[\langle n| \hat{I}|i\rangle + \lambda \left(-\frac{i}{\hbar} \right) \int_{t_0}^t dt_1 \langle n| \hat{V}_I(t_1) |i\rangle \right. \\ &\quad \left. + \lambda^2 \left(-\frac{i}{\hbar} \right)^2 \int_{t_0}^t dt_1 \int_{t_0}^{t_1} dt_2 \langle n| \hat{V}_I(t_1) \hat{V}_I(t_2) |i\rangle + \dots \right] |n\rangle. \end{aligned} \quad (5.2.50)$$

Also, by making correspondence with Eqs. (5.2.39) and (5.2.40)

$$\begin{aligned} |\psi(t)\rangle_I &= \sum_n c_n(t) |n\rangle \\ &= \sum_n (c_n^0(t) + \lambda c_n^1(t) + \lambda^2 c_n^2(t) + \dots) |n\rangle, \end{aligned} \quad (5.2.51)$$

each term $c_n^i(t)$ can now be derived as

$$c_n^0(t) = \langle n| \hat{I}|i\rangle = \delta_{ni} \quad (5.2.52)$$

$$\begin{aligned} c_n^1(t) &= -\frac{i}{\hbar} \int_{t_0}^t dt_1 \langle n| \hat{V}_I(t_1) |i\rangle \\ &= -\frac{i}{\hbar} \int_{t_0}^t dt_1 \langle n| \hat{V}(t_1) |i\rangle e^{i\omega_{ni} t_1} \end{aligned} \quad (5.2.53)$$

$$\begin{aligned} c_n^2(t) &= -\frac{1}{\hbar^2} \int_{t_0}^t dt_1 \int_{t_0}^{t_1} dt_2 \langle n| \hat{V}_I(t_1) \hat{V}_I(t_2) |i\rangle \\ &= -\frac{1}{\hbar^2} \sum_m \int_{t_0}^t dt_1 \int_{t_0}^{t_1} dt_2 \langle n| \hat{V}_I(t_1) |m\rangle \langle m| \hat{V}_I(t_2) |i\rangle \\ &= -\frac{1}{\hbar^2} \sum_m \int_{t_0}^t dt_1 \int_{t_0}^{t_1} dt_2 \langle n| \hat{V}(t_1) |m\rangle \langle m| \hat{V}(t_2) |i\rangle e^{i\omega_{nm} t_1 + i\omega_{mi} t_2}. \end{aligned} \quad (5.2.54)$$

While the derivation, $\hat{V}_I = e^{i\hat{\mathcal{H}}^0 t/\hbar} \hat{V} e^{-i\hat{\mathcal{H}}^0 t/\hbar}$ is used to modify $\langle n| \hat{V}_I(t) |i\rangle$ as

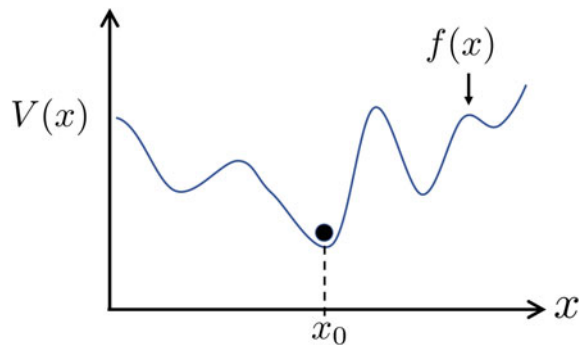
$$\langle n| \hat{V}_I(t) |i\rangle = \langle n| e^{i\hat{\mathcal{H}}^0 t/\hbar} \hat{V} e^{-i\hat{\mathcal{H}}^0 t/\hbar} |i\rangle \quad (5.2.55)$$

$$= \langle n| \hat{V}(t) |i\rangle e^{i\omega_{ni} t}, \quad (5.2.56)$$

where $\omega_{ni} = \omega_n - \omega_i$.

Time-dependent perturbation theory is often used to calculate the transition probability to state $|n\rangle$ from an initial state $|i\rangle$. When the final state $|n\rangle$ of interest is

Fig. 5.6 A particle located at the bottom of the potential landscape



different from the initial state, $c_n^0(t) = 0$ and the first-order approximation $c_n^1(t)$ is important. The first-order approximation of the transition probability $P_{i \rightarrow n}$ is

$$P_{i \rightarrow n} = \left| \frac{1}{i\hbar} \int_0^t dt' \langle n | \hat{V}(t') | i \rangle e^{i\omega_n t'} \right|^2. \quad (5.2.57)$$

Problems

Problem 5-1 In order to observe quantum phenomena, the experimental system or a sample of interest is often cooled by a refrigerator or some active method, such as laser cooling. At a low enough temperature, the system of interest should be in a ground state, meaning the bottom of a potential well as shown in Fig. 5.6. The particle position in ground state is $x = x_0$ at the bottom of the well defined by a potential curve $f(x)$.

Show that for a small amplitude (or energy), the system can always be expressed as a harmonic oscillator. (This is not a quantum problem, but important to recognize why we use the harmonic oscillator as the building blocks in quantum technology.)

[Hint: Use Taylor expansion.]

Problem 5-2 Consider adding an extra “push” to a harmonic oscillator so the classical energy of the system reads

$$E = \frac{p^2}{2m} + \frac{m\omega^2 x^2}{2} + \alpha x.$$

This equation can be rewritten with a displaced equilibrium position $x = 0 \rightarrow x_0$ as

$$E = \frac{p^2}{2m} + \frac{m\omega^2(x - x_0)^2}{2} - E_{\text{offset}}.$$

Now consider the same situation for a quantum harmonic oscillator, where the system Hamiltonian is described as

$$\begin{aligned}\hat{\mathcal{H}} &= \hat{\mathcal{H}}_0 + \hat{V} \\ &= \hbar\omega\hat{a}^\dagger\hat{a} + \alpha\hat{x} \\ &= \hbar\omega\hat{a}^\dagger\hat{a} + \alpha x_{\text{zpf}}(\hat{a} + \hat{a}^\dagger),\end{aligned}$$

where $x_{\text{zpf}} = \sqrt{\frac{\hbar}{2m\omega}}$ is zero-point displacement fluctuation of the harmonic oscillator.

- (i) Solve the classical equilibrium position x_0 and energy offset E_{offset} .
- (ii) Use perturbation theory to calculate the first-order correction for the wavefunction $|\psi_n^1\rangle$.
- (iii) Use the result in (ii) to calculate the new ground state $|0'\rangle$.
- (iv) Find the new ground state energy E_0 by calculating up to second-order correction.
- (v) Find the expectation value of position $\langle x \rangle$ for $|0'\rangle$.
- (vi) Compare E_0 and $\langle x \rangle$ with x_0 and E_{offset} obtained in (i).

Problem 5-3 The Hamiltonian and eigenenergy of a harmonic oscillator is given as

$$\begin{aligned}\hat{\mathcal{H}}_0 &= \hbar\omega_0\hat{a}^\dagger\hat{a} \\ E_n &= \hbar n\omega_0\end{aligned}$$

and the energy spacing between states $\Delta E_n = E_n - E_{n-1} = \hbar\omega_0$ are all the same. *LC* circuit (or *LC* resonator) is a harmonic oscillator and have the same Hamiltonian and the energy spacing. In a superconducting circuits, there is a nonlinear circuit component called Josephson junction and its variants, which can introduce a nonlinear response to the harmonic system.

Suppose, a nonlinear circuit component added to a *LC* resonator has a perturbation a form

$$\hat{V} = \hbar\alpha\hat{a}^\dagger\hat{a}\hat{a}^\dagger\hat{a}.$$

- (i) Write a system Hamiltonian $\hat{\mathcal{H}} = \hat{\mathcal{H}}_0 + \hat{V}$.
- (ii) Find the eigenenergy of the system $E_n = E_n^0 + E_n^1$ including up to a first-order energy correction.
- (iii) Find the energy separation ΔE_n of the system.
- (iv) Discuss that this system can actually be used as a qubit.

Problem 5-4 External control is applied to a qubit forming a new Hamiltonian

$$\hat{\mathcal{H}} = \hat{\mathcal{H}}_0 + \hat{V} = \frac{\hbar\omega_q}{2}\hat{\sigma}_z + \hbar\alpha\hat{\sigma}_x,$$

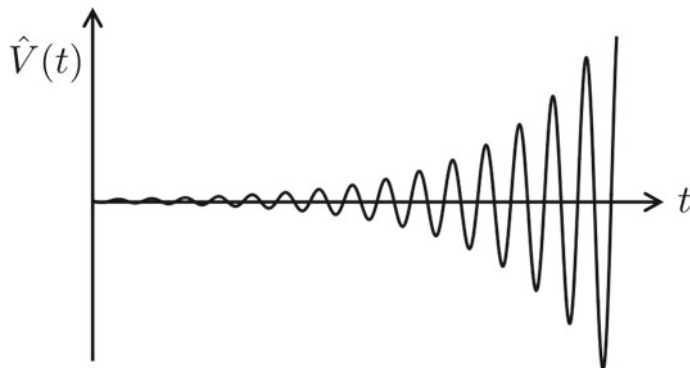


Fig. 5.7 Sinusoidal perturbation being slowly turned on

where $\alpha \ll \omega_q$.

- Find the new state $|0'\rangle$ and $|1'\rangle$ in terms of the original qubit state $|0\rangle$ and $|1\rangle$, using up to a first-order perturbation.
- Find the energies of the new states $E_{0'}$ and $E_{1'}$.
- Can the new states $|0'\rangle$ and $|1'\rangle$ be used as a basis for qubit, other words, are they orthogonal?

Problem 5-5 Consider a slow turn-on of a sinusoidal perturbation

$$\hat{V}(t) = \hat{V}_0 e^{-i\omega t} e^{\gamma t} \quad (5.2.58)$$

as shown in Fig. 5.7.

- Calculate the transition probability $P_{i \rightarrow f}$.

[Hint: Since it is a “slow” turn-on, take the time integral from $t' = -\infty$].

- Find the transition rate Γ_f .

Part II

Harmonic Oscillator, Qubit and Coupled Quantum Systems



Harmonic Oscillator

6

6.1 Harmonic Oscillator and Its Hamiltonian

Lights, sounds, vibrations—such waves we meet in our daily lives are mostly understood as harmonic oscillations supported in various media. Harmonic oscillators are frequently expressed in the form of Hamiltonian with canonical variables q and p , as¹

$$\mathcal{H} = \frac{p^2}{2m} + \frac{1}{2}m\omega^2 q^2.$$

Here m is the mass of an object and ω is the angular frequency of the harmonic oscillation. To switch to quantum mechanics, canonical variables should be replaced by operators $q \rightarrow \hat{q}$ and $p \rightarrow \hat{p} = (\hbar/i)d/dq$. Whenever there is no confusion, we omit hats on the operators.

By defining annihilation and creation operators by $a = \sqrt{m\omega/2\hbar}[q + (i/m\omega)p]$ and $a^\dagger = \sqrt{m\omega/2\hbar}[q - (i/m\omega)p]$, above Hamiltonian can be rewritten as

$$\mathcal{H} = \hbar\omega \left(a^\dagger a + \frac{1}{2} \right)$$

with a set of eigenstates $\{|n\rangle ; n = 0, 1, 2, \dots\}$ which are called Fock states. Since the index n in $|n\rangle$ represents the number of quanta of the harmonic oscillation, the Fock states are also dubbed as number states.

Supplementary Information The online version contains supplementary material available at https://doi.org/10.1007/978-981-19-4641-7_6.

¹ Light quantum, photon, is an exception for its massless nature. Nevertheless, we can theoretically understand it as a harmonic oscillator with slightly different but essentially the same Hamiltonian.

Fock states constitute a complete orthonormal basis. Fock state $|n\rangle$ has the mean photon number n and vanishing standard deviation. For these properties and their physical comprehensibility, Fock states are often used as a fundamental tool to expand and analyze other quantum states given in this section.

6.2 Electromagnetic Waves and Ladder Operators

6.2.1 Quantization of Electromagnetic Waves

For a quantum-engineering purpose, there is a need to flip the state between the ground state and excited state, or generate superposition of them by some means. In general, the ground ($|g\rangle$) and excited ($|e\rangle$) states are non-degenerate, separated in energy by $\hbar\omega_q$, and in most systems in reality the quantum state refers to the electronic and/or spin states. Therefore, the flip operation is done by applying electromagnetic waves with its frequency around ω_q , the transition frequency.

Again for the purpose of quantum engineering, it is often necessary to treat electromagnetic fields in a quantum fashion. The quantum theory of light is really insightful and delightful to learn; however, it is beyond the scope of this book to fully describe it without messing up the main streamline of the story. So that we shall only scratch the surface of it and pick several useful topics up. For more detail, please find them in the literature [8].

We shall focus first on a confined optical mode, or a cavity mode, where one might imagine an optical resonance mode such as the one in the Fabry–Perót resonator and any other types of it. To simplify the situation, a single cavity mode is considered that yields the energy

$$\mathcal{E} = \frac{1}{2} \int_{\text{cavity}} \left(\epsilon_0 \mathbf{E}^2 + \frac{1}{\mu_0} \mathbf{B}^2 \right) dV \quad (6.2.1)$$

$$= 2\epsilon_0 V_{\text{cavity}} \omega_c^2 \mathbf{A}_0 \cdot \mathbf{A}_0^* \quad (6.2.2)$$

where \mathbf{E} , \mathbf{B} , and \mathbf{A}_0 denote the electric field, magnetic field, and amplitude of vector potential,² ϵ_0 and μ_0 the vacuum permittivity and permeability, V_{cavity} and ω_c the mode volume and the resonant frequency of the cavity mode under concern. By introducing canonical variables q and p together with the polarization vector $\boldsymbol{\varepsilon}$ to rewrite $A_0 = \sqrt{1/4\epsilon_0 V_{\text{cavity}} \omega_c^2} (\omega_c q + i p) \boldsymbol{\varepsilon}$, the energy reads

$$\mathcal{E} = \frac{1}{2} (p^2 + \omega_c^2 q^2) \quad (6.2.3)$$

which is manifestly a harmonic oscillator. The canonical variables q and p are replaced by operators \hat{q} and \hat{p} to make this Hamiltonian quantum mechanical.³ With

² It is assumed that vector potential have the form $\mathbf{A}_0 e^{-i\omega_c t + i\mathbf{k} \cdot \mathbf{r}} + \mathbf{A}_0^* e^{i\omega_c t - i\mathbf{k} \cdot \mathbf{r}}$. Coulomb gauge and the relations $\mathbf{E} = -\partial \mathbf{A}/\partial t$ and $\mathbf{B} = \nabla \times \mathbf{A}$ are used as well.

³ All “hats” in the quantum-mechanical operators are not shown throughout this book unless there is a confusing situation.

in the classical picture, one can imagine continuous trajectory of (q, p) in classical harmonic oscillator. There q and p are oscillating with the relative phase of $\pi/2$ to enclose a circle in the phase space. In quantum-theoretic treatment, the state of photon is not a point in a phase space but rather a distribution. In analogy with the classical wave-like understandings of light the variables q and p are called *in-phase* and *quadrature* components of the quantum states. As in the usual prescription, we can define alternatively $\mathbf{A}_0 = \sqrt{\hbar/2\varepsilon_0 V_{\text{cavity}}\omega_c} a \boldsymbol{\varepsilon}$ using annihilation operator a to obtain

$$\mathcal{E} = \hbar\omega_c \left(a^\dagger a + \frac{1}{2} \right). \quad (6.2.4)$$

This is a familiar expression of a harmonic oscillator in quantum mechanics and we mostly omit the zero-point energy $\hbar\omega_c/2$. This expression is well-understood by noticing that the operator $\hat{n} = a^\dagger a$ counts the number of photons in the mode. In such an expression, the electric and magnetic fields are written as

$$\mathbf{E} = i \sqrt{\frac{\hbar\omega_c}{2\varepsilon_0 V_{\text{cavity}}}} \boldsymbol{\varepsilon} (ae^{-i\omega_c t + i\mathbf{k}\cdot\mathbf{r}} - a^\dagger e^{i\omega_c t - i\mathbf{k}\cdot\mathbf{r}}), \quad (6.2.5)$$

$$\mathbf{B} = i \sqrt{\frac{\hbar\omega_c}{2\varepsilon_0 V_{\text{cavity}} c^2}} \hat{\mathbf{k}} \times \boldsymbol{\varepsilon} (ae^{-i\omega_c t + i\mathbf{k}\cdot\mathbf{r}} - a^\dagger e^{i\omega_c t - i\mathbf{k}\cdot\mathbf{r}}). \quad (6.2.6)$$

Here $\hat{\mathbf{k}}$ is a unit vector parallel to the wavevector. Note that in the rotating frame such that the time-dependent factors associated with a and a^\dagger are hidden, and properly choosing the phase, these reduce to

$$\mathbf{E} = E_{\text{zpf}} (a + a^\dagger) \boldsymbol{\varepsilon}, \quad (6.2.7)$$

$$\mathbf{B} = B_{\text{zpf}} (a + a^\dagger) \hat{\mathbf{k}} \times \boldsymbol{\varepsilon}. \quad (6.2.8)$$

where $E_{\text{zpf}} = \sqrt{\hbar\omega_c/2\varepsilon_0 V_{\text{cavity}}}$ and $B_{\text{zpf}} = \sqrt{\hbar\omega_c/2\varepsilon_0 V_{\text{cavity}} c^2}$ are vacuum amplitudes or the zero-point fluctuations of the cavity field: the smaller the cavity, the larger the vacuum amplitudes. The subscript “zpf” stands for the zero-point fluctuation.

6.2.2 Ladder Operators of a Harmonic Oscillator

At this point, let us review the properties of the annihilation and creation operators a and a^\dagger . From the commutation relation $[a, a^\dagger] = 1$, we can immediately see that $[\hat{n}, a] = -a$ and $[\hat{n}, a^\dagger] = a^\dagger$. Now we want to consider the eigenstate $|n\rangle$ of the

number operator $\hat{n} = a^\dagger a$. As the reader can see, we discriminate the number operator \hat{n} and its eigenvalue n in this section. The eigenvalue n is the number of quanta: $\hat{n} |n\rangle = n |n\rangle$. Then let us try operating above commutation relations on $|n\rangle$:

$$\begin{aligned}\hat{n}(a - a\hat{n}) |n\rangle &= (\hat{n}a - na) |n\rangle = -a |n\rangle, \\ (\hat{n}a^\dagger - a^\dagger \hat{n}) |n\rangle &= (\hat{n}a^\dagger - na^\dagger) |n\rangle = a^\dagger |n\rangle.\end{aligned}$$

These are rewritten as

$$\hat{n}(a |n\rangle) = (n - 1)(a |n\rangle), \quad (6.2.9)$$

$$\hat{n}(a^\dagger |n\rangle) = (n + 1)(a^\dagger |n\rangle), \quad (6.2.10)$$

which can be interpreted as follows. The quantum states $(a |n\rangle)$ and $(a^\dagger |n\rangle)$ are eigenstates of the number operator \hat{n} , respectively, with the eigenvalues $n - 1$ and $n + 1$. In other words, the operator a makes the number of quanta decrease by 1 and a^\dagger does the number of quanta increase by 1, manifesting themselves as ladder operators.

6.3 Quantum States of a Harmonic Oscillator

6.3.1 Coherent State

Fock states are the eigenstates of the harmonic oscillator, but in real life it is hard to encounter them. Real life's single-mode harmonic oscillations mostly appear as sinusoidal, monochromatic waves. Then what quantum state is the closest to the classical, monochromatic wave? Remember that the monochromatic wave in the classical mechanics can be generated by the forced oscillation. Therefore, we would like to consider the forced oscillation in a quantum manner.

Driving a harmonic oscillator can be done by injecting energy into the oscillator by a beam-splitter interaction $\mathcal{H}_d = i\hbar\Omega(ba^\dagger - b^\dagger a)$, where b denotes the annihilation operator of the driving field. The driving field is usually quite intense that it is replaced by the classical amplitude β . By mocking up the coefficients as $\Omega\beta = \alpha/\tau$ with τ being the time duration of the drive, the interaction reads $\mathcal{H}_d = i\hbar[(\alpha/\tau)a^\dagger - (\alpha^*/\tau)a]$ and gives the unitary evolution

$$D(\alpha) = e^{-i\frac{\mathcal{H}_d}{\hbar}\tau} = e^{\alpha a^\dagger - \alpha^* a}.$$

The unitary operator $D(\alpha)$ is called the displacement operator. To see why it is “displacement,” we shall see important properties of $D(\alpha)$.

First, suppose that the vacuum $|0\rangle$ is subject to the forced oscillation. The resultant state is $|\alpha\rangle \stackrel{\text{def}}{=} D(\alpha)|0\rangle$ and we expect $|\alpha\rangle$ is the closest quantum analogue of the

classical oscillation. Then let us make a act on $|\alpha\rangle$:

$$\begin{aligned} a|\alpha\rangle &= ae^{\alpha a^\dagger - \alpha^* a} |0\rangle \\ &= ae^{\alpha a^\dagger} e^{-\alpha^* a} e^{-\frac{|\alpha|^2}{2}} |0\rangle \\ &= \alpha e^{\alpha a^\dagger} e^{-\alpha^* a} e^{-\frac{|\alpha|^2}{2}} |0\rangle \\ &= \alpha e^{\alpha a^\dagger - \alpha^* a} |0\rangle \\ &= \alpha |\alpha\rangle. \end{aligned}$$

In the second and fourth lines, the Baker–Campbell–Hausdorff formula $e^A e^B = e^{A+B+[A,B]/2}$ is used. In the third line, the factor $ae^{\alpha a^\dagger}$ is Taylor-expanded and the repetitive use of commutation relation $[a, a^\dagger] = 1$ yields $e^{\alpha a^\dagger}a + \alpha e^{\alpha a^\dagger}$. The first of the two terms acts on $|0\rangle$ to give zero. From above calculation, $|\alpha\rangle$ is revealed to be an eigenstate of the annihilation operator a .

Now, estimating the expectation values of $q = \sqrt{2\hbar/m\omega}(a + a^\dagger)/2$ and $p = \sqrt{2m\hbar\omega}(a - a^\dagger)/2i$ is not so difficult. Since $a|\alpha\rangle = \alpha|\alpha\rangle$ and $\langle\alpha|a^\dagger = \langle\alpha|\alpha^*$,

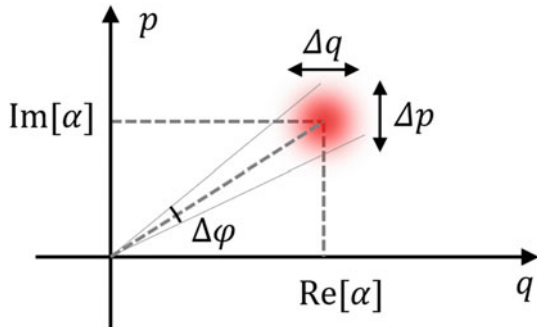
$$\begin{aligned} \langle q \rangle &= \langle\alpha|q|\alpha\rangle = \sqrt{\frac{2\hbar}{m\omega}} \frac{\alpha + \alpha^*}{2} = \sqrt{\frac{2\hbar}{m\omega}} \text{Re}[\alpha], \\ \langle p \rangle &= \langle\alpha|p|\alpha\rangle = \sqrt{2m\hbar\omega} \frac{\alpha - \alpha^*}{2i} = \sqrt{2m\hbar\omega} \text{Im}[\alpha]. \end{aligned}$$

In order to calculate the standard deviations of q and p , we can utilize the equalities $\langle\alpha|aa|\alpha\rangle = \alpha^2$, $\langle\alpha|a^\dagger a|\alpha\rangle = |\alpha|^2$ and $\langle\alpha|aa^\dagger|\alpha\rangle = |\alpha|^2 + 1$ to get

$$\begin{aligned} \Delta q &\equiv \sqrt{\langle q^2 \rangle - \langle q \rangle^2} \\ &= \sqrt{\frac{2\hbar}{m\omega} \frac{\alpha^2 + \alpha^{*2} + 2|\alpha|^2 + 1 - \alpha^2 - 2|\alpha|^2 - \alpha^{*2}}{4}} \\ &= \sqrt{\frac{\hbar}{2m\omega}}, \\ \Delta p &\equiv \sqrt{\langle p^2 \rangle - \langle p \rangle^2} \\ &= \sqrt{2m\hbar\omega \frac{-\alpha^2 - \alpha^{*2} + 2|\alpha|^2 + 1 + \alpha^2 + \alpha^{*2} - 2|\alpha|^2}{4}} \\ &= \sqrt{\frac{m\hbar\omega}{2}}. \end{aligned}$$

If we consider the phase space, or qp plane, the state $|\alpha\rangle$ is represented as a distribution located at $(\sqrt{2\hbar/m\omega}\text{Re}[\alpha], \sqrt{2m\hbar\omega}\text{Im}[\alpha])$ with the extent $\sqrt{\hbar/2m\omega}$ in q - and $\sqrt{m\hbar\omega}/2$ in p -axes. Note that $\Delta q \Delta p = \hbar/2$, implying that the state $|\alpha\rangle$ is the minimum-uncertainty state. Remembering the classical harmonic oscillation, where

Fig. 6.1 Schematic illustration of the coherent state in the phase space



the phase-space representation is a point in a rotating frame, the state $|\alpha\rangle$ certainly seems to be the quantum version of the forced oscillation of the harmonic oscillator. The state $|\alpha\rangle$ is thus deduced to be phase-coherent, by which the term coherent state is given (Fig. 6.1).

We shall rewrite the state $|\alpha\rangle$ in terms of the Fock states: $|\alpha\rangle = \sum_{n=0}^{\infty} A_n |n\rangle$. From the equality $a |\alpha\rangle = \alpha |\alpha\rangle$, one can get the recurrence relation $A_{n+1} = \alpha A_n / \sqrt{n+1}$ and deduce $A_n = \alpha^n A_0 / \sqrt{n!}$. Therefore, $|\alpha\rangle = \sum_{n=0}^{\infty} (\alpha^n / \sqrt{n!}) A_0 |n\rangle$. The coefficient A_0 can be determined by the normalization condition $\langle \alpha | \alpha \rangle = 1$ as $A_0 = e^{-|\alpha|^2/2}$, so that the final form is

$$|\alpha\rangle = \sum_{n=0}^{\infty} \frac{\alpha^n}{\sqrt{n!}} e^{-\frac{|\alpha|^2}{2}} |n\rangle. \quad (6.3.1)$$

The coefficient squared represents the number distribution of the coherent state:

$$P_n = \frac{|\alpha|^{2n}}{n!} e^{-|\alpha|^2}.$$

The standard deviation of the photon number reads

$$\Delta n \equiv \sqrt{\langle (a^\dagger a)^2 \rangle - \langle a^\dagger a \rangle^2} = |\alpha|$$

and together with P_n , the number distribution of the coherent state is revealed to be a Poissonian one.

We should keep in mind that the set of coherent state $\{|\alpha\rangle ; \alpha \in \mathbb{C}\}$ is said to be overcomplete. This stands for the fact that with this basis set one can express any quantum state composed of a harmonic oscillator; however, any two coherent states are not rigorously orthogonal to each other. Let us check this by calculating $\langle \beta | \alpha \rangle$ for $\alpha, \beta \in \mathbb{C}$. To do this math, we can use the following formula:

$$D(\alpha) D(\beta) = e^{(\alpha\beta^* - \alpha^*\beta)/2} D(\alpha + \beta)$$

which states that the two sequential application of displacement operators with α and β results in the displacement by $\alpha + \beta$ with a global phase acquired. This leads to the following result:

$$\begin{aligned}\langle \beta | \alpha \rangle &= \langle 0 | D^\dagger(\beta) D(\alpha) | 0 \rangle \\ &= \langle 0 | e^{(-\beta\alpha^* + \beta^*\alpha)/2} D(\alpha - \beta) | 0 \rangle \\ &= e^{(-\beta\alpha^* + \beta^*\alpha)/2} \langle 0 | \alpha - \beta \rangle \\ &= e^{(-\beta\alpha^* + \beta^*\alpha)/2} e^{-|\alpha - \beta|^2/2} \langle 0 | (|0\rangle + |\alpha - \beta| |1\rangle + \dots) \\ &= e^{-(|\alpha|^2 + |\beta|^2 - 2\beta^*\alpha)/2} \\ &\neq \delta(\alpha - \beta).\end{aligned}$$

Another thing to note here in the end of this section is that the coherent state analyzed here is a quantum analogue of the classical sinusoidal, forced oscillation, as described in the beginning. Then why are we dealing with such a stuff? How such a “classical” state appear in the quantum technology that we are to learn? We have a simple answer that the electromagnetic waves we have in laboratories and even in daily lives are the coherent states and principal tool we can poke the quantum object with is lasers and microwaves in the coherent states. We need to understand our indispensable tool of electromagnetic waves in terms of the coherent state and apply the knowledge to properly control the quantum states of photons, atoms, and artificial quantum systems.

6.3.2 Schrödinger's Cat State

An interesting states are realized by superposing two coherent states $|\alpha\rangle$ and $|-\alpha\rangle$, which are called Schrödinger's cat states, or simply the cat states. Here for simplicity we take the complex number α to be real and consider two cats:

$$\begin{aligned}|\text{cat}_{\text{even}}\rangle &= \frac{|\alpha\rangle + |-\alpha\rangle}{A_{\text{even}}}, \\ |\text{cat}_{\text{odd}}\rangle &= \frac{|\alpha\rangle - |-\alpha\rangle}{A_{\text{odd}}}\end{aligned}$$

which are called even cat and odd cat, respectively. A_{even} and A_{odd} normalizes the states here. Let us express these states in the Fock basis $\{|n\rangle\}$. By looking at Eq. (6.3.1), it can be seen that the even (odd) cat state contains only the even (odd) number Fock states and concrete expressions are given as

$$\begin{aligned}|\text{cat}_{\text{even}}\rangle &= \frac{2}{A_{\text{even}}} \sum_{n=0}^{\infty} \frac{\alpha^{2n}}{\sqrt{(2n)!}} e^{-\frac{\alpha^2}{2}} |2n\rangle, \\ |\text{cat}_{\text{odd}}\rangle &= \frac{2}{A_{\text{odd}}} \sum_{n=0}^{\infty} \frac{\alpha^{2n+1}}{\sqrt{(2n+1)!}} e^{-\frac{\alpha^2}{2}} |2n+1\rangle.\end{aligned}$$

These even and odd cat states are apparently orthogonal to each other, manifesting themselves as a simplest example of qubit encoding in the infinite-dimensional Hilbert space held by a harmonic oscillator.

6.3.3 Squeezed State

Light-matter interaction is so diverse that various nonlinear interactions among photons can take place. Nonlinear optical phenomena are characterized by their order m where $m + 1$ photons are involved in the nonlinear process with strength characterized by nonlinear coefficient $\chi^{(m)}$. The most simple, exemplary process is m th harmonic generation where m -photon absorption (emission) and one-photon emission (absorption) occurs at once in a two-level system or certain crystals. Sum- and difference-frequency generation are classified as $\chi^{(2)}$ processes. Frequently appearing nonlinearities are $\chi^{(2)}$ nonlinearity, which gives the interaction Hamiltonian with the products of three operators $i\hbar g(aaa^\dagger - a^\dagger a^\dagger a)$, and $\chi^{(3)}$ nonlinearity with four operators. By applying a monochromatic drivings and replace one or two operators by classical numbers in $\chi^{(2)}$ or $\chi^{(3)}$ Hamiltonian, one can get so-called squeezing Hamiltonian

$$\mathcal{H}_s = i\hbar \frac{r}{2\tau} (e^{i\phi} a^2 - e^{-i\phi} a^\dagger)^2.$$

and squeezing operator

$$S(r) = e^{-i\frac{\mathcal{H}_s}{\hbar}\tau} = e^{\frac{r}{2}(e^{i\phi} a^2 - e^{-i\phi} a^\dagger)^2}.$$

for the unitary evolution.

Though its action on an arbitrary state is very tough to calculate, we can deduce some properties by inspecting the action on the coherent state. Let us work out a calculation of $S^\dagger(r)aS(r)$ for this purpose. With the use of the Baker–Campbell–Hausdorff formula, $\tilde{S} = (\tilde{r}a^2 - \tilde{r}^*a^\dagger)^2$, and $\tilde{r} = re^{i\phi}/2$, this reads

$$\begin{aligned} S^\dagger(r)aS(r) &= e^{-\tilde{S}}ae^{\tilde{S}} \\ &= a - [\tilde{S}, a] + \frac{1}{2!} [\tilde{S}, [\tilde{S}, a]] - \frac{1}{3!} [\tilde{S}, [\tilde{S}, [\tilde{S}, a]]] + \dots \\ &= a + \frac{1}{2!} 2^2 |\tilde{r}|^2 a + \frac{1}{4!} 2^4 |\tilde{r}|^4 a + \dots \\ &\quad - 2\tilde{r}^* a^\dagger - \frac{1}{3!} 2^3 \tilde{r}^* |\tilde{r}|^2 a^\dagger - \frac{1}{5!} 2^5 \tilde{r}^* |\tilde{r}|^4 a^\dagger - \dots \\ &= a \sum_{n=0}^{\infty} \frac{|2\tilde{r}|^{2n}}{(2n)!} - a^\dagger \frac{\tilde{r}^*}{|\tilde{r}|} \sum_{n=0}^{\infty} \frac{|2\tilde{r}|^{2n+1}}{(2n+1)!} \\ &= a \cosh r - a^\dagger e^{-i\phi} \sinh r. \end{aligned}$$

Then we are able to calculate the expectation values of q and p with the state $|r, \alpha\rangle \equiv S(r)|\alpha\rangle$ as

$$\begin{aligned}\langle q \rangle &\equiv \langle r, \alpha | q | r, \alpha \rangle \\&= \sqrt{\frac{\hbar}{2m\omega}} \langle \alpha | S^\dagger(r)(a + a^\dagger)S(r) | \alpha \rangle \\&= \sqrt{\frac{\hbar}{2m\omega}} (\alpha \cosh r - \alpha^* e^{-i\phi} \sinh r + \alpha^* \cosh r - \alpha e^{i\phi} \sinh r) \\&= \sqrt{\frac{\hbar}{2m\omega}} [(\alpha + \alpha^*) \cosh r - (\alpha e^{i\phi} + \alpha^* e^{-i\phi}) \sinh r]\end{aligned}$$

and similarly

$$\begin{aligned}\langle p \rangle &\equiv \langle r, \alpha | p | r, \alpha \rangle \\&= \sqrt{\frac{m\hbar\omega}{2}} [(\alpha - \alpha^*) \cosh r + (\alpha e^{i\phi} - \alpha^* e^{-i\phi}) \sinh r].\end{aligned}$$

Furthermore, we want to evaluate $\langle q^2 \rangle \equiv \langle r, \alpha | q^2 | r, \alpha \rangle = \langle \alpha | S^\dagger(r)q^2S(r) | \alpha \rangle$ and $\langle p^2 \rangle \equiv \langle r, \alpha | p^2 | r, \alpha \rangle = \langle \alpha | S^\dagger(r)p^2S(r) | \alpha \rangle$ in order to assess the standard deviations. $S^\dagger(r)q^2S(r)$ consists of terms like $S^\dagger(r)aaS(r)$ and the maths get rather straightforward by inserting $S(r)S^\dagger(r) = 1$ in the middle. For example, $S^\dagger(r)aaS(r) = S^\dagger(r)aS(r)S^\dagger(r)aS(r) = (a \cosh r - a^\dagger e^{-i\phi} \sinh r)^2$. Using such relations, one finally obtains

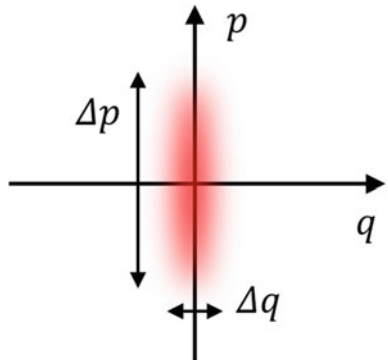
$$\begin{aligned}\Delta q &= \sqrt{\langle q^2 \rangle - \langle q \rangle^2} \\&= \sqrt{\frac{\hbar}{2m\omega} (\cosh 2r - \cos \phi \sinh 2r)}, \\ \Delta p &= \sqrt{\langle p^2 \rangle - \langle p \rangle^2} \\&= \sqrt{\frac{m\hbar\omega}{2} (\cosh 2r + \cos \phi \sinh 2r)}.\end{aligned}$$

Note that $\Delta q \Delta p = (\hbar/2)\sqrt{\cosh^2 2r - \cos^2 \phi \sinh^2 2r}$, which takes the minimal value $\hbar/2$ when $\phi = 0$ or $r = 0$. Looking at Δq for $\phi = 0$, $\Delta q = \sqrt{\hbar/2m\omega}e^{-r}$. This value is indeed smaller than that of coherent state by a factor of e^{-r} . On the other hand, $\Delta p = \sqrt{m\hbar\omega/2}e^r$, which is larger than that of the coherent state by a factor of e^r , hence the state $|r, \alpha\rangle$ is prolate in the phase space, one quadrature even being smaller than the vacuum fluctuation. In particular, the state $|r, 0\rangle = S(r)|0\rangle \equiv |r\rangle$ looks squeezed in q direction, thence is called the squeezed vacuum (Fig. 6.2).

For more characterization, let us express the squeezed vacuum $|r\rangle$ by the Fock states. For preparation,

$$S(r)aS^\dagger(r) = a \cosh r + a^\dagger e^{-i\phi} \sinh r.$$

Fig. 6.2 Schematic illustration of the squeezed vacuum state in the phase space



as has been done before. This operates on the squeezed vacuum to yield zero, namely $S(r)aS^\dagger(r)S(r)|0\rangle = S(r)a|0\rangle = 0$. Therefore, the squeezed vacuum is an eigenstate of the operator $a \cosh r + a^\dagger e^{-i\phi} \sinh r \equiv \mu a + \nu a^\dagger$. Expanding the squeezed vacuum as $|r\rangle = \sum_{n=0}^{\infty} C_n |n\rangle$ and operating $\mu a + \nu a^\dagger$ on it, we obtain recurrence relations

$$\mu\sqrt{n+2}C_{n+2} + \nu\sqrt{n}C_n = 0.$$

Then the coefficients to be determined are C_0 and C_1 , however, $(\mu a + \nu a^\dagger)C_1|1\rangle = C_1\mu|0\rangle + \sqrt{2}\nu C_2|2\rangle$ implies that $C_1 = 0$, so that $C_{2n+1} = 0$. Thus, the expanded squeezed vacuum is dictated to be

$$|r\rangle = \frac{1}{\sqrt{\cosh r}} \sum_{n=0}^{\infty} (-1)^n e^{-in\phi} (\tanh r)^n \frac{\sqrt{(2n)!}}{2^n n!} |2n\rangle$$

with $C_0 = 1/\sqrt{\cosh r}$ is determined by the normalization condition.

6.3.4 Thermal State

Thermal state is not a pure state, but a mixed state with probability of the system being in $|n\rangle$ reads

$$p_n = \frac{e^{-n\beta\hbar\omega}}{\sum_{n=0}^{\infty} e^{-n\beta\hbar\omega}} = e^{-n\beta\hbar\omega}(1 - e^{-\beta\hbar\omega})$$

as statistical mechanics states about the thermal distribution. Here $\beta = 1/k_B T$ is the inverse temperature and k_B and T are the Boltzmann constant and system temperature, respectively. With these probabilities, the thermal state is well described by the density operator

$$\rho_{\text{th}} = \sum_{n=0}^{\infty} p_n |n\rangle \langle n|.$$

As is usually done in the statistical mechanics, the average photon number $\langle n \rangle = \sum_{n=0}^{\infty} p_n \langle n | a^\dagger a | n \rangle = \sum_{n=0}^{\infty} np_n$ and the standard deviation $\Delta n = \sqrt{\langle n^2 \rangle - \langle n \rangle^2}$ are easily calculated using the relation $\sum_{n=0}^{\infty} ne^{-n\beta\hbar\omega} = \sum_{n=0}^{\infty} (-1/\hbar\omega)(\partial/\partial\beta)e^{-n\beta\hbar\omega} = (-1/\hbar\omega)(\partial/\partial\beta)(1 - e^{-\beta\hbar\omega})$. The results are

$$\langle n \rangle = \frac{e^{-\beta\hbar\omega}}{1 - e^{-\beta\hbar\omega}},$$

$$\Delta n = \sqrt{\langle n \rangle^2 + \langle n \rangle}.$$

These results show that for the thermal state, the fluctuation of the photon number is almost equal to the average photon number.

6.4 Photon Correlations

What is classical and what is quantum? How coherent a state is? Two correlation functions frequently used in the quantum optics give, to some extent, measures of the “quantumness” and coherence.

6.4.1 Amplitude Correlation/First-Order Coherence

Quantum analogue of amplitude autocorrelation is called the first-order coherence and is defined by

$$g^{(1)}(\tau) = \frac{\langle a^\dagger(t)a(t+\tau) \rangle}{\sqrt{\langle a^\dagger(t)a(t) \rangle \langle a^\dagger(t+\tau)a(t+\tau) \rangle}}.$$

For the coherent state, since $a(t) = ae^{-i\omega t}$ in the Heisenberg picture,

$$g^{(1)}(\tau) = \frac{\langle a^\dagger a \rangle e^{-i\omega\tau}}{\langle a^\dagger a \rangle} = e^{-i\omega\tau}.$$

Let us consider another example. Suppose we have two modes a_1 and a_2 and see amplitude cross-correlation

$$g_{12}^{(1)}(\tau) = \frac{\langle a_1^\dagger(t)a_2(t+\tau) \rangle}{\sqrt{\langle a_1^\dagger(t)a_1(t) \rangle \langle a_2^\dagger(t+\tau)a_2(t+\tau) \rangle}}.$$

For such a situation with both of the two modes being coherent states, $g_{12}^{(1)}(\tau) = e^{-i\omega\tau}$ as well. However, for the Fock state $|n_1, n_2\rangle$, straightforward calculation shows that

$g_{12}^{(1)}(\tau) = 0$. Recall that the amplitude correlation signals the interference effect, that is, it tells us that the state has maximal ability of interference when $|g^{(1)}| = 1$ and the system lacks interference when $g^{(1)} = 0$. Thus, the former and the latter cases are said to be coherent and incoherent, respectively. In other cases, $0 < g^{(1)} < 1$, the state is said to be partially coherent.

Physically, the first-order coherence is nothing but a result of interference of waves. Therefore, the first-order coherence can be observed if one prepares the double-slit experiment or its equivalent alternatives.

6.4.2 Intensity Correlation/Second-Order Coherence

Quantum analogue of intensity autocorrelation is called the second-order coherence and is defined by

$$g^{(2)}(\tau) = \frac{\langle a^\dagger(t)a^\dagger(t+\tau)a(t)a(t+\tau) \rangle}{\sqrt{\langle a^\dagger(t)a(t) \rangle \langle a^\dagger(t+\tau)a(t+\tau) \rangle}}.$$

For a monochromatic wave, $\langle a^\dagger(t)a^\dagger(t+\tau)a(t)a(t+\tau) \rangle = \langle a^\dagger a^\dagger aa \rangle = \langle a^\dagger(aa^\dagger - 1)a \rangle = \langle n^2 \rangle - \langle n \rangle$. Therefore, the second-order coherence reduces to

$$g^{(2)}(\tau) = \frac{\langle n^2 \rangle - \langle n \rangle}{\langle n \rangle^2} = 1 + \left(\frac{\Delta n}{\langle n \rangle} \right)^2 - \frac{1}{\langle n \rangle}.$$

For the coherent state, $\Delta n = \sqrt{\langle n \rangle}$ and $g^{(2)}(\tau) = 1$. For the thermal state, $\Delta n = \sqrt{\langle n \rangle^2 + \langle n \rangle}$ so that $g^{(2)}(\tau) = 2$. In general, classical intensity correlation function always takes values larger than 1, and inversely there is some classical analogue of the quantum state under consideration whenever $g^{(2)}(\tau) \geq 1$. For the Fock state $|n\rangle$, there is no fluctuation of the photon number and $g^{(2)}(\tau) = 1 - 1/n < 1$. This does not have any classical analogue and is definitely of quantum nature. Thus, the second-order coherence is a measure of the quantumness of a quantum state under concern.

Intensity correlation is interpreted as a particle-like statistics of a harmonic oscillator. For a photonic mode, it can be measured by preparing two photon-counting modules and measuring the coincidence.

6.5 Wigner Function

6.5.1 General Remarks

Density matrix contains the complete information about the quantum state, and now we would like to express it in a phase space. Let us apply Wigner transformation to

the density matrix:

$$W(q, p) = \frac{1}{2\pi\hbar} \int_{-\infty}^{\infty} e^{-ipq'} \left\langle q + \frac{q'}{2} \middle| \rho \middle| q - \frac{q'}{2} \right\rangle dq'.$$

$W(q, p)$ is known as Wigner function. One might immediately see that the Wigner function is real but not necessarily positive.

Marginal distributions are obtained by integrating with respect to one variable. For example,

$$\begin{aligned} W(q) &= \int_{-\infty}^{\infty} W(q, p) dp \\ &= \frac{1}{2\pi\hbar} \int_{-\infty}^{\infty} dp \int_{-\infty}^{\infty} dq' e^{-ipq'} \left\langle q + \frac{q'}{2} \middle| \rho \middle| q - \frac{q'}{2} \right\rangle \\ &= \int_{-\infty}^{\infty} dq' \delta(q') \left\langle q + \frac{q'}{2} \middle| \rho \middle| q - \frac{q'}{2} \right\rangle \\ &= \langle q | \rho | q \rangle. \end{aligned}$$

Here the identity $2\pi\delta(q) = \int_{-\infty}^{\infty} dp e^{-ipq}$ is used. $W(q)$ is obviously non-negative.⁴ For a pure state, $W(q)$ is a squared wavefunction in q -representation. How about $W(p) = \int_{-\infty}^{\infty} W(q, p) dq$? The calculation is a bit tricky but by properly inserting $\int_{-\infty}^{\infty} |p\rangle \langle p| dp = 1$ twice and using $\langle q | p \rangle = e^{ipq/\hbar} / \sqrt{2\pi\hbar}$, one can see

$$W(q) = \langle p | \rho | p \rangle.$$

This, as well, is non-negative and equals a squared wavefunction in p -representation for a pure state. Thus, the marginal distributions are probability distributions, satisfying

$$\int_{-\infty}^{\infty} W(q) dq = \int_{-\infty}^{\infty} W(p) dp = \int_{-\infty}^{\infty} \int_{-\infty}^{\infty} W(q, p) dq dp = 1$$

The Wigner function itself can take negative values, therefore it is not a probability distribution. Instead, it is said to be a quasi-probability distribution, for it is normalized. But do not overlook the importance of the Wigner function itself, since the quantum states accompanied with the classical counterpart yield positive Wigner function. In other words, the negativity of the Wigner function is an evidence of the non-classicality.

⁴ Check for $\rho = \sum |c_i|^2 |\psi_i\rangle \langle \psi_i|$, $\sum |c_i|^2 = 1$.

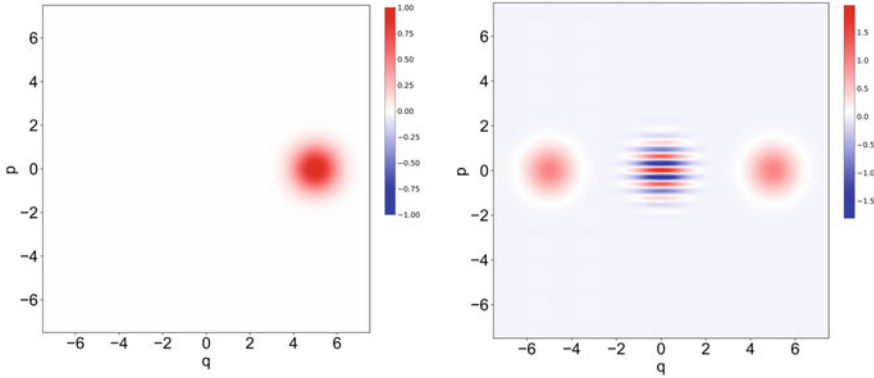


Fig. 6.3 Wigner functions of coherent state $|\alpha\rangle$ (left) and superposition $|\alpha\rangle + |-\alpha\rangle$ (right)

6.5.2 Examples

We pick up a few examples of Wigner function for pure states. For a pure state $|\psi\rangle$, the Wigner function reduces to

$$W(q, p) = \frac{1}{2\pi\hbar} \int_{-\infty}^{\infty} e^{-ipq'} \psi\left(q + \frac{q'}{2}\right) \rho \psi^*\left(q - \frac{q'}{2}\right) dq'.$$

Coherent State

First example is a coherent state. First we should derive the q -representation of the coherent state by evaluating $\langle q | \alpha \rangle$.

$$\begin{aligned} \langle q | \alpha \rangle &= \langle x | \sum_{n=0}^{\infty} \frac{\alpha^n}{\sqrt{n!}} e^{-\frac{|\alpha|^2}{2}} | n \rangle \\ &= \langle x | \sum_{n=0}^{\infty} \frac{\alpha^n}{n!} e^{-\frac{|\alpha|^2}{2}} a^{\dagger n} | 0 \rangle \\ &= \langle x | e^{-\frac{|\alpha|^2}{2}} e^{\alpha a^\dagger} | 0 \rangle \\ &= e^{-\frac{|\alpha|^2}{2}} \langle x | e^{\alpha \sqrt{\frac{m\omega}{2\hbar}} (\hat{q} - i \frac{\hat{p}}{m\omega})} | 0 \rangle \\ &= e^{-\frac{|\alpha|^2}{2}} e^{-\frac{\alpha^2}{4}} \langle x | e^{\alpha \sqrt{\frac{m\omega}{2\hbar}} \hat{q}} e^{-i\alpha \frac{\hat{p}}{\sqrt{2m\hbar\omega}}} | 0 \rangle \\ &= e^{-\frac{|\alpha|^2}{2}} e^{-\frac{\alpha^2}{4}} e^{\alpha \sqrt{\frac{m\omega}{2\hbar}} q} e^{\frac{-i\alpha}{\sqrt{2m\hbar\omega}} \frac{\hbar}{i} \frac{d}{dq}} \langle x | 0 \rangle \\ &= e^{-\frac{|\alpha|^2}{2}} e^{-\frac{\alpha^2}{4}} e^{\alpha \sqrt{\frac{m\omega}{2\hbar}} q} \left\langle x - \alpha \sqrt{\frac{\hbar}{2m\omega}} | 0 \right\rangle \end{aligned}$$

$$\begin{aligned}
&= Ae^{-\frac{|\alpha|^2}{2}} e^{-\frac{\alpha^2}{4}} e^{\alpha\sqrt{\frac{m\omega}{2\hbar}}q} e^{-\frac{m\omega}{2\hbar}\left(q-\alpha\sqrt{\frac{\hbar}{2m\omega}}\right)^2} \\
&= Ae^{-\frac{m\omega}{2\hbar}\left(q-\alpha\sqrt{\frac{2\hbar}{m\omega}}\right)^2}
\end{aligned}$$

In this calculation, identities $e^{\gamma(d/dq)}f(q) = f(q + \gamma)$ and $\langle x | 0 \rangle = Ae^{-\frac{m\omega}{2\hbar}q^2}$ are used. In the last line, α is assumed to be real to simplify the situation.

Now, let us evaluate the Wigner function. With the knowledge of $\int_{-\infty}^{\infty} e^{-a(x+b)^2} dx = \sqrt{\pi/a}$ for real a and complex b , one can straightforwardly derive

$$W_\alpha(q, p) = \frac{\sqrt{2}A^2}{\sqrt{\pi m \hbar \omega}} e^{-\frac{m\omega}{\hbar}\left(q-\alpha\sqrt{\frac{2\hbar}{m\omega}}\right)^2} e^{-\frac{p^2}{m\hbar\omega}}$$

which is the Gaussian distribution with its peak located at $(\alpha\sqrt{2\hbar/m\omega}, 0)$ and its widths being $\sqrt{\hbar/2m\omega}$ in q - and $\sqrt{m\hbar\omega/2}$ in p -axes. See the left panel of Fig. 6.3.

Schrödinger's Cat State

Let us next consider the Wigner function of a Schrödinger's cat state $|\alpha\rangle + e^{i\theta}|-\alpha\rangle$, a coherent superposition of two coherent states. The normalization factor is omitted here. The calculation of the Wigner function is a bit lengthier than that of the simple coherent state, but it basically reduces to Gaussian integrals. The final expression is

$$W(q, p) = W_\alpha(q, p) + W_{-\alpha}(q, p) + \tilde{A}e^{-\frac{m\omega}{\hbar}q^2} e^{-\frac{p^2}{m\hbar\omega}} \cos\left(2p\sqrt{\frac{2\hbar}{m\omega}}\alpha + \theta\right).$$

The Wigner function of the Schrödinger's cat state is shown in the right panel of Fig. 6.3. In addition to the Wigner function of each coherent state W_α or $W_{-\alpha}$, there is an “interference fringe” in p direction in the middle which originates in the third term.

Fock State

The wavefunctions of the Fock states are given as

$$\begin{aligned}
|\psi_n(q)|^2 &= \frac{1}{2^n n!} \sqrt{\frac{m\omega}{\pi\hbar}} e^{-\frac{m\omega q^2}{\hbar}} H_n\left(\sqrt{\frac{m\omega}{\hbar}}q\right) \\
|\psi_n(p)|^2 &= \frac{1}{2^n n!} \sqrt{\frac{1}{\pi m \hbar \omega}} e^{-\frac{p^2}{m\hbar\omega}} H_n\left(\sqrt{\frac{1}{m\hbar\omega}}p\right)
\end{aligned}$$

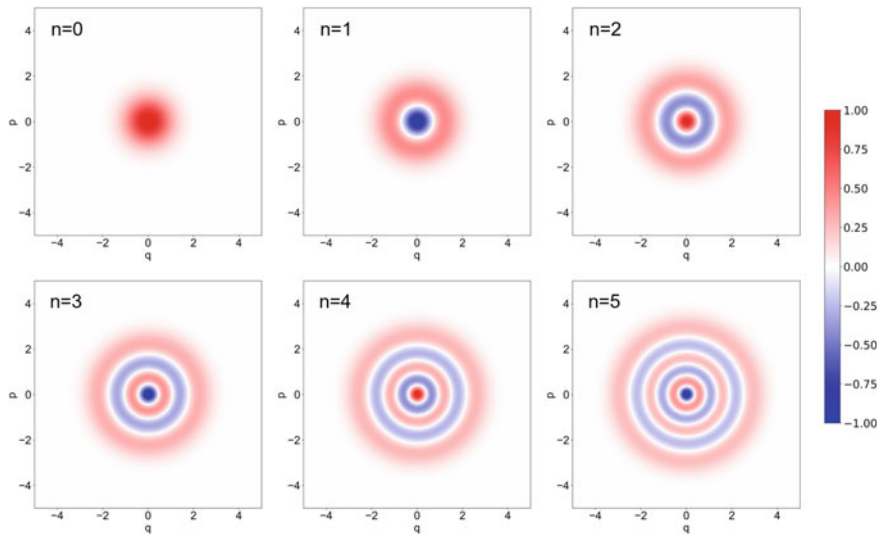


Fig. 6.4 Wigner functions of Fock states $|n\rangle$

using Hermite polynomials $H_n(x) = (-1)^n e^{x^2/2} (\partial^n / \partial x^n) e^{x^2/2}$. The Wigner function which generates these as marginals is the following:

$$W_n(q, p) = \frac{(-1)^n}{\pi \hbar} e^{-\frac{1}{\hbar} \left(m\omega q^2 + \frac{p^2}{m\omega} \right)} L_n \left(\frac{2}{\hbar} \left(m\omega q^2 + \frac{p^2}{m\omega} \right) \right).$$

Here $L_n(x) = \sum_{j=0}^n {}_n C_j (-x)^j / j!$ are Laguerre polynomials.

As it was mentioned in the beginning of this section, a quantum state with Wigner function taking negative values does not have corresponding classical analogue. In this perspective, the Schrödinger's cat state and the Fock state (Fig. 6.4) both take negative values and thus are genuinely quantum mechanical states. On the other hand, the coherent state and squeezed state does not have intrinsic negativity in the Wigner function and there are corresponding classical phenomena.

Problems

Problem 6-1 (i) Derive $[q, p] = i\hbar$ using $p = (\hbar/i)d/dq$.
(ii) Show $[a, a^\dagger] = 1$.

Problem 6-2 Show that the creation operator a^\dagger does not have any nontrivial eigenstate, that is, the eigenstate other than the null vector.

Problem 6-3 We define superoperators $(S*)$, $(*S)$ and $[S,]$ for an operator S such that for any operator A they act as

$$(S*)A = SA, \quad (*S)A = AS, \quad [S,]A = [S, A]. \quad (6.5.1)$$

- (i) Check that $[S,] = (S*) - (*S)$ and $(S*)(*S) = (*S)(S*)$ hold.
- (ii) Prove the Baker–Campbell–Hausdorff formula

$$e^{-S} A e^S = A - [S, A] + \frac{1}{2!} [S, [S, A]] - \frac{1}{3!} [S, [S, [S, A]]] + \dots \quad (6.5.2)$$

Problem 6-4 Check that the coherent state has standard deviation $|\alpha|$ of its number.

Problem 6-5 Prove that a marginal distribution $W(q)$ of a Wigner function is non-negative, here for a state in q -representation $\rho = \sum |c_i|^2 |\psi_i(q)\rangle\langle\psi_i(q)|$, $\sum |c_i|^2 = 1$.

Problem 6-6 Let us consider a Wigner function of a thermal state with average number of quanta n_{th} .

- (i) Discuss qualitatively what it should look like.
- (ii) Quantitatively confirm your physical intuition by explicitly calculating the Wigner function of the thermal state starting from the density-matrix representation of it. The following identities might be useful:

$$e^{-n\beta\hbar\omega}(1 - e^{-\beta\hbar\omega}) = \frac{\langle n \rangle^n}{(1 + \langle n \rangle)^{n+1}} \quad (6.5.3)$$

$$\sum_n c^n L_n(x) = \frac{e^{\frac{-cx}{1-c}}}{1 - c}. \quad (6.5.4)$$

Then discuss the similarities and differences with other quantum states such as the coherent state.

Problem 6-7 Calculate the normalization constants A_{even} and A_{odd} of the Schrödinger's cat states.



Two-level System and Interaction with Electromagnetic Waves

7

7.1 Two-level System, Spin, and Bloch Sphere

First of all, what we are interested in is a quantum bit, or a qubit, which is to be controlled in the quantum engineering activities. A qubit consists of two orthogonal quantum states $|g\rangle$ and $|e\rangle$, that is, $\langle g|g\rangle = \langle e|e\rangle = 1$ and $\langle g|e\rangle = 0$. This set of states

$$|g\rangle = \begin{pmatrix} 0 \\ 1 \end{pmatrix},$$
$$|e\rangle = \begin{pmatrix} 1 \\ 0 \end{pmatrix},$$

or the two-level system is usually constructed by picking-up two orthogonal quantum states among many others residing in an individual quantum system regarding the ability of manipulation, excited-state lifetime and coherence, and any other merits regarding the quantum control of the qubit. Note that labels g and e are often interchanged depending on the convention used. Quantum information can be registered in the complex vector space called Hilbert space, spanned by these two orthonormal bases set $\{|g\rangle, |e\rangle\}$, or more generally by an assembly of them. Let us, then, write down the Hamiltonian of the qubit which is the sum of the energies, $\hbar\omega_g$ for the ground state and $\hbar\omega_e$ for the excited state (Fig. 7.1), associated with the projectors $|g\rangle\langle g|$ and $|e\rangle\langle e|$:

$$\mathcal{H} = \hbar\omega_g|g\rangle\langle g| + \hbar\omega_e|e\rangle\langle e|. \quad (7.1.1)$$

Supplementary Information The online version contains supplementary material available at https://doi.org/10.1007/978-981-19-4641-7_7.

One can easily verify that if the Hamiltonian is evaluated (sandwiched) by $|g\rangle$, the value is the ground-state energy, and so for the excited state as well. Here we want to try rewriting this Hamiltonian by the Pauli operators defined by

$$\sigma_x = \begin{pmatrix} 0 & 1 \\ 1 & 0 \end{pmatrix} = |e\rangle\langle g| + |g\rangle\langle e|, \quad (7.1.2)$$

$$\sigma_y = \begin{pmatrix} 0 & -i \\ i & 0 \end{pmatrix} = -i|e\rangle\langle g| + i|g\rangle\langle e|, \quad (7.1.3)$$

$$\sigma_z = \begin{pmatrix} 1 & 0 \\ 0 & -1 \end{pmatrix} = -|g\rangle\langle g| + |e\rangle\langle e| \quad (7.1.4)$$

to get an alternative expression of the Hamiltonian as

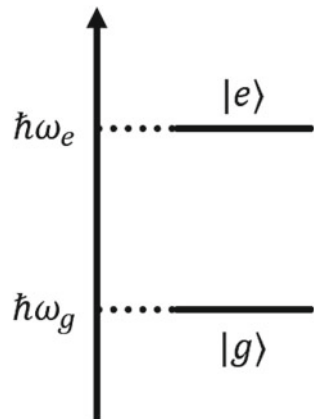
$$\begin{aligned} \mathcal{H} &= \frac{\hbar(\omega_e - \omega_g)}{2}\sigma_z + \frac{\hbar(\omega_e + \omega_g)}{2}I \\ &= \frac{\hbar\omega_q}{2}\sigma_z + \text{const.} \end{aligned} \quad (7.1.5)$$

where the second term in the first line is neglected since it, being proportional to the identity matrix I , only accounts for the energy shift imposed on the whole system that only redefines the reference of the energy. Here $\omega_q = \omega_e - \omega_g$ is the transition frequency, which specifies the frequency of the electromagnetic wave to be applied in order to flip the qubit, as detailed in later section.

Let us pose here gazing at Pauli operators given in Eqs. (7.1.2)–(7.1.4). First of all, they are all Hermitian: $\sigma_\xi^\dagger = \sigma_\xi$ ($\xi = x, y, z$). This means that the eigenvalues of the Pauli operators can be interpreted as being some physically observable quantities. Next point is less obvious but essential. With the commutator $[A, B] = AB - BA$, they have relations

$$[\sigma_x, \sigma_y] = 2i\sigma_z, \quad [\sigma_y, \sigma_z] = 2i\sigma_x, \quad [\sigma_z, \sigma_x] = 2i\sigma_y. \quad (7.1.6)$$

Fig. 7.1 Energy levels of a quantum bit



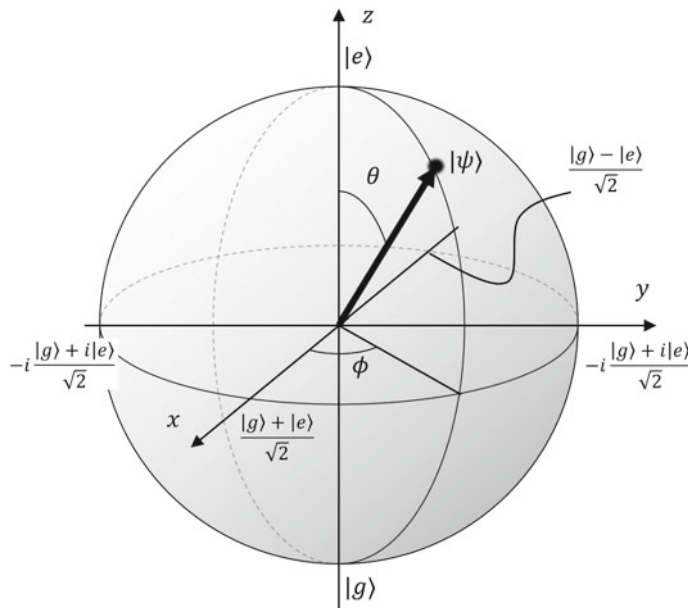


Fig. 7.2 Illustration of a Bloch sphere

These relations are summarized into following form:

$$[\sigma_i, \sigma_j] = 2i\epsilon_{ijk}\sigma_k. \quad (7.1.7)$$

Pauli operators are indeed the generators of the special unitary group SU(2), which is known to be a good group-theoretical description of a spin-1/2 system. In other words, a qubit can be identified as a spin-1/2 system! We are glad to see this correspondence, since the expectation value of the Pauli operator σ_ξ is now read as the spin component in ξ axis and we are allowed to draw a quantum state of the qubit within a Bloch sphere (see Fig. 7.2), likewise for a single spin-1/2 system. In the Bloch sphere, three sets of orthogonal bases $\{(|g> + |e>)/\sqrt{2}, (|g> - |e>)/\sqrt{2}\}$, $\{-i(|g> + i|e>)/\sqrt{2}, -i(|g> - i|e>)/\sqrt{2}\}$ and $\{|e>, |g>\}$ are taken, respectively, to be x , y , and z axes.¹ If a qubit is in a pure state $|\psi>$, it can be rewritten as $|\psi> = \cos(\theta/2)|e> + e^{i\phi}\sin(\theta/2)|g>$ with parameters θ and ϕ , or equivalently in the Bloch sphere as $(\sin\theta\cos\phi, \sin\theta\sin\phi, \cos\theta) = (\langle\psi|\sigma_x|\psi\rangle, \langle\psi|\sigma_y|\psi\rangle, \langle\psi|\sigma_z|\psi\rangle)$.

7.2 Interaction Between Two-level System and Electromagnetic Field

The quantum states constructing a qubit are ideally orthogonal to each other, as mentioned in the previous section. Some mechanism is needed to “mix” these two

¹ It is straightforward to check that these bases are eigenvectors of σ_x , σ_y and σ_z , respectively.

states to transform a naturally prepared state, say $|g\rangle$, into a desired state like $|e\rangle$, $(|g\rangle + |e\rangle)/\sqrt{2}$, and so on. In many cases, $|g\rangle$ is the ground state and $|e\rangle$ the excited state of some anharmonic oscillator, and sometimes they are spin down and spin up. However, one thing seems to be very common: the two states are coupled via transition dipole moment which is driven by an electromagnetic field resonant on the transition.^{2,3} The transition dipole moment d is intuitively the classical dipole moment $q\mathbf{r}$ with charge q and some maths will give the correctly quantized expression of it. However, we dictate the final expression as given, since it is also intuitive. The dipole operator d is given as [9]

$$d = \mu (|e\rangle\langle g| + |g\rangle\langle e|) \quad (7.2.1)$$

$$= \mu(\sigma_+ + \sigma_-). \quad (7.2.2)$$

In this expression, the following two operators are newly defined:

$$\sigma_+ = |e\rangle\langle g| = \begin{pmatrix} 0 & 1 \\ 0 & 0 \end{pmatrix} = \frac{\sigma_x + i\sigma_y}{2} \quad (7.2.3)$$

$$\sigma_- = |g\rangle\langle e| = \begin{pmatrix} 0 & 0 \\ 1 & 0 \end{pmatrix} = \frac{\sigma_x - i\sigma_y}{2}. \quad (7.2.4)$$

These operators act as raising and lowering operators, so that we can control qubit by “stimulating” the dipole moment that includes these operators by an external field.

Suppose that the electromagnetic field with its polarization parallel to the transition dipole moment is applied to the two-level system. Then the interaction terms are generated in the Hamiltonian that is generally described by a polynomial function of the applied field, say, an electromagnetic field \mathbf{E} . To first-order approximation the interaction term reads $d \cdot E$ and let us neglect other higher-order terms.⁴ Plugging the operator expressions of $d = \mu(\sigma_+ + \sigma_-)$ and $E = E_{\text{zpf}}(a + a^\dagger)$, we have an interaction Hamiltonian

$$\mathcal{H}_{\text{int}} = \mu E_{\text{zpf}}(\sigma_+ + \sigma_-)(a + a^\dagger). \quad (7.2.5)$$

Furthermore, we assume that the frequency of the electric field ω_c and the transition frequency ω_q are close together. Products such as $\sigma_+ a^\dagger$ are “rapidly oscillating” at

² There are cases with quadrupole moment taking place, however, the resultant interaction Hamiltonian will be of the same form so that we focus on the dipole transitions.

³ There are cases where the auxiliary level $|r\rangle$ mediates the transition between $|g\rangle$ and $|e\rangle$. In such a case the system can be treated as a two-level system as well. After reading through this Chapter, readers interested in are recommended to refer to Appendix C.

⁴ This prescription is called the “electric dipole approximation” in the case of electric dipole moment under concern.

$\omega_q + \omega_c$ and we neglect here. This procedure is called the rotating-wave approximation. Then the final expression is

$$\begin{aligned}\mathcal{H}_{\text{int}} &= \mu E_{\text{zpf}} (\sigma_+ a + \sigma_- a^\dagger) \\ &= \hbar g (\sigma_+ a + \sigma_- a^\dagger)\end{aligned}\quad (7.2.6)$$

which is the celebrated Jaynes–Cummings interaction [10] with coupling strength $g = \mu E_{\text{zpf}} / \hbar$. The physical situation is really simple. The first term represents the process that a photon is absorbed (a) by the qubit and the qubit is excited (σ_+) and the reverse in the second.

Sometimes the anti-Jaynes–Cummings interaction appears depending on the context.⁵ It is of the form

$$\mathcal{H}_{\text{int}} = \hbar g' (\sigma_+ a^\dagger + \sigma_- a). \quad (7.2.7)$$

Keep in mind that whether the Jaynes–Cummings or anti-Jaynes–Cummings interaction, or both, survives depends on what system and what “driving” electromagnetic waves you take into account. By driving the nonlinear system with $\omega_q + \omega_c$ strongly, the nonlinear process may allow simultaneous creation of a photon in the cavity and the qubit excitation and *vice versa*. For example, both of them can be realized by applying the two-tone driving to the trapped atomic ions to implement Mølmer–Sørensen gate [11], which enables the highest-ever-achieved-fidelity two-qubit gate [12].

7.2.1 Spontaneous and Stimulated Emission

Here we introduce two kinds of processes, spontaneous emission and stimulated emission/absorption, as the ones involving electromagnetic waves in close relation to the two-level system. Spontaneous emission is a process that the excited state decays into the ground state by emitting one photon. This happens due to the coupling of the dipole moment of the two-level system to the vacuum field surrounding it. This can be interpreted as the stimulated emission caused by the vacuum fluctuation, as introduced in the next paragraph.

Intuitive picture of this process in the classical physics point of view is that with an atom as an example, the orbiting electron around the nucleus, for instance, generates the oscillating electromagnetic field and loses its energy. Of course, this is incorrect interpretation of the dynamics of electron in an atom and the quantum mechanics

⁵ Here we make a note on the terminology. The (anti-)Jaynes–Cummings interaction usually refers to those between a qubit and a harmonic oscillator. Similar interactions involving two harmonic oscillators, whose annihilation operators are a and b , are represented by $\hbar g(a^\dagger b + ab^\dagger)$ and $\hbar g(a^\dagger b^\dagger + ab)$, and called *beam-splitter* and *two-mode squeezing interaction*, respectively. For qubit-qubit interactions such as the ones proportional to $\sigma_x \otimes \sigma_x$ and $\sigma_x \otimes \sigma_y$, names like *XX* and *XY* interactions are frequently used.

should take place. In the spontaneous emission process, a single photon is emitted and the phase of the emitted photon is completely at random. This results in the dephasing, as we will refer to in the later Section.

The spontaneous emission or spontaneous decay is responsible for the de-excitation of the qubit with its transition frequency in the optical regime. However, the de-excitation process itself is actually not limited to the spontaneous decay. For example, the energy transfer between the qubit and some particle in the environment results in irreversible loss of excitation energy from the qubit system. The general name of the de-excitation processes is longitudinal decay or longitudinal relaxation which is complementary to the dephasing processes or transverse decay/relaxation.

Another important process is stimulated emission and absorption which occur when a coherent electromagnetic wave is applied to the two-level system. The processes under concern are the absorption and emission of photons by the two-level system, and these two processes are reciprocal to each other and occur at the same rate proportional to the square root of the intensity of the incident electromagnetic wave. Therefore, however strongly we apply continuous electromagnetic wave, the two-level system does not end in a situation that the occupation probability of the excited state gets unity. The occupation probabilities of the ground and excited states should be 1/2, or less if the driving field is not sufficiently intense. As it is important in the Rabi oscillation and Ramsey interference introduced in later Chapter, the stimulated emission and absorption are coherent processes in which the phases of the electromagnetic waves and the qubit state have one-to-one correspondence.

7.3 Two-level Systems and Electromagnetic Waves in Practice

7.3.1 Two-level Systems in Nuclear Magnetic Resonance

Nuclear magnetic resonance (NMR) is frequently utilized in a spectroscopic method in material sciences, but also in a very familiar method of medical application known as magnetic resonance imaging (MRI). In NMR, a two-level system is constructed by two states $|\uparrow\rangle$ and $|\downarrow\rangle$ of a nuclear spin of an atom in a properly chosen molecule. Energies of these two nuclear-spin states are split by Zeeman effect under applied magnetic field. Molecules containing nuclear spins usually take a form of aqueous or other solutions, and nuclear spins of phosphor and hydrogen atoms are frequently shed light (through radio frequency, as we mention later on). Magnetic field of the order of 1 T is applied to the solution containing nuclear spins, with which the spin states are Zeeman-split. Then radio-frequency waves of tens or hundreds of MHz, equivalent to the Zeeman splitting mentioned just above, are applied to implement the interaction between a two-level system and electromagnetic waves in the form of magnetic dipole interaction. Coherence time of nuclear-spin state depends on molecules and solvents used. In some combinations, the coherence time becomes too long to be measured, verifying that the nuclear spins are quite nicely isolated quantum systems even in condensed matter systems.

7.3.2 Two-level Systems in Atomic Gases

In systems utilizing neutral and singly ionized atomic gases, their rich internal structures allow us to construct various two-level systems. Here we focus on two-level systems operated in the optical regime and in microwave regime, that appear frequently in the trapped ion quantum systems. Appendix D might help readers unfamiliar with atomic levels such as hyperfine structures and more details will be found in e.g. Ref. [9].

What we want to introduce first is an optically operated two-level system. For such a purpose, we summarize the frequently-used quantum states and optical transitions of a singly-charged calcium ion in Fig. 7.3. A calcium ion, an alkaline-halide atom with one valence electron removed, possesses one valence electron and so that it has S state as its electronic ground state. It also has P state as an excited state with a lifetime of several nanoseconds, and the optical transition from S state to P state ($S-P$ transition) is dipole-allowed. This ion has D state which is metastable, since the $S-D$ transition is dipole forbidden. The $S-D$ transition, which is only allowed by an electric quadrupole transition, has very narrow linewidth of around 1 Hz and thus D state has very long lifetime of around 1 s. This is one of the benefits of building a qubit with S state as $|g\rangle$ and D state as $|e\rangle$.

For the purpose of introducing a two-level system operated in microwave regime, we consider an singly-ionized ytterbium atom, especially a specific isotope of $^{171}\text{Yb}^+$. Its electronic ground state is S state and its nuclear spin is $1/2$. Therefore, hyperfine structure has two manifolds $F = 0$ and $F = 1$, where F denotes the total angular momentum including electronic spin, electronic orbital, and nuclear spin degrees of freedom. The hyperfine splitting is about 12.6 GHz in frequency. Though the $F = 0$ state has only one spin state with $m_F = 0$ where m_F stands for the component of the angular momentum along the quantization axis, $F = 1$ manifold consists of three states $m_F = -1, 0, +1$. Since the energies of two $m_F = 0$ states are insensitive to the magnetic field for the absence of the angular momentum component along the quantization axis, $|F, m_F\rangle = |0, 0\rangle$ and $|F, m_F\rangle = |1, 0\rangle$

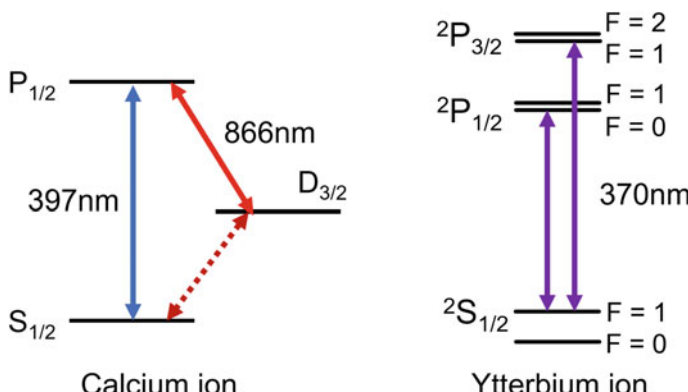


Fig. 7.3 Partial energy diagram of calcium ion and ytterbium ion

are frequently used as a bases constructing a qubit. By irradiating microwaves of 12.6 GHz frequency or by using optical Raman transition, the qubit state can be controlled. Since both the $|0, 0\rangle$ and $|1, 0\rangle$ states are electronic ground state, the lifetime of the qubit excited state is nearly infinite. Therefore, the coherence time of such a hyperfine qubit is limited by dephasing, mainly due to the fluctuation of the transition frequency accompanied with the fluctuating magnetic field bias.

Atomic gas or atomic ions as qubits provides us with uniform, long-lived two-level systems by nature. Cons are the complex experimental systems using frequency-stabilized lasers and optics for their adjustment, and ultrahigh vacuum setup down to 10^{-9} Pa or less. The atomic quantum technologies are fronting these difficulties of the stability and the scalability.

7.3.3 Two-level Systems in Solid-state Quantum Defects

Atomic defects or impurities in the non-metallic solid materials are called quantum defects. The optical transition of such a defect center has energy levels within the bandgap and can be coherently controlled, since it is relatively isolated from the environment, or bulk phonons and electrons supported by the substrate materials. However, the isolation is not complete: the optical transitions are in many cases broadened by phonons, and the spin states are disturbed by surrounding electronic and/or nuclear spins. The site-controlled preparation of the quantum defects is also a technical challenge.

7.3.4 Two-level System in an Optically Controlled Semiconductor Quantum Dot

Semiconductor crystal growth technology has enabled us crystal growth at single-atom-layer level. This technology has been applied to realize nanoscale material region with narrower bandgap, indium arsenide for instance, than that of the substrate such as gallium arsenide. If such a nanoscale region confines the electron in 3 dimensions, such a nanostructure is called a quantum dot. Only a single electron or two can be trapped inside the quantum dot, the optical transition and quantum manipulation of electronic spin state have gathered attention.

Figure 7.4 depicts the band structure of the quantum dot. An electron in a quantum dot is localized in a region of around 10 nm, so that only a single electron is trapped in most cases. The excited state of the quantum dot electron just below the conduction-band edge exhibits the lifetime of a few hundreds of picoseconds to a few nanoseconds.

An electron confined in the quantum dot energetically close to the valence band has a spin degree of freedom, so that it can also be used as a qubit. The coherence time of such a spin qubit is about a few microseconds; therefore, the spin qubit can be controlled by using laser technique such as stimulated Raman transition.

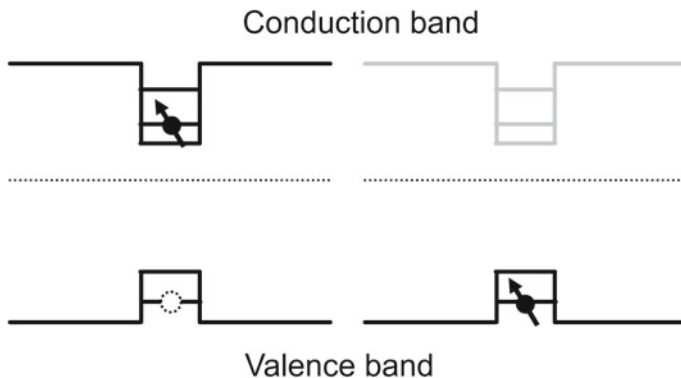


Fig. 7.4 Exciton in a quantum dot (left) and an electron confined in a quantum dot (right). Broken horizontal line represents the Fermi energy

Although semiconductor quantum dot fits well with the semiconductor-based nanophotonics, the short coherence time and the dot-to-dot fluctuation of its position, lifetime, and emission wavelength hinder the straightforward scaling up of the quantum dot quantum technology.

7.3.5 Two-level System in Superconducting Circuit

As detailed later in Sect. 9.3, a ultra-low loss, nonlinear LC resonator can be constructed by the parallel connection of a capacitor and a Josephson junction using superconducting wiring. In such a superconducting circuit, anharmonicity of the resonator results in such situation that the energy difference between the ground state and the first excited state and that of the first and the second excited states are quite large to allow us for utilizing the ground and the first excited state as a two-level system, which is often referred to as a superconducting qubit. The transition energy of this qubit depends on the circuit design, however, generally it is within a few to 10 GHz. An advantage of the superconducting qubit is that by properly designing a circuit, the interaction between microwave field and the qubit can be very large that the coupled qubit-cavity system (circuit QED system) is often in a strong dispersive regime.

7.4 Dynamics and Relaxations of Two-level Systems

7.4.1 Bloch Equations and Relaxations

In the previous section, we saw that a qubit can be identified as a spin. Primary dynamics that the spin undergoes is, in the context of quantum engineering, due to the interaction with applied electromagnetic fields. Or we consider relaxation of it when it is subject to the interaction with some environment, such as stray electromagnetic

fields for highly isolated systems and thermal phonons or surrounding spin degree of freedom for solid-state systems. In 1946, Felix Bloch constructed a set of equations describing the spin, or more concretely the magnetization, precession about the applied magnetic field. This theory was developed principally for the “real” spin systems such as nuclear magnetic resonance, electron spin resonance for instance, however, in 1957 Richard P. Feynman realized that the Bloch equation is also a good description of the dynamics of a fictitious spin-1/2 system, or a qubit. Here we introduce a density matrix first, rewriting it as a spin-1/2 object, and analyze its behavior using a fundamental equation named master equation. Then, as a concrete case, the Bloch equations are derived.

Let us first define a density matrix ρ for a quantum state $|\psi\rangle = c_g|g\rangle + c_e|e\rangle$ as

$$\rho = |\psi\rangle\langle\psi| \quad (7.4.1)$$

$$= \rho_{gg}|g\rangle\langle g| + \rho_{ge}|g\rangle\langle e| + \rho_{eg}|e\rangle\langle g| + \rho_{ee}|e\rangle\langle e| \quad (7.4.2)$$

$$= \begin{pmatrix} |c_e|^2 & c_g^*c_e \\ c_gc_e^* & |c_g|^2 \end{pmatrix}. \quad (7.4.3)$$

A density matrix can treat the probabilistic realization of some states $\sum_i p_i |\psi_i\rangle\langle\psi_i|$, called the mixed state, in contrast to the pure state. How about the dynamics of the density matrix? To address this, we depart from the state vector in the Schrödinger picture, where the time evolution of the state reads $|\psi(t)\rangle = e^{-i(\mathcal{H}/\hbar)t}|\psi\rangle = U_t|\psi\rangle$ with the system Hamiltonian \mathcal{H} . Let us differentiate the density matrix evolving with $\rho(t) = U_t\rho U_t^\dagger$:

$$\frac{d\rho(t)}{dt} = \frac{dU_t}{dt}\rho U_t^\dagger + U_t\rho\frac{dU_t^\dagger}{dt} = -\frac{i}{\hbar}\mathcal{H}\rho(t) + \frac{i}{\hbar}\rho(t)\mathcal{H} = \frac{1}{i\hbar}[\mathcal{H}, \rho(t)] \quad (7.4.4)$$

which leads us to the von Neumann equation

$$i\hbar\frac{d\rho}{dt} = [\mathcal{H}, \rho]. \quad (7.4.5)$$

Note the difference between the von Neumann equation for a state and the Heisenberg equation of motion for an operator A : $i\hbar dA/dt = [A, \mathcal{H}]$.

Let us now consider a driven qubit, at a first step without the relaxations. Our Hamiltonian for the driven qubit is dictated as⁶

$$\mathcal{H} = \frac{\hbar\omega_q}{2}\sigma_z + \frac{\hbar\Omega}{2}(\sigma_+e^{-i\omega_dt} + \sigma_-e^{i\omega_dt}). \quad (7.4.6)$$

Here the parameter $\Omega = \mu E_d$ is introduced with the electric field strength E_d , which is in close connection with the coupling strength g of the Jaynes–Cummings interaction. Moving onto the rotating frame (see Appendix B) by the unitary transformation

⁶Please refer to the Appendix C for the derivation of the driving term.

$U\mathcal{H}U^\dagger - i\hbar U\dot{U}^\dagger$ with $U = \exp[i(\omega_d/2)\sigma_z t]$, we get a modified one:

$$\mathcal{H}' = \frac{\hbar\Delta_q}{2}\sigma_z + \frac{\hbar\Omega}{2}(\sigma_+ + \sigma_-), \quad (7.4.7)$$

where the detuning is defined by $\Delta_q = \omega_q - \omega_d$. Substituting this into the von Neumann equation (7.4.5) and evaluating it by sandwiching with $|g\rangle$'s and $|e\rangle$'s, one can obtain a set of equations

$$\frac{d\rho_{ee}}{dt} = i\frac{\Omega}{2}(\rho_{eg} - \rho_{ge}), \quad (7.4.8)$$

$$\frac{d\rho_{gg}}{dt} = -i\frac{\Omega}{2}(\rho_{eg} - \rho_{ge}), \quad (7.4.9)$$

$$\frac{d\rho_{eg}}{dt} = -i\Delta_q\rho_{eg} - i\frac{\Omega}{2}(\rho_{gg} - \rho_{ee}), \quad (7.4.10)$$

$$\frac{d\rho_{ge}}{dt} = +i\Delta_q\rho_{ge} + i\frac{\Omega}{2}(\rho_{gg} - \rho_{ee}), \quad (7.4.11)$$

where $\rho_{ij} = \langle i|\rho|j\rangle$. Let us define some quantities that look like the components of the pseudo-spin:

$$s_x = \rho_{ge} + \rho_{eg}, \quad s_y = -i(\rho_{ge} - \rho_{eg}), \quad s_z = \rho_{ee} - \rho_{gg}.$$

Note that there is an intrinsic relation of the density matrix of a pure state $\rho_{gg} + \rho_{ee} = 1$. The reason why we can regard this as components of the pseudo-spin can be seen by noting that

$$\rho = \rho_{gg}|g\rangle\langle g| + \rho_{ge}|g\rangle\langle e| + \rho_{eg}|e\rangle\langle g| + \rho_{ee}|e\rangle\langle e| \quad (7.4.12)$$

$$= \frac{1}{2}(I + s_x\sigma_x + s_y\sigma_y + s_z\sigma_z). \quad (7.4.13)$$

Furthermore, these quantities allow us to rewrite above differential equations in the following neat form, thanks to the transformation onto the rotating frame:

$$\frac{ds_x}{dt} = -\Delta_q s_y, \quad (7.4.14)$$

$$\frac{ds_y}{dt} = +\Delta_q s_x - \Omega s_z, \quad (7.4.15)$$

$$\frac{ds_z}{dt} = \Omega s_y \quad (7.4.16)$$

$$\iff \frac{d}{dt} \begin{pmatrix} s_x \\ s_y \\ s_z \\ \Delta_q \end{pmatrix} = \begin{pmatrix} \Omega \\ 0 \\ 0 \\ -\Omega \end{pmatrix} \times \begin{pmatrix} s_x \\ s_y \\ s_z \\ \Delta_q \end{pmatrix} \iff \frac{d\mathbf{s}}{dt} = \mathbf{B} \times \mathbf{s}. \quad (7.4.17)$$

This is the Bloch equation without relaxations that Feynman found valid for the two-level system, and it resembles the Bloch equation for real spin systems. The

two-level system and the vector $\mathbf{B} = (\Omega, 0, \Delta_q)$ act like a spin and applied static magnetic field, just as the Larmor precession.

Master equation (see Appendix E) goes a step further by incorporating a loss characterized by a dissipator Λ and Lindblad superoperator $\mathcal{L}[\Lambda]\rho = 2\Lambda\rho\Lambda^\dagger - \Lambda^\dagger\Lambda\rho - \rho\Lambda^\dagger\Lambda$ added in the von Neumann equation to describe the lossy dynamics of the system. Suppose the dissipator is Λ with its spontaneous and thermal-bath-induced decay rates Γ and Γ' , respectively, the master equation has the general form of

$$\frac{d\rho}{dt} = -\frac{i}{\hbar} [\mathcal{H}, \rho] + \frac{1}{2}\mathcal{L}[\sqrt{\Gamma + \Gamma'}\Lambda]\rho + \frac{1}{2}\mathcal{L}[\sqrt{\Gamma'}\Lambda^\dagger]\rho. \quad (7.4.18)$$

The effect of thermal bath, Γ' , is mostly negligible in the quantum engineering experiments, since the whole environment is usually cooled down to sufficiently low temperature. Therefore, we shall ignore this from now on. We now consider two sources of relaxations. One is the spontaneous decay or longitudinal relaxation, which originates in the finite lifetime of the excited state $|e\rangle$ and is represented by a Lindblad superoperator $\mathcal{L}[\sqrt{\Gamma_1}\sigma_-]$. The other is the dephasing or the transverse relaxation, whose origins are diverse ranging from fast fluctuations of an environment to slow variation of applied electromagnetic fields. This is taken into account by a superoperator $\mathcal{L}[\sqrt{2\Gamma_2}\sigma_z/2]$. Putting these together, we shall investigate the specific but ubiquitous master equation

$$\frac{d\rho}{dt} = -\frac{i}{\hbar} [\mathcal{H}, \rho] + \frac{1}{2}\mathcal{L}[\sqrt{\Gamma_1}\sigma_-]\rho + \frac{1}{2}\mathcal{L}[\sqrt{\Gamma_2}\sigma_z]\rho. \quad (7.4.19)$$

As has been done when the Bloch equation was derived, both sides of the equation are evaluated and reinterpreted in terms of s_x , s_y , and s_z to become Bloch equations with relaxations:

$$\frac{ds_x}{dt} = -\Delta_q s_y - \frac{\Gamma_1 + 2\Gamma_2}{2} s_x \quad (7.4.20)$$

$$\frac{ds_y}{dt} = +\Delta_q s_x - \Omega s_z - \frac{\Gamma_1 + 2\Gamma_2}{2} s_y \quad (7.4.21)$$

$$\frac{ds_z}{dt} = \Omega s_y - \Gamma_1(s_z + 1) \quad (7.4.22)$$

$$\iff \frac{d\mathbf{s}}{dt} = \mathbf{B} \times \mathbf{s} - \begin{pmatrix} \frac{\Gamma_1+2\Gamma_2}{2}s_x \\ \frac{\Gamma_1+2\Gamma_2}{2}s_y \\ \Gamma_1(s_z + 1) \end{pmatrix}. \quad (7.4.23)$$

As can be seen in above expressions, Γ_1 is principally responsible for the decay from $|e\rangle$ to $|g\rangle$. Γ_2 does not account for the population decay but the Bloch sphere “shrinks” in s_x and s_y directions as a result of the loss of phase coherence of a qubit (see Fig. 7.5).

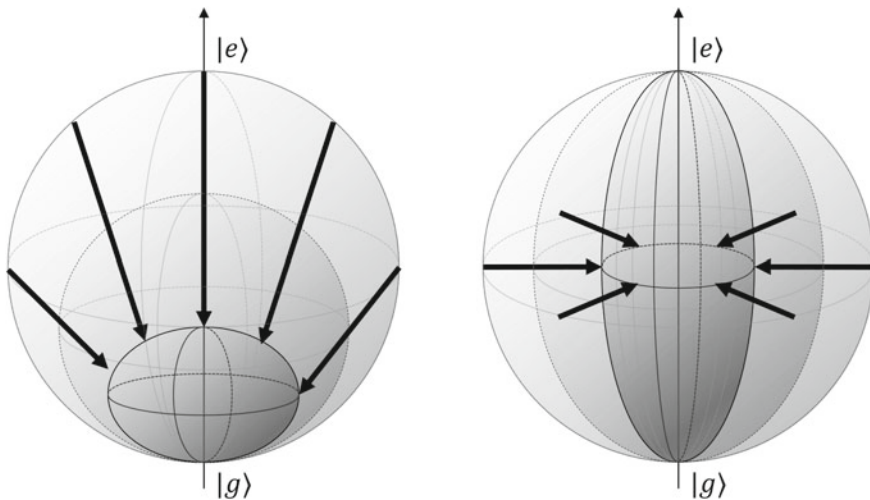


Fig. 7.5 Evolution of the Bloch sphere with spontaneous emission (left) and dephasing (right)

7.4.2 Rabi Oscillation

Given a set of equations that describes the spin dynamics in the presence of driving field and losses, we are to analyze it in practice. However, the Bloch equation cannot be solved analytically except for some special situations. We here solve this for idealized case of no detuning ($\Delta_q = 0$) and no relaxations ($\Gamma_1 = \Gamma_2 = 0$). Then the Bloch equations are simplified as

$$\frac{ds_x}{dt} = 0, \quad \frac{ds_y}{dt} = -\Omega s_z, \quad \frac{ds_z}{dt} = \Omega s_y$$

which yield $s_x = \text{const.}$ and $s_z = -\cos(\Omega t)$, $s_y = \sin(\Omega t)$ with an initial condition $s_z(t=0) = -1$, meaning that the qubit is in $|g\rangle$ at $t=0$. Intuitively in the Bloch sphere, the qubit state, first in $|g\rangle$, is rotated about the vector $(\Omega, 0, 0)$, the “x” axis, see left panel of Fig. 7.6. One can easily recognize that Ω determines how rapidly the qubit is rotated in the Bloch sphere, justifying the notion of the Rabi frequency. Recall that the Rabi frequency Ω is related to the applied field strength by $\Omega = \mu E_d / 2\hbar$, the product of the transition dipole moment and the applied electric field strength. Therefore, how much the qubit is rotated with an applied pulse, being assumed to be square-shaped, is under control of the pulse duration Δt and electric field strength E_d . In general, the phase of rotation is determined by the pulse area, the integrated pulse envelope over relevant time.

We give some remarks on a bit more general case, firstly for a finite detuning $\Delta_q \neq 0$. As mentioned previously, the Bloch vector, the qubit state represented in the Bloch sphere, is rotated about the vector $(\Omega, 0, -\Delta_q)$, which is inclined by an angle $\theta = -\arctan(\Delta_q / \Omega)$ with respect to the x axis, see right panel of Fig. 7.6. Therefore, the population dynamics can be easily deduced from the above consideration: the

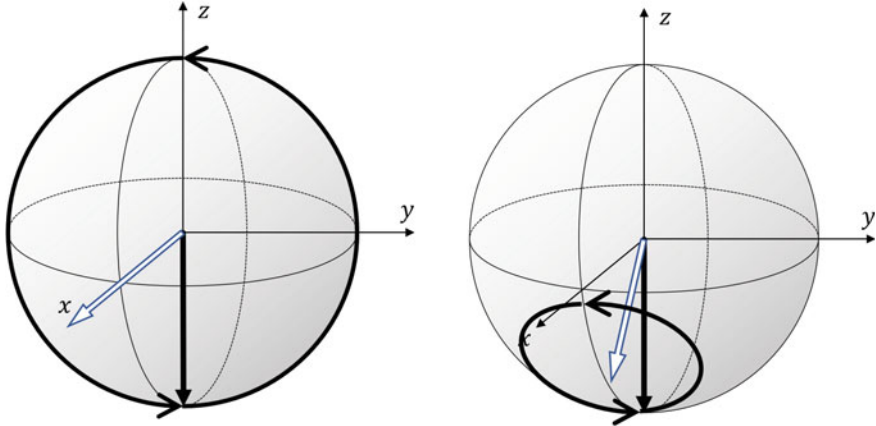


Fig. 7.6 Rabi oscillation without (left) and with (right) the detuning

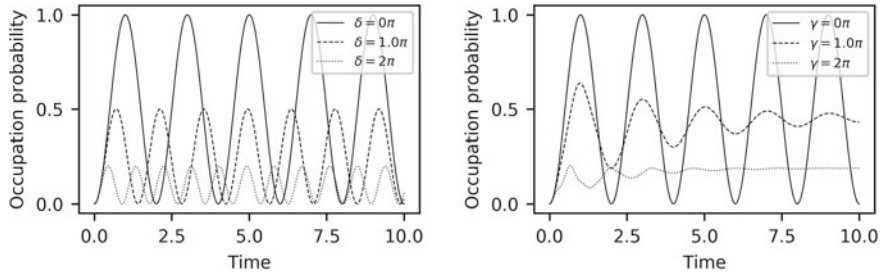


Fig. 7.7 Population dynamics in $|e\rangle$ during the Rabi oscillation. Left panel: Rabi oscillation for various detunings δ without spontaneous decay. Right panel: Rabi oscillation for various spontaneous decay rates γ without detuning. Simulation is done with the help of QuTiP [13]

Bloch vector of the qubit is rotated about $(\Omega, 0, \Delta_q)$ and the population, initially in $|g\rangle$, is not completely transferred to $|e\rangle$ unlike the case of $\Delta_q = 0$, and the angular frequency of the rotation is given by the length of the vector $(\Omega, 0, \Delta_q)$, namely $\sqrt{\Omega^2 + \Delta_q^2}$ which is called the generalized Rabi frequency. The situation is depicted in the right panel of Fig. 7.6. In the case of finite losses, namely Γ_1 and Γ_2 are not equal to zero, the Rabi oscillation gradually loses its amplitude and final population $s_z(t = \infty)$ is determined by the balance between the driving intensity Ω and the decay Γ_1 . Such a situation is illustrated in the left panel of Fig. 7.7. Numerical evaluation of the system dynamics is useful in such general cases.⁷

⁷ For example, a package called Quantum Toolbox In Python (QuTiP) [13] is a good choice if you are familiar with python (or even if not!).

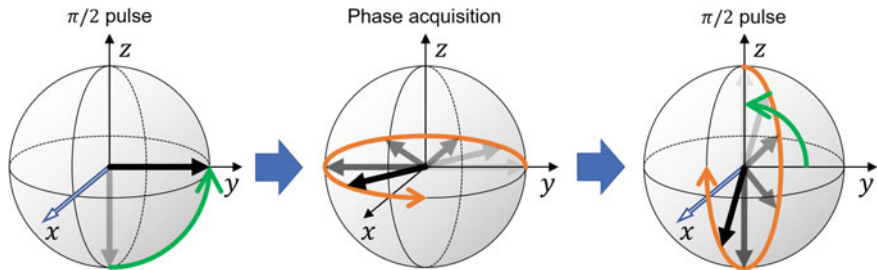


Fig. 7.8 Schematics of the Ramsey interference

7.4.3 Ramsey Interference

We would like to introduce another important quantum-mechanical phenomena⁸ called Ramsey interference, named after Norman Ramsey. In the Ramsey interference, the qubit is transformed into a superposition of ground and excited states and the interference phenomenon can be observed between these states experiencing different phase shifts. First we apply a resonant electromagnetic pulse of duration $\Delta t = \pi/2\Omega$ to the qubit so that it acquires the phase of $\pi/2$ in the Rabi oscillation. This pulse is called the $\pi/2$ -pulse. The Bloch vector, initially in $|g\rangle$, is then transferred to $|-\rangle = (|g\rangle - i|e\rangle)/\sqrt{2}$ (left panel of Fig. 7.8). Then for some time duration the qubit is subject to the “free” evolution, that is, we do nothing. At the final stage, the $\pi/2$ -pulse is again applied to the qubit that maps the phase information in xy plane onto zx plane and the projective measurement along z axis is executed. If the qubit is not subject to any fluctuating environment and/or stray field, the Bloch vector stays where it is just after the first $\pi/2$ -pulse and is transferred to $|e\rangle$ by the second $\pi/2$ -pulse, which gives $s_z = 1$.

If, e.g., the slow variation of the applied field, the phase drift occurs during the time we leave the qubit between the two $\pi/2$ -pulses, the phase rotation in the xy plane is transformed to the one in the zx plane and the final measurement result of s_z oscillates (co-)sinusoidally between 1 and -1 (see middle and right panels of Fig. 7.9) according to the acquired phase, showing an interference fringe. Or if the pure dephasing instead of the phase drift is experienced by the qubit, random phase “diffusion” in xy plane makes s_x and s_y decrease and finally results in $s_x = s_y = 0$ with sufficiently long duration between the two $\pi/2$ -pulses.

7.4.4 Spin Echo

Even if there are some sources of the phase drifts mentioned above during the time evolution of the quantum systems, their effects can be canceled by a spin-echo method, though under a few conditions. The essential idea is simple. The phase drift

⁸ Originally the Ramsey interference was invented for spectroscopic purpose.

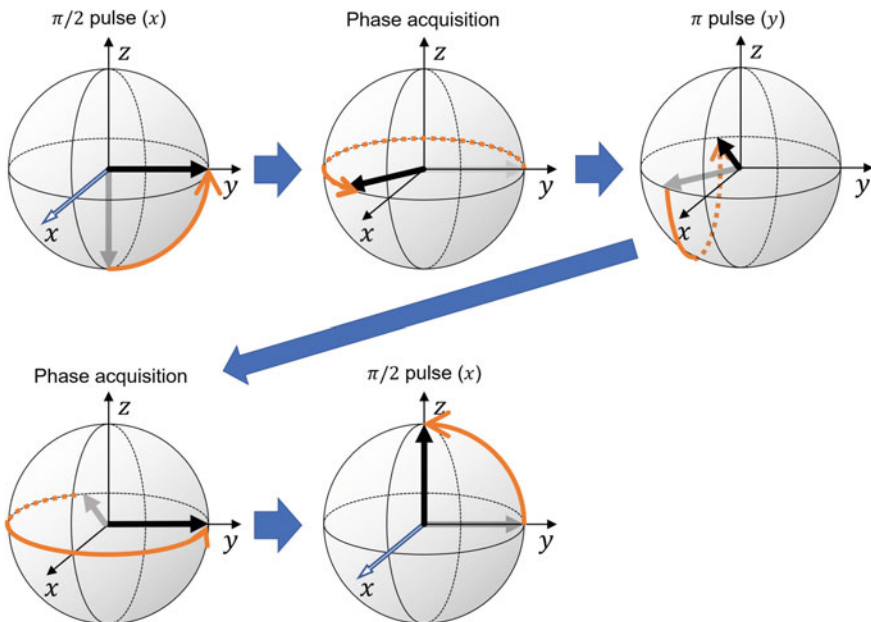


Fig. 7.9 Schematics of the spin-echo sequence

of the qubit is intuitively recognized as a rotation around z axis in the Bloch sphere. Then, if typical timescales of the phase drift are sufficiently long, or in other words the phase drift is constant over the time duration under concern, we can effectively “rewind” them by applying a π pulse around x or y axis.

The spin-echo method is particularly useful when, for example, the qubit is subject to the slowly varying noise during the quantum operations such as π rotation around x axis. Since the phase drift adds small z rotation during the x -rotation sequence, it gives rise to an operational error. To avoid this error, spin-echo method tells us that we can cancel the phase drift by dividing the π pulse into two $\pi/2$ pulses temporarily separated by some duration τ and insert a π pulse around y axis in between, delayed from the first $\pi/2$ pulse by $\tau/2$. To see what is going on in this sequence, see Fig. 7.9. Let us suppose the qubit is initialized in $|g\rangle$. The first $\pi/2$ pulse let the quantum state in $| -i \rangle$ and in the succeeding $\tau/2$ free evolution the Bloch vector is rotated around z axis by some angle ϕ . The π pulse in between the two $\pi/2$ pulses flips the Bloch vector around y axis. Here, if the source of the phase drift is constant over the whole sequence, the Bloch vector again rotates about z axis by exactly the same angle ϕ to get back to $| -i \rangle$ state. Eventually, the last $\pi/2$ pulse let $| -i \rangle$ evolve into $|e\rangle$. In the above discussion, of course, a fact that the phase drift occurs during every pulse sequence is neglected. Even so, the fine tuning of the pulse durations could help achieve phase-drift-free qubit operation in actual experiments.

The spin-echo method is originally invented for the spectroscopy of an ensemble of spins in the presence of the inhomogeneous environment, where the inhomogeneous phase evolutions of the spins here and there are all “rewinded” to have

echo-like revival of the signals of the spin ensemble. For a single spin, or a qubit, unwanted phase acquisition is prevented by this pulse sequence, however, the loss of the phase coherence by the pure dephasing still remains. Therefore, in combination with the ordinary Ramsey interference, the spin-echo method is frequently used for the measurement of pure dephasing rate separately from the systematic phase noises.

Problems

Problem 7-1 Find eigenvectors for the Pauli operators σ_x , σ_y and σ_z .

Problem 7-2 Show that the density matrix of a qubit can be written as

$$\rho = \frac{1}{2}(I + s_x\sigma_x + s_y\sigma_y + s_z\sigma_z). \quad (7.4.24)$$

Problem 7-3 Discuss what happens for the Bloch vector (s_x, s_y, s_z) when ρ is mixed state. What if $\rho = I/2$?

Problem 7-4 Discuss the nature of the Bloch equation (7.4.23) for $\Gamma_2 = 0$, and $s_z(t=0) = 1$ and explain the physical situation and consequence.

Problem 7-5 Consider the steady state of the Bloch equation (7.4.23), namely $ds/dt = 0$ to calculate the excited-state population ρ_{ee} . It will be of Lorentzian lineshape with respect to the detuning Δ_q and check that power broadening occurs, that is, the linewidth gets thicker as the Rabi frequency increases.



Electromagnetic Cavities and Cavity Quantum Electrodynamics

8

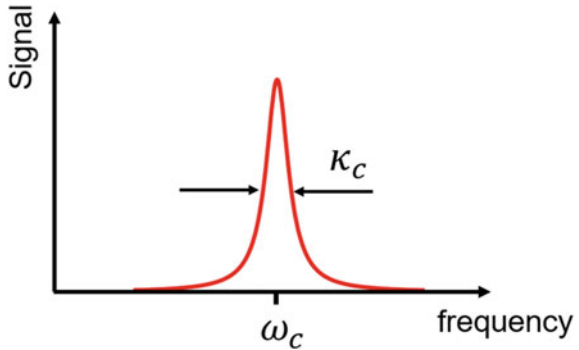
Only for the sake of manipulating a single quantum system, one can realize it by applying intense electromagnetic waves such as lasers and/or microwaves, except for the photon itself as a quantum system. However, this is not the case when one wants to convert quantum states back and forth between a fixed quantum system and a photon, in a deterministic and efficient manner. For such a purpose, electromagnetic cavities, or electromagnetic resonators, are outstandingly significant components in quantum technologies for their ability to enhance the interaction between a single quantum system and a single photon. In this chapter, we will describe some properties of electromagnetic cavities and general schemes of cavity measurements. To put it concretely, We will introduce quality factor and lifetime of a cavity, finesse of a Fabry-Perót cavity, internal loss and external coupling, and input-output theory with applications to some types of cavities. Succeeding Sections are devoted to the introduction of cavity quantum electrodynamics where Jaynes–Cummings and Tavis–Cummings models are introduced and weak, strong and strong dispersive regimes are analyzed.

8.1 Properties of Cavities

An electromagnetic resonator/cavity, or simply a cavity, is characterized by its resonant (angular) frequency ω_c and the lifetime τ_c of a cavity photon. The lifetime of the cavity photon characterizes the $1/e$ time scale of the exponential decay of

Supplementary Information The online version contains supplementary material available at https://doi.org/10.1007/978-981-19-4641-7_8.

Fig. 8.1 Typical frequency spectrum of a cavity mode



the cavity photon number. Despite we introduced the lifetime, the cavity is rarely evaluated by the lifetime itself. We instead often consider a loss rate $\kappa_c = 2\pi/\tau_c$ of the cavity photon which is proportional to the inverse of the cavity lifetime. In terms of the electric field of the cavity mode, it oscillates at the frequency $\omega_c/2\pi$ and its amplitude decays exponentially with the rate $\kappa_c/2$. This exponential decay assumes that the loss rate is independent of the number of photons inside the cavity, which is justified in almost every situation since the photon–photon interaction, or the self-Kerr effect, is usually very weak. Frequency spectrum $S_c(\omega)$ of such a cavity mode is, by noting that the exponential function is Fourier transformed to yield a Lorentzian function, expected to have a form

$$S_c(\omega) \propto \frac{1}{(\omega - \omega_c)^2 + (\kappa_c/2)^2}. \quad (8.1.1)$$

As can be seen in this spectral shape (see Fig. 8.1), the loss rate κ_c is the full-width-half-maximum value of this Lorentzian spectrum.

An electromagnetic cavity is a tool for confining electromagnetic waves inside a definite spatial region. As mentioned above, one of its characteristics is how long it can trap electromagnetic waves inside it, and frequently used quantities are quality factor or Q factor Q and finesse \mathcal{F} , both being proportional to the lifetime and inversely proportional to the loss rate of the cavity. Which of these two we should consider depends on various situations and losses involved in the cavity, however, basic policy to decide which is somewhat simple, as detailed in the later Section. To evaluate these quantities, time-domain or frequency-domain measurement is performed where appropriate one is adopted in the actual experiment.

Another quantity to characterize the cavity is the mode volume V , which indicates that in how small region it can confine electromagnetic waves. As we learned in Sect. 6.2, vacuum fluctuation of the electric field of a cavity mode is proportional to $1/\sqrt{V}$, so that it is preferable to make the mode volume as small as possible for the sake of enhancing electromagnetic waves–matter interaction in the cavity mode. The mode volume is determined by the shape and size of the cavity.

8.1.1 Q Factor

Q factor is a quantity given by the ratio of the center frequency and the loss rate (full-width-half-maximum) of the Lorentzian spectrum of a cavity mode

$$Q = \frac{\omega_c}{\kappa_c}.$$

Its physical meaning becomes clear when we rewrite it as $Q = \tau_{\text{loss}}/\tau_c$, with $\tau_c = 2\pi/\omega_c$ and $\tau_{\text{loss}} = 2\pi/\kappa_c$, respectively, denote the oscillation period of the cavity electric field and the time constant of the cavity loss. This expression suggests that the Q factor tells how many times the resonant electromagnetic field can oscillate until it escapes from the cavity. It is implied that this quantity is a good measure if the cavity photon is continuously exposed to the loss, which is true in most cases except for the Fabry-Perot cavity.

Q factor gets infinity for a lossless cavity, however, in reality, various loss mechanisms make the Q factor finite. Let multiple loss mechanisms with loss rates $\kappa_i = \omega_c/Q_i$ join the system, which give rise to the total cavity loss rate $\sum_i \kappa_i$. By noting that the loss rate is inversely proportional to the Q factor, therefore, the Q factor of the cavity becomes

$$Q_{\text{tot}} = \left(\sum_i \frac{1}{Q_i} \right)^{-1}. \quad (8.1.2)$$

Nonetheless, when one designs experimental systems in practice including internal loss and external coupling as is done in the input-output theory (see Sect. 8.3), it might be intuitive to go with the loss rates.

8.1.2 Finesse

The simplest optical cavity is a Fabry-Perot resonator, which consists of a pair of mirrors that traps light in between (see Fig. 8.2). In this cavity, light wave resonates when the phase acquisition during a single turnaround in the resonator equals an integer multiple of 2π , by which the light wave inside the cavity can constructively

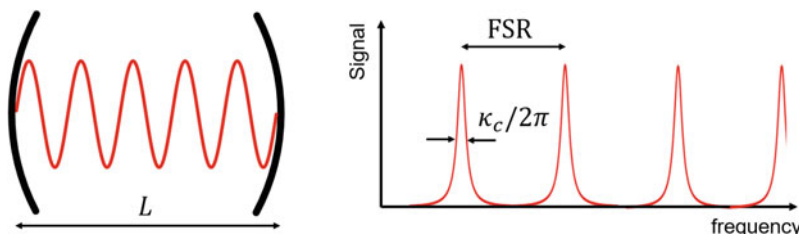


Fig. 8.2 Fabry-Perot cavity and its spectra

interfere to build up. In other words, the light waves in the cavity otherwise interfere with various phases modulo 2π to cancel out, which means that the light wave cannot exist in the cavity. The resonance condition reads

$$2nL = \lambda \mathbb{N} \quad \Leftrightarrow \quad v = \frac{c}{\lambda} = \frac{c}{2nL} \mathbb{N}, \quad (8.1.3)$$

by reinterpreting the above condition as the round-trip optical length being equal to the integer multiple of the optical wavelength. Here \mathbb{N} denotes the non-negative integer. One can immediately see that the cavity mode aligns equidistantly in the frequency domain, and the frequency interval $c/2nL$ is called the free spectral range or FSR. Taking into account the loss of the cavity, each spectrum has a Lorentzian lineshape with its full-width-half-maximum corresponding to the loss rate.

Let us pose here a bit thinking about the loss of the Fabry-Perot cavity. When the light propagates in the region between the mirrors, the atmosphere between the mirrors hardly causes loss by light scattering, as long as the wavelength is in the visible or near-infrared region. The main origin of the loss in the Fabry-Perot cavity is the cavity mirror, where light unwantedly flies out of the cavity due to various mechanisms, such as surface roughness and imperfect reflectivity. Therefore, the loss rate of the Fabry-Perot cavity is proportional to the number of times that light is reflected by cavity mirrors within 1 s. Given this observation, the longer the cavity, the larger the Q factor. In such a situation, the Q factor still represents a loss rate, but not a good parameter characterizing a quality of Fabry-Perot cavity. Finesse \mathcal{F} is used in such a situation, instead of the Q factor. The finesse is represented by using FSR as

$$\mathcal{F} = \frac{\text{FSR}}{\kappa_c/2\pi}. \quad (8.1.4)$$

The quantity $1/\text{FSR} = 2nL/c$ stands for how long it takes for light to go around the cavity and $2\pi/\kappa_c$ does for the time constant of the loss. Therefore, finesse quantifies how many times the light can go around the cavity.

8.2 Measurement of a Cavity

Cavities often appear in experimental attempts of quantum technologies and their measurement take various forms depending on the physical systems. However, every measurement technique has an essential thing in common, that is, one inputs electromagnetic waves to the cavity and inspects the response. This will be clarified more using input-output theory in the later section, however, let us see basic measurement schemes here as a preparation.

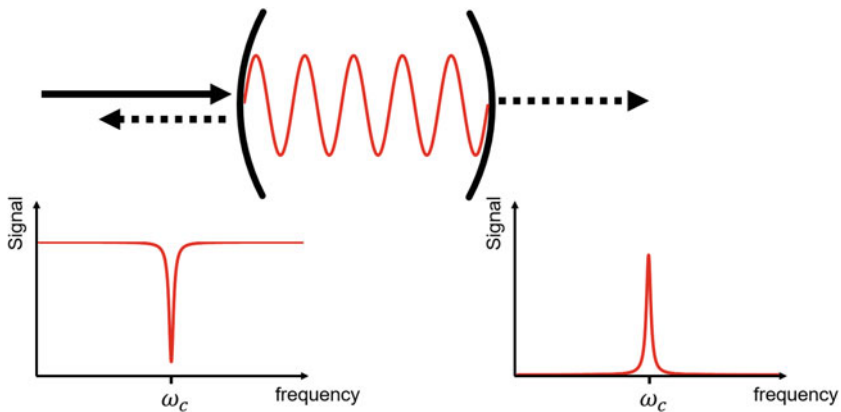


Fig. 8.3 Schematic representation of reflection and transmission measurements

8.2.1 Reflection and Transmission Measurements

Cavity has a structure that traps electromagnetic waves inside, so that the electromagnetic waves injected from outside are repelled out ideally. However, with a proper design one can inject a fraction of electromagnetic waves into the cavity. Hence, the amount of electromagnetic waves reflected back from the cavity is reduced, and the measurement of this signal reduction is referred to as the reflection measurement. If we have another outcoupling port incorporated in a cavity, the injected electromagnetic waves can transmit from the input port to that port. These transmitted waves are also useful for cavity measurement since it allows for the background-free measurement of the cavity. This latter method is called the transmission measurement. A schematics in Fig. 8.3 might help the readers to grab a concept.

Spectrum measurement

The most common method of measuring a cavity is to measure its electromagnetic response in the frequency domain. In concrete, reflection or transmission signal of the electromagnetic waves is measured with the frequency $\omega/2\pi$ of the incident wave swept over the resonance, see Fig. 8.3.

This method is valid when the cavity linewidth is broader than that of the incident electromagnetic wave, which is the case in most experiments. In contrast, if such a situation is not realized in the experiment, the measured spectrum shows the linewidth of the incident wave as well and the cavity linewidth is hidden in such a noise.¹ Even in such a case, we can measure the linewidth of the cavity by ring-down method, a time-domain measurement introduced in the next section.

¹ Rather we can measure the linewidth of the electromagnetic wave in this situation

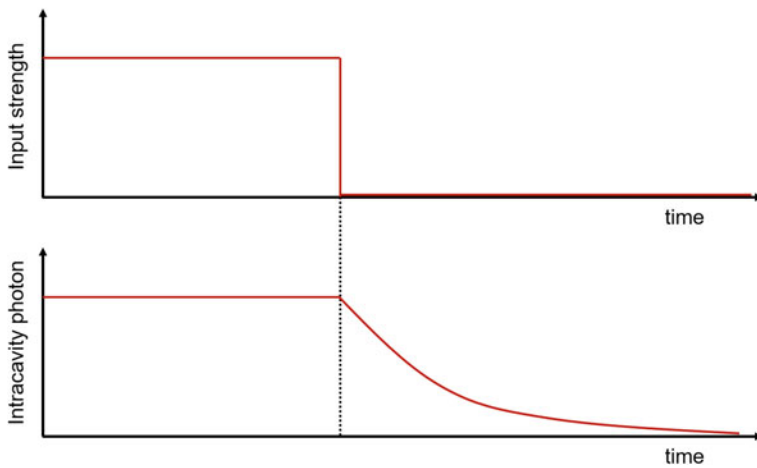


Fig. 8.4 Timeline of the input electromagnetic wave (upper panel) and observed signal (lower panel) in the ring-down experiment

Ringdown measurement

If we continuously inject electromagnetic waves into the cavity resonance, a steady state is realized such that a certain amount of photons are accumulated in the cavity. The number of photons stored inside the cavity is determined by the balance between the photon injection rate and the loss rate and detailed calculation can be done by using the input-output theory later. Then we suddenly turn off the electromagnetic wave or tune the frequency of the electromagnetic wave off-resonant. After such an operation, photon injection no longer exists and the stored photons inside the cavity leak out. The photon number decreases exponentially as inferred by the Fourier transformation of the Lorentzian spectrum of the cavity mode. Therefore, the signal from the cavity also decreases exponentially. This type of measurement is called the ring-down measurement which is an analogy of ringing down the bell and examining the decay of the sound of the bell. A schematic illustration of what we observe in the ring-down measurement is indicated in Fig. 8.4.

In the ring-down measurement, we must quickly modulate or turn off the electromagnetic wave into the cavity in time domain. This is difficult for the measurement of a cavity with thick linewidth, or equivalently a cavity with short lifetime. On the other hand, ring-down measurement is suitable for a cavity with narrow linewidth, or long lifetime, manifesting itself as a useful method of the cavity measurement complimentary to the frequency-domain measurement.

8.2.2 Actual Measurement Systems

Let us take an overview of the measurements for optical cavities. As a typical case, we pick up Fabry-Perot and ring cavities here. For a Fabry-Perot cavity, a laser beam is incident on one of the mirrors with the same direction and the same beam profile as

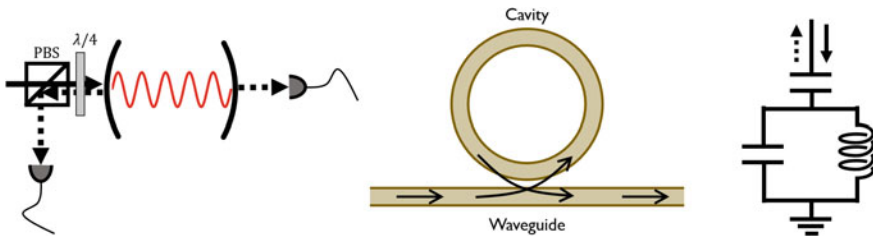


Fig. 8.5 Schematics of the actual measurement systems of a Fabry-Perot resonator (left), a ring resonator (center) and an LC resonator (right)

leaked optical mode out of a cavity. The reflection measurement can be implemented by collecting the reflected light at the first mirror by properly setting the polarization of the incident optical beam. If we collect the leakage of cavity-mode light through the second mirror instead, this measurement becomes the transmission measurement. The leakage rate of photons of the cavity mode is dependent on the reflectances of the mirrors. The injection rate of photons into the cavity is additionally dependent on the spatial overlap between the input mode and leakage mode.

As for the ring cavity (center of Fig. 8.5), it is not easy to have an access to a cavity mode from free space. In such a case, one can introduce light into the ring cavity by putting an optical waveguide next to the ring cavity, so that the evanescent wave of the optical waveguide overlaps that of the cavity mode which results in the coupling between the modes of the optical waveguide and ring cavity. With this configuration, one can observe dips in the transmission spectrum of the optical waveguide, which originates in the resonance of the cavity modes of the ring cavity that extracts light from the optical waveguide.

Next, we will describe the measurement systems for the cavity constructed by electrical circuits. Right panel of Fig. 8.5 displays an LC circuit. By adding a capacitor and sending radio-frequency waves or microwaves from one side of that coupling capacitor, we can get the reflection from the LC resonator and implement the reflection measurement. Furthermore, if we add other coupling elements and monitor leakage signals of electromagnetic waves, the transmission measurement is feasible. The coupling element is not necessarily capacitors, but inductors can also be used to couple to the LC resonator by utilizing the mutual inductance. The difference between the use of capacitor and inductor is merely whether the LC resonator is accessed through its electric or magnetic field. Which one to use is up to the electromagnetic-field profiles of the resonator and to the actual design parameters and purposes. Such circumstances are common in various cavities using electrical components, for example, a coplanar cavity, three-dimensional cavity, and loop-gap cavity.

8.3 Input-Output Theory

8.3.1 Propagating Mode and Input-Output Theory

In this Section, we investigate what signals we should expect in the reflection and transmission measurements and what information we can deduce about the cavity from the measurement outcome. In relation to this purpose, we have a problem that we only know, or have learned through this book, how to treat spatially localized physical systems, e.g. a qubit that is supposed to be at rest and a cavity confining electromagnetic waves in some region. However, we want to analyze the situation that traveling photons in the propagating mode are coupled into and out of the cavity. We should utilize boundary conditions at which a localized mode and a propagating mode exchange photons to analyze the system. Below, we overview the basics of the input-output theory treating such boundary conditions called input–output relations together with its applications for practical cavity measurements.

Here let annihilation and creation operators of one-dimensional propagating mode be $c(\omega)$ and $c(\omega)^\dagger$, respectively, with a commutation relation $[c(\omega), c^\dagger(\omega')] = 2\pi\delta(\omega - \omega')$. The operators are dependent on the frequency of the propagating mode, reflecting the fact that a propagating mode has a continuous spectrum. With this setup, we shall describe a model of cavity measurement including the coupling of the cavity mode to the propagating mode [26].

First, Hamiltonian of the whole system including a cavity mode, a propagating mode and the coupling between them is dictated as

$$\mathcal{H}_{\text{tot}} = \hbar\omega_c a^\dagger a + \int_{-\infty}^{\infty} \frac{d\omega}{2\pi} \hbar\omega c^\dagger(\omega)c(\omega) - i\hbar\sqrt{\kappa} \int_{-\infty}^{\infty} \frac{d\omega}{2\pi} [a^\dagger c(\omega) - c^\dagger(\omega)a]. \quad (8.3.1)$$

First term represents the cavity mode and the second one the propagating mode. The coupling between the cavity mode and the propagating mode is incorporated in the third term with the rate of photon exchange being represented by the quantity called external coupling rate κ . We pose here for a moment to clarify the reason why the external coupling rate is included in the third term by its square root. Consider the situation where the cavity is pumped and the number of photons are stored inside it. The quantity κ is the rate that the cavity photon leaks out toward the propagating mode, which can be in principle evaluated using Fermi's golden rule. Therefore, the squared value of the coefficient of the interaction Hamiltonian should coincide with the rate κ , so that $\sqrt{\kappa}$ appears in the coefficient of the third term.

To return to our subject, let us write down the Heisenberg equation of motion about the propagating-mode operator $c(\omega)$

$$\begin{aligned} \frac{dc(\omega)}{dt} &= \frac{i}{\hbar} [\mathcal{H}_{\text{tot}}, c(\omega, t)] = \frac{i}{\hbar} \left[\int_{-\infty}^{\infty} \frac{d\omega'}{2\pi} \hbar\omega' c^\dagger(\omega')c(\omega'), c(\omega) \right] \\ &\quad + \frac{i}{\hbar} \left[-i\hbar\sqrt{\kappa} \int_{-\infty}^{\infty} \frac{d\omega'}{2\pi} [a^\dagger c(\omega') - c^\dagger(\omega')a], c(\omega) \right] \end{aligned}$$

$$\begin{aligned}
&= \int_{-\infty}^{\infty} \frac{d\omega'}{2\pi} i\omega' \left[c^\dagger(\omega') c(\omega'), c(\omega) \right] + \int_{-\infty}^{\infty} \frac{d\omega'}{2\pi} \sqrt{\kappa} \left[a^\dagger c(\omega') - c^\dagger(\omega') a, c(\omega) \right] \\
&= - \int_{-\infty}^{\infty} \frac{d\omega'}{2\pi} i\omega' (2\pi) \delta(\omega - \omega') c(\omega') + \int_{-\infty}^{\infty} \frac{d\omega'}{2\pi} \sqrt{\kappa} (2\pi) \delta(\omega - \omega') a \\
&= -i\omega c(\omega) + \sqrt{\kappa} a.
\end{aligned} \tag{8.3.2}$$

On the other hand, the Heisenberg equation of motion for the cavity mode reads by denoting the system Hamiltonian by \mathcal{H}_s

$$\frac{da}{dt} = \frac{i}{\hbar} [\mathcal{H}_s, a] - \sqrt{\kappa} \int_{-\infty}^{\infty} \frac{d\omega}{2\pi} c(\omega). \tag{8.3.3}$$

What we do next is to formally solve the Heisenberg equation of motion for the propagating mode. In doing this, we have two solutions, namely c_{in} referring to a past time $t_0 < t$ and c_{out} referring to a future time $t_1 > t$. These can be written as, by making use of the equality $\int (d\omega/2\pi) e^{-i\omega(t-\tau)} = \delta(t - \tau)$

$$c_{\text{in}}(\omega, t) = e^{-i\omega(t-t_0)} c(\omega, t_0) + \sqrt{\kappa} \int_{t_0}^t d\tau e^{-i\omega(t-\tau)} a(\tau), \tag{8.3.4}$$

$$c_{\text{out}}(\omega, t) = e^{-i\omega(t-t_1)} c(\omega, t_1) - \sqrt{\kappa} \int_t^{t_1} d\tau e^{-i\omega(t-\tau)} a(\tau). \tag{8.3.5}$$

Substituting these into the Heisenberg equation of motion for the cavity mode, we obtain

$$\frac{da}{dt} = \frac{i}{\hbar} [\mathcal{H}_s, a] - \frac{\kappa}{2} a - \sqrt{\kappa} c_{\text{in}} e^{-i\Omega t}, \tag{8.3.6}$$

$$\frac{da}{dt} = \frac{i}{\hbar} [\mathcal{H}_s, a] + \frac{\kappa}{2} a - \sqrt{\kappa} c_{\text{out}} e^{-i\Omega t}. \tag{8.3.7}$$

The derivation is aided by the Markov approximation that allows us to neglect m -fold integrals ($m \geq 2$) and the substitutions

$$c_{\text{in}} e^{-i\Omega t} = \int_{-\infty}^{\infty} \frac{d\omega}{2\pi} e^{-i\omega(t-t_0)} c(\omega, t_0), \tag{8.3.8}$$

$$c_{\text{out}} e^{i\Omega t} = \int_{-\infty}^{\infty} \frac{d\omega}{2\pi} e^{-i\omega(t-t_1)} c(\omega, t_1). \tag{8.3.9}$$

There is one thing to note here about c_{in} and c_{out} . These operators are now integrated with respect to frequency. As a result, these have a unit of [$\sqrt{\text{Hz}}$]. An operator $n_{\text{in/out}} = c_{\text{in/out}}^\dagger c_{\text{in/out}}$ hence possesses a unit of [Hz], implying that $n_{\text{in/out}}$ stands for a photon flux operator.

By combining the above two differential equations, the following input-output relation can be obtained:

$$c_{\text{out}} = c_{\text{in}} + \sqrt{\kappa} a e^{i\Omega t}. \tag{8.3.10}$$

The set of the Heisenberg equation of motion and input–output relation allows us to calculate various experimentally measurable quantities such as absorption and emission spectra. The input–output relation is often rewritten as $c_{\text{out}} = c_{\text{in}} + \sqrt{\kappa}a$ in rotating frames with frequency Ω for both c_{in} and c_{out} . In the following sections, we will see how to use this method for understanding how cavity measurement works.

8.3.2 Single-Port Measurement

We here consider what we call single-port measurement as a simple and useful situation. What we call the single-port measurement here refers to the circumstance that the cavity is intended to couple to only a single propagating mode, e.g., an optical microring resonator coupled to an optical waveguide, an electrical circuit resonator with a capacitively or inductively coupling wiring, and so on.

As a Hamiltonian, we only have to take the cavity one $\mathcal{H} = \hbar\Delta_c a^\dagger a$ into account and do not have to explicitly include the propagating mode, for we know how it affects the Heisenberg equation of motion of a . Whenever it becomes unclear what the equation should look like with the propagating mode, one would follow the discussion in the previous Section again to obtain the correct equation. Here we define the relaxation rate of the cavity photon without the external coupling, or intrinsic loss, as κ_{in} and the external coupling rate between the cavity and the propagating mode, here for convenience supposed to be the one inside a waveguide of some electromagnetic field, as κ_{ex} ; see Fig. 8.6. The Heisenberg equation of motion of a reads

$$\frac{da}{dt} = -i\Delta_c a - \frac{\kappa_{\text{in}}}{2}a - \frac{\kappa_{\text{ex}}}{2}a - \sqrt{\kappa_{\text{ex}}}a_{\text{in}}. \quad (8.3.11)$$

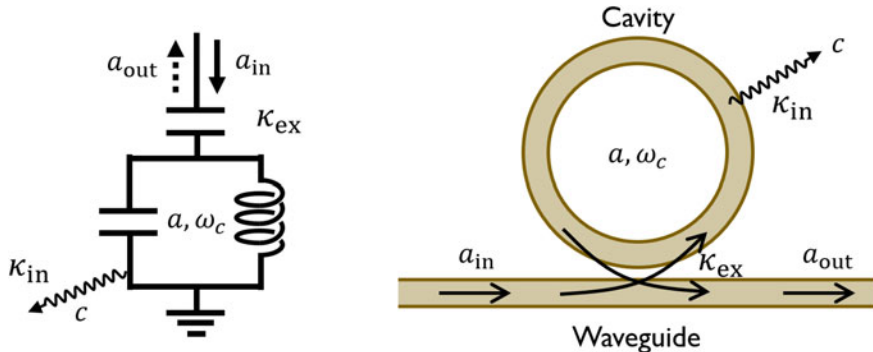


Fig. 8.6 Schematics of a single-port measurement

and the input-output relation is obtained to be $a_{\text{out}} = a_{\text{in}} + \sqrt{\kappa_{\text{ex}}}a$. In a steady state, $da/dt = 0$ and this yields

$$a = -\frac{\sqrt{\kappa_{\text{ex}}}}{i\Delta_c + \frac{\kappa_{\text{in}} + \kappa_{\text{ex}}}{2}}a_{\text{in}}. \quad (8.3.12)$$

By taking the product of this and its Hermitian conjugate, we obtain a relationship between the intra-cavity photon number $n_{\text{cav}} = a^\dagger a$ and input photon flux $n_{\text{in}} = a_{\text{in}}^\dagger a_{\text{in}}$ as

$$n_{\text{cav}} = \frac{\kappa_{\text{ex}}}{\Delta_c^2 + [(\kappa_{\text{in}} + \kappa_{\text{ex}})/2]^2} n_{\text{in}}. \quad (8.3.13)$$

From this expression, we see that the intra-cavity photon number roughly equals the input photon flux divided by the relaxation rate of the cavity when the driving frequency is in resonance with the cavity and the intrinsic loss κ_{in} is negligible compared to the external coupling.

Furthermore, by substituting the expression of a into the input-output relation, we get

$$\begin{aligned} a_{\text{out}} &= \left(1 - \frac{\kappa_{\text{ex}}}{i\Delta_c + \frac{\kappa_{\text{in}} + \kappa_{\text{ex}}}{2}}\right) a_{\text{in}} \\ &= \frac{i\Delta_c + \frac{\kappa_{\text{in}} - \kappa_{\text{ex}}}{2}}{i\Delta_c + \frac{\kappa_{\text{in}} + \kappa_{\text{ex}}}{2}} a_{\text{in}}. \end{aligned} \quad (8.3.14)$$

The transmittance T of the waveguide can be calculated as the ratio of output photon number/flux to the input photon number/flux. Then by using $\langle n_{\text{out}} \rangle / \langle n_{\text{in}} \rangle = \langle a_{\text{out}}^\dagger a_{\text{out}} \rangle / \langle a_{\text{in}}^\dagger a_{\text{in}} \rangle$, the transmittance is revealed to be

$$T = \frac{\Delta_c^2 + \left(\frac{\kappa_{\text{in}} - \kappa_{\text{ex}}}{2}\right)^2}{\Delta_c^2 + \left(\frac{\kappa_{\text{in}} + \kappa_{\text{ex}}}{2}\right)^2} = 1 - \frac{\kappa_{\text{in}}\kappa_{\text{ex}}}{\Delta_c^2 + \left(\frac{\kappa_{\text{in}} + \kappa_{\text{ex}}}{2}\right)^2}. \quad (8.3.15)$$

As can be seen immediately from this expression, a Lorentzian dip appears in a transmission spectrum, manifesting itself as a signal of the cavity mode.

Related to this spectrum, we make a brief note of the three coupling regimes of the coupled cavity-waveguide system. First, if the external coupling rate κ_{ex} is smaller than the intrinsic loss rate κ_{in} of the cavity, namely if $\kappa_{\text{ex}} < \kappa_{\text{in}}$, the system is said to be in an under coupling regime or one would state that the cavity is under coupled. The left panel of Fig. 8.7 displays $\langle a_{\text{out}} \rangle / \langle a_{\text{in}} \rangle$ in the complex plane or phase space, using the relationship

$$a_{\text{out}} = \left(1 - \frac{\kappa_{\text{ex}}}{i\Delta_c + \frac{\kappa_{\text{in}} + \kappa_{\text{ex}}}{2}}\right) a_{\text{in}}. \quad (8.3.16)$$

The quantity $\langle a_{\text{out}} \rangle / \langle a_{\text{in}} \rangle$ as a function of the driving frequency forms a circle in the phase space. In the under coupling regime, the circle does not enclose the origin of the phase space, hence the spectral dip does not reach zero and the phase variation is obviously below π . This can be intuitively understood as follows: photons in the propagating mode transmit more without coupling into the cavity in the under coupling regime, so that not all photons can be consumed by the cavity.

When $\kappa_{\text{ex}} = \kappa_{\text{in}}$, that is, the intrinsic loss and the external coupling balances, the system is said to be in the critical coupling. In such a situation, the resonance circle in the phase space reaches the origin, resulting in a zero transmittance at the very resonance of the cavity mode and π -phase variation, see the middle panel of Fig. 8.7. This means that the photons in the propagating mode are completely consumed in the cavity mode. In other words, the impedance matching from the propagating mode to the intrinsic loss channel of the cavity mode is realized. The spectral linewidth of the cavity mode in the critical coupling becomes $\kappa_{\text{in}} + \kappa_{\text{ex}} = 2\kappa_{\text{in}}$. This situation is convenient in the experiment because when the spectral dip of the cavity mode shows Lorentzian lineshape with its linewidth Γ_{exp} and zero transmittance at resonance, one can immediately see that the intrinsic loss rate of the cavity mode is $\Gamma_{\text{exp}}/2$. If one has a single transmission spectrum alone without the phase information, one can uniquely determine the intrinsic loss rate of the cavity mode only when the measuring system is in the critical coupling regime.

The third and last regime is the over coupling regime, where the external coupling rate overwhelms the intrinsic loss rate, namely $\kappa_{\text{ex}} > \kappa_{\text{in}}$. The resonance circle, in this coupling regime encircles the origin of the phase space. This leads to a situation that the transmittance does not reach zero at resonance while the phase variation always yields 2π . The linewidth of the measured cavity mode is more than two times thicker than its intrinsic one, solely due to the coupling to the propagating mode. An over coupled cavity extracts many photons from the waveguide and at the same time returns many photons back to it. This is the reason why the over coupled cavity mode shows nonzero transmittance at resonance. The transmission spectra for various coupling parameters are shown in Fig. 8.8.

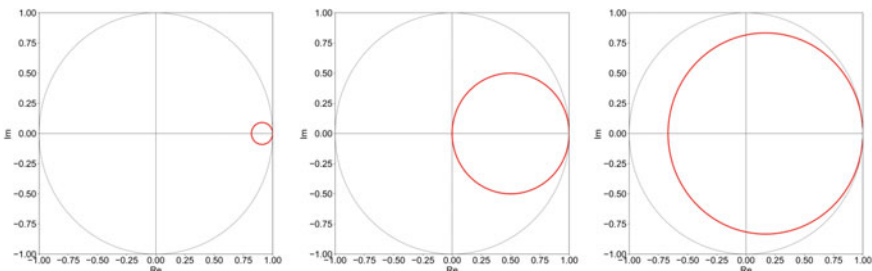


Fig. 8.7 Transmission signals in the phase space for the cavity mode in under-(left), critical (middle), and overcoupling regimes

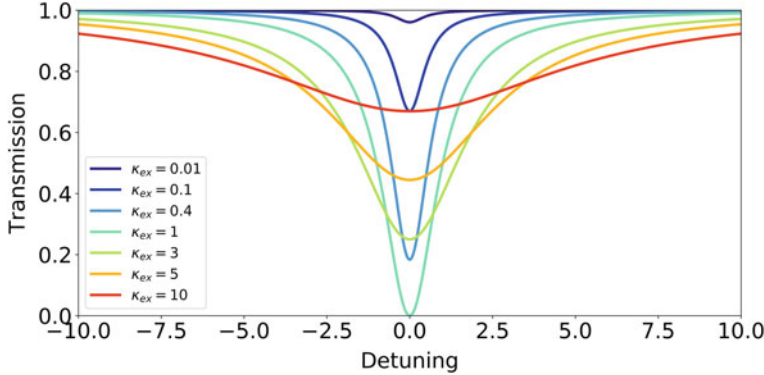


Fig. 8.8 Transmission spectra for various κ_{ex} for $\kappa_{\text{in}} = 1$

8.3.3 Dual-Port Measurement

The next cavity measurement under concern is what we call dual-port measurement here, including two-sided Fabry-Perot cavities and LC resonators with two coupling elements (Fig. 8.9). The input-output relations are considered in this case for two input-output ports of the electromagnetic waves, as two boundary conditions. At a port to which the electromagnetic waves are injected, the external coupling rate is defined as κ_1 . The annihilation operators for incident and reflected waves are written as a_{in} and a_{out} , respectively. At the other port with external coupling rate κ_2 , the transmitted electromagnetic waves are monitored and the annihilation operator of this field is written as b_{out} . Heisenberg equation of motion for cavity operator a reads, as in the previous Section

$$\frac{da}{dt} = -i\Delta_c a - \frac{\kappa}{2}a - \sqrt{\kappa_1}a_{\text{in}}. \quad (8.3.17)$$

Here, $\kappa = \kappa_{\text{in}} + \kappa_1 + \kappa_2$ is the total decay rate of the cavity, meaning that in addition to the intrinsic loss rate of the cavity, photons can escape from the cavity through the two ports. The input-output relations at the two ports are

$$a_{\text{out}} = a_{\text{in}} + \sqrt{\kappa_1}a, \quad (8.3.18)$$

$$b_{\text{out}} = \sqrt{\kappa_2}a \quad (8.3.19)$$

reflecting the incoming and outgoing fields at the two ports, where the one including b_{out} does not contain the incident field since there is no input field for this port. We shall consider the steady state to put $\frac{da}{dt} = 0$ and calculate the reflectance $R = \langle a_{\text{out}}^\dagger a_{\text{out}} \rangle / \langle a_{\text{in}}^\dagger a_{\text{in}} \rangle$ and the transmittance $T = \langle b_{\text{out}}^\dagger b_{\text{out}} \rangle / \langle a_{\text{in}}^\dagger a_{\text{in}} \rangle$. After some

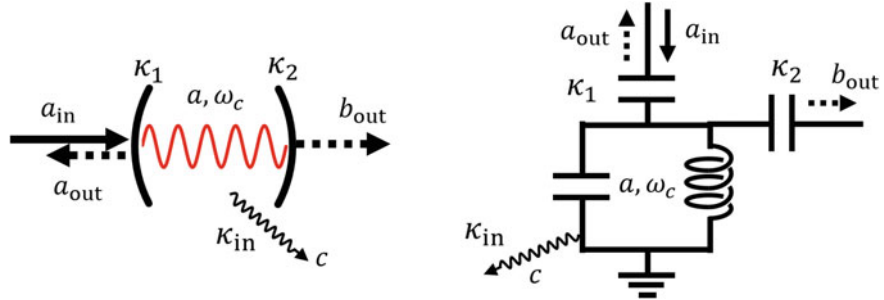


Fig. 8.9 Schematics of a dual-port measurement

maths, we obtain

$$R = 1 - \frac{\kappa_1(\kappa_{\text{in}} + \kappa_2)}{\Delta_c^2 + (\kappa/2)^2}, \quad (8.3.20)$$

$$T = \frac{\kappa_1 \kappa_2}{\Delta_c^2 + (\kappa/2)^2}. \quad (8.3.21)$$

Here the sum of the reflectance and transmittance is not unity: $R + T = 1 - \kappa_{\text{in}} \kappa_1 / (\Delta_c^2 + (\kappa/2)^2)$, simply because the intrinsic loss throws photons away in neither mode a_{out} nor mode b_{out} . One might well note that when $\kappa_1 = \kappa_{\text{in}} + \kappa_2$, the reflectance gets zero and the transmittance is maximized at resonance $\Delta_c = 0$. This is the “impedance matching” from the input port to the output port.

8.4 Cavity Quantum Electrodynamics

8.4.1 Jaynes–Cummings Model

Cavity quantum electrodynamics deals with the two-level system(s) interacting with a cavity to investigate quantum nature of photons inside the cavity or rather to control the two-level system in between by a cavity photon. Such a physical system is well described by the Jaynes–Cummings model

$$\mathcal{H}_{\text{JC}} = \frac{\hbar \omega_q}{2} \sigma_z + \hbar \omega_c a^\dagger a + \hbar g (\sigma_+ a + a^\dagger \sigma_-). \quad (8.4.1)$$

and let us analyze this model here to learn most simple but powerful platform of engineering a quantum system.

First of all, let us assume a lossless system and see what the eigenenergies of the Jaynes–Cummings Hamiltonian look like. Here the state vector with a qubit being in $|\xi\rangle$ ($\xi = g, e$) and n photons is denoted by $|\xi, n\rangle$. It is straightforward to inspect the matrix elements $\langle \xi', m | \mathcal{H}_{\text{JC}} | \xi, n \rangle$ and one will find that this Hamiltonian is block-diagonal. This is because the off-diagonal part, $\sigma_+ a + a^\dagger \sigma_-$, only connects $|g, n\rangle$

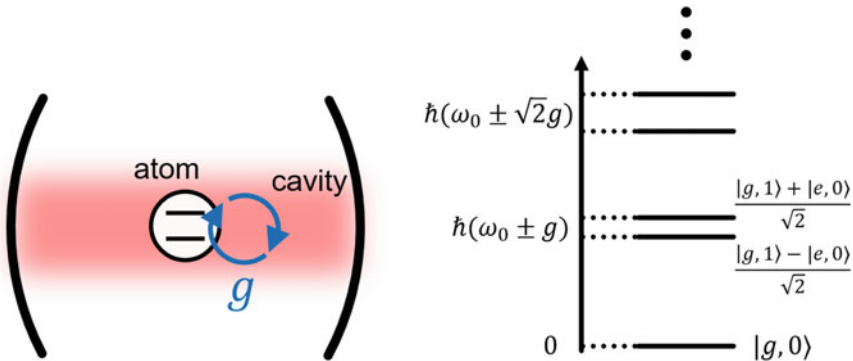


Fig. 8.10 Jaynes-Cummings model and Jaynes-Cummings ladder

and $|e, n-1\rangle$. By explicitly writing down the block $\mathcal{H}_{\text{JC}}^{(n)}$,

$$\mathcal{H}_{\text{JC}}^{(n)} = \begin{pmatrix} -\frac{\hbar\omega_q}{2} + \hbar\omega_c n & \hbar g \sqrt{n} \\ \hbar g \sqrt{n} & \frac{\hbar\omega_q}{2} + \hbar\omega_c(n-1) \end{pmatrix} \quad (8.4.2)$$

where the first and second column/row indicate the elements in bases $|g, n\rangle$ and $|e, n-1\rangle$, respectively, and $n \geq 1$. This matrix has eigenvalues $\lambda_{\pm} = \hbar\omega_c(n-1/2) \pm (\hbar/2)\sqrt{(\omega_c - \omega_q)^2 + 4g^2n}$, which reads, in the case of atom-cavity resonance $\omega_c = \omega_q = \omega_0$,

$$\lambda_{\pm} = \hbar\omega_0 \pm \hbar g \sqrt{n}. \quad (8.4.3)$$

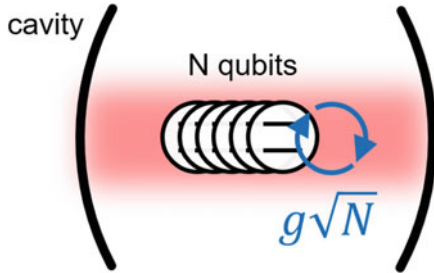
Thus the n -th excited manifold formed by $|g, n\rangle$ and $|e, n-1\rangle$ has (of course) two eigenstates energetically split by $2\hbar g \sqrt{n}$. Thus, the coupled system of a harmonic oscillator and a two-level system described by the Jaynes–Cummings model yields an anharmonic spectrum dubbed as the Jaynes–Cummings ladder. The energy splitting $2g$ of the first two excited states is called the vacuum Rabi splitting.

As for the eigenstate, the states $|\psi_{\pm}^n\rangle = (|g, n\rangle \pm |e, n-1\rangle)/\sqrt{2}$ represent the symmetric and anti-symmetric modes, much like the bonding and antibonding orbitals in molecules. If one somehow excites only the qubit or only injects photons into the cavity, the quantum state of the system oscillates among these symmetric and anti-symmetric modes (Fig. 8.10).

8.4.2 Tavis–Cummings Model

Let us consider another situation that N qubits are coupled to a single cavity mode with Jaynes–Cummings interaction, as schematically shown in Fig. 8.11. For simplicity, we assume here that every qubit has its transition frequency ω_q and that the coupling strengths for qubits, being inhomogeneous in actual experiments, are supposed to be the same value g . Hamiltonian of the whole system is then written as

Fig. 8.11 Tavis–Cummings model



$$\mathcal{H} = \sum_i \frac{\hbar\omega_q}{2} \sigma_z^{(i)} + \hbar\omega_c a^\dagger a + \sum_i \hbar g(a^\dagger \sigma_+^{(i)} + a \sigma_-^{(i)})$$

with superscript i on the Pauli operators indicate those for i -th qubit. Note here that by considering N qubits, the Pauli operator such as $\sigma_z^{(i)}$ should be rigorously $I \otimes \dots I \otimes \sigma_z^{(i)} \otimes I \otimes \dots I$. We should only keep it in mind and usually abbreviate I 's. Since the frequencies and coupling strengths for the qubits are identical, we cannot spectrally distinguish the qubits through the measurement of the cavity's response. This situation justifies the use of collective Pauli operators

$$S_+ = \frac{1}{\sqrt{N}} \sum_i \sigma_+^{(i)},$$

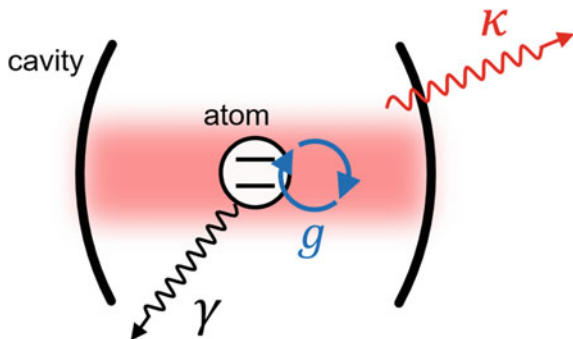
$$S_- = \frac{1}{\sqrt{N}} \sum_i \sigma_-^{(i)}.$$

We also assume that qubits do not interact directly with each other, that is, terms like $\sigma_+^{(i)} \sigma_-^{(j)}$ ($i \neq j$) does not have contributions in the Hamiltonian. We further assume that only one qubit out of N qubits is excited at most, justifying that the first term in the Hamiltonian can be rewritten as $(\hbar\omega_q/2)S_+S_-$. The interaction terms can be rewritten as well using $\sum_i \sigma_\pm^{(i)} = \sqrt{N}S_\pm$ and the Hamiltonian now reads

$$\mathcal{H} = \frac{\hbar\omega_q}{2} S_+ S_- + \hbar\omega_c a^\dagger a + \hbar\tilde{g}(a^\dagger S_+ + a S_-).$$

This looks much like a Jaynes–Cummings Hamiltonian with the modified coupling strength $\tilde{g} = g\sqrt{N}$. This enhancement of the coupling strength is owing to the presence of multiple identical qubits and is called the collective enhancement. The Hamiltonian shown above is called Tavis–Cummings Hamiltonian and the physical system modeled by this Hamiltonian is called Tavis–Cummings model. The vacuum Rabi splitting with $2\tilde{g}$ and related physics are the same as those in the Jaynes–Cummings model as long as the above assumptions are valid.

Fig. 8.12 Jaynes–Cummings model with losses



8.4.3 Weak and Strong Coupling Regimes

Let us analyze Jaynes–Cummings model further here with losses incorporated. We consider a qubit residing in a cavity as shown in Fig. 8.12, where the longitudinal decays of the qubit (γ) and the cavity (κ) are considered. We depart from the Jaynes–Cummings Hamiltonian in the rotating frame at frequency ω . The transformation matrix is $U = \exp [i\omega a^\dagger a t + i(\omega/2)\sigma_z t]$. Do not be afraid of multiple terms in the exponent since they commute. One can do such transformations one by one. We have, as a result

$$\mathcal{H}_{JC} = \frac{\hbar\Delta_q}{2}\sigma_z + \hbar\Delta_c a^\dagger a + \hbar g(\sigma_+ a + a^\dagger \sigma_-). \quad (8.4.4)$$

Here $\Delta_q = \omega_q - \omega$ and $\Delta_c = \omega_c - \omega$.² From this Hamiltonian, we obtain coupled Heisenberg equations of motion for a and σ_- that appear as

$$\frac{da}{dt} = -i\Delta_c a - \frac{\kappa}{2}a - ig\sigma_-, \quad (8.4.5)$$

$$\frac{d\sigma_-}{dt} = -i\frac{\Delta_q}{2}\sigma_- - \frac{\gamma}{2}\sigma_- + ig\sigma_z a. \quad (8.4.6)$$

The loss terms are introduced on the right-hand side as the second terms. At this point, we make an approximation that the qubit is mostly in the ground state, that is, the expectation value of σ_z is -1 , which is valid when the qubit is very weakly excited. By assuming this nonlinear term $+ig\sigma_z a$ in the second equation is simplified as $-iga$ and we here consider the situation that the multiphoton states are negligible. Above equations of motion lead to the coupled linear differential equations

$$\frac{d}{dt} \begin{pmatrix} a \\ \sigma_- \end{pmatrix} = \begin{pmatrix} -(i\Delta_c + \frac{\kappa}{2}) & -ig \\ -ig & -\left(i\frac{\Delta_q}{2} + \frac{\gamma}{2}\right) \end{pmatrix} \begin{pmatrix} a \\ \sigma_- \end{pmatrix}. \quad (8.4.7)$$

² Note the phase convention of the interaction term. See also the Problems.

Note the resemblance of these equations to the Schrödinger equation when the Hermitian conjugate of the two lines of equations are taken and they act on the state $|g, 0\rangle$. Therefore, it can be deduced that the eigenvalues of the matrix in the right hand side are closely related to the energies of the cavity-qubit coupled system. By an ordinary diagonalization procedure yields eigenvalues

$$\frac{E_{\pm}}{i\hbar} = -\frac{1}{2} \left[\left(i\Delta_c + \frac{\kappa}{2} \right) + \left(i\Delta_q + \frac{\gamma}{2} \right) \right] \pm \sqrt{\left[\frac{1}{2} \left(i\Delta_c + \frac{\kappa}{2} \right) - \frac{1}{2} \left(i\frac{\Delta_q}{2} + \frac{\gamma}{2} \right) \right]^2 - g^2} \quad (8.4.8)$$

with eigenvectors

$$|\psi_{\pm}\rangle = \frac{1}{\sqrt{A_{\pm}}} \left\{ \left[\frac{1}{2} \left(i\Delta_c + \frac{\kappa}{2} \right) - \left(i\frac{\Delta_q}{2} + \frac{\gamma}{2} \right) \right] \right. \quad (8.4.9)$$

$$\left. \pm \sqrt{\left[\frac{1}{2} \left(i\Delta_c + \frac{\kappa}{2} \right) - \frac{1}{2} \left(i\frac{\Delta_q}{2} + \frac{\gamma}{2} \right) \right]^2 - g^2} \right] |g, 1\rangle - g|e, 0\rangle \quad (8.4.10)$$

where the factor $1/\sqrt{A_{\pm}}$ is present for the normalization. As the loss terms are involved, the eigenenergies E_{\pm} are complex-valued in general. Their real and complex parts are regarded as the energies and losses, respectively.

Here we can discuss interesting regimes of this cavity QED system; weak and strong coupling regimes. These are discriminated by whether the real parts of E_{\pm} exhibit the same value or not. For brevity, we restrict ourselves in the case $\Delta_c = \Delta_q = 0$. When the coupling strength g is smaller than $|\kappa/4 - \gamma/4|$, the weak coupling regime, the quantity in the square root is always positive and hence $\text{Re}[E_{\pm}]$ is equal. In other words, the qubit and the cavity spectrally coincide with each other except for the linewidths and there is no frequency shift for either due to the weakness of the coupling compared to the losses. This situation in turn makes the loss rates of the qubit and the cavity deviate from the original ones. Let us consider the bad cavity limit $\kappa/4 \gg \gamma/4 \gg g$ and expand the square-root term as follows:

$$\frac{E_{\pm}}{i\hbar} = -\frac{1}{2} \left(\frac{\kappa}{2} + \frac{\gamma}{2} \right) \pm \frac{1}{2} \left(\frac{\kappa}{2} - \frac{\gamma}{2} \right) \left[1 - \frac{1}{2} \frac{g^2}{\left(\frac{\kappa-\gamma}{4} \right)^2} \right] \quad (8.4.11)$$

$$= -\frac{\kappa \mp \gamma}{4} - \frac{\gamma \pm \gamma}{4} \mp \frac{1}{2} \frac{g^2}{\frac{\kappa-\gamma}{4}} \quad (8.4.12)$$

Now we write down $\Gamma_+ = E_+/i\hbar$ and $\Gamma_- = E_-/i\hbar$ separately

$$\Gamma_+ = -\frac{\gamma}{2} \left(1 + \frac{g^2}{\frac{\kappa}{2} \frac{\kappa-\gamma}{2}} \right) \simeq -\frac{\gamma}{2} \left(1 + \frac{4g^2}{\kappa\gamma} \right), \quad (8.4.13)$$

$$\Gamma_- = -\frac{\kappa}{2} \left(1 - \frac{g^2}{\frac{\kappa}{2} \frac{\kappa-\gamma}{2}} \right) \simeq -\frac{\kappa}{2} \left(1 - \frac{4g^2}{\kappa^2} \right). \quad (8.4.14)$$

The first thing we can say is that Γ_+ and Γ_- , respectively, correspond to the qubit and cavity loss rates, since their absolute values approach their original values as the coupling strength g vanishes. In the presence of the finite coupling strength, they are modified from their intrinsic values, e.g., atomic loss increases by $\mathcal{F}_p = 4g^2/\kappa\gamma$. This enhancement factor \mathcal{F}_p is called the Purcell factor, or the atomic cooperativity in the context of the cavity QED.

Next, we shall see what happens when the coupling strength g is greater than $|\kappa/4 - \gamma/4|$, the strong coupling regime. In this situation, the quantity in the square root becomes negative and the real parts of E_+ and E_- are no longer the same. This is an implication of the fact that the atom and the cavity is hybridized to form two coupled modes. Again we consider the case $\Delta_c = \Delta_q = 0$ to simplify the maths. Given the above circumstances, we rewrite the eigenenergies as

$$E_{\pm} = \mp\hbar\sqrt{g^2 - \left(\frac{\kappa - \gamma}{4}\right)^2} - i\frac{\hbar}{2}\left(\frac{\kappa}{2} + \frac{\gamma}{2}\right) \quad (8.4.15)$$

from which it can be seen that the loss rates of the two modes take the simple average of those of them. The energetic shifts are $\Delta E_{\pm} = \mp\hbar\Omega_0 = \mp\hbar\sqrt{g^2 - [(\kappa - \gamma)/4]^2}$ and the energy splitting given by an amount of $2\hbar\Omega_0$ is called the vacuum Rabi splitting. How linewidths and the energies behave in the strong coupling regime are plotted in Fig. 8.13.

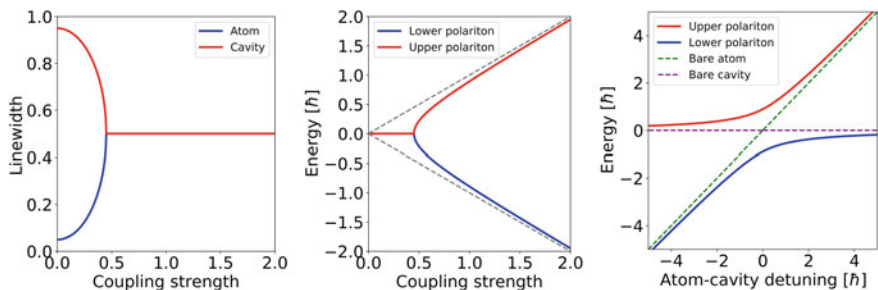


Fig. 8.13 Linewidths (left, Imaginary part of E_{\pm}), energies (center, Imaginary part of E_{\pm}) and their dependence on the detuning (right). Parameters are chosen so that the cavity and qubit linewidths are 1 and 0.05

8.4.4 Dispersive Regime

In the previous Section, the Jaynes–Cummings Hamiltonian is investigated when the qubit and the cavity are on- or near-resonance. In this Section, however, let us consider an interesting, alternative regime in which the qubit and the cavity are far-off resonant, but the coupling constant is moderately large enough so that the qubit and the cavity couple dispersively with each other.

The consequences of the analysis shown in this subsection are somehow related to the dressed-state picture and ac Stark shift or light shift therein. We will see that, as a result of the dispersive coupling, the energy of the cavity is shifted by the qubit and the amount of the shift depends on whether the qubit is in $|g\rangle$ or $|e\rangle$, on one hand. On the other hand, the energy of the qubit will be shifted as well, and the energy shift depends on the number of photons, just as in the light shift. Indeed, what we are going to see here is a fully quantum-mechanical treatment of a light shift.

Let us depart again from the Jaynes–Cummings Hamiltonian

$$\mathcal{H} = \frac{\hbar\omega_q}{2}\sigma_z + \hbar\omega_c a^\dagger a + \hbar g(\sigma_+ a + \sigma_- a^\dagger). \quad (8.4.16)$$

Riding onto the frame rotating at ω_c by $U = \exp[i\omega_c a^\dagger at + i(\omega_c/2)\sigma_z t]$, the Hamiltonian in the rotating frame gets $\mathcal{H}' = (\hbar\Delta/2)\sigma_z + \hbar g(\sigma_+ a + \sigma_- a^\dagger)$ where $\Delta = \omega_q - \omega_c$. Then we approximately diagonalize the Hamiltonian by Schrieffer–Wolff transformation³ using $e^S = \exp[(g/\Delta)(\sigma_+ a - \sigma_- a^\dagger)]$,⁴ which is meaningful only when $|g/\Delta| \ll 1$. The truncated Hamiltonian reads $\mathcal{H}'' = (\hbar\Delta/2)\sigma_z + \hbar(g^2/\Delta)(a^\dagger a + 1/2)\sigma_z$ and back to the original frame,

$$\mathcal{H}''' = \frac{\hbar\omega_q}{2}\sigma_z + \hbar\omega_c a^\dagger a + \frac{\hbar g^2}{\Delta} \left(a^\dagger a + \frac{1}{2} \right) \sigma_z. \quad (8.4.17)$$

This is often called the dispersive Hamiltonian and according to our intention it is apparently diagonal, that is, the Hamiltonian consists only of σ_z and $a^\dagger a$. We shall interpret this Hamiltonian in two ways: first

$$\mathcal{H}''' = \frac{\hbar}{2} \left(\omega_q + \frac{g^2}{\Delta} \right) \sigma_z + \hbar \left[\omega_c + \frac{g^2}{\Delta} \sigma_z \right] a^\dagger a. \quad (8.4.18)$$

There can be seen two types of frequency shifts of qubit and cavity nature. The frequency shift of the qubit by g^2/Δ is caused by the coupling of the qubit to the vacuum fluctuation, which is read as the Lamb shift. The one of the cavity by an amount $(g^2/\Delta)\sigma_z$ is interpreted as the frequency shift depending on the state of the qubit, which is called the dispersive shift. With this expression, it is apparent that the cavity peak will split into two, representing the ground and excited states of the qubit.

³ see Appendix F.

⁴ For consistency with Appendix F, one might put $e^{gS} = \exp[(g/\Delta)(\sigma_+ a - \sigma_- a^\dagger)]$.

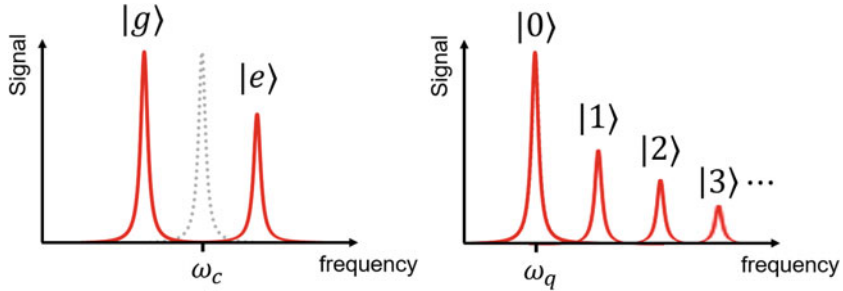


Fig. 8.14 Spectral features (schematic) of Jaynes–Cummings model in the strong dispersive regime. Left: cavity spectrum. Right: qubit spectrum

This spectral feature is schematically illustrated in Fig. 8.14. The two resonances are resolved when $2g^2/\Delta > \gamma$. Next, the Hamiltonian can also be written in the form

$$\mathcal{H}''' = \hbar \left[\omega_q + \frac{g^2}{\Delta} \left(a^\dagger a + \frac{1}{2} \right) \right] \sigma_z + \hbar \omega_c a^\dagger a. \quad (8.4.19)$$

This form tells us that other than the Lamb shift, the qubit frequency is shifted discretely and exhibits multiple peaks, each of which corresponds to the photon number (see right panel of Fig. 8.14). Using this property, the photon-number resolving experiments are implemented using a superconducting qubit [16] under the condition that the peaks are resolved, $g^2/\Delta > \kappa$. One can see that if we drive the cavity strongly, we can make a replacement $a \rightarrow \alpha + a$ with α being a classical, complex amplitude and a after the replacement is only responsible for the quantum noise that is negligibly small compared to the amplitude $|\alpha|$. Then we define the Rabi frequency $g\alpha = \Omega$ to get the frequency shift of the qubit by the classical driving as Ω^2/Δ which is the very thing we saw in the discussion of the dressed-state picture.

8.4.5 Waveguide-Coupled Cavity QED System

We here consider a system where a coupled qubit-cavity system is further coupled to a propagating mode in a waveguide and analyze what kind of signal one can see and how the cavity QED system looks like through the transmission measurement with the waveguide as depicted in Fig. 8.15.

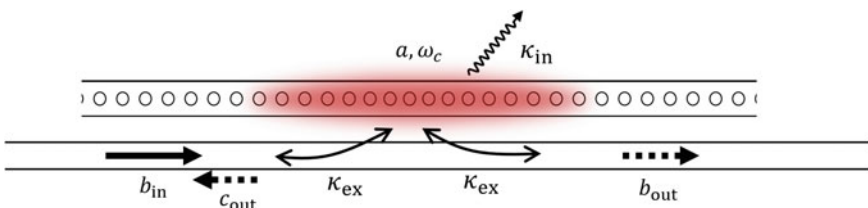


Fig. 8.15 Waveguide-coupled cavity QED system

Here, for instance, we suppose that a photonic-crystal cavity is evanescently coupled to the optical waveguide. The Hamiltonian of the system is simply of Jaynes–Cummings type, that is

$$\mathcal{H} = \frac{\hbar\omega_a}{2}\sigma_z + \hbar a^\dagger a - i\hbar g(\sigma_+a - \sigma_-a^\dagger) \quad (8.4.20)$$

In this Section, we write the intrinsic loss rate of the cavity as κ_{in} and the external coupling rate to the waveguide as κ_{ex} . Total loss rate of the cavity mode is $\kappa = \kappa_{\text{in}} + 2\kappa_{\text{ex}}$. The factor of 2 for the external coupling rate originates in the fact that the cavity photons couple to both of the left-going and right-going propagating modes. We assume the incident waveguide mode b_{in} is coming from the left and transmitted mode and reflected mode are denoted by b_{out} and c_{out} , respectively. In a rotating frame with angular frequency ω , the drive frequency, for qubit and cavity operators, the Heisenberg equations of motion are

$$\frac{da}{dt} = -i\Delta_c a - \frac{\kappa}{2}a - g\sigma_- - \sqrt{\kappa_{\text{ex}}}b_{\text{in}}, \quad (8.4.21)$$

$$\frac{d\sigma_-}{dt} = -i\frac{\Delta_a}{2}\sigma_- - \frac{\gamma}{2}\sigma_- - g\sigma_z a, \quad (8.4.22)$$

$$\frac{d\sigma_z}{dt} = 2g(\sigma_+a + \sigma_-a^\dagger) \quad (8.4.23)$$

where $\Delta_a = \omega_q - \omega$ and $\Delta_c = \omega_c - \omega$ are detunings of the qubit and the cavity. Input-output relations are

$$b_{\text{out}} = b_{\text{in}} + \sqrt{\kappa_{\text{ex}}}a, \quad (8.4.24)$$

$$c_{\text{out}} = \sqrt{\kappa_{\text{ex}}}a \quad (8.4.25)$$

from which we want to calculate the transmittance and reflectance. However, this equation is not linear due to the presence of σ_z in (8.4.22). Furthermore, here we do not assume that the qubit is only weakly excited and $\langle\sigma_z\rangle = -1$. In other words, we want to consider the situation that the qubit can be strongly driven to make $\langle\sigma_z\rangle \neq -1$. Keeping this in mind, let us regard coherent electromagnetic waves b_{in} , b_{out} and c_{out} as classical quantities with the same terminologies, and also the Pauli operators σ_z and σ_- of the coherently driven qubit as s_z and s , respectively [17]. By this prescription, we lose the single-photon-level response of the cavity and the qubit but can know how the coupled system behaves with the classical input and output electromagnetic waves. After a bit lengthy calculation, one obtains

$$c_{\text{out}} = -r(\Delta_c, \Delta_a)b_{\text{in}}, \quad (8.4.26)$$

$$b_{\text{out}} = [1 - r(\Delta_c, \Delta_a)]b_{\text{in}}, \quad (8.4.27)$$

$$s_z = -\frac{1}{1 + X}, \quad (8.4.28)$$

$$s = -\sqrt{\frac{1}{\eta}} \frac{1}{1 + X} \frac{2\eta r_0(\Delta_c)}{2\eta r_0(\Delta_c) + 2(i\Delta_a + \gamma/2)} b_{\text{in}}. \quad (8.4.29)$$

Here the following parameters are defined:

$$\eta = \frac{g^2}{\kappa_{\text{ex}}}, \quad (8.4.30)$$

$$r_0(\Delta_c) = \frac{\kappa_{\text{ex}}}{i\Delta_c + \kappa/2}, \quad (8.4.31)$$

$$r(\Delta_c, \Delta_a) = \left[1 - \frac{2\eta r_0(\Delta_c)}{2\eta r_0(\Delta_c) + 2(i\Delta_a + \gamma/2)} \frac{1}{1+X} \right] r_0(\Delta_c), \quad (8.4.32)$$

$$X = \frac{|b_{\text{in}}|^2}{P_s}, \quad (8.4.33)$$

$$P_s = \frac{1}{8\eta\kappa_{\text{ex}}^2} \left\{ \left[\Delta_a^2 + \left(\frac{\gamma}{2} \right)^2 \right] \left[\Delta_c^2 + \left(\frac{\kappa}{2} \right)^2 \right] + \eta^2 \kappa_{\text{ex}}^2 - 2\eta\kappa_{\text{ex}}\Delta_a\Delta_c + \frac{\gamma\eta\kappa_{\text{ex}}\kappa}{2} \right\} \quad (8.4.34)$$

$r(\Delta_c, \Delta_q)$ represents the reflectance of the coupled qubit-cavity system and $r_0(\Delta_c)$ the reflectance in the absence of the qubit. P_s is a value of photon flux with which the qubit is saturated and X denotes a photon flux normalized by P_s .

By using above expressions, we can now examine the behavior of the coupled qubit-cavity system by evaluating the transmittance $|b_{\text{out}}|^2/|b_{\text{in}}|^2$ and the reflectance $|c_{\text{out}}|^2/|b_{\text{in}}|^2$. These spectra are plotted in Fig. 8.16 for various values of X in the case of the frequencies of the qubit and the cavity coincides and $\kappa > \gamma$. Let us look at the lower panel of Fig. 8.16, where the transmission spectra are displayed. For small X , that is, when the incident electromagnetic waves are weak enough to only weakly excite the qubit, the coupled qubit-cavity system exhibits a gross resonance dip structure of the cavity with a steep peak at resonance as a result of the destructive interference of the photons from the qubit and the cavity. In other words, the cavity becomes transparent at resonance as a result of the coupling to the qubit, which is dubbed as the dipole-induced transparency. Corresponding to this, a reflection dip appears in the reflection spectrum.

Next, let us take a look at the dependence of the reflection spectrum on the coupling strength g and the qubit detuning Δ_a with Δ_c set to be zero (lower panel of Fig. 8.17). As the coupling strength gets larger, the dip at the center of the cavity peak becomes larger and the spectrum exhibits two peaks split by $2g$ (see the upper panel of Fig. 8.17), implying that the coupled qubit-cavity system is in the strong coupling regime. The lower panel of Fig. 8.17 plots the spectra when the qubit frequency is swept over the cavity spectrum. When the qubit-cavity detuning is large, the spectrum possesses two peaks, i.e., sharp one by the qubit and a thick one by the cavity. As the qubit peak approaches the cavity one, the lineshape of the qubit peak appears dispersive, in other words, it exhibits Fano lineshape, at the shoulders of the cavity peak.

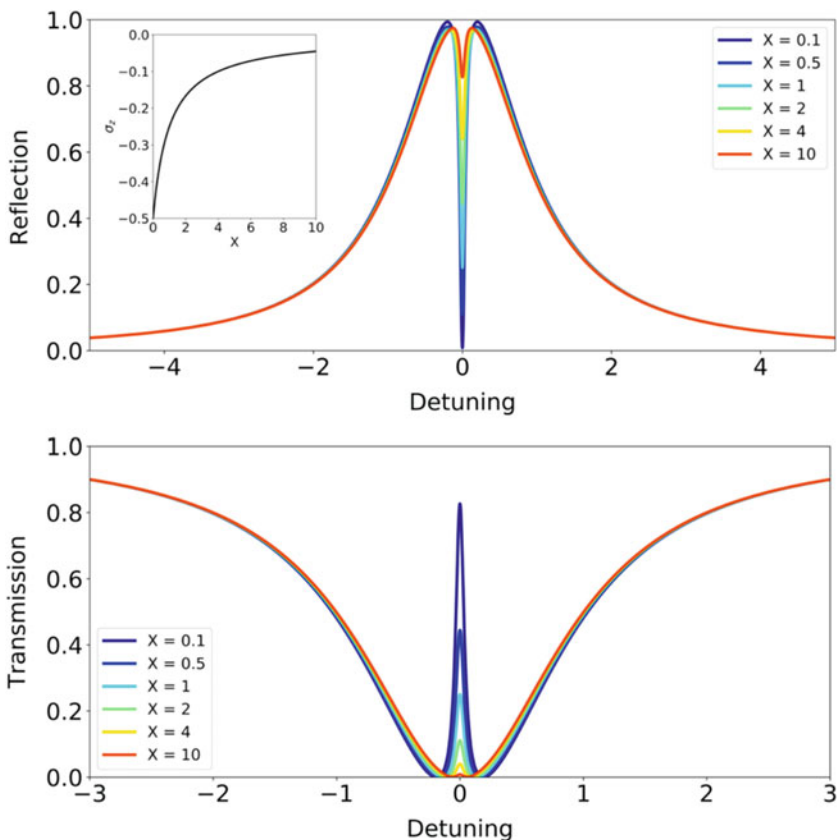


Fig. 8.16 Upper panel and its inset, respectively, show the waveguide reflection spectra and expectation values of σ_z for various normalized input photon flux X . The lower panel shows the waveguide transmission spectra for various X

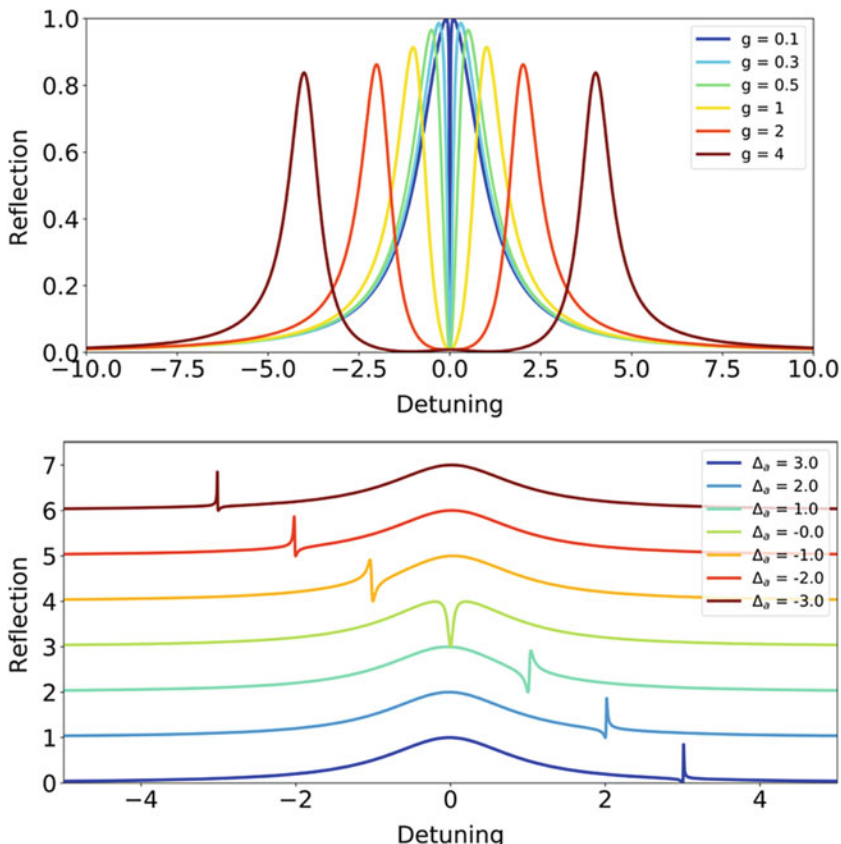


Fig. 8.17 Reflection spectra for various coupling strengths g (upper panel) and qubit-cavity detuning (lower panel)

Problems

- Problem 8-1** Suppose one executes the reflection measurement of a cavity that has only a single coupling port. Then they obtain a cavity spectrum like the one shown in Fig. 8.18 by measuring the reflected signal which is proportional to the number of reflected photons. Given this spectrum, express the intrinsic loss rate and external coupling rate of the cavity.
- Problem 8-2** Discuss what information is required to determine the external coupling rate uniquely in the single-port measurement.
- Problem 8-3** Suppose one executes the reflection and transmission measurements of a cavity that has two coupling ports. Then they obtain a cavity

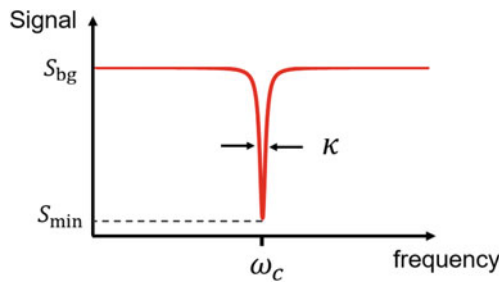


Fig. 8.18 Cavity spectrum with a single-port measurement

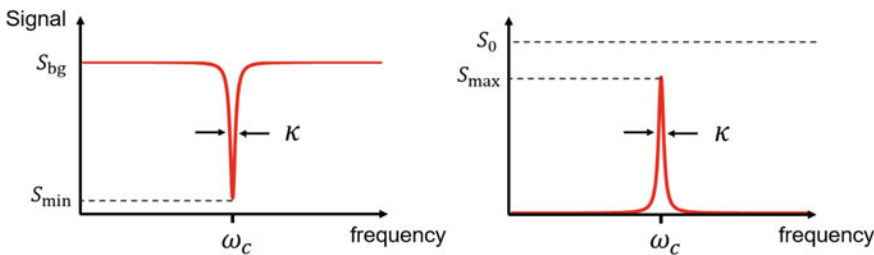


Fig. 8.19 Cavity spectra with a dual-port measurement

spectra like the one shown in Fig. 8.19 by measuring the reflected and transmitted signals which are proportional to the number of reflected photons. Here left and right panels of Fig. 8.19 show the reflection and transmission spectra, respectively. The S_0 is the signal level at which all the input electromagnetic waves are detected. Given these spectra, express the intrinsic loss rate and external coupling rates of the cavity.

Problem 8-4

- (i) Discuss what assumption is made for the decay process when one says that the system decays exponentially.
- (ii) Show that Fourier transformation of an exponential function is a Lorentzian function.

Problem 8-5

Interaction terms like $\hbar g(\sigma_+a + a^\dagger\sigma_-)$ sometimes appear in other context as $-i\hbar g(\sigma_+a - a^\dagger\sigma_-)$. Show that these can be regarded as equivalent under the transformation $U = \exp[i(\pi/2)a^\dagger a]$ or $U = \exp[i(\pi/2)\sigma_z]$. This phase difference is not significant as long as the relative phases of each terms in the Hamiltonian do not matter.

Problem 8-6

Derive Eq. (8.4.17) by applying Schrieffer-Wolff transformation (see Appendix F).



Various Couplings in Quantum Systems

9

In this chapter, we pick up several quantum systems to see examples of interactions, or couplings, among quantum systems and estimate the values of the coupling strengths in practice. The basic strategy is to consider classical interaction energies first, then quantize them to derive interaction Hamiltonians, and finally get the coupling strengths which include susceptibilities of the particles to an applied field and/or vacuum fluctuations of the field.

9.1 Interaction Hamiltonians

Before diving into the concrete physical systems, we would like to introduce several types of interaction Hamiltonians to which their specific names are given. To “read” or deduce what is going on with the given interaction Hamiltonian, it is important to grasp the involved quantum systems first and then interpret the products of operators as describing concrete processes that can happen in the coupled system under concern. Keeping this in mind, let us take an overview of various interactions Hamiltonians frequently appear in quantum technologies.

Throughout this section, the following notations are used. First, $a, a^\dagger, b, b^\dagger, \dots$ represent annihilation and creation operators of harmonic oscillators with eigenfrequencies $\omega_a, \omega_b, \dots$. Pauli operators σ with proper subscripts $x, y, z, +$ and $-$ and superscripts (i) are assigned for i -th qubit, while the superscript is not attached when only a single qubit is under concern. In most examples, g denotes the coupling strength, however, keep in mind that they are all different and have their

Supplementary Information The online version contains supplementary material available at https://doi.org/10.1007/978-981-19-4641-7_9.

own expression in terms of susceptibilities and vacuum fluctuations, as introduced in later Sections. The interaction Hamiltonian is commonly denoted by \mathcal{H}_{int} .

9.1.1 Jaynes–Cummings and Anti-Jaynes–Cummings Interactions

Interaction Hamiltonian of a Jaynes–Cummings interaction involves a qubit and a harmonic oscillator, exchanging their energy

$$\mathcal{H}_{\text{int}} = \hbar g(a^\dagger \sigma_- + a \sigma_+) \quad (9.1.1)$$

This type of interaction is ubiquitous for a coupled quantum system of a harmonic oscillator and a two-level system. The figure below depicts the physical process realized by the Jaynes–Cummings interaction.

$$\mathcal{H}_{\text{int}} = \hbar g \left(\begin{array}{c} |n+1\rangle \xrightarrow{\quad} |e\rangle \xrightarrow{\quad} \\ |n\rangle \quad |g\rangle \end{array} + \begin{array}{c} |n+1\rangle \xrightarrow{\quad} |e\rangle \xrightarrow{\quad} \\ |n\rangle \quad |g\rangle \end{array} \right)$$

Anti-Jaynes–Cummings interaction is a complementary one to the Jaynes–Cummings interaction in a sense that “counter-rotating” terms are taken from the original quantum Rabi interaction $\hbar g(a + a^\dagger)(\sigma_- + \sigma_+)$, from which the Jaynes–Cummings interaction can be derived through the rotating-wave approximation. It expresses the simultaneous creation or annihilation of the excitations and the concrete form reads

$$\mathcal{H}_{\text{int}} = \hbar g(a^\dagger \sigma_+ + a \sigma_-). \quad (9.1.2)$$

and is schematically represented as in the following figure.

$$\mathcal{H}_{\text{int}} = \hbar g \left(\begin{array}{c} |n+1\rangle \xrightarrow{\quad} |e\rangle \xrightarrow{\quad} \\ |n\rangle \quad |g\rangle \end{array} + \begin{array}{c} |n+1\rangle \xleftarrow{\quad} |e\rangle \xleftarrow{\quad} \\ |n\rangle \quad |g\rangle \end{array} \right)$$

In the next section, we introduce the trapped ion system as a first example. In that system, the phonon mode and the internal state of an ion are coupled by properly utilizing the energy and momentum of the incident laser. The coupling is either Jaynes–Cummings or anti-Jaynes–Cummings interaction depending on whether the frequency of the laser is slightly red-detuned or blue-detuned, respectively. This will be seen later in Sect. 9.2.2.

9.1.2 Beam-Splitter and Two-Mode-Squeezing Interactions

Two modes of harmonic oscillators can interact with each other and they can exchange their energy quanta when their eigenfrequencies are sufficiently close together. This

process is described by a beam-splitter interaction

$$\mathcal{H}_{\text{int}} = \hbar g(a^\dagger b + ab^\dagger). \quad (9.1.3)$$

which allows an intuitive interpretation as shown below.

$$\mathcal{H}_{\text{int}} = \hbar g \left(\begin{array}{c} |n+1\rangle \text{---} \circ \\ |n\rangle \end{array} \begin{array}{c} |m+1\rangle \text{---} \circ \\ |m\rangle \end{array} \begin{array}{c} \uparrow \\ \downarrow \end{array} + \begin{array}{c} |n+1\rangle \text{---} \circ \\ |n\rangle \end{array} \begin{array}{c} |m+1\rangle \text{---} \circ \\ |m\rangle \end{array} \begin{array}{c} \downarrow \\ \uparrow \end{array} \right)$$

The two-mode-squeezing interaction can be introduced in almost the same spirit as the anti-Jaynes-Cummings interaction, since the beam-splitter interaction is obtained via an application of a rotating-wave approximation to the original coupling of the form $\hbar g(a + a^\dagger)(b + b^\dagger)$. The interaction Hamiltonian

$$\mathcal{H}_{\text{int}} = \hbar g(a^\dagger b^\dagger + ab) \quad (9.1.4)$$

manifest itself as the one of two-mode-squeezing interaction and graphically it can be shown as below.

$$\mathcal{H}_{\text{int}} = \hbar g \left(\begin{array}{c} |n+1\rangle \text{---} \circ \\ |n\rangle \end{array} \begin{array}{c} |m+1\rangle \text{---} \circ \\ |m\rangle \end{array} \begin{array}{c} \uparrow \\ \uparrow \end{array} + \begin{array}{c} |n+1\rangle \text{---} \circ \\ |n\rangle \end{array} \begin{array}{c} |m+1\rangle \text{---} \circ \\ |m\rangle \end{array} \begin{array}{c} \downarrow \\ \downarrow \end{array} \right)$$

If the two modes involved in the two-mode-squeezing interaction are identical, the interaction Hamiltonian reads

$$\mathcal{H}_{\text{int}} = \hbar g[(a^\dagger)^2 + a^2] \quad (9.1.5)$$

that is called the squeezing interaction. Since this interaction makes two quanta created or annihilated simultaneously, the physical situation is interpreted as depicted in the following figure.

$$\mathcal{H}_{\text{int}} = \hbar g \left(\begin{array}{c} |n+2\rangle \text{---} \circ \\ |n+1\rangle \text{---} \circ \\ |n\rangle \end{array} \begin{array}{c} \uparrow \\ \uparrow \end{array} + \begin{array}{c} |n+2\rangle \text{---} \circ \\ |n+1\rangle \text{---} \circ \\ |n\rangle \end{array} \begin{array}{c} \downarrow \\ \downarrow \end{array} \right)$$

Likewise, the two-mode-squeezing interaction correlates the quantum states of two harmonic oscillators, and the squeezing interaction correlates a quantum state of a harmonic oscillator to itself in the phase-space: a Wigner function of it will be transformed, or squeezed, as in Sect. 6.3.3.

9.1.3 Interaction Between Qubits

Interaction terms such as $\hbar g \sigma_x^{(1)} \sigma_x^{(2)}$, $\hbar g \sigma_z^{(1)} \sigma_z^{(2)}$ and $\hbar g \sigma_x^{(1)} \sigma_z^{(2)}$ are respectively called by their rotation axes as XX , ZZ and XZ interactions. These are literally the simultaneous rotations of Bloch vectors about the X axes of the two qubits. If the interaction Hamiltonian is given as some combination of qubit-qubit interaction, say, $\hbar g(\sigma_x^{(1)} \sigma_x^{(2)} + \sigma_y^{(1)} \sigma_y^{(2)})$, this is never simple, separate rotations of Bloch vectors about some axes. This becomes clear if we recognize that the time evolution with the interaction Hamiltonian \mathcal{H}_{int} is described by the unitary operation $U(t) = e^{-i\mathcal{H}_{\text{int}}t/\hbar}$, as will be discussed later in detail in Sect. 10.1.2.

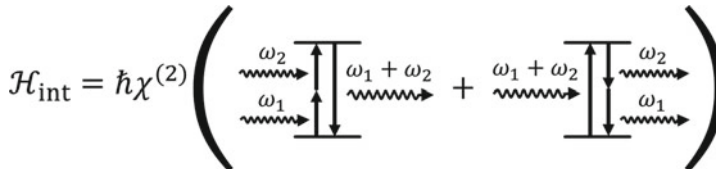
9.1.4 Nonlinear Interactions

The last type of interaction is nonlinear interaction, in which the effect of the interaction depends on the number of quanta. Nonlinear interaction is literally diverse, and we here only pick up two simplest examples of $\chi^{(2)}$ and $\chi^{(3)}$ nonlinear interactions.

The first example is the $\chi^{(2)}$ interaction within a single harmonic oscillator:

$$\mathcal{H}_{\text{int}} = \hbar \chi^{(2)} [a^\dagger a^2 + (a^\dagger)^2 a]. \quad (9.1.6)$$

This interaction Hamiltonian represents the three-wave mixing, where two quanta with energies $\hbar\omega_1$ and $\hbar\omega_2$ are absorbed (emitted) and a single quantum with energy $\hbar\omega_1 + \hbar\omega_2$ is emitted (absorbed) by some media (see the figure below).



The most frequently appearing $\chi^{(2)}$ process takes place in the second-harmonic generation, often abbreviated as SHG, where for instance an intense 1064 nm-wavelength laser beam optically pumps the nonlinear crystal and transforms two such near-infrared photons into a green, 532 nm-wavelength photon. By regarding a strong pump photons as a classical wave with its complex amplitude α to substitute $\alpha + a$ into a and apply rotating-wave approximation, we can replace one of the three operators to get a squeezing Hamiltonian. The optomechanical interaction

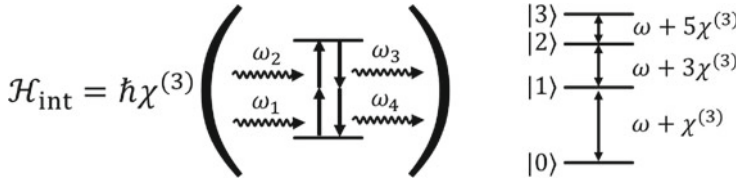
$$\mathcal{H}_{\text{int}} = \hbar g a^\dagger a (b + b^\dagger) \quad (9.1.7)$$

is also understood as a $\chi^{(2)}$ interaction. Strong pump laser allow us to replace a by $\alpha + a$ again. Depending on the pump detuning, the rotating-wave approximation then leads to beam-splitter or two-mode-squeezing interaction.

Next we would like to introduce the $\chi^{(3)}$ interaction in a single harmonic oscillator, which is also known as a self-Kerr effect. The interaction Hamiltonian is

$$\mathcal{H}_{\text{int}} = \hbar \chi^{(3)} a^\dagger a a^\dagger a \quad (9.1.8)$$

that implies that the four-wave mixing with the absorption of quanta with energies $\hbar\omega_1$ and $\hbar\omega_2$ are absorbed and those with $\hbar\omega_3$ and $\hbar\omega_4$ are absorbed. Note that the energy conservation requires $\omega_1 + \omega_2 = \omega_3 + \omega_4$. This situation is depicted in the left panel of the figure below.



Its meaning will become clear if the total Hamiltonian $\mathcal{H}_{\text{tot}} = \hbar\omega a^\dagger a + \hbar\chi^{(3)} a^\dagger a a^\dagger a = \hbar(\omega + \chi^{(3)} n)\hat{n}$ is considered. Its eigenenergy reads $\hbar(\omega + \chi^{(3)} n)n$ and the level spacing does not become equidistant, as indicated in the right panel of above figure where $\chi^{(3)}$ is assumed to be negative in this case. This means that the presence of even a single quanta affects the energy of another quanta. In such a situation, we can regard the quanta interact with themselves to shift their energy according to the number of quanta present.

As another example, let us think about the interaction Hamiltonian

$$\mathcal{H}_{\text{int}} = \hbar \chi^{(3)} a^\dagger b^\dagger b a. \quad (9.1.9)$$

By combining with the bare energies $\hbar\omega_a a^\dagger a + \hbar\omega_b b^\dagger b$, we see that the presence of one quanta shifts the energy of the quanta of the other harmonic oscillator. This interaction is called the cross-Kerr effect.

9.2 Atomic Ions

In most cases, atomic or atomic-ion systems allow us to derive analytical expressions of the coupling strengths that agree well with the experimentally implemented ones. Let us see the atomic-ion system for example, in which ion interacts with light by its electric dipole moment, ions' motional degrees of freedom can be coupled to each other as well as to light.

9.2.1 Atom-Light Interaction

Let us dictate here again the results of Sect. 7.2 about the light-atom interaction. When we consider the electric dipole interaction $d \cdot E$, $d = \mu(\sigma_+ + \sigma_-)$ and

$E = E_{\text{zpf}}(a + a^\dagger)$ yield the interaction Hamiltonian

$$\mathcal{H}_{\text{int}} = \mu E_{\text{zpf}}(\sigma_+ + \sigma_-)(a + a^\dagger). \quad (9.2.1)$$

Furthermore, rotating-wave approximation is applicable to this Hamiltonian when the frequencies of the optical transition of the ion ω_q and the cavity ω_c is close to each other. The interaction Hamiltonian reads then the Jaynes-Cummings Hamiltonian

$$\begin{aligned} \mathcal{H}_{\text{int}} &= \mu E_{\text{zpf}}(\sigma_+ a + \sigma_- a^\dagger) \\ &= \hbar g(\sigma_+ a + \sigma_- a^\dagger). \end{aligned} \quad (9.2.2)$$

with the coupling strength $g = \mu E_{\text{zpf}}/\hbar$. This coupling strength of the Jaynes-Cummings interaction is obviously a product of the transition dipole moment and the vacuum fluctuation of the electric field of the cavity mode.

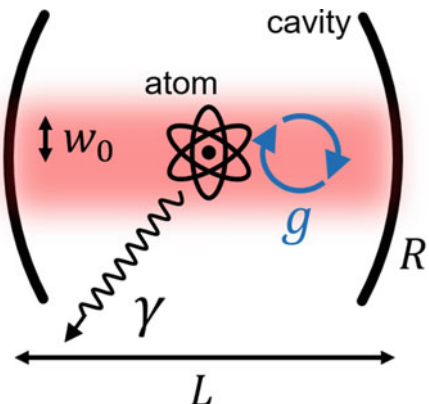
The transition dipole moment μ and the inverse of the excited-state lifetime, denoted by Γ , have a relationship

$$\Gamma = \frac{\mu^2 \omega_q^3}{3\pi \hbar \epsilon_0 c^3} \iff \mu = \sqrt{\frac{3\pi \hbar \epsilon_0 c^3 \Gamma}{\omega_q^3}} \quad (9.2.3)$$

only if the excited-state lifetime is dominated by the radiative recombination and nonradiative recombination can be neglected. For instance, a 422 nm-wavelength optical transition of the strontium ion has $\Gamma = 2\pi \times 23$ MHz, which is equivalent to the transition dipole moment of this transition being 1.39×10^{-29} C·m.

Next, let us consider a Fabry-Perót cavity with its length being L , radii of curvature R and the beam-waist radius w_0 , as depicted in Fig. 9.1. The mirrors are usually made of multiple layers of dielectric coatings and the effective cavity length should include the optical penetration depth at the mirrors, however, the penetration depth is comparable to the wavelength of light, and in most cases, it is far smaller than L . The optical penetration can thus be neglected and the effective length is here set to be L . The electric-field amplitude of the fundamental mode of this cavity is written

Fig. 9.1 Schematic of a cavity QED system with an atom inside a Fabry-Perót cavity



under the assumption that the cavity length L and the radii of curvature of the mirrors R are sufficiently large compared to the wavelength λ

$$E(\mathbf{r}) = E_0 \sin \frac{2\pi x}{\lambda} \exp \left[-\frac{y^2 + z^2}{w_0^2} \right]. \quad (9.2.4)$$

The mode volume of the cavity mode is defined by the integral of the squared electric field and simple calculation yields

$$V = \frac{1}{E_{\max}^2} \int_0^L dx \int_{-\infty}^{\infty} dy \int_{-\infty}^{\infty} dz E(\mathbf{r})^2 = \frac{\pi w_0^2}{4} L. \quad (9.2.5)$$

This mode volume is an important quantity since the vacuum fluctuation of the electric field of the cavity mode is defined as $E_{\text{zpf}} = \sqrt{\hbar\omega_c/2\varepsilon_0 V}$, as we mentioned earlier. Since the beam radius w_0 can be written as [14]

$$w_0 = \sqrt{\frac{L\lambda}{2\pi}} \left(\frac{2R - L}{L} \right)^{\frac{1}{4}}, \quad (9.2.6)$$

the mode volume reads

$$V = \frac{\lambda}{8} \sqrt{L^3(2R - L)}. \quad (9.2.7)$$

Assuming that $\lambda = 422$ nm, $L = 200$ μm and $R = 1$ mm, we have $V = 6.3 \times 10^6$ μm³.

By putting above parameters in $g = \mu E_{\text{zpf}}/\hbar$, we can estimate the coupling strength of the optical transition of the ion and the cavity mode as $g/2\pi = 0.96$ MHz. Since the natural linewidth, or the inverse of the excited-state lifetime, under concern is $2\pi \times 23$ MHz, the coupling strength is inferior to the natural linewidth and this cavity QED system is in the weak coupling regime regardless of the decay rate of the cavity mode. In order to increase the ratio of the coupling strength to the natural linewidth and the cavity one, we should make some efforts as illustrated below. One prescription is to use an optical transition with narrower natural linewidth. At first sight, the narrower linewidth is equivalent to the smaller transition dipole moment and it seems that the coupling strength gets smaller. However, if the wavelength of the transition is long enough, it may rather enhance the coupling strength, see Eq. (9.2.3). Furthermore, the narrower linewidth makes it easy for the system to get into the strong coupling regime, even if the enhancement is just incremental or not achieved. Another straightforward prescription is to make a smaller cavity to make the mode volume smaller and the vacuum fluctuation E_{zpf} larger, to enhance the coupling strength. The use of mirrors with smaller radii of curvature R is also beneficial for this purpose.

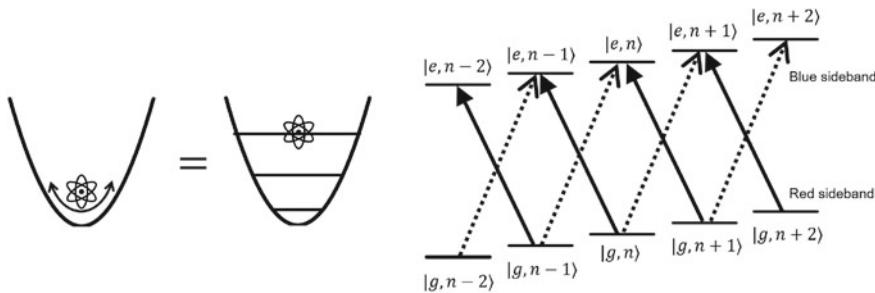


Fig. 9.2 Quantized motion of an ion and the sideband transitions

9.2.2 Sideband Transitions: Optomechanics with an Ion

Paul trap is an ion-trapping technique that confines atomic ions in an effective harmonic potential generated by an oscillating quadrupolar electric field. Ions then exhibit harmonic oscillations, whose quanta are called phonons. If only a single ion is trapped, three phonon modes exist, and if there are N ions, $3N$ phonon modes are supported by the chunk of the ions connected through Coulomb interaction. In this section, we consider the situation that only a single ion is trapped, and a phonon mode only in one direction is taken into account (Fig. 9.2).

By the presence of phonon mode, the ion can oscillate with frequency ω_m and its position fluctuates even if the ion is in its motional ground state by the vacuum fluctuation of the phonon. Then if the laser is irradiated on the ion, the phase of the laser field sensed by the ion can vary according to the ion's position x . We can take this effect into account by including the ion's position in the phase factor of the laser field to rewrite as $E(x) = E_{\text{zpf}} e^{ikx} (a + a^\dagger)$.¹ Here $k = 2\pi/\lambda$ is the wavevector of the laser beam. We now denote an annihilation operator of the phonon mode as b and the vacuum fluctuation of the phonon as x_{zpf} to rewrite the dipole transition term $\mu E(x)$ as

$$\begin{aligned}
 & \hbar g e^{ikx} (\sigma_+ + \sigma_-)(a + a^\dagger) \\
 &= \hbar g e^{ikx_{\text{zpf}}(b+b^\dagger)} (\sigma_+ + \sigma_-)(a + a^\dagger) \\
 &\simeq \hbar g [1 + ikx_{\text{zpf}}(b + b^\dagger)] (\sigma_+ + \sigma_-)(a + a^\dagger) \\
 &= \hbar g (\sigma_+ + \sigma_-)(a + a^\dagger) \\
 &\quad + i\hbar\eta g(b + b^\dagger)(\sigma_+ + \sigma_-)(a + a^\dagger).
 \end{aligned} \tag{9.2.8}$$

Here the dimensionless parameter $\eta = kx_{\text{zpf}}$ is defined, which is called Lamb-Dicke parameter. The first term in the above expression yields Jaynes-Cummings

¹ Here for the simplicity the laser field is rewritten as if it is a localized mode, or cavity mode, however, we can switch to the propagating mode just by replacing localized photon operators a and a^\dagger by corresponding ones.

interaction via a rotating-wave approximation as usual, and is called the carrier transition that does not have something to do with the phonons.

What we are interested in here is the phonon-related transitions contained in the second term. To simplify the problem, we shall assume that the irradiated laser light is intense, continuous one, and the photon operators can be replaced by a coherent amplitude α that is assumed to be real-valued here, multiplied by a time-evolution factor. In such a situation, if the irradiated laser field has a frequency $\omega_q - \omega_m$, rotating-wave approximation allows us to eliminate the terms oscillating with $\omega_q + \omega_m$ to yield

$$i\hbar\eta g\alpha(\sigma_+ b + \sigma_- b^\dagger). \quad (9.2.9)$$

This is a Jaynes–Cummings interaction between the ion's optical transition and the phonon mode. Since the process described by the above interaction can be driven by the laser with frequency $\omega_q - \omega_m$ that is red-detuned from the carrier transition frequency ω_q , this process is called the red-sideband transition.

On the other hand, if the ion is driven with the frequency $\omega_q + \omega_m$, this time we obtain

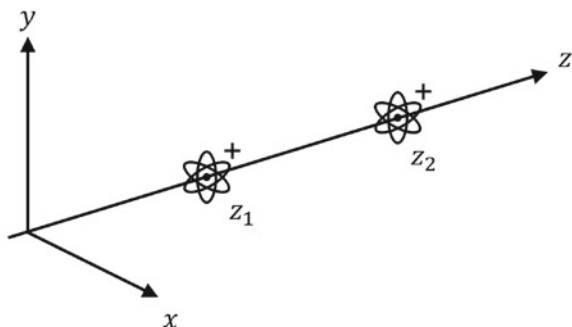
$$i\hbar\eta g\alpha(\sigma_+ b^\dagger + \sigma_- b). \quad (9.2.10)$$

This is an anti-Jaynes–Cummings interaction between the ion's optical transition and the phonon mode again. Since the drive frequency $\omega_q + \omega_m$ is blue-detuned from the carrier transition frequency ω_q , this process is called the blue-sideband transition. If the two-tone driving with $\omega_q - \omega_m$ and $\omega_q + \omega_m$ is executed on the ion, red- and blue-sideband transitions are driven at the same time.

9.2.3 Phonon–Phonon Interaction

When two monovalence ions are interacting with each other by Coulomb force in a harmonic potential, phonon–phonon interaction is significant. We here derive the phonon–phonon interaction Hamiltonian and its coupling strength by considering the position-dependent electrostatic energy between the two ions. As in Fig. 9.3, ions

Fig. 9.3 Ions' phonons interacting with each other in a harmonic potential



at Z_1 and Z_2 are separated by a distance $Z = Z_2 - Z_1$ and the displacements from their equilibrium positions are denoted by $\mathbf{r}_1 = (x_1, y_1, z_1)$ and $\mathbf{r}_2 = (x_2, y_2, z_2)$. Then we shall calculate the Coulomb energy $E_{\text{ph-ph}}$ between these two ions as

$$\begin{aligned} E_{\text{ph-ph}} &= \frac{1}{2} \frac{e^2}{4\pi\epsilon_0} \frac{1}{|\mathbf{r}_1 - \mathbf{r}_2|} \\ &= \frac{e^2}{8\pi\epsilon_0} \frac{1}{\sqrt{(x_1 - x_2)^2 + (y_1 - y_2)^2 + (Z + z_1 - z_2)^2}} \\ &= \frac{e^2}{8\pi\epsilon_0 Z} \left[1 + \frac{2(z_1 - z_2)}{Z} + \frac{(z_1 - z_2)^2}{Z^2} + \frac{(x_1 - x_2)^2}{Z^2} + \frac{(y_1 - y_2)^2}{Z^2} \right]^{-\frac{1}{2}} \\ &\simeq \frac{e^2}{8\pi\epsilon_0 Z} \left[1 - \frac{z_1 - z_2}{Z} - \frac{1}{2} \frac{(z_1 - z_2)^2}{Z^2} - \frac{1}{2} \frac{(x_1 - x_2)^2}{Z^2} - \frac{1}{2} \frac{(y_1 - y_2)^2}{Z^2} \right]. \end{aligned} \quad (9.2.11)$$

In this case, we consider phonons only in z -direction and set $x_1 = x_2 = y_1 = y_2 = 0$. Then above energy can be simplified as

$$E_{\text{ph-ph}} = \frac{e^2}{8\pi\epsilon_0 Z} \left[1 - \frac{z_1 - z_2}{Z} - \frac{1}{2} \frac{(z_1 - z_2)^2}{Z^2} \right]. \quad (9.2.12)$$

Here it is the time for the substitution of the displacements by operators, namely $z_i = z_{zpf}^i (a_i^\dagger + a_i)$ for $i = 1, 2$. a_i are the annihilation operators of the phonons. We focus on the third term alone, since the phonon–phonon interaction resides there but not in the first two terms. The phonon–phonon interaction Hamiltonian $\mathcal{H}_{\text{ph-ph}}$ at this stage reads

$$\begin{aligned} \mathcal{H}_{\text{ph-ph}} &= \frac{e^2}{16\pi\epsilon_0 Z} \frac{(z_1 - z_2)^2}{Z^2} \\ &= \frac{e^2 z_{zpf}^1 z_{zpf}^2}{16\pi\epsilon_0 Z^3} \left[(a_1^\dagger)^2 + a_1^2 + (a_2^\dagger)^2 + a_2^2 + (2a_1^\dagger a_1 + 1) + (2a_2^\dagger a_2 + 1) \right. \\ &\quad \left. - 2(a_1^\dagger a_2^\dagger + a_1 a_2) - 2(a_1^\dagger a_2 + a_1 a_2^\dagger) \right]. \end{aligned} \quad (9.2.13)$$

Among the terms, we can eliminate about a half of them by assuming that two phonon modes have the same oscillation frequency ω_m

$$\mathcal{H}_{\text{ph-ph}} = \frac{e^2 z_{zpf}^1 z_{zpf}^2}{8\pi\epsilon_0 Z^3} \left[a_1^\dagger a_1 + a_2^\dagger a_2 - a_1^\dagger a_2 - a_1 a_2^\dagger \right]. \quad (9.2.14)$$

The first two terms of above expression just shift the energies of the phonons, therefore, we omit them. The final form of the interaction Hamiltonian reads

$$\mathcal{H}_{\text{ph-ph}} = -\hbar g_{\text{ph-ph}} (a_1^\dagger a_2 + a_1 a_2^\dagger) \quad (9.2.15)$$

which is obviously a beam-splitter-type interaction. This interaction is also physically intuitive since it expresses the exchange of phonons between the two phonon modes. The phonon-phonon coupling strength is now defined as $g_{\text{ph-ph}} = e^2 z_{\text{zpf}}^1 z_{\text{zpf}}^2 / 8\hbar\pi\epsilon_0 Z^3$. Therefore, by plugging the expressions of the vacuum fluctuations of the phonon modes $z_{\text{zpf}}^i = \sqrt{\hbar/2m\omega_m}$, which can be quickly derived by equating a half of the zero-point energy and the potential energy of the harmonic oscillation: $\hbar\omega_m/2 = m\omega_m^2(z_{\text{zpf}}^i)^2/2$, we can obtain concrete expression of the coupling constant as

$$g_{\text{ph-ph}} = \frac{e^2}{16\pi\epsilon_0 m \omega_m Z^3}. \quad (9.2.16)$$

This is the case for the circumstance that the two ions have the same mass, however, one can obtain the coupling strengths for more general situations by replacing the expressions of the vacuum fluctuation of phonons.

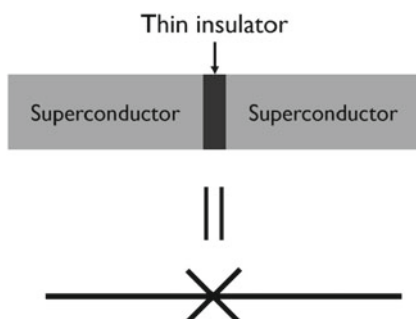
Let us evaluate the coupling strength with realistic parameters at last. As typical values, we set $Z = 10 \mu\text{m}$, $m = 40m_p$ with m_p being proton mass and $\omega_m/2\pi = 100 \text{ kHz}$, the coupling strength is evaluated to be $g_{\text{ph-ph}}/2\pi = 220 \text{ kHz}$.

9.3 Superconducting Circuits

In a superconducting material, where Bardeen–Cooper–Schrieffer theory is valid, electrons form so-called Cooper pairs with the help of attractive interaction in a momentum space that is mediated by electron–phonon interaction. Cooper pairs share a macroscopic wavefunction over the entire superconductor to exhibit quantum-mechanical behavior such as interference effect. The fact that the resistance of the superconductor is nearly equal to zero means that the quality factor of the LC resonator drastically increases, which is otherwise limited by the Joule heating with parasitic resistance.

In addition to this, Josephson junction, which consists of a nanometer-thick insulating layer sandwiched by superconductors (Fig. 9.4) plays an important role in the context of quantum technology. Cooper pairs can transmit the insulating film of the Josephson junction by tunneling effect and exhibit finite conductivity across

Fig. 9.4 Josephson junction and its circuit diagram



the insulating film, which is the celebrated Josephson effect. The AC Josephson effect, in particular, states that the tunneling current $I(t)$ oscillates with respect to the magnetic flux Φ_J piercing the circuit as $I(t) = I_0 \sin(2\pi\Phi_J/\Phi_0)$ with I_0 being a constant in the unit of current and $\Phi_0 = h/2e$ is a flux quantum, where $e (< 0)$ is the elementary charge. For a back-of-the-envelope derivation of the Josephson effect can be found in Ref. [15]. In an ordinary inductor with inductance L , the current through it is proportional to L . In the AC Josephson effect, one can immediately see that there is no simple proportionality between the current and inductance, and indeed the Josephson junction is acting as a nonlinear inductor. By replacing the linear inductor of the LC resonator by such a Josephson junction, one can realize the anharmonic resonator whose ground state and the first excited state can be utilized for qubit construction. In this Section, we review the quantum-mechanical treatment of an LC resonator, an anharmonic resonator described above which is also called a transmon, and coupling between an LC resonator and a transmon.

9.3.1 Quantum-Mechanical Treatment of an LC Resonator

Let us consider an LC resonator with an inductor L and a capacitor C connected in parallel, as shown in Fig. 9.5. The resonance frequency is, of course, given by $1/2\pi\sqrt{LC}$. The purpose of this chapter is to quantize the LC resonator and to obtain a Hamiltonian describing it as a harmonic oscillator. The charge accumulated in the capacitor is here denoted by Q and magnetic flux, or simply “flux” below, in the resonator by Φ . These quantities are related to voltage V and current I as

$$Q = CV, \quad \Phi = LI. \quad (9.3.1)$$

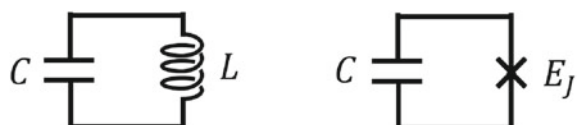
The voltage V and current I are further related to the time derivatives of the charge Q and magnetic flux Φ , respectively as

$$I = -\frac{dQ}{dt}, \quad V = \frac{d\Phi}{dt}. \quad (9.3.2)$$

By combining these equalities, a differential equation for Q can be obtained as

$$\frac{d^2Q}{dt^2} = -\frac{Q}{LC} \quad (9.3.3)$$

Fig. 9.5 LC resonator (left) and transmon qubit (right)



which actually yields solutions oscillating at the frequency $1/2\pi\sqrt{LC}$. In the same manner, the flux Φ obeys a differential equation

$$\frac{d^2\Phi}{dt^2} = -\frac{\Phi}{LC}. \quad (9.3.4)$$

At this stage, we would like to think about Lagrangian that yields above differential equations as Euler-Lagrange equations. Such a Lagrangian \mathcal{L} is

$$\mathcal{L} = \frac{Q^2}{2C} - \frac{L}{2} \left(\frac{dQ}{dt} \right)^2 \quad (9.3.5)$$

and by noting the apparent fact that the canonical conjugate variable of the charge Q is the flux Φ , Hamiltonian \mathcal{H}_{LC} reads

$$\mathcal{H}_{LC} = \frac{Q^2}{2C} + \frac{\Phi^2}{2L} \quad (9.3.6)$$

where one can see that the first term stands for the energy stored in the capacitor, and the second term does for the energy in the inductor.

Here we succeeded in expressing the LC resonator by the Hamiltonian of a harmonic oscillator with canonical variables Q and Φ . Then, we require a commutation relation $[Q, \Phi] = i\hbar$ to complete the quantization of the LC resonator. The annihilation and creation operators of a photon in the LC resonator are defined as

$$a = \frac{1}{2\hbar} \sqrt{\frac{L}{C}} Q + \frac{i}{2\hbar} \sqrt{\frac{C}{L}} \Phi \quad (9.3.7)$$

$$a^\dagger = \frac{1}{2\hbar} \sqrt{\frac{L}{C}} Q - \frac{i}{2\hbar} \sqrt{\frac{C}{L}} \Phi \quad (9.3.8)$$

that fulfills the commutation relation $[a, a^\dagger] = 1$ and the Hamiltonian is rewritten as

$$\mathcal{H}_{LC} = \hbar\omega_{LC} \left(a^\dagger a + \frac{1}{2} \right). \quad (9.3.9)$$

9.3.2 Superconducting Quantum Bit

Next, let us consider the circuit shown in the right panel of Fig. 9.5 in which the inductor is replaced by a Josephson junction. The Josephson effect tells us that current I and voltage V across the Josephson junction can be written by the phase difference θ of the macroscopic wavefunction across the junction as

$$I = I_0 \sin \theta, \quad V = \frac{\hbar}{2e} \frac{d\theta}{dt}. \quad (9.3.10)$$

By using the flux quantum $\Phi_0 = h/2e$ and defining the flux as $\Phi_J = (\theta/2\pi)\Phi_0$, we can rewrite above expressions as

$$I(t) = I_0 \sin\left(2\pi \frac{\Phi_J}{\Phi_0}\right), \quad V = \frac{d\Phi_J}{dt}. \quad (9.3.11)$$

Then by noting that the current is given by the time derivative of the charge, we get

$$\frac{dQ}{dt} = C \frac{dV}{dt} = -I_0 \sin\left(2\pi \frac{\Phi_J}{\Phi_0}\right) \quad (9.3.12)$$

and further by using $V = d\Phi_J/dt$ we obtain

$$C \frac{d^2\Phi_J}{dt^2} = -I_0 \sin\left(2\pi \frac{\Phi_J}{\Phi_0}\right) \quad (9.3.13)$$

as a differential equation for Φ_J . Lagrangian \mathcal{L}_q that yields such an Euler-Lagrange equation is

$$\mathcal{L}_q = \frac{C}{2} \left(\frac{d\Phi_J}{dt} \right)^2 + \frac{I_0 \Phi_0}{2\pi} \cos\left(2\pi \frac{\Phi_J}{\Phi_0}\right). \quad (9.3.14)$$

The first term is immediately reinterpreted as the energy of the capacitor $Q^2/2C$ and the second term is interpreted as the energy involving Cooper pair tunneling across the junction. The prefactor $E_J = I_0 \Phi_0 / 2\pi$ of the second term is called Josephson energy. We further define charge energy $E_C = e^2/2C$ and number of Cooper pairs $n_C = Q/2e$ to obtain a Hamiltonian \mathcal{H}_q of the circuit under concern as

$$\mathcal{H}_q = 4E_C n_C^2 + E_J \cos\theta \quad (9.3.15)$$

where the argument of the second term is written by θ again. If we expand the cosinusoidal function as $\cos\theta = 1 - \theta^2/2! + \theta^4/4! - \dots$ and truncate the series to keep terms up to θ^2 , we see that this Hamiltonian reduces to a one describing mere harmonic oscillator.

Here we shall make an assumption: we suppose that the Josephson energy is much larger than the charge energy, namely $E_J/E_C \gg 1$. The resonance circuit has originally become a nonlinear or anharmonic oscillator by the incorporation of the Josephson junction, a nonlinear inductor. However, above assumption implies that the nonlinearity is so small that physical quantities of the circuit can be approximated by the ones of the harmonic oscillator, which turns out to be not so bad as we shall see below. In such an approximation, the commutation relation $[Q, \Phi_J] = i\hbar$ is required to hold as was done in the quantization procedure of the LC resonator. $[n_C, \theta] = i$ is

immediately derived from this commutation relation and we define the annihilation and creation operators a and a^\dagger as follows:

$$n_C = \left(\frac{E_J}{8E_C} \right)^{\frac{1}{4}} \frac{a + a^\dagger}{\sqrt{2}}, \quad (9.3.16)$$

$$\theta = \left(\frac{8E_C}{E_J} \right)^{\frac{1}{4}} \frac{a - a^\dagger}{i\sqrt{2}}. \quad (9.3.17)$$

Since we assumed that the nonlinearity caused by the Josephson junction is small, it is reasonable to put $\cos \theta \simeq 1 - \theta^2/2! + \theta^4/4!$ by truncating the Taylor expansion. The reason that we keep the term proportional to θ^4 is that this term is the lowest-order one which brings the nonlinearity into the circuit. Then by plugging n_C and θ into the Hamiltonian we finally get

$$\begin{aligned} \mathcal{H}_q &= (\sqrt{8E_C E_J} - E_C) a^\dagger a - \frac{E_C}{2} a^\dagger a^\dagger a a \\ &= \hbar\omega_q a^\dagger a + \frac{\hbar\alpha_q}{2} a^\dagger a^\dagger a a \end{aligned} \quad (9.3.18)$$

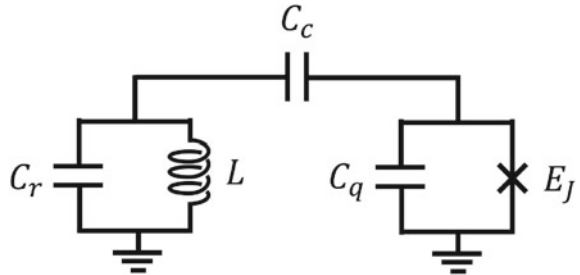
which manifests itself as a harmonic oscillator-like resonator in the first term while a weakly nonlinear one in the second term. Therefore, the energy levels of this system are energetically not equidistantly aligned and we can only pick up the lowermost two levels to construct a qubit. The qubit energy reads $\hbar\omega_q = \sqrt{8E_C E_J} - E_C$ and the quantity $\alpha_q = -E_C/\hbar$ represents the magnitude of the nonlinearity since the energy difference between the first excited state and the second one is given by $\hbar\omega_q + \hbar\alpha_q$. As typical parameters, $\omega_q \simeq 10$ GHz, $E_J/E_C \geq 50$, $\alpha_q \sim -200$ MHz.

We here make a brief comment on the assumption $E_J/E_C \gg 1$ made in the above discussion. The statement that the Josephson energy E_J is much larger than the charge energy E_C means that the nonlinearity of the circuit is very weak, as implied in the coefficient of θ including a factor $(E_J/E_C)^{1/4}$. One can acquire deeper intuition by considering the vacuum fluctuation of the charge operator $\delta n_C = (E_J/8E_C)^{1/4}$. When the E_J/E_C is small, δn_C is also small and a tiny difference of n_C , even by a single quantum, has non-negligible effect on the state and energy of the circuit. Therefore, the nonlinearity is understood to be large. In contrast to this, δn_C is very large if $E_J/E_C \gg 1$ and a small change of n_C does not affect the state and energy of the circuit, meaning that the circuit is almost linear. The superconducting circuit considered above where $E_J/E_C \gg 1$ holds is called a transmon. On the contrary, if $E_J/E_C \gg 1$ do not hold, the nonlinearity gets large and such a circuit is called a Cooper-pair box.

9.3.3 Coupling Between a Transmon and an LC Resonator

Let us consider here the situation that the transmon and the LC resonator is electrically connected by a capacitor as depicted in Fig. 9.6. Parameters such as voltages, charges

Fig. 9.6 Coupled system of a transmon and an LC resonator



in capacitors and fluxes are defined as indicated in the figure. A key point is how to treat the coupling capacitor with capacitance C_c . Here we assume that the coupling capacitance is negligibly small compared to C_q and C_r , so that the Hamiltonian can be given by the sum of energies of the transmon, the LC resonator and the coupling capacitor. The voltage across the coupling capacitor is $V_c = V_r - V_q = Q_r/C_r - Q_q/C_q$ and the energy of the coupling capacitor is given by $C_c V_c^2/2$ using V_c . Then, the Hamiltonian of the whole system reads

$$\begin{aligned} \mathcal{H} &= \frac{Q_r^2}{2C_r} \left(1 + \frac{C_c}{C_r}\right) + \frac{\Phi_r^2}{2L} + \frac{Q_q^2}{2C_q} \left(1 + \frac{C_c}{C_q}\right) + E_J \cos \theta - C_c V_r V_q \\ &= \frac{Q_r^2}{2C'_r} + \frac{\Phi_r^2}{2L} + \frac{Q_q^2}{2C'_q} + E_J \cos \theta - C_c V_r V_q. \end{aligned} \quad (9.3.19)$$

Here $C'_\xi = C_\xi C_c / (C_\xi + C_c)$ ($\xi = r, c$) are defined and the expression of the last term is intended to be in terms of the voltages. Let us now replace the charges and fluxes by the annihilation and creation operators of the LC resonator (c^\dagger, c) and the transmon (a^\dagger, a), namely by

$$Q_r = \hbar \sqrt{\frac{C'_r}{L}} (c + c^\dagger), \quad \Phi_r = \frac{\hbar}{i} \sqrt{\frac{L}{C'_r}} (c - c^\dagger), \quad (9.3.20)$$

$$Q_q = \left(\frac{E_J}{8E_C}\right)^{\frac{1}{4}} \frac{a + a^\dagger}{\sqrt{2}}, \quad \theta = \left(\frac{8E_C}{E_J}\right)^{\frac{1}{4}} \frac{a - a^\dagger}{i\sqrt{2}}. \quad (9.3.21)$$

By ignoring the constants, we obtain

$$\mathcal{H} = \hbar \omega_{LC} c^\dagger c + \hbar \omega_q a^\dagger a + \frac{\hbar \alpha_q}{2} a^\dagger a^\dagger a a - \hbar g(c + c^\dagger)(a + a^\dagger) \quad (9.3.22)$$

where coupling strength g is defined as

$$g = \frac{C_c}{\hbar} \left(\frac{\hbar}{C'_r} \sqrt{\frac{C'_r}{L}} \right) \left[\frac{2e}{C'_q} \left(\frac{E_J}{8E_C} \right)^{\frac{1}{4}} \frac{1}{\sqrt{2}} \right]. \quad (9.3.23)$$

This coupling constant is proportional to the coupling capacitance C_c , the vacuum fluctuation of the voltage of the LC resonator, and the vacuum fluctuation of the voltage of the transmon. Further application of rotating-wave approximation to this Hamiltonian yields the Jaynes-Cummings Hamiltonian.

In realistic designs of the superconducting circuits and their couplings, tiny capacitor, inductors, and Josephson junctions should be characterized by numerical simulations and empirical values. This is because the capacitance and inductance held by wirings other than the capacitor and inductor are not negligible. The original assumption of $C_c \ll C_q, C_r$ is not the case as well in most situations, hence the numerical simulations are indispensable at last when one deals with the superconducting circuits.

9.4 Optomechanical Interaction

9.4.1 Brief Introduction

A gravitational-wave detector consists of a number of mirrors that form an astonishingly large Michelson interferometer extending over kilometers to pickup an unimaginably tiny amount of “noise” created in the spacetime by gravitational waves. The mirrors form extremely high-finesse, coupled optical resonators in order to enhance the sensitivity of the detector to such noises. Enough disgustingly, the detector should sense the deviation of the cavity lengths with a precision well below the lattice constants of solids!—and hence, the vibrational motion of the mirrors and even of the collective motion of atoms on the surface of mirrors, both are described universally as phonons, may cause fatal noises on the detector that hide the faint signals. To avoid such unwanted noises, the mirrors are kept in a vacuum, cooled down to a cryogenic temperature, and suspended by thin wires. Being highly isolated from the environment, the mirrors embrace the vibrational modes with extremely high-quality factors. The effect of these vibrational modes on optical signals was studied by Braginsky, focusing on the quantum-limited measurement of the position of the mirror.

In the series of this kind of study, the cavity optomechanics [30] raised the cry. It anticipates the interaction between cavity photons and mechanical phonons, where photons can control phonons and *vice versa*. Phonons scatter the cavity photons inelastically to make optical sidebands, which are spectrally discriminated from the cavity spectrum when the mechanical frequency is much larger than the linewidth of the cavity. Researchers have searched for high-frequency mechanical modes in the micromechanical devices to deal with nicely resolved sidebands. Resolved-sideband regime allows the cooling rate to be maximized to even achieve ground-state cooling of the mechanical modes where the phonons can be manipulated in the quantum regime.

Here we introduce the optomechanical interaction and its linearization. These play essential roles in the rapidly growing field of cavity optomechanics that enchant the quantum optical systems with novel degrees of freedom.

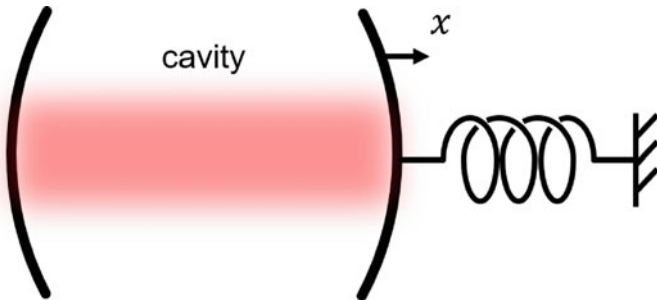


Fig. 9.7 Schematics of the system of cavity optomechanics

9.4.2 Optomechanical Interaction

We first dictate the basic Hamiltonian that only includes the energies of cavity photons ($\hbar\omega_c a^\dagger a$) and mechanical phonons ($\hbar\omega_m b^\dagger b$);

$$\mathcal{H} = \hbar\omega_c(x)a^\dagger a + \hbar\omega_m b^\dagger b \quad (9.4.1)$$

in which we assume that the resonant frequency of the cavity $\omega_c(x)$ is dependent on the position x of the mechanical oscillator. This assumption applies to the situation that the cavity length is modulated by the oscillatory motion of some part of the cavity, e.g., that one of the mirrors which form a Fabry-Perót resonator is ideally fixed and the other is supported by a spring (see Fig. 9.7). There we can expand the resonant frequency as $\omega_c(x) = \omega_c - Gx + \dots$ with the structure-dependent coefficient G to get the “perturbed” Hamiltonian

$$\mathcal{H} = \hbar(\omega_c - Gx)a^\dagger a + \hbar\omega_m b^\dagger b \quad (9.4.2)$$

$$= \hbar\omega_c a^\dagger a + \hbar\omega_m b^\dagger b - \hbar G a^\dagger a x \quad (9.4.3)$$

$$= \hbar\omega_c a^\dagger a + \hbar\omega_m b^\dagger b - \hbar g_0 a^\dagger a(b + b^\dagger) \quad (9.4.4)$$

within the linear regime in the expansion of $\omega_c(x)$. Here we utilized the fact that the mechanical displacement is written as $x = x_{\text{zpf}}(b + b^\dagger)$ where $x_{\text{zpf}} = \sqrt{\hbar/2m\omega_m}$ represents the amplitude of the zero-point fluctuation. The effective mass m of the mechanical oscillator is used in this expression. The coupling strength is thus written as $g_0 = x_{\text{zpf}} G$. This Hamiltonian is widely applicable to the cavity optomechanical systems including Fabry-Perót type cavities with moving mirrors, membrane-in-the-middle system, photonic-phononic crystal cavities, and even the electromechanical systems where the LC resonator involving a trembling capacitor.

Let us look at the form of the optomechanical interaction \mathcal{H}_{int} . It is a coupling term between photon number in the cavity and the mechanical displacement, hence its static nature is the radiation pressure, i.e. the mechanical object is pushed by the momentum kicks exerted by the cavity photons. Since the radiation pressure pushes back the mechanical object slightly to make the equilibrium position shift, it is also called the optical spring effect. Its dynamical nature results in the situation that the

phonon is either created or annihilated in the virtual absorption and emission of the cavity photon to result in the Stokes and anti-Stokes scattering. These inelastic scatterings are frequently called the red- and blue-sideband transitions with the terms “red” and “blue” referring to the detuning relative to the carrier (phonon-number conserving) transition. The highlight of the cavity optomechanics is the cooling of the mechanical modes down close to its motional ground state by imposing the strong imbalance between red- and blue-sideband transitions.

9.4.3 Linearized Optomechanical Interaction

We would like to see the linearized versions of the optomechanical interaction. We for brevity ride on a rotating frame of the laser drive frequency ω_l . The first term is transformed to $\hbar(\omega_c - \omega_l)a^\dagger a = \hbar\Delta_c a^\dagger a$ while other two remain unchanged. We consider the circumstance that the cavity mode is driven by the laser with sufficiently narrow linewidth, so that the cavity operator a can be replaced by $\alpha + \delta a$, where $\alpha \in \mathbb{C}$ is the amplitude of the coherent state and δa is the noise or fluctuation operator superposed on the amplitude. By doing this, we have

$$\mathcal{H}_{int} = -\hbar g_0 (|\alpha|^2 + \alpha^* \delta a + \alpha \delta a^\dagger + \delta a^\dagger \delta a) (b + b^\dagger) \quad (9.4.5)$$

$$= -\hbar g_0 n_{cav} (b + b^\dagger) - \hbar g_0 \sqrt{n_{cav}} (\delta a + \delta a^\dagger) (b + b^\dagger) \quad (9.4.6)$$

by neglecting the term in second order of the fluctuation and defining $n_{cav} = |\alpha|^2$. The coupling strength often include this driving amplitude to be $g = g_0 \sqrt{n_{cav}}$. The first term gives the static shift of the resonant frequency of the cavity, that is, the radiation pressure and dropped in the following discussion. The second term represents the linearized optomechanical interaction and takes two forms depending on the frequency of the driving laser. It might be helpful to explicitly write down the time-dependent factors as

$$\mathcal{H}_{int} = -\hbar g (\delta a e^{-i\Delta_c t} + \delta a^\dagger e^{i\Delta_c t}) (b e^{-i\omega_m t} + b^\dagger e^{i\omega_m t}) \quad (9.4.7)$$

$$= \begin{cases} -\hbar g (\delta a b^\dagger + \delta a^\dagger b) & \text{when } \Delta_c = \omega_m \Rightarrow \omega = \omega_c - \omega_m \\ -\hbar g (\delta a^\dagger b^\dagger + \delta a b) & \text{when } \Delta_c = -\omega_m \Rightarrow \omega = \omega_c + \omega_m \end{cases} \quad (9.4.8)$$

Apparently these are read as the beam-splitter and two-mode-squeezing interactions. The intuitive understanding is straightforward: when the driving laser is red-detuned ($\omega_l = \omega_c - \omega_m$), the driving photon at $\omega_c - \omega_m$ is annihilated, the “noise” at ω_c is created and the phonon is annihilated, see Fig. 9.8a. The “noise” at $\omega_c - 2\omega_m$ is also present, however, it is not nicely supported by the cavity. This asymmetry of the inelastic scattering make the phonon mode to be cooled, even down to the motional ground state as detailed in Appendix H. The reverse process takes place when the driving laser is resonant on the cavity. On the other hand, if the driving laser is blue-detuned ($\omega_l = \omega_c + \omega_m$), the simultaneous creation or annihilation of the “noise” at ω_c and the phonon occurs with entanglement between them [see

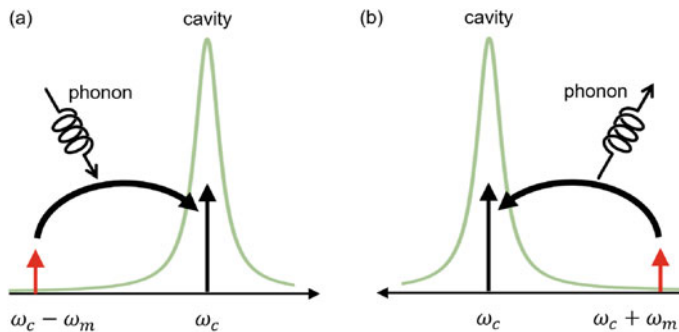


Fig. 9.8 **a** Beam-splitter and **b** entangling interactions

Fig. 9.8b]. Due to the presence of the density of states of the cavity, phonon creation process overwhelms the annihilation one, leading to the motional heating. As the phonon number increases, the nonlinear nature of the phonon mode ($b^\dagger b^\dagger b b$ term) gets relevant and the phonon-phonon interaction has non-negligible effect. Further phonon pumping results in the observation of phonon lasing.

9.5 Hybrid Quantum Systems and Cooperativity

In the previous section, an interesting “hybrid” quantum system composed of a harmonic oscillator and an optical cavity is introduced. Such hybrid quantum systems, where different quantum systems are somehow coupled to each other, provide many kinds of interesting applications based on the conversion of the quantum state from one to the other. Then the characteristic quantity should be defined for the hybrid quantum system representing how efficient the conversion of the quantum state is. This can be given by the quantity called cooperativity, which we shall introduce in the following.

First, we shall consider a hybrid system where two harmonic oscillators A and B are coupled with a beam-splitter interaction as schematically shown in Fig. 9.9. Frequencies of the harmonic oscillators are denoted as ω_a and ω_b , and a (a^\dagger) and b

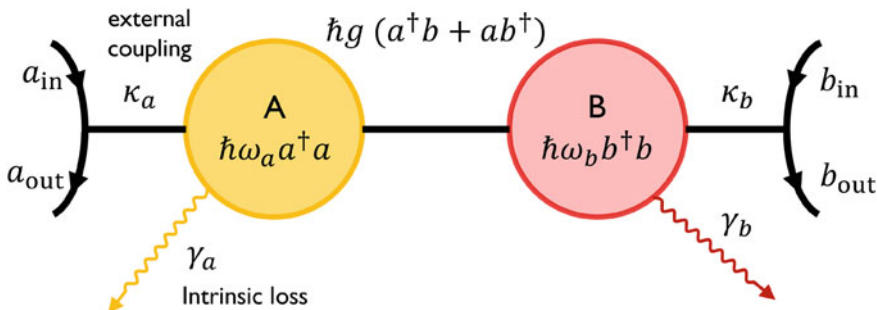


Fig. 9.9 Schematics of a coupled harmonic oscillator

(b^\dagger) are annihilation (creation) operators. Intrinsic loss rates γ_a and γ_b are present for the systems A and B, respectively. Propagating-mode operators a_{in} (a_{out}) and b_{in} (b_{out}) represent the input and output waves for the corresponding harmonic oscillator, with external coupling rate κ_a for A and κ_b for B. Further with the coupling strength g of the beam-splitter interaction, we can write down the full Hamiltonian of this system as

$$\mathcal{H} = \hbar\omega_a a^\dagger a + \hbar\omega_b b^\dagger b + \hbar g(a^\dagger b + ab^\dagger).$$

What we want to find out with this model system is how efficiently the input waves from a_{in} can be transmitted to b_{out} by quantifying the ratio of the photon flux $\langle b_{\text{out}}^\dagger b_{\text{out}} \rangle / \langle a_{\text{in}}^\dagger a_{\text{in}} \rangle$. Therefore, we have no input from b_{in} so that this propagating-mode operator is neglected hereafter.

Let us then think of driving the system A with frequency ω_d . Riding on the rotating frame with this frequency for both systems A and B by applying unitary transformation with $U(t) = \exp[i\omega_d a^\dagger at + i\omega_d b^\dagger bt]$, we get

$$\mathcal{H}' = \hbar\Delta_a a^\dagger a + \hbar\Delta_b b^\dagger b + \hbar g(a^\dagger b + ab^\dagger)$$

where $\Delta_a = \omega_a - \omega_d$ and $\Delta_b = \omega_b - \omega_d$. Heisenberg equations of motion are then considered next. For our purpose here, we take into account the input with a_{in} in the Heisenberg equations of motion using input-output theory:

$$\frac{da}{dt} = - \left(i\Delta_a + \frac{\Gamma_a}{2} \right) a - igb + \sqrt{\kappa_a} a_{\text{in}}, \quad (9.5.1)$$

$$\frac{db}{dt} = - \left(i\Delta_b + \frac{\Gamma_b}{2} \right) b - ig a. \quad (9.5.2)$$

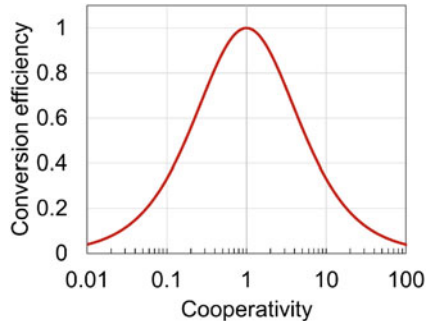
Here the total loss rates of the systems are defined as $\Gamma_a = \gamma_a + \kappa_a$ for the system A and $\Gamma_b = \gamma_b + \kappa_b$ for B. Given these and input-output relations

$$\begin{aligned} a_{\text{out}} &= a_{\text{in}} + \sqrt{\kappa_a} a, \\ b_{\text{out}} &= \sqrt{\kappa_b} b, \end{aligned}$$

we analyze the behavior of the hybrid system. We consider the situation with $da/dt = 0$ and $db/dt = 0$ here, which corresponds to the steady state of the driven system. Then above equations result in an easy-going set of linear algebraic equations. Solving these yields

$$b_{\text{out}} = - \frac{ig\sqrt{\kappa_a \kappa_b}}{\left(i\Delta_a + \frac{\Gamma_a}{2} \right) \left(i\Delta_b + \frac{\Gamma_b}{2} \right) + g^2} a_{\text{in}}$$

Fig. 9.10 Conversion efficiency as a function of the cooperativity C



and becomes simpler if we suppose the system is driven resonantly: $\Delta_a = \Delta_b = 0$. With this assumption, the quantum conversion efficiency $\eta = \langle b_{\text{out}}^\dagger b_{\text{out}} \rangle / \langle a_{\text{in}}^\dagger a_{\text{in}} \rangle$ is then written as

$$\eta = \eta_a \eta_b \frac{4C}{(1+C)^2}$$

with newly introduced parameters being given as $\eta_a = \kappa_a / \Gamma_a$, $\eta_b = \kappa_b / \Gamma_b$ and

$$C = \frac{4g^2}{\Gamma_a \Gamma_b}$$

which is called cooperativity.

Figure 9.10 displays the conversion efficiency as a function of the cooperativity, when $\eta_a, \eta_b \sim 1$ which means that the external coupling rates are dominant over the intrinsic loss rates for both systems A and B. One can immediately see that the conversion efficiency reaches unity only if $C = 1$. To see what this situation looks like, we revisit the Heisenberg equations of motion (9.5.1) and (9.5.2) where b in Eq. (9.5.1) is now to be rewritten by a . For brevity we put $\Delta_a = \Delta_b = 0$, $\gamma_a = \gamma_b = 0$ and $da/dt = 0$ and get

$$\frac{da}{dt} = - \left(i \Delta_a + \frac{\kappa_a}{2} - \frac{2g^2}{\kappa_b} \right) a + \sqrt{\kappa_a} a_{\text{in}} \quad (9.5.3)$$

where the loss term of A, originally $\kappa_a/2$, is now modified as $\kappa_a/2 - 2g^2/\kappa_b$. The unity cooperativity $C = 1$ in this situation means that the original loss rate of A, $\kappa_a/2$, is equal to the newly added loss rate due to the coupling, $2g^2/\kappa_b$, where a kind of impedance matching from a_{in} to b_{out} is fulfilled. In real experiments, neither of γ_a nor γ_b equals to zero but finite. Hence, $\eta_a, \eta_b < 1$ always makes the conversion efficiency less than 1 even if $C = 1$ is fulfilled. It is important for achieving high conversion efficiency to get large coupling strength and to tune external coupling rates at will to make them dominant over the intrinsic loss rates and at the same time to make $C = 1$.

Problems

Problem 9-1 Red- and blue-sideband transitions of trapped ion and cavity optomechanical systems allow us to manipulate mechanical oscillations.

- Explain what happens with these transitions in terms of the ion's internal state.
- Continuously driving the red-sideband transition leads to the cooling of ion's motion. Verify this statement qualitatively.
- Address above two issues in the system of cavity optomechanics.

Problem 9-2 Let us consider a system of coupled Harmonic oscillators A and B with annihilation operators a and b , respectively. The Hamiltonian is given as

$$\mathcal{H}' = \hbar\omega_a^\dagger a + \hbar\omega_b^\dagger b + \hbar g(a^\dagger b + ab^\dagger)$$

where two oscillators are coupled via beam-splitter interaction. Diagonalize this Hamiltonian and examine the energy spectrum.

Problem 9-3 Calculate the transition frequencies of the transmon qubit from the ground state to the first excited state and from the first excited state to the second excited state. Given $\alpha/2\pi = 100$ MHz, how long should the transmon qubit's lifetime be for above two transitions spectrally resolve?

Problem 9-4 Consider a coupled system of three harmonic oscillators as shown below (Fig. 9.11):

Calculate the quantum conversion efficiency of this system.

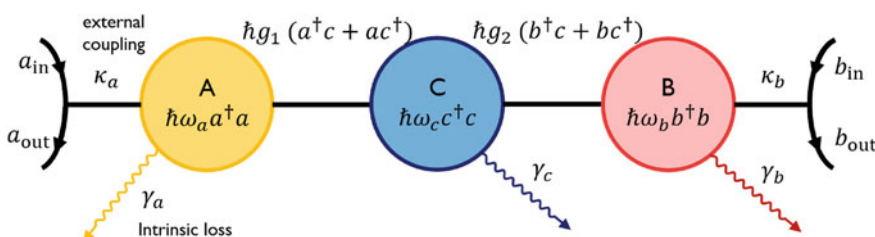


Fig. 9.11 A schematic and parameters of three harmonic oscillators coupled in series

Part III

Quantum Information Processing and Quantum Technologies



Basics of Quantum Information Processing

10

10.1 Quantum Gates

As mentioned before, an applied electromagnetic field can rotate the qubit state in a Bloch sphere and the rotation angle is at our will, by tuning the pulse area of the applied field. However, this is not everything we should do. In quantum technologies, one will frequently desire to make any single-qubit state in the Bloch sphere, or more generally any multi-qubit quantum states which may include heavily entangled states. For the sake of such an attempt, fortunately, we only have to prepare a few quantum operations, called the quantum gates, to realize any quantum states. This set of quantum gates is termed a universal set of quantum gates and is not unique [18]. For example, single-qubit unitary gates and CNOT gate, which will be described later, establish a universal set. In this Section, we introduce several frequently used single- and two-qubit gates.

One thing should be noted before we proceed. In the community of quantum information processing, the convention about the density matrix is different from what we have adopted so far. In short, the density matrix reads

$$\rho = \begin{pmatrix} |c_g|^2 & c_e^* c_g \\ c_e c_g^* & |c_e|^2 \end{pmatrix}, \quad (10.1.1)$$

where the ordering of $|g\rangle$ and $|e\rangle$ are exchanged. Only in this chapter, we rather switch to this convention in order for the expression of the quantum gates to be in common forms seen in other literatures.

Supplementary Information The online version contains supplementary material available at https://doi.org/10.1007/978-981-19-4641-7_10.

10.1.1 Single-Qubit Gates

A quantum state of a single qubit is represented by a point in a Bloch sphere, therefore any single-qubit gate is a product of a rotation matrix that maps one point on the Bloch sphere to another, and a global phase shift. The former is given by using a unit vector $\mathbf{n} = (n_x, n_y, n_z)$ as

$$\begin{aligned} R_{\mathbf{n}}(\theta) &= e^{-i\frac{\theta}{2}(n_x\sigma_x+n_y\sigma_y+n_z\sigma_z)} = I \cos \frac{\theta}{2} - i(n_x\sigma_x + n_y\sigma_y + n_z\sigma_z) \sin \frac{\theta}{2} \\ &= \begin{pmatrix} \cos \frac{\theta}{2} - in_z \sin \frac{\theta}{2} & -(n_y + in_x) \sin \frac{\theta}{2} \\ (n_y - in_x) \sin \frac{\theta}{2} & \cos \frac{\theta}{2} + in_z \sin \frac{\theta}{2} \end{pmatrix} \end{aligned} \quad (10.1.2)$$

Here, the unit vector \mathbf{n} act as an axis about which the rotation by an angle θ takes place.¹ We shall describe special cases where the rotation axes are simply x or z . Indeed the rotation about y -axis can be decomposed into a product of rotations about X and Z axes.²

X Gate

First single-qubit quantum gate we consider is the X gate which is defined as

$$R_x(\pi) = \begin{pmatrix} 0 & -i \\ -i & 0 \end{pmatrix} = -iX = -i(|e\rangle\langle g| + |g\rangle\langle e|) \quad (10.1.3)$$

and simply flips the qubit from $|g\rangle$ to $|e\rangle$ and $|e\rangle$ to $|g\rangle$. The X gate often refers to the operation $X = iR_x(\pi)$, but in a practical experiment the π -rotation about the x axis executes the operation $-iX$. Therefore, it can be easily noticed that the resonant Rabi oscillation with pulse duration $\Delta t = \pi/\Omega$ realizes this operation. This applied pulse is often called the π -pulse since the acquired phase is π . In the Bloch sphere, X gate corresponds to the π -rotation around the x axis.

Z Gate

Next we consider the Z gate, which is defined by

$$R_z(\pi) = -i \begin{pmatrix} 1 & 0 \\ 0 & -1 \end{pmatrix} = -iZ = -i(|g\rangle\langle g| - |e\rangle\langle e|). \quad (10.1.4)$$

This operation imposes π -phase shift on $|e\rangle$ but leave $|g\rangle$ unaffected. This operation is understood as a π -rotation around z axis, and Z gate often refers to the operation $Z = iR_z(\pi)$ as well. Then what procedure is needed to implement the rotation around z axis? Before answering this question let us remind that the Bloch vector “stops” at some point in a Bloch sphere only when we are in the rotating frame at the frequency

¹ \mathbf{n} is indeed equivalent to \mathbf{s} .

² $Y = R_z(\frac{\pi}{2})XR_z(-\frac{\pi}{2})$.

ω_q . Namely, the phase of the qubit is at any time evolving in other frames and one answer to above question comes up with our mind: just wait for time duration π/ω_q . However, for ω_q ranging from a few tens of MHz to hundreds of THz, it is tough to wait precisely for a half-period of the oscillation of the light field. Another way is to shift the phase convention of the overall experimental sequence by π , which is relatively easier and quicker. Nonetheless, it is still difficult to achieve ultimately stable phase of the electromagnetic field especially in the optical domain. In such a case, active irradiation of the electromagnetic field might be another way. Looking at the vector causing Rabi oscillation $(\Omega, 0, -\Delta_q)$, one might drive qubit by an off-resonant drive with $\Omega \ll \Delta_q$ for a duration π/Δ_q to get a π -phase shift, though this inevitably leads to errors such as X and Y with tiny but finite possibilities.

Hadamard Gate H , Phase Gate S and $\pi/8$ Gate T

Although not being simple rotations, we list three single-qubit gates of frequent use. The first is the Hadamard gate

$$H = \frac{1}{\sqrt{2}} \begin{pmatrix} 1 & 1 \\ 1 & -1 \end{pmatrix} = \frac{X+Z}{\sqrt{2}}. \quad (10.1.5)$$

Hadamard gate transforms $|g\rangle \rightarrow (|g\rangle + |e\rangle)/\sqrt{2}$ and $|e\rangle \rightarrow (|g\rangle - |e\rangle)/\sqrt{2}$, that corresponds to π -rotation around the vector $\mathbf{n} = (1/\sqrt{2}, 0, 1/\sqrt{2})$. Hadamard gate satisfies $H^\dagger = H$ and transforms X and Z to each other, namely $H X H = Z$ and $H Z H = X$.

The other two are related to the Z gate:

$$S = \begin{pmatrix} 1 & 0 \\ 0 & i \end{pmatrix} = e^{i\frac{\pi}{4}} R_z\left(\frac{\pi}{2}\right), \quad (10.1.6)$$

$$T = \begin{pmatrix} 1 & 0 \\ 0 & e^{i\frac{\pi}{4}} \end{pmatrix} = e^{i\frac{\pi}{8}} R_z\left(\frac{\pi}{4}\right) \quad (10.1.7)$$

where $S^2 = Z$, $T^2 = S$ are satisfied. These are two specific cases of the phase gate which gives a phase factor $e^{i\phi}$ to $|e\rangle$ and leave $|g\rangle$ unchanged. By using the S gate, the Y gate is decomposed into $Y = SX S^\dagger$.

10.1.2 Two-Qubit Gates

Two-qubit gate is in general a quantum gate acting on a two-qubit system $|\psi_1\rangle \otimes |\psi_2\rangle$ consisting of the first $|\psi_1\rangle$ and the second $|\psi_2\rangle$ qubits.³ For operations like $X_1 \otimes X_2$ by which X_i act on i -th qubit, it is simply a simultaneous action of two single-qubit operations. Another interesting two-qubit operation is a controlled gate where

³ “ \otimes ” is a tensor product.

the “target” qubit (say, the second qubit) undergoes some single-qubit gate if the “control” qubit (say, the first qubit) is $|e\rangle$. We shall focus on this kind of gates here.

Controlled-NOT (CNOT) Gate

Controlled-NOT gate, or CX gate, is a gate that acts as the X gate on the target qubit for the control-qubit state $|e\rangle$. The matrix form of this gate is, by using 2^2 by 2^2 matrix,

$$\text{CNOT} = \begin{pmatrix} 1 & 0 & 0 & 0 \\ 0 & 1 & 0 & 0 \\ 0 & 0 & 0 & 1 \\ 0 & 0 & 1 & 0 \end{pmatrix} = |g\rangle\langle g| \otimes I + |e\rangle\langle e| \otimes X, \quad (10.1.8)$$

or more concretely, the operations are the replacements $|gg\rangle \rightarrow |gg\rangle$, $|ge\rangle \rightarrow |ge\rangle$, $|eg\rangle \rightarrow |ee\rangle$ and $|ee\rangle \rightarrow |eg\rangle$.

Controlled-Z Gate

Controlled-Z gate, or CZ gate, is a gate that acts as the Z gate on the target qubit if the control-qubit state is $|e\rangle$. The matrix form of this gate is

$$CZ = \begin{pmatrix} 1 & 0 & 0 & 0 \\ 0 & 1 & 0 & 0 \\ 0 & 0 & 1 & 0 \\ 0 & 0 & 0 & -1 \end{pmatrix} = |g\rangle\langle g| \otimes I + |e\rangle\langle e| \otimes Z. \quad (10.1.9)$$

*i*SWAP and SWAP Gates

*i*SWAP and SWAP gates are defined as follows:

$$i\text{SWAP} = \begin{pmatrix} 1 & 0 & 0 & 0 \\ 0 & 0 & i & 0 \\ 0 & i & 0 & 0 \\ 0 & 0 & 0 & 1 \end{pmatrix}, \quad (10.1.10)$$

$$\text{SWAP} = \begin{pmatrix} 1 & 0 & 0 & 0 \\ 0 & 0 & 1 & 0 \\ 0 & 1 & 0 & 0 \\ 0 & 0 & 0 & 1 \end{pmatrix}. \quad (10.1.11)$$

It can be easily seen that SWAP gate exchanges the state between the two qubit, while the *i*SWAP gate does this with phase factor of i .

XX and ZZ Gates

XX and ZZ gates are defined as follows:

$$XX(\theta) = \begin{pmatrix} \cos \frac{\theta}{2} & 0 & 0 & -i \sin \frac{\theta}{2} \\ 0 & \cos \frac{\theta}{2} & -i \sin \frac{\theta}{2} & 0 \\ 0 & -i \sin \frac{\theta}{2} & \cos \frac{\theta}{2} & 0 \\ -i \sin \frac{\theta}{2} & 0 & 0 & \cos \frac{\theta}{2} \end{pmatrix} = I \otimes I \cos \frac{\theta}{2} - i X \otimes X \sin \frac{\theta}{2}, \quad (10.1.12)$$

$$ZZ(\theta) = \begin{pmatrix} e^{i \frac{\theta}{2}} & 0 & 0 & 0 \\ 0 & e^{-i \frac{\theta}{2}} & 0 & 0 \\ 0 & 0 & e^{-i \frac{\theta}{2}} & 0 \\ 0 & 0 & 0 & e^{i \frac{\theta}{2}} \end{pmatrix} = I \otimes I \cos \frac{\theta}{2} + i Z \otimes Z \sin \frac{\theta}{2}. \quad (10.1.13)$$

These are also called Ising coupling gates since they mimic the time evolution of the system generated by the Ising interaction.

From Hamiltonian to Gate Operation

Every physical system implementing qubits possesses its own ways of interaction between qubits. Then a question arises: how above-listed two-qubit gates are realized with given interaction Hamiltonian \mathcal{H}_{int} ? To address this question, let us remind of the fact that the quantum system evolves according to the master equation, or Schrödinger equation if we neglect the loss terms. Formally the Schrödinger equation in the interaction picture⁴ $i\hbar(\partial/\partial t)|\psi\rangle = \mathcal{H}_{\text{int}}|\psi\rangle$ can be solved as $|\psi(t)\rangle = \exp[-i(\mathcal{H}_{\text{int}}/\hbar)t]|\psi(0)\rangle$. Therefore, in the following argument what we will do is really simple: put \mathcal{H}_{int} in the exponent to clarify the action of $\exp[-i(\mathcal{H}_{\text{int}}/\hbar)t]$ on target qubit(s).

First, we shall consider “incomplete” but very common, beam-splitter-like qubit-qubit interaction

$$\mathcal{H}_{\text{int}} = \hbar g(\sigma_+ \sigma_- + \sigma_- \sigma_+) = \frac{\hbar g}{2}(\sigma_x \sigma_x + \sigma_y \sigma_y). \quad (10.1.14)$$

Here the terms like $\sigma_+ \sigma_-$ and $\sigma_x \sigma_x$ should be written as $\sigma_+ \otimes \sigma_-$ and $\sigma_x \otimes \sigma_x$ rigorously, indicating that the first operator acts on the first qubit and the second to the other qubit. We shall omit the symbol \otimes whenever there is no risk of confusion. We will follow the whole maths for this first example. Let us see the explicit form of $(\sigma_x \sigma_x + \sigma_y \sigma_y)/2$:

⁴ Dubbed as the Tomonaga-Schwinger equation.

$$\frac{\sigma_x \sigma_x + \sigma_y \sigma_y}{2} = \frac{1}{2} \begin{pmatrix} 0 & 0 & 1 \\ 0 & 1 & 0 \\ 0 & 0 & 0 \end{pmatrix} + \frac{1}{2} \begin{pmatrix} 0 & 0 & -1 \\ 0 & 1 & 0 \\ -1 & 0 & 0 \end{pmatrix} = \begin{pmatrix} 0 & 0 & 0 \\ 0 & 1 & 0 \\ 0 & 0 & 0 \end{pmatrix} \equiv A. \quad (10.1.15)$$

Simple algebra shows that $A^2 = \text{diag}(0, 1, 1, 0)$ and $A^3 = A$. Now the $\exp[-i(\mathcal{H}_{\text{int}}/\hbar)t] = \exp[-igAt]$ reads

$$e^{-igAt} = 1 - igtA - \frac{(gt)^2}{2!}A^2 + i \frac{(gt)^3}{3!}A^3 + \frac{(gt)^4}{4!}A^4 + \dots \quad (10.1.16)$$

$$= 1 - igtA - \frac{(gt)^2}{2!}A^2 + i \frac{(gt)^3}{3!}A + \frac{(gt)^4}{4!}A^2 + \dots \quad (10.1.17)$$

$$= \text{diag}(1, 0, 0, 1) + \left(1 - \frac{(gt)^2}{2!} + \frac{(gt)^4}{4!} - \dots\right) \text{diag}(0, 1, 1, 0) \quad (10.1.18)$$

$$- i \left((gt) - \frac{(gt)^3}{3!} + \frac{(gt)^5}{5!} - \dots \right) A \quad (10.1.19)$$

$$= \begin{pmatrix} 1 & 0 & 0 & 0 \\ 0 & \cos gt & -i \sin gt & 0 \\ 0 & -i \sin gt & \cos gt & 0 \\ 0 & 0 & 0 & 1 \end{pmatrix}. \quad (10.1.20)$$

With this, the states $|gg\rangle$ and $|ee\rangle$ are unaffected but ‘‘Rabi oscillation’’ between $|ge\rangle$ and $|eg\rangle$ occurs. By setting $t = 3\pi/2g$, this reads the *iSWAP* gate:

$$e^{-i\frac{3\pi}{2}A} = \begin{pmatrix} 1 & 0 & 0 & 0 \\ 0 & 0 & i & 0 \\ 0 & i & 0 & 0 \\ 0 & 0 & 0 & 1 \end{pmatrix}. \quad (10.1.21)$$

Next we consider the two-mode-squeezing-like, counter-rotating interaction

$$\mathcal{H}_{\text{int}} = \hbar g(\sigma_+ \sigma_+ + \sigma_- \sigma_-) = \frac{\hbar g}{2}(\sigma_x \sigma_x - \sigma_y \sigma_y). \quad (10.1.22)$$

Almost the same procedure applies to this and we get

$$e^{-ig\frac{(\sigma_x \sigma_x - \sigma_y \sigma_y)}{2}t} = \begin{pmatrix} \cos gt & 0 & 0 & -i \sin gt \\ 0 & 1 & 0 & 0 \\ 0 & 0 & 1 & 0 \\ -i \sin gt & 0 & 0 & \cos gt \end{pmatrix}, \quad (10.1.23)$$

that leads to the oscillation in the subspace $\{|gg\rangle, |ee\rangle\}$. As a special case, this operation with $t = 3\pi/2g$ is called the *bSWAP* gate.

Let us consider a simultaneous implementation of above two interactions. This can be done in practice in quantum systems such as trapped ions and superconducting qubits. The Hamiltonian reads

$$\mathcal{H}_{\text{int}} = \hbar g(\sigma_+ \sigma_- + \sigma_- \sigma_+) + \hbar g(\sigma_+ \sigma_+ + \sigma_- \sigma_-) = \hbar g \sigma_x \sigma_x. \quad (10.1.24)$$

This can be immediately exponentiated by using the formula⁵ $\exp[-i\sigma_\xi \sigma_\xi \alpha] = \cos \alpha I \otimes I - i \sin \alpha \sigma_\xi \otimes \sigma_\xi$

$$e^{-ig\sigma_x \sigma_x t} = \begin{pmatrix} \cos gt & 0 & 0 & -i \sin gt \\ 0 & \cos gt & -i \sin gt & 0 \\ 0 & -i \sin gt & \cos gt & 0 \\ -i \sin gt & 0 & 0 & \cos gt \end{pmatrix} \quad (10.1.25)$$

which is identified as an XX gate. Likewise the ZZ gate can also be obtained, which originates in the state-dependent phase shifts of the ZZ interaction.

The “complete” Ising interaction between qubits is the Heisenberg interaction dictated as

$$\mathcal{H}_{\text{int}} = \hbar g \frac{\sigma_x \sigma_x + \sigma_y \sigma_y + \sigma_z \sigma_z}{2}. \quad (10.1.26)$$

This Hamiltonian gives the following time evolution⁶:

$$e^{-ig \frac{\sigma_x \sigma_x + \sigma_y \sigma_y + \sigma_z \sigma_z}{2} t} = \begin{pmatrix} e^{-i \frac{g}{2} t} & 0 & 0 & 0 \\ 0 & \frac{e^{-i \frac{g}{2} t} + e^{3i \frac{g}{2} t}}{2} & \frac{e^{-i \frac{g}{2} t} - e^{3i \frac{g}{2} t}}{2} & 0 \\ 0 & \frac{e^{-i \frac{g}{2} t} - e^{3i \frac{g}{2} t}}{2} & \frac{e^{-i \frac{g}{2} t} + e^{3i \frac{g}{2} t}}{2} & 0 \\ 0 & 0 & 0 & e^{-i \frac{g}{2} t} \end{pmatrix} \quad (10.1.27)$$

which gives the SWAP gate when $t = \pi/2g$, up to a global phase on two qubits.

$$e^{-ig \frac{\sigma_x \sigma_x + \sigma_y \sigma_y + \sigma_z \sigma_z}{2} \frac{\pi}{2g}} = e^{-i \frac{\pi}{4}} \begin{pmatrix} 1 & 0 & 0 & 0 \\ 0 & 0 & 1 & 0 \\ 0 & 1 & 0 & 0 \\ 0 & 0 & 0 & 1 \end{pmatrix}. \quad (10.1.28)$$

The readers might notice that the two-qubit gates such as CNOT and CZ gate—the controlled gate—do not appear as “natural” quantum gates of frequently used interaction Hamiltonians. Usually, these controlled gates are implemented by sequential application of the above-given two-qubit gates in combination with the single-qubit gates.

⁵ You can easily check this!

⁶ Derivation is not as straight as before. See Appendix G.

10.1.3 Clifford and Non-Clifford Gates

We shall now mention briefly about a more general aspect of the quantum gates. First we introduce the n -qubit Pauli group⁷ \mathcal{P}_n acting on an n -qubit state by

$$\mathcal{P}_n = \{ e^{i\frac{\pi}{2}\Theta} \Xi_1 \otimes \cdots \otimes \Xi_n \mid \Theta = 0, 1, 2, 3; \Xi_i = I_i, X_i, Y_i, Z_i \} \quad (10.1.29)$$

where the subscript i indicates that the operator acts on i -th qubit. Elements in \mathcal{P}_n are tensor products of n single-qubit gates with overall factors $1, i, -1$ or $-i$. Given this Pauli group, a Clifford group \mathcal{C}_n is defined as a set of unitary operations that transforms an element in a Pauli group into an element in a Pauli group. If we write all n -qubit unitaries by U_n , this definition takes the form

$$\mathcal{C}_n = \{ V \in U_n \mid V\mathcal{P}_nV^\dagger = \mathcal{P}_n \}. \quad (10.1.30)$$

For example, from $HXH = Z$, $HZH = X$ and $SXS^\dagger = Y$, the Hadamard gate H and the phase gate S are the Clifford gates. There are $6 \times 4 = 24$ elements in \mathcal{C}_1 corresponding to how we assign x and z axes on three-dimensional space. How about the two-qubit gates? For instance, we can see that $\text{CNOT}(X \otimes I)\text{CNOT} = X \otimes X$ and $\text{CNOT}(I \otimes Z)\text{CNOT} = Z \otimes Z$. These imply the CNOT gate is also a Clifford gate, and actually it is [18]! Two-qubit gates such as CNOT and CZ gates are the Clifford gates, indeed. What is the number of elements in \mathcal{C}_2 ? Counting up the number of Clifford gates is not so simple as in the case of \mathcal{C}_1 . Indeed, there are 11 520 elements in \mathcal{C}_2 and in general, \mathcal{C}_n has superexponentially larger number of elements as n increases.

Unfortunately, the celebrated Gottesman-Knill theorem states that, starting with an eigenstate of a Pauli operator, the quantum computation only with the Clifford gates is simulatable in polynomial time with the probabilistic classical computer. Furthermore, it is known that Clifford gates alone cannot produce arbitrary quantum states. Therefore, for the aim of realizing universal quantum computation that might exceed the classical computer in certain tasks, *non-Clifford* quantum gates are indispensable.⁸ Fortunately, a non-Clifford gate is already at our hand—the T gate. T gate is combined with H gate to form a gate $THHT$ which has a rotation angle of $\theta_{THHT} = 2 \arccos [\cos^2(\pi/8)]$ that is an irrational number times π . This, unlike the rational number, can cover $\text{SU}(2)$ densely and Solovay-Kitaev theorem ensures that this coverage can be done efficiently, that is, for any given rotation angles one might reach it with polynomial steps with sufficient precision. Reference [18] provides more information about above theorems.

⁷ Group is here a mathematical concept. Readers unfamiliar to this concept may refer to some literature on group theory or google it to catch a flavor.

⁸ With a magic state $|\psi_m\rangle = \cos \frac{\theta}{8}|g\rangle + \sin \frac{\theta}{8}|e\rangle$ as an initial state, one can execute the universal quantum computation only using Clifford gates.

10.2 Quantum Circuit Model

In the previous section, we took an overview of quantum gates and physical implementation of them using time evolution of interaction Hamiltonians. The quantum operations are described by operators acting on state vectors; however, it will be messy when the system scales up, that is, the number of quantum operations and controlled quantum bits increase. Thence a graphical method of representing a chunk of quantum operations is desired to facilitate the design of protocols for quantum technologies. Such a method is called quantum circuit in which quantum gates and quantum measurements are represented as boxes operating on the quantum state represented by lines incoming from the left, see Fig. 10.1. A line outgoing on the right of the quantum operation represents a resultant state, which is a quantum state for the quantum gate and a classical bit state for the quantum measurement, usually written as a double line.

Let us coin a few concrete elements of the quantum circuit. A single-qubit gate is depicted by a box and lines attached to it, with a character indicating the gate operation such as X , Y , Z , H , S , T , $R_x(\theta)$, $R_z(\theta)$, and so on. The circuit depicted in Fig. 10.1a yields the output state $X|\psi\rangle$. Since the state flows from left to right to sequentially experience the quantum gates, the quantum circuit in Fig. 10.1b results in the state $ZX|\psi\rangle$.

Next, let us take a look at a two-qubit gate, especially a Controlled-NOT gate, a CNOT gate, as an example. The CNOT gate deals with two-qubit state as an input and an output state as well. In this perspective, a way to represent it is as the one displayed in the left panel of Fig. 10.1c. Another way to represent the CNOT gate is to regard it as an X gate acting on the target qubit conditionally with the quantum states of the control qubit. This representation is visualized in the middle of Fig. 10.1c. The rightmost representation is the most frequently used one, mimicking the Boolean algebra to imply that the CNOT operation conditionally executes the flip-flop between $|g\rangle = |0\rangle$ and $|e\rangle = |1\rangle$.

The last element is the quantum measurement, whose description will be given in the next section. The quantum-circuit representation of the quantum measurement is shown in Fig. 10.1. It consists of an icon indicating the measurement and two

Fig. 10.1 Quantum circuits.

- a A single-qubit gate. b Sequential application of two quantum gates. c A two-qubit gate

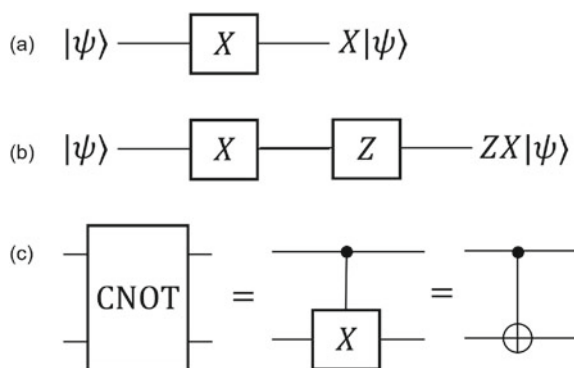


Fig. 10.2 Quantum-circuit representation of a quantum measurement



lines attached to it, one on the left side representing a qubit measured and the other indicating the classical bit information obtained by the measurement. The double line on the right is often hidden unless it is utilized for controlling other qubits (Fig. 10.2).

10.3 Measurement and Imperfections of Quantum States

10.3.1 Projective and Generalized Measurement

Measurement of a quantum state affects the measured state significantly, in general. This is the principal reason why we devote one Section to the quantum measurement, however, it is also because the proper formalism⁹ of the quantum measurement can describe the quantum states after the measurement, by which the quantum error correction has been established [18].

Suppose we have a quantum state $|\psi\rangle = \sum_i c_i |\varphi_i\rangle$ (not necessarily being a qubit here) that is subject to the measurement. The projective measurement is the one that extracts the probability $p_i = |c_i|^2$ of being in a basis state $|\varphi_i\rangle$ and leave the measured state in that basis. Let the projection operator be $P_i = |\varphi_i\rangle\langle\varphi_i|$. Projective measurement makes the state $|\psi\rangle \rightarrow P_i|\psi\rangle = c_i|\varphi_i\rangle$ without normalization, and with the normalization we have the state vector and the density matrix

$$|\psi\rangle \rightarrow \frac{P_i|\psi\rangle}{\sqrt{p_i}}, \quad (10.3.1)$$

$$\rho = |\psi\rangle\langle\psi| \rightarrow \frac{P_i|\psi\rangle\langle\psi|P_i}{p_i} \quad (10.3.2)$$

after the projective measurement. So far so good for a pure state. For a more general situation, generalized measurement should be introduced. In order to do that, Kraus operators are introduced first. Aside from the rigorous definition of the Kraus operators, it is fair to say that the Kraus operators represent how the measured quantum states end up by the measurement. For example, since the projective measurement leaves the quantum state as it is measured, $M_g = |g\rangle\langle g|$ and $M_e = |e\rangle\langle e|$ constitute the Kraus operators. Here it can be seen that the number of Kraus operator equals the number of bases of the measured system, therefore two Kraus operators M_i ($i = g, e$) are assigned to the projective measurement of the qubit. The density operator after a quantum measurement with the measurement outcome $|i\rangle$ becomes $M_i\rho M_i^\dagger$ and by

⁹ Currently thought so.

normalizing it with the probability p_i that we find the qubit in the state $|i\rangle$, we have

$$\rho \rightarrow \frac{M_i \rho M_i^\dagger}{p_i} \quad (10.3.3)$$

Another important concept is positive operator-valued measure (POVM). POVM are operators that are defined using Kraus operators as $E_i = M_i^\dagger M_i$ that satisfies $\sum_i E_i = I$. The probability p_i is written by using POVM as $p_i = \text{Tr} [M_i \rho M_i^\dagger] = \text{Tr} [E_i \rho]$. POVM coincides with the projection operators if the measurement does not include errors. Passing the details to the literature like Ref. [18], we would like to describe a simple example of measurement with errors. WIth the projection measurement, one might encounter two types of errors. One is the error that we missed the signal and the other is the one that we have counted a noise as a signal. Here we assume these two errors occur with the same probablity ϵ . Then the Kraus operators read

$$M_g = \sqrt{1 - \epsilon}|g\rangle\langle g| + \sqrt{\epsilon}|e\rangle\langle e|, \quad (10.3.4)$$

$$M_e = \sqrt{1 - \epsilon}|e\rangle\langle e| + \sqrt{\epsilon}|g\rangle\langle g|. \quad (10.3.5)$$

We shall make a brief comment on a quantum non-demolition (QND) measurement. QND measurement refers to a projective measurement that preserves the probability distribution of the measured system. In the quantum engineering community, one often measures σ_z of a target system using a probe system interacting with it. If the interaction is of type $ZZ = \sigma_z \otimes \sigma_z$, it does not affect s_z of the target state and the QND measurement is possible. In the community, QND measurement almost always refers to the measurement of σ_z using the ZZ interaction.

10.3.2 State Tomography

As mentioned previously, the density matrix of a single-qubit system is given in the form $\rho = (1/2)(I + s_x\sigma_x + s_y\sigma_y + s_z\sigma_z)$. All we have to do in identifying the quantum state is to determine the coefficients s_x , s_y and s_z . Using the fact that the Pauli matrices σ_ξ and thus their product $\sigma_\xi\sigma_\zeta$ ($\xi \neq \zeta$) are traceless and $\sigma_\xi^2 = I$, we can obtain the spin components s_ξ by using the equality $s_\xi = 2\text{Tr} [\rho\sigma_\xi]$. Then, how this can be done in actual experiments? Firstly we note that in most experiment, what we extract from the measured signal about the quantum state is the population, or in other words s_z . Other components s_x and s_y cannot be obtained from this measurement unless the measurement basis is changed. This can be done rather by rotating the Bloch vector of a qubit in order for the desired x or y component to align in z direction. For s_x measurement, first the gate $R_y(\pi/2)$ is applied to the quantum state so that the transformations $|+\rangle = (|g\rangle + |e\rangle)/\sqrt{2} \rightarrow |g\rangle$ and $|-\rangle = (|g\rangle - |e\rangle)/\sqrt{2} \rightarrow |e\rangle$ take place. That is, the x component of the Bloch vector is transformed into the z component and now the s_x is measurable with the measurement

of z component. Similarly, $R_x(\pi/2)$ gate makes $|+i\rangle = (|g\rangle + i|e\rangle)/\sqrt{2} \rightarrow |g\rangle$ and $|-i\rangle = (|g\rangle - i|e\rangle)/\sqrt{2} \rightarrow |e\rangle$, so that the s_y measurement becomes feasible by successive s_z measurement. In this manner, the quantity $\mathbf{s} = (s_x, s_y, s_z)$ is determined through multiple attempts and one acquires the complete information of the quantum state in terms of the density matrix ρ . This procedure is known as the quantum state tomography.

10.3.3 Fidelity

Once the quantum state is identified by the state tomography, one needs to evaluate how close it is to the desired state by using some quantity. A frequently used quantity for such a purpose is the fidelity. Fidelity does not fulfill the mathematical conditions of distance between quantum states. However, it yields zero for orthogonal state and 1 for identical states, so that the fidelity is frequently used as an intuitive and easy-to-calculate characteristics.

For general quantum states represented as density matrices ρ and σ , the fidelity F is defined by

$$F = \text{Tr} [\rho\sigma]. \quad (10.3.6)$$

It can be immediately seen that for identical states we have $F = \text{Tr} [\rho^2] = 1$. If the two states are orthogonal, the two states are pure states and orthogonality leads to $F = 0$. The inverse is actually true that one gets $F = 0$ only if the two quantum states are orthogonal to each other. Suppose that ρ is unknown quantum state and $\sigma = |\psi\rangle\langle\psi|$ is known. The fidelity reads

$$F = \text{Tr} [\rho|\psi\rangle\langle\psi|] = \text{Tr} [\langle\psi|\rho|\psi\rangle] = \langle\psi|\rho|\psi\rangle. \quad (10.3.7)$$

Further simplifying the above expression by assuming ρ as a pure state $\rho = |\phi\rangle\langle\phi|$, we get $F = |\langle\psi|\phi\rangle|^2$ and the fidelity is merely a squared value of the inner product of the two states.

We shall refer to the fidelity evaluated for two completely mixed states. Since the completely mixed state for a single qubit is $I/2$, the fidelity reads $F = 1/2$ by simply taking a trace of the matrix $I \otimes I/4$. The completely mixed state is a state with no coherence; however, the fidelity outputs a value of $1/2$. If we consider a many-qubit system, the completely mixed state reads $I^{\otimes n}/2^n$ and the fidelity for two such states becomes $2^n(1/2^n)(1/2^n) = 1/2^n$.

One might encounter another definition of the fidelity. Fidelity is defined above as the trace of product of density matrices; however, here we define it as a trace of square-root of product of density matrices:

$$f = \text{Tr} \left[\sqrt{\sqrt{\rho}\sigma\sqrt{\rho}} \right]. \quad (10.3.8)$$

By assuming that ρ is unknown and $\sigma = |\psi\rangle\langle\psi|$ is known, the fidelity reads $f = \text{Tr} [\sqrt{\sqrt{\rho}|\psi\rangle\langle\psi|\sqrt{\rho}}] = \sqrt{\langle\psi|\rho|\psi\rangle} \text{Tr} [|\psi\rangle\langle\psi|] = \sqrt{\langle\psi|\rho|\psi\rangle}$ using the cyclic property of the trace operation. Further assumption of $\rho = |\phi\rangle\langle\phi|$ makes $f = |\langle\psi|\phi\rangle|$, from which we can catch a flavor that f is a square-root version of F .

10.3.4 Estimation of Gate Errors

Quantum gates, such as single-qubit gates, can be implemented by applying a pulse of electromagnetic wave with a designed pulse area. However, there are many factors that the desired gate deviates from the ideal one. For example, the fluctuation of pulse duration or pulse height gives rise to the improper rotation. Or, the drifted phase would result in the improper rotation axis. Therefore, a method for the evaluation of gate errors must be developed in order to access how good the gates are. In this section, we describe such methods.

Noise Superoperators

Quantum processes can be described by applying some operator on a quantum state $|\psi\rangle$ only in the case of pure states under consideration. If one wants more general prescription applicable to the mixed state, operation on the density matrix should be dealt with. This is done by writing it as

$$\mathcal{E}(\rho) = \sum_i A_i \rho A_i^\dagger \quad (10.3.9)$$

where A_i describing the physical process is called the Kraus operator which should satisfy the conservation of probability. For example, the process described by $\mathcal{E}(\rho) = X\rho X$ corresponds to the qubit flip process¹⁰ with probability 1. In contrast to this perfect operation, realistic operation always suffers from noisy processes expressed as operations on a density matrix. This operation Λ is expressed as a “superoperator” since the noise process is an operator on a matrix, an operator as well. If a noise process flips the qubit with probability p , the noise superoperator Λ_x of the bit-flip error is

$$\Lambda_x \rho = (1 - p)\rho + pX\rho X. \quad (10.3.10)$$

When, on the other hand, the phase of the qubit is rotated by π by accident, the noise superoperator Λ_z of the phase-flip error reads

$$\Lambda_z \rho = (1 - p)\rho + pZ\rho Z. \quad (10.3.11)$$

¹⁰ See $X\rho X = X|\psi\rangle\langle\psi|X^\dagger$, which is just a density matrix of $X|\psi\rangle$.

Another typical noise is the bit-phase-flip error that is

$$\Lambda_y \rho = (1 - p)\rho + pY\rho Y. \quad (10.3.12)$$

The depolarizing error,

$$\Lambda_d \rho = (1 - p)\rho + \frac{p}{3}(X\rho X + Y\rho Y + Z\rho Z), \quad (10.3.13)$$

where all of the bit-, phase-, and bit-phase-flip noise occur, is not practical in most experiments. Nevertheless, it is occasionally used because of its symmetry that facilitates the theoretical treatment.

The spontaneous decay, often dubbed as the amplitude damping in this context, requires a bit complicated treatment. It is described by

$$\Lambda_{\text{amp}} \rho = A_0 \rho A_0^\dagger + A_1 \rho A_1^\dagger \quad (10.3.14)$$

with Kraus operators

$$A_0 = \begin{pmatrix} 1 & 0 \\ 0 & \sqrt{1-p} \end{pmatrix}, \quad A_1 = \begin{pmatrix} 0 & \sqrt{p} \\ 0 & 0 \end{pmatrix}. \quad (10.3.15)$$

The first Kraus operator A_0 represents the loss of population in $|e\rangle$, and A_1 implies it is due to the transition from $|e\rangle$ to $|g\rangle$, both of which are simultaneous processes with probability p .

Quantum Process Tomography

Quantum process tomography is, like the state tomography, a method for the complete characterization of the quantum process. The goal is to find a way to quantify how well an experimentally implemented gate resembles the ideal one. First we apply a quantum gate on a system and write this “unknown” quantum operation as a result of various noises as $\mathcal{E}(\rho) = \sum_i A_i \rho A_i^\dagger$. The unknown Kraus operators on d -dimensional Hilbert space can always be decomposed by orthogonal basis of operators as $A_i = \sum_m a_{im} E_m$, $m = 1, 2, \dots, d^2$. Plugging this into $\mathcal{E}(\rho)$, we can rewrite it as

$$\mathcal{E}(\rho) = \sum_{m,n} \chi_{mn} E_m \rho E_n^\dagger \quad (10.3.16)$$

where $\chi_{mn} = \sum_i a_{im} a_{in}^*$ is called a χ -matrix which thoroughly characterizes the unknown quantum operation in terms of a handy set of orthogonal bases, which are usually the Pauli matrices together with an identity operator.

Experimentally, first the qubit is prepared in some state ρ_j chosen out of a linearly independent set of states $\{\rho_j\}$ and the gate operation is executed on it. Then the qubit state is evaluated by state tomography to obtain an output. When this is all

done, the output state can be written as $\mathcal{E}(\rho_j) = \sum_k c_{jk} \rho_k$. Furthermore, since it can be said that, by the linear independence of ρ_j 's $E_m \rho_k E_n^\dagger = \sum_k \beta_{mnjk} \rho_k$, we have

$$\sum_k c_{jk} \rho_k = \sum_{m,n} \sum_k \chi_{mn} \beta_{mnjk} \rho_k \quad \Leftrightarrow \quad c_{jk} = \sum_{m,n} \chi_{mn} \beta_{mnjk}. \quad (10.3.17)$$

Then inverting β_{mnjk} , we achieve

$$\chi_{mn} = \sum_{j,k} \beta_{mnjk}^{-1} c_{jk}. \quad (10.3.18)$$

On the right-hand side, c_{jk} are experimentally available values through the state tomography and β_{mnjk} is given by $E_m \rho_k E_n^\dagger = \sum_k \beta_{mnjk} \rho_k$ assuming that the ρ_k is ideal. Therefore, χ -matrix can be evaluated by repetitive attempts for all ρ_k 's and the unknown quantum operation can now be completely determined. For single- and two-qubit gates the $\{E_i\}$ are respectively $\{I, X, Y, Z\}$ and $\{II, IX, \dots, YZ, ZZ\}$ hence the χ -matrices are 4×4 for single-qubit gates and 16×16 matrices for two-qubit ones.

There is one thing to note about quantum process tomography. Quantum computation proceeds firstly with state preparation, secondly the gate operation and in the end the state is measured, and sometimes the measurement result is fed back into the system by reflecting it to the gate operation. What errors the quantum process tomography senses is *the total errors throughout these procedures*. In other words, the errors given rise to in the state preparation and measurement, frequently abbreviated as SPAM error, are not separately calibrated.

Gate Fidelity

Once the gate is characterized by some means such as quantum process tomography, a measure is needed to quantify how the implemented gate generating $\mathcal{E}(\rho)$ is close to the ideal gate U which results in $U \rho U^\dagger$. One such measure seems to be

$$F'_g = \text{Tr} [U \rho U^\dagger \mathcal{E}(\rho)]$$

which reads

$$F'_g = \text{Tr} [U \rho U^\dagger \mathcal{E}(\rho)] = \text{Tr} \left[U \rho U^\dagger \sum_m \chi_m E_m \rho E_m^\dagger \right] \quad (10.3.19)$$

$$= \text{Tr} \left[U \rho \sum_m \chi_{mm} U^\dagger E_m \rho E_m^\dagger U U^\dagger \right] \quad (10.3.20)$$

$$= \text{Tr} \left[\rho \sum_m \chi_{mm} U^\dagger E_m \rho E_m^\dagger U U^\dagger U \right] \quad (10.3.21)$$

$$= \text{Tr} \left[\rho \sum_m \chi_{mm} U^\dagger E_m \rho E_m^\dagger U \right] \quad (10.3.22)$$

$$= \text{Tr} [\rho \Lambda] \quad (10.3.23)$$

where we defined the noise superoperator $\Lambda = \sum_m \chi_{mm} L_m \rho L_m^\dagger$ with $L_m = U^\dagger E_m$. If the implemented gates were ideal and $\mathcal{E}(\rho) = U \rho U^\dagger$, the quantity F'_g becomes $F'_g = \text{Tr} [\rho^2]$ and is 1 for a pure state. In practice the error comes in and even if the initial state is a pure state, the errors make the final state ends up with a mixed state, meaning that the quantity F'_g degrades to be less than 1.

One thing we should keep in mind is that the gate fidelity depends on the basis taken in the trace operation. For example, let the desired operation be a phase-flip Z gate but with small probability p it appears to be a bit-flip X gate. By taking the trace with basis set $\{|g\rangle, |e\rangle\}$ the gate fidelity is $1 - p/2 < 1$, however, with $\{(|g\rangle + i|e\rangle)/\sqrt{2}, (|g\rangle - i|e\rangle)/\sqrt{2}\}$ the gate fidelity gets 1! In order to make things straight, we should define the gate fidelity not as F'_g itself but the minimum value of it evaluated for any pure state $|\psi\rangle$:

$$F_g = \min_{|\psi\rangle} \text{Tr} [U |\psi\rangle \langle \psi| U^\dagger \mathcal{E}(|\psi\rangle \langle \psi|)]. \quad (10.3.24)$$

This allows us to avoid underestimation of the gate errors. For example, let us check with the example that the X gate is contaminated by the Z gate with probability p . F_g is calculated as

$$F_g = \min_{|\psi\rangle} \text{Tr} [X |\psi\rangle \langle \psi| X \mathcal{E}(|\psi\rangle \langle \psi|)] \quad (10.3.25)$$

$$= \min_{|\psi\rangle} \text{Tr} [\langle \psi | X [(1-p)X |\psi\rangle \langle \psi| + pZ |\psi\rangle \langle \psi| Z] X |\psi\rangle] \quad (10.3.26)$$

$$= (1-p) + p \min_{|\psi\rangle} \text{Tr} [\langle \psi | Y |\psi\rangle \langle \psi | Y |\psi\rangle] \quad (10.3.27)$$

$$= 1 - p \quad (10.3.28)$$

so that the gate fidelity is now evaluated to be $1 - p$.

Randomized Benchmarking

In the quantum process tomography, gate errors are not discriminated from the SPAM errors. Another problem is that as the number of qubit grows, the dimension of χ matrix rapidly grows and becomes hard to implement full process tomography. To mitigate these problems, a technique called randomized benchmarking is of frequent use. Randomized benchmarking has several assumptions and procedures that should be sufficed, however, the merit of this method is that the gate errors can be separately extracted from the various errors including SPAM errors.

The procedures for the randomized benchmarking are listed below.

- Initialize the qubit(s) to $|\psi_i\rangle$

- Apply randomly-chosen $l \in \mathbb{N}$ Clifford gates
- Apply a gate that inverts the above Clifford gates
- Check if the final state $|\psi_f\rangle$ is the same as the initial one

As the number of Clifford gates l increases, the error accumulates and the fidelity of the quantum states¹¹ $F = \max_{\text{all purification of } |\psi_f\rangle} |\langle\psi_f|\psi_i\rangle|^2$ decreases exponentially. Then by fitting this exponential decrease we can extract the gate fidelity in a manner discriminated from the SPAM errors!

Randomized benchmarking looks such powerful, however, there is of course a limitation that the assumption made in above argument seems to be not so relevant in the realistic experiments. The assumptions to be fulfilled are

- All noise superoperators are equally contained in every Clifford gates.
- Average gate fidelity is calculated as if the noise was the depolarizing error.
- Noises are Markovian, namely the noises are memoryless.

These assumptions, especially the first and the second ones, seem ridiculous from the experimental viewpoint. For instance, for the first point, certain quantum system is good at performing some gates but not at others. As for the second issue the modeling of error solely as the depolarizing noise does not seem to be the case, rather the spontaneous decay and dephasing are more likely to be the actual ones. The noise process is not proven to be Markovian regarding the third one, though experimentally it is fair to assume so. Nonetheless, randomized benchmarking is routinely used in obtaining the gate fidelities. One might also notice that there is always spontaneous emission that might let coverage of the state space inhomogeneous. This can be mitigated by adopting a technique called “twirling”, see literature for the detail [19].

10.4 Essential Idea of Quantum Error Correction

Qubits are always subject to the errors as well as the classical bits are. Realistic applications of quantum technologies may require numerous, say millions of, state preparations, quantum gates and measurements applied to the system, so that even if we have quantum operation of a gate fidelity 0.9999, success probability of a series of 1 000 gate operations is about 0.9, while 100 000 operations make it on the order of 10^{-5} ! Therefore, the errors of the quantum manipulations should be corrected somehow, as is routinely done in the classical information processing. In the classical information processing, the error correction can be done by preparing multiple copies of the bits and adopting majority, assuming the low error rate. In contrast, quantum

¹¹ First, any mixed states can be made pure state by attaching another qubit state. Next, for the pure states $|\psi_i\rangle$ and $|\psi_f\rangle$ the fidelity reads $F = |\langle\psi_f|\psi_i\rangle|^2$. Uhlmann's theorem states that this fidelity of the quantum states can be estimated by above equation.

error correction is not that straightforward as it should be implemented under the following conditions:

- (i) Errors are continuous in a Bloch sphere
- (ii) No-cloning theorem inhibits the simple redundancy
- (iii) Measurement destroys the quantum state

Quantum error correction elegantly avoids violating these conditions. In other words, one can “digitize” the errors and sense them to implement quantum error correction, without destroying the quantum state. A drawback is the fact that it requires redundancy by multiple qubits like the classical majority voting,¹² and the error threshold, over which the quantum error correction does not work, is somehow stringent with current technology—in other words, the fidelity of the quantum operation must be incredibly high. In this Section, we introduce some essential ideas of quantum error correction to just scratch the surface of it. More details are found in the literature [18, 20].

10.4.1 Stabilizer Formalism

Before proceeding to the error correcting codes, it is instructive to take several paragraphs about the stabilizer formalism. The stabilizer group \mathcal{S} is an Abelian, or commutable, subgroup of n -qubit Pauli group \mathcal{P}_n such that

$$\mathcal{S} = \{ S_i \mid -I \notin \mathcal{S}, [S_i, S_j] = 0 \text{ for all } S_i, S_j \in \mathcal{S} \} \leq \mathcal{P}_n. \quad (10.4.1)$$

Here “ \leq ” means that the group on the left-hand side is a subgroup of the one on the right-hand side. Since $\mathcal{S} \leq \mathcal{P}_n$, $S \in \mathcal{S}$ is an n -qubit Pauli operator possessing the eigenvalues ± 1 . A group is characterized by a generators whose products cover the entire group. The subset made of generators \mathcal{S}_g , or a generator itself, of the stabilizer group is called the stabilizer generator. By construction any generator cannot be decomposed into a product of other generators. The stabilizer group contains the stabilizer generators, $\mathcal{S} = \langle \mathcal{S}_g \rangle$, and the number of generators required to reproduce \mathcal{S} is known to be at most $\log |\mathcal{S}|$ where $|\mathcal{S}|$ denotes the order, the number of elements, of \mathcal{S} . Here comes one of the merits using stabilizer group to describe the quantum system, namely we expect economic description of quantum states using stabilizer formalism rather than writing down the bras and kets of many-qubit system explicitly.

Stabilizer operators all commute with each other by definition, hence have common eigenstates spanning the eigenspace in common as well. The common eigenstates are stabilizer states that satisfy $S_i |\psi\rangle = |\psi\rangle$ for any $S_i \in \mathcal{S}$, with the common eigenvalue $+1$. The eigenspace spanned by the stabilizer states is said to be the stabilizer subspace V_s stabilized by \mathcal{S} . There is another subspace spanned by eigenstates with the eigenvalue -1 , which are denoted by V'_s for convenience.

¹²Though it is not majority voting in quantum case.

Let us see an example with stabilizer group $\mathcal{S} = \langle\{Z_1 \cdots Z_n, X_1 \cdots X_n\}\rangle$ with even n .¹³ The stabilizer subspace is the “cat state”¹⁴

$$|\text{cat}\rangle = \frac{|g \cdots g\rangle + |e \cdots e\rangle}{\sqrt{2}}.$$

As another example, let us omit $X_1 \cdots X_n$ from the stabilizer generator and let $\mathcal{S} = \langle Z_1 \cdots Z_n \rangle$, whose stabilizer subspace is $\{|g \cdots g\rangle, |e \cdots e\rangle\}$. If one of the qubit is flipped, the states will be in the subspace spanned by $\{|eg \cdots g\rangle, |ge \cdots g\rangle, \dots, |gg \cdots e\rangle, |ge \cdots e\rangle, |eg \cdots e\rangle, \dots, |ee \cdots g\rangle\}$. Since these are eigenstates of $Z_1 \cdots Z_n$ with the eigenvalue -1 , we can see that a single-bit-flip error maps the system from V_s into V'_s , and thus this error can be detected by measuring $Z_1 \cdots Z_n$. However, we cannot tell which qubit is flipped only with this measurement. To correct the error, there are more tricks to develop the quantum error correction codes.

The quantum error correction code stands for the qubits constructed in the subspace of the n -qubit Hilbert space, and error correction codes can be neatly described by the stabilizer formalism: the logical qubit is encoded in the stabilizer subspace and the error can be sensed by the measurements of the stabilizer generators, by which the quantum state can be set back to the original one through the proper feedback operation.

10.4.2 Three-Qubit Repetition Code

There is one more step to go before the complete¹⁵ quantum error correction. We here see the three-qubit repetition code by which the bit-flip error can be detected and corrected in a manner capable of keeping the coherence of the qubit.

The stabilizer group for the three-qubit repetition code is $\mathcal{S} = \langle\{Z_1 Z_2, Z_2 Z_3\}\rangle$ and the stabilizer subspace reads $V_s = \{|ggg\rangle, |eee\rangle\}$. The logical qubit $\{|0_L\rangle, |1_L\rangle\}$ is encoded as $|0_L\rangle = |ggg\rangle$ and $|1_L\rangle = |eee\rangle$, whose logical Pauli operators are $X_L = X_1 X_2 X_3$ and $Z_L = Z_1 Z_2 Z_3$. Then, we shall see what happens and what is inferred from the measurements of the stabilizer generators. First, the measurement results of $Z_1 Z_2$ and $Z_2 Z_3$ with the states in the stabilizer subspace V_s always return $+1$ because a single Pauli-Z operator returns $+1$ for $|g\rangle$ and -1 for $|e\rangle$, and the stabilizer generators are the product of two single Pauli-Z operators. This is somewhat trivial from the definition of V_s .

Next we consider the states after the bit-flip error. If the first qubit is subject to the bit-flip error, the state $a|ggg\rangle + b|eee\rangle$ is turned into $a|egg\rangle + b|gee\rangle$. Then the measurement of $Z_1 Z_2$ returns -1 and that of $Z_2 Z_3$ returns $+1$. Readers might notice that $Z_i Z_j$ judges whether i -th and j -th qubits are in the same state ($+1$) or not (-1), justifying such a measurement as the parity measurement. By these two parity measurements, we know qubits 1 and 2 are different but 2 and 3 are the same.

¹³ More details of this example and the stabilizer formalism itself is found in Ref. [20].

¹⁴ $|\xi_1\rangle \otimes |\xi_2\rangle \otimes \cdots \otimes |\xi_n\rangle$ is denoted by $|\xi_1 \xi_2 \cdots \xi_n\rangle$.

¹⁵ Regardless of the feasibility.

Under the assumption that only one bit-flip error occurs, we can tell from this set of measurements that the first qubit is flipped and to be corrected again. This set of parity measurements is thus called the syndrome measurement and even if the bit-flip error occurs on qubit 2 or 3, the syndrome measurement can specify which qubit is bit-flipped.

The bit-flipped qubit is then flipped to bring the state back again into the stabilizer subspace, which constitutes the quantum error correction against the bit-flip error. Let us see the probability of having the correct state of qubit after the error correction. The probability of having no errors in all three physical qubits is $(1 - p)^3$ given that the single-qubit error occurs with probability p . If the error is not corrected, this contains a term linear in p . If the error is corrected, the single-bit-flip event can be corrected and the probability of having the correct state is $(1 - p)^3 + 3(1 - p)^2 p = 1 - 3p^2 + 2p^3$, where the term linear in p vanishes and when $p < 1/2$ this gives larger probability than without the error correction.

Note that the three-qubit repetition code can correct the bit-flip error; however, the phase-flip and the bit-phase-flip errors cannot be addressed in this logical-qubit encoding. If one have a stabilizer group $\mathcal{S} = \langle\{X_1X_2, X_2X_3\}\rangle$, then the code space is $\{|+++ \rangle, |---\rangle\}$ and the phase-flip error can be addressed in expense of the ability to correct the bit-flip error. Another important point is that in actual experiment, we should prepare an auxiliary qubit that is subject to the syndrome measurements.

10.4.3 Nine-Qubit Shor Code

The three-qubit repetition code is capable of correcting only the bit-flip error. Here we introduce one of the most popular codes, the nine-qubit Shor code named after Peter Shor invented it, for it affords the complete correction of single-qubit errors.¹⁶ In the nine-qubit Shor code, logical qubit is constructed as follows:

$$|0_L\rangle = \frac{(|ggg\rangle + |eee\rangle)(|ggg\rangle + |eee\rangle)(|ggg\rangle + |eee\rangle)}{2\sqrt{2}}, \quad (10.4.2)$$

$$|1_L\rangle = \frac{(|ggg\rangle - |eee\rangle)(|ggg\rangle - |eee\rangle)(|ggg\rangle - |eee\rangle)}{2\sqrt{2}}. \quad (10.4.3)$$

These are the stabilizer states of the stabilizer group

$$\begin{aligned} \mathcal{S} = &\langle\{Z_1Z_2, Z_2Z_3, Z_4Z_5, Z_5Z_6, Z_7Z_8, Z_8Z_9, \\ &X_1X_2X_3X_4X_5X_6, X_4X_5X_6X_7X_8X_9\}\rangle \end{aligned}$$

and the logical Pauli operators are

$$Z_L = X_1X_2X_3X_4X_5X_6X_7X_8X_9, \quad (10.4.4)$$

$$X_L = Z_1Z_2Z_3Z_4Z_5Z_6Z_7Z_8Z_9. \quad (10.4.5)$$

¹⁶ And it appeared as a first demonstration that the quantum computer can be, in principle, fault-tolerant.

This Shor code looks like a phase-flip code constructed by a bit-flip code. Such a code concatenation is a straightforward, powerful way to enhance the fault tolerance of the logical qubit. Actually, syndrome measurements of $Z^{\otimes 2}$ stabilizer generators, which contains two Z operators, detect the bit-flip errors in one of the three qubits in the three blocks, and syndrome measurements of two $X^{\otimes 6}$ stabilizer generators sense the phase-flip errors.

Naive thought leads us to think that in order to execute the quantum operations fault-tolerantly, that is, in the way the errors are corrected, the required gate fidelity seems not so high because no two- or more-qubit error out of nine qubits is sufficient for the error correction to work. However, in scaling up the quantum operation one might have millions of gates and errors can be distributed among the physical qubits through, say, CNOT gates and so on. This error propagation should be avoided by making the probability of the error propagation square of the error probability itself, to ultimately make the quantum operations fault-tolerant. Proper analysis shows that there is a threshold theorem [18] for a specific quantum error correction code that specifies how much error is admissible to implement the fault-tolerant quantum computations, the error threshold. It is known that with the Shor code the error threshold is on the order of 10^{-7} , just an incredibly tiny amount of errors are formidable!

10.4.4 Advanced Quantum Error Correction Codes

The nine-qubit Shor code is a relatively simple code that is not so hard to understand, however, the error threshold of $\sim 10^{-7}$ is so stringent that near-term realization is desperate given that the current best gate error achieved for the single-qubit operation of a trapped ion is just $\sim 10^{-6}$ and a few-orders-of-magnitude larger for the two-qubit gates. The error correcting code with a moderate error threshold, or that may demand less physical resources by utilizing the Fock space of a harmonic oscillator is under intensive investigation to provide less stringent forms of the fault-tolerant quantum devices. Two representatives of such are the surface code and the Gottesman-Kitaev-Preskill code.

The surface code is also called as topological code and toric code, in which a large number of physical qubits in a two-dimensional array span logical qubits. An attractive point of the surface code is its high error threshold which amounts to ~ 0.01 . It also has relation to the condensed matter physics, opening up a new application of quantum information theory to new avenue of condensed matter theory. A drawback is the number of physical qubits required for the implementation of the surface code is no less than 1 000 that imposes the currently stringent scale-up of the quantum systems. It is important to estimate how the error rate scales with the number of connected qubits and how the electrical and/or optical wirings and control units does, which are under intense investigation.

The second example of the advanced quantum error correction code, the GKP code [22], gathers attention as a way to implement a logical qubit in a Fock space of a harmonic oscillator. It utilizes quantum states represented by two-dimensional arrays of points in the phase space. The spanned logical qubit is also called GKP qubit. A point in a phase space stands for the situation that $+\infty$ -dB squeezing is

available and not realistic. Therefore, distributions with finite width aligning in a grid are generated to form approximately orthogonal two GKP qubit states. By now there are some attempts of GKP qubit generation using an oscillatory motion or phonon of a trapped ion [23] and a microwave cavity coupled to a superconducting qubit [24].

10.5 DiVincenzo Criteria

In order to assess how a quantum system is suitable for applications in quantum technologies, criteria have been coined by David P. DiVincenzo which are listed below [29]:

(i) **Scalable, well-characterized qubit**

The system should be almost always settled within a two quantum states among others. Furthermore, a numerous number of this element of qubit should be assembled together, in the scope of realistic applications.¹⁷

(ii) **Initialization of qubits to a fiducial state**

Preparation of a system in a proper subspace spanning qubits is as important as the precise operations on it. If the system cannot be initialized properly, one might start the quantum operations conditionally when they get some signal telling the completed initialization. However, this tends to be probabilistic and the “firing” events become rarer and rarer as the system size grows.

(iii) **Long coherence times¹⁸**

In the experiment, one should fight against decoherences exerted by surrounding environment, including experimental equipments. This process literally lets the quantum state “decohere” and transforms it gradually into undesired state. Quantum gates must be executed within the duration much shorter than this coherence time and the lifetime and, roughly speaking, the ratio of the gate pulse duration to the coherence time gives the estimation of the gate fidelity.

(iv) **A universal gate set**

Universal gate set is given by arbitrary single-qubit gates, necessarily including at least one non-Clifford gate, and two-qubit gates. Single-qubit gates require phase-coherent, individual control of physical qubits, while the two-qubit gates are usually implemented by some coherent interaction between physical qubits.

(v) **A qubit-specific measurement capability**

A physical qubit can usually be measured by a projective measurement and pro-

¹⁷ Sloppy estimation: if a single logical qubit is spanned by thousands of physical qubits and one desires to factorize a thousand-digit number by Shor’s algorithm executed fault-tolerantly, then thousands of logical qubits are required and millions of physical qubits should be integrated into the system.

¹⁸ or “decoherence times”.

jective measurement combined with single-qubit Pauli gates enables the state tomography.

(vi) **Interconversion between stationary and flying qubits and faithful transmission of flying qubits**

This criterion together with former five criteria constitutes the necessary conditions for the construction of quantum networks [25].

Problems

Problem 10-1 Verify Eq. (10.1.2).

Problem 10-2 Show that $Y = SX S^\dagger$ holds.

Problem 10-3 Derive the matrix representation of YY and ZX gates.

Problem 10-4 Calculate explicitly the resultant two-qubit state by the quantum circuit shown in Fig. 10.3.

Problem 10-5 What are the Kraus operators for the luminescence measurement, where one measures whether a photon is detected or not to determine the two-level system was in its excited or ground states, respectively? Is the luminescence measurement projective one?

Problem 10-6 In the quantum process tomography, how many matrix elements do you have to determine for an n -qubit system?

Problem 10-7 In the randomized benchmarking, we should invert the quantum operations in the last sequence. How many gates are needed for such an inversion?

Problem 10-8 Discuss how the random errors and coherent errors can be detected in the randomized benchmarking. The random error refers to the random fluctuation of the rotation angle of the quantum gate and coherent one does to a fixed glitch of the rotation angle.

Problem 10-9 What states are generated by the quantum circuits shown in Fig. 10.4?

Problem 10-10 Show that the quantum circuit in Fig. 10.5 encodes $|\psi\rangle$ into the logical qubit of the Shor code. Furthermore, find out how to decode the logical state of the Shor code.

Fig. 10.3 Quantum circuit with a Hadamard gate and a CNOT gate

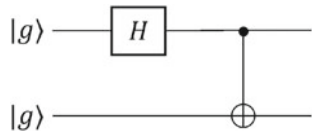


Fig. 10.4 Quantum circuits with different input states

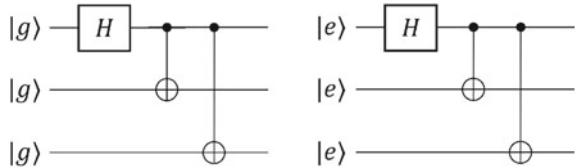
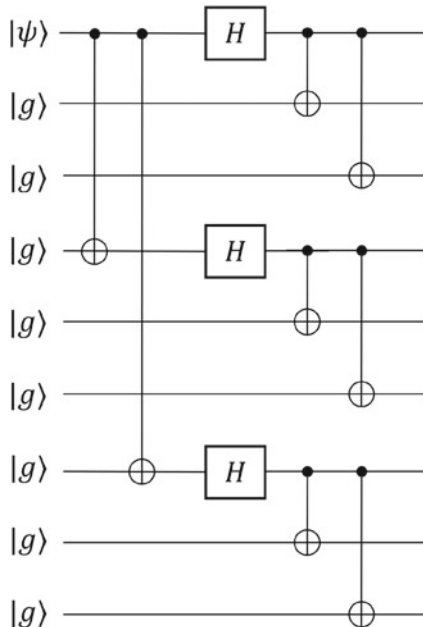


Fig. 10.5 Quantum circuit for Shor encoding





In this chapter, we will introduce some of the applications that can be realized by the quantum technologies described so far.

11.1 Quantum Computer

By using quantum systems, it is possible to perform certain kinds of computational tasks at a speed overwhelming the classical computer. A quantum computer is a device that implements such tasks. Qubits play the role of fundamental information carriers in quantum computation. As we have seen, the output of the projective measurement on a qubit is a discrete number, 0 or 1. Although these values tell us the output of the quantum computation, the qubit is in superposition states during calculation and has essentially analog information in the form of complex coefficients of them. In this sense, quantum computation is very different from the conventional digital computation.

All physical manipulations have finite errors, therefore, errors cannot be avoided in the actual quantum computers. These of error are not unique to the quantum world and the conventional digital computers also suffer from them. However, the errors become a larger issue, especially for quantum computation due to the analog nature of qubits. Even if the errors are tiny, they accumulate with each operation, and making the final output unreliable. In a large-scale quantum computation, which could be considered as a huge quantum interferometer, a very small error will propagate and change the output result. To solve this problem, a quantum computation with error correcting capability, as current digital computations operate under a finite error, is being considered. This is called error-tolerant (digital) quantum computation, achieved by correcting the state of the qubit and the errors in each operation by quantum error correction. When the various quantum operations are performed with a error rate less than a certain threshold, the quantum error correction enables the execution of quantum algorithm without being affected by imperfections in the quantum operations.

The quantum error correction will definitely be a game changer, however, the hardware demand is still high and would take some time to perform a large-scale quantum error correction. Mean while analog quantum computation, in which computation is performed under accumulating errors, has also been studied. The analog quantum computer such as quantum annealing [33] and NISQ (Noisy Intermediate-Scale Quantum) [34] computer, are capable of sampling problems and evaluation and the characteristics on of the ground state of some physical system that are difficult to calculate with the current state-of-the-art classical super computer. These analog quantum computers, outputs the computation results without constructing a huge quantum interferometer.

11.1.1 Grover's Algorithm

We introduce Grover's quantum search algorithm as an example of the quantum algorithm.

Consider the problem of determining integer x_0 for a function f as

$$f(x) = \begin{cases} 1 & x = x_0 \\ 0 & x \neq x_0, \end{cases} \quad (11.1.1)$$

where $x = 0, 1, \dots, 2^n - 1$ is the integer expressed by n bits. We can find x_0 by brute force, substituting all number from 0 for x until function f returns 1. It requires $2^n/2$ trials on average, and $2^n - 1$ times in the worst case.

Here we consider the case of $n = 2$ for simplicity. The Grover's algorithm searches x_0 with only a single trial. We define operators \hat{U} and \hat{W} acting on $|x\rangle$ as

$$\hat{U}|x\rangle = \exp(if(x)\pi)|x\rangle = \begin{cases} -|x\rangle & x = x_0 \\ |x\rangle & x \neq x_0 \end{cases} \quad (11.1.2)$$

$$\hat{W}|x\rangle = \begin{cases} -|0\rangle & x = 0 \\ |x\rangle & x \neq 0. \end{cases} \quad (11.1.3)$$

Note that, only \hat{U} depends on the function f .

These two operators and the Hadamard gate act on the initial state $|0, 0\rangle$ in turn, so that

$$\hat{H}^{\otimes 2}\hat{W}\hat{H}^{\otimes 2}\hat{U}\hat{H}^{\otimes 2}|0, 0\rangle = |x_0\rangle, \quad (11.1.4)$$

where $\hat{H}^{\otimes 2}$ expresses the simultaneous operations of Hadamard gates on both qubits. We get integer x_0 by measuring the final state $|x_0\rangle$. We need only one \hat{U} operator to find x_0 , which is smaller than the number of trials that classical calculations needs to be done. For general n qubit case and more details, please refer to Reference [18].

11.1.2 Phase Estimation Algorithm

Controlled Unitary Operations
Suppose we want to find the eigenvalues of a unitary operator \hat{U} .¹

The controlled unitary operation with a unitary operator \hat{U} can be formed as

$$\hat{U}_c = |0\rangle_c \langle 0| \hat{U} + |1\rangle_c \langle 1| \hat{U}. \quad (11.1.5)$$

Consider this controlled unitary operation is performed on a initial state

$$|\psi_{\text{in}}\rangle = \frac{1}{\sqrt{2}} (|0\rangle_c + |1\rangle_c) |u_k\rangle, \quad (11.1.6)$$

where $|u_k\rangle$ is the eigenstate of the operator \hat{U} and its eigenvalue is u_k . The output state is

$$\hat{U}_c |\psi_{\text{in}}\rangle = \frac{1}{\sqrt{2}} (|0\rangle_c + \exp(iu_k) |1\rangle_c) |u_k\rangle. \quad (11.1.7)$$

The eigenvalue u_k is imparted in the phase of the control qubit. We can determine these eigenvalues u_k by measuring the phase of the control qubit with the quantum state tomography.

Accuracy

Since each measurement on a single qubit returns only “0” or “1”, it is necessary to obtain the expectation value of many measurements.

Suppose the each trial are independent, the accuracy of phase estimation, $\Delta\phi$ is calculated by a binomial distribution as

$$\Delta\phi \propto 1/\sqrt{N}, \quad (11.1.8)$$

where N is the number of the measurement. The number of measurements needs to be increased by two digits to improve the accuracy by one digit, and an exponentially large number of measurements is required for the large number of digits of the phase to be obtained.

Phase Estimation Algorithm

In a phase estimation algorithm, the number of control qubits used determines the number of digits of the eigenvalue you would like to calculate. The j -th control qubit control the unitary operator $\hat{U}_{(j)}^{2^j}$ to the target qubits. This leads

$$\hat{U}_{(j)}^{2^j} \frac{1}{\sqrt{2}} (|0\rangle_j + |1\rangle_j) |u_k\rangle = \frac{1}{\sqrt{2}} \left(|0\rangle_j + \exp(2^j i u_k) |1\rangle_j \right) |u_k\rangle. \quad (11.1.9)$$

¹ For example, from the eigenvalues of the time evolution operator $\hat{U}_t = \exp(-it\hat{H}/\hbar)$, the energy eigenvalues are obtained. Here, \hat{H} is the Hamiltonian of the system.

Performing these controlled operators to all control qubits, the final state is obtained as

$$\hat{U}_{(0)}^{2^0} \hat{U}_{(1)}^{2^1} \cdots \hat{U}_{(N-1)}^{2^{N-1}} \frac{1}{\sqrt{2^N}} (|0\rangle_0 + |1\rangle_0) \cdots (|0\rangle_{N-1} + |1\rangle_{N-1}) |u_k\rangle = \frac{1}{\sqrt{2^N}} (|0\rangle_0 + \exp(iu_k)|1\rangle_0) \cdots (|0\rangle_{N-1} + \exp(2^nu_k)|1\rangle_{N-1}) |u_k\rangle \quad (11.1.10)$$

where N is the number of control qubits. The eigenvalues are written into the phase of the control bits, digit by digit. There are two methods for extracting the information of each digit: quantum state tomography and quantum inverse Fourier transform. As in the previous section, the quantum state tomography method estimates the state of the qubit that represents each digit and measures the phase. Unlike the previous section, the number of measurements required for tomography is constant regardless of the number of digits, since each digit of the eigenvalue expressed as a binary number can be obtained from the estimation of each qubit.

Quantum Fourier transform is an unitary operation,

$$|j\rangle \rightarrow \frac{1}{\sqrt{N}} \sum_{k=0}^{N-1} \exp(2\pi i j k / N) |k\rangle. \quad (11.1.11)$$

Here, $|j\rangle$ express the quantum state of N qubit system such as

$$|j\rangle = |j_1, j_2, \dots, j_N\rangle \quad (j = j_1 2^{N-1} + j_2 2^{N-2} + \dots + j_N 2^0). \quad (11.1.12)$$

With a little algebra, this definition of the quantum Fourier transformation leads to following expression [18],

$$|j\rangle \rightarrow \frac{1}{\sqrt{2^N}} (|0\rangle_0 + \exp(2\pi i j / 2^1) |1\rangle_0) \cdots (|0\rangle_{N-1} + \exp(2\pi i j / 2^N) |1\rangle_{N-1}). \quad (11.1.13)$$

Comparing this equation and Eq. (11.1.10), we can see the eigenvalue will be written in the state of the control qubits through the reverse quantum Fourier transformation.

These methods require the preparation of number of qubits enough to obtain the precision that we want. The algorithm also require number of measurements which does not grow exponential with respect to the number of digits (qubits) required.

11.1.3 Shor's Algorithm

An application of the phase estimation algorithm is Shor's algorithm for prime factorization. Consider an operator that performs the following operation on an input bitstring x ,

$$\hat{U}_{\text{shor}} |x\rangle = |yx \bmod N\rangle. \quad (11.1.14)$$

Table 11.1 Encoding for BB84

	0	1
A. linear	Horizontal	Vertical
B. inclined	+45 degree	-45 degree

This operator is unitary and the order $r (> 0)$ is the minimum integer, which following equation will satisfy,

$$\hat{U}_{\text{shor}}^r |x\rangle = |y^r x \bmod N\rangle = |x \bmod N\rangle. \quad (11.1.15)$$

The phase estimation algorithm for the operator \hat{U}_{shor} finds the order r and the result can be used for the prime factorization. For more details, please refer to Reference [18].

11.2 Quantum Key Distribution

In the quantum mechanics, successive measurements of non-commutable operators induce the backaction and make outputs probabilistic. For example, when we measure the $|0\rangle$ state in Z basis, the output is always 0. On the other hand, we add a measurement with X basis before that, the outputs become 0 and 1 with a probability of 50 % for each output. Using this feature of the quantum world, we can share the secret key for detecting a wiretap. This technique is called quantum key distribution (QKD) [35]. These shared secret keys are useful for secure cryptography. The first QKD protocol (BB84) was proposed by Charles Bennett and Gilles Brassard in 1984 [7].

11.2.1 BB84

In BB84, we use the polarization of photons is used for the encoding in two different ways expressed in Table 11.1.

A sender creates a set of random numbers and sends a series of randomly encoded photons to the receiver using method A or method B for each data. A set of random numbers and their encoding methods should be recorded one by one by the sender. The receiver detects the polarization of photons with method A or B, which is randomly chosen. The output of the measurements and their basis should be recorded.

If the method on the sender and the receiver is matched, the output on the receiver must be the same as the sender's bit. If not, the output of the receiver is completely random, because the linear polarization state is the superposition of the two inclined linear polarization states like

$$|H\rangle = \frac{1}{\sqrt{2}} (|+45\rangle + |-45\rangle). \quad (11.2.1)$$

To check whether there is a wiretap in the communication channel or not, the receiver randomly picks up some of the measured results and sends the results and their methods to the sender over a classical insecure channel. The sender checks the correlation between the sent data and the receiver's results only for trials where the methods were identical between them. If someone peeks at the photon to wiretap a communication, the state of the photon changes according to the result of someone's measurement and breaks the correlation between the data. The sender can know by the correlation whether the photon has been peeked at or not. If the correlations are perfect, the rest of the data can be shared with secret keys.

11.3 Quantum Sensing

A method of precisely measuring an object using a quantum system is called quantum sensing [36]. In quantum sensing, quantum technologies such as quantum state manipulation and quantum measurement are used to construct a sensor. The typical examples of the currently used quantum sensors are the following:

- Color center in a diamond (NV center) [37,38]
- Superconducting quantum interference device [39–41]
- Atomic gas [42–44]
- Cavity optomechanics [45,46]

In many quantum sensing methods, a shift of the resonant frequency of the quantum systems are measured. For example, from the shift of the resonant frequency of the spin, we can sense the magnetic field. Ramsey interference is one of the most widely used methods to precisely measure the frequency change using quantum coherence.

11.3.1 Ramsey Interference

The frequency shift $\delta\omega$ induces Z rotation to a qubit and corresponds to the operation as

$$\hat{U}_{\text{shift}} = \exp\left(\frac{\delta\omega t}{2}\hat{\sigma}_z\right), \quad (11.3.1)$$

where t is the interaction time and $\hat{\sigma}_z$ is the Pauli operator of the z component.

The Ramsey interferometer consists of successive $\pi/2$ X-rotations and the operator \hat{U}_{shift} between them. The output state of the interferometer is

$$|\psi\rangle = R_x(\pi/2)\hat{U}_{\text{shift}}R_x(\pi/2)|0\rangle, \quad (11.3.2)$$

and the probability for the 0 state of the output state is

$$p_0 = |\langle 0 | \psi \rangle|^2 = \cos^2 \frac{\delta\omega t}{2}. \quad (11.3.3)$$

This leads to frequency detection and senses the external field. Note that, the probability becomes most sensitive for the frequency shift at the condition of $\delta\omega t/2 = \pi/4$.

Since the measurement of the quantum state outputs only 0 or 1, the measurement results have statistical fluctuations. The frequency shift proportional to the probability of the final state and the fluctuation of the measurement at the condition of $\delta\omega t/2 = \pi/4$

$$\Delta\omega \propto \Delta p_0 \geq \frac{\Delta N_{\text{bin}}}{N} = \frac{1}{2\sqrt{N}}, \quad (11.3.4)$$

where N is the number of measurements and ΔN_{bin} is the statistical fluctuation of the binomial distribution. This precision limit is called a projection noise limit or shot noise limit [36].

11.3.2 Quantum Sensing with Entanglement

Entanglement can be used to improve the metrological sensitivity. As described in the previous section, N independent measurements improve sensitivity by \sqrt{N} . This can be achieved by making N measurements in succession, or it can also be achieved by increasing the number of qubits to N qubits. When these N qubits are independent, the sensitivity increases by the same amount as simply making N measurements, or \sqrt{N} . However, when the N qubits are not independent, or other words correlated in some special way it may be possible to make measurements that exceed the sensitivity of \sqrt{N} . In the following, we will discuss such ultra-sensitive measurements.

Here we consider a following entangle state of n qubit system,

$$|\psi\rangle = \frac{1}{\sqrt{2}}(|111\dots 1\rangle + |000\dots 0\rangle). \quad (11.3.5)$$

When the n qubits are subject to the perturbation causing the same frequency shifts, the probability of the $|00\dots 0\rangle$ state is

$$p_{00\dots 0} = \langle 0| R_x(\pi/2)^{\otimes n} \hat{U}_{\text{shift}}^{\otimes n} R_x(\pi/2)^{\otimes n} |0\rangle = \cos^2 \frac{n\delta\omega t}{2}. \quad (11.3.6)$$

The sensitivity for frequency measurement is enhanced by n times;

$$\Delta\omega \propto \frac{\Delta p_{00\dots 0}}{n} \geq \frac{\Delta N_{\text{bin}}}{nN} = \frac{1}{2n\sqrt{N}}. \quad (11.3.7)$$

This shows that for large n , quantum sensing can be more sensitive than sensors using n independent qubits. This limitation is called Heisenberg limit [36].

11.4 Quantum Simulation

In theoretical physics, simulation of the physical systems are performed to understand and predict physical phenomena. In many cases, the simulations are done by digital computer, but the complexity of the quantum system increases exponentially with the number of particles because of the superposition nature of the quantum world. Even a handful of particles require a supercomputer to simulate [58].

Therefore, in order to simulate complex quantum behaviors, we prepare an ideal quantum system to model the system. We examine the behavior of the model system instead of the actual system. This type of calculation method is called quantum simulation [47,48]. Quantum simulations of several models such as the Hubbard model and the Heisenberg model of spin have been reported experimentally [59,60] as well as observations of their quantum phase transitions.

There are not only quantum simulations that actually create the corresponding quantum system, but also quantum simulations that calculate time evolution and energy eigenstates on the quantum computer. These algorithms, such as quantum chemical calculations, have been actively studied in recent years as an application for NISQ computers.

11.5 Quantum Internet

The Internet has become an indispensable part of our daily lives, either directly or indirectly. Just as the Internet connects our information devices, we can think about networks that connect quantum devices. When we think of a network that combines various quantum technologies such as quantum computers, quantum sensors, and quantum key delivery, it is important to realize a quantum network that allows the exchange of quantum states as a communication channel. Such a system consisting of an entire quantum network is called a quantum Internet [52]. In the quantum internet, more powerful quantum functions will emerge, such as cloud-based quantum computation [53], quantum secret computation [61], quantum dense coding communication [62,63], and increased sensitivity of quantum sensors [54,55]. The quantum internet will require ultimate quantum technologies such as quantum media conversion from photons to spins, spins to microwaves, etc., [49–51] and quantum error correction. These technologies are currently only at the proof-of-principle level and will require the realization of a test bed and a high-performance interface that can accommodate the different environments and time scales of individual quantum systems.

Because of the loss of communication channel, signal repeaters are installed even in the classical communication. The repeaters placed at some distance amplify the optical signal and compensate for the loss. However, the quantum information cannot be amplified and relayed because of a property in quantum mechanics called *no cloning theorem*, which claims that quantum information cannot be copied without noise. Instead of installing the amplifier, the entanglement swapping [56,57] and quantum teleportation [4,5] play an important role for the quantum repeaters. By the

quantum teleportation, the quantum state can be transferred to a remote place without loss with an entangled pair and lossy classical channel. Remote entangled pairs will be prepared by the entanglement swapping technique. The interested readers might refer to the Appendix I for detailed explanations.

Position and Momentum Representations

A

In the Dirac notation using bras and kets, a quantum state is represented by a ket vector $|\Psi\rangle$ as long as it is a pure state. Indeed, this is a more abstract representation of the quantum state than the wavefunction like $\Psi(q)$,¹ since the state vector $|\Psi\rangle$ is defined as an object that yields the wavefunction $\Psi(q)$ in the position representation and $\Psi(p)$ in the momentum representation. Such position and momentum representations are of frequent use and let us quickly summarize the basic properties here.

First, let the eigenstate of the position operator \hat{q} be $|q\rangle$, with its eigenvalue being q :

$$\hat{q} |q\rangle = q |q\rangle. \quad (\text{A.1})$$

In the same manner, we define the eigenvector $|p\rangle$ and eigenvalue p for the momentum operator \hat{p} as

$$\hat{p} |p\rangle = p |p\rangle. \quad (\text{A.2})$$

Then the position and momentum representations of the quantum state $|\Psi\rangle$, respectively, read

$$\Psi(q) = \langle q | \Psi \rangle, \quad \Psi(p) = \langle p | \Psi \rangle \quad (\text{A.3})$$

which result in wavefunctions as functions of position and momentum, respectively. $|q\rangle$ ($|p\rangle$) forms a basis set with continuous variable, so that the completeness relations are dictated as

$$\int dq |q\rangle \langle q| = \hat{1}, \quad \int dp |p\rangle \langle p| = \hat{1}. \quad (\text{A.4})$$

¹ Position and momentum are, respectively, denoted by q and p in this appendix.

Wavefunctions $\Psi(p)$ and $\Psi(q)$ can be derived from each other by the Fourier transformation

$$\langle q | \Psi \rangle = \frac{1}{\sqrt{2\pi\hbar}} \int dp e^{ipq/\hbar} \langle p | \Psi \rangle \quad (\text{A.5})$$

and on the other hand, by sandwiching $\int dp |p\rangle \langle p| = \hat{1}$ by $\langle q |$ and $|\Psi\rangle$ we obtain

$$\langle q | \Psi \rangle = \int dp \langle q | p \rangle \langle p | \Psi \rangle. \quad (\text{A.6})$$

If we compare this with Eq. (A.5), we see that

$$\langle q | p \rangle = \frac{1}{\sqrt{2\pi\hbar}} e^{ipq/\hbar}, \quad (\text{A.7})$$

namely the position representation of the momentum eigenvector $|p\rangle$ results in a plane wave, or equivalently the state with definite momentum. This is a physically trivial result, however, above equality is useful in many calculations such as in Sect. 6.5.

Unitary Transformation to a Rotating Frame

B

It is often preferable to analyze the dynamics of the system in the “frame” rotating at the driving frequency. The unitary transformation that let the frame rotating at the driving frequency ω_d is given by $U(t) = \exp[i(\mathcal{H}_s(\omega_d)/\hbar)t]$ with the system Hamiltonian. A state vector $|\psi\rangle$ is transformed as $|\phi\rangle = U(t)|\psi\rangle$ and the Schrödinger equation for $|\phi\rangle$ reads

$$i\hbar \frac{d|\phi\rangle}{dt} = i\hbar \frac{dU}{dt} |\psi\rangle + i\hbar U \frac{d|\psi\rangle}{dt} \quad (\text{B.1})$$

$$= i\hbar \dot{U} |\psi\rangle + U \mathcal{H} |\psi\rangle \quad (\text{B.2})$$

$$= i\hbar \dot{U} U^\dagger |\phi\rangle + U \mathcal{H} U^\dagger |\phi\rangle \quad (\text{B.3})$$

$$= (U \mathcal{H} U^\dagger - i\hbar U \dot{U}^\dagger) |\phi\rangle \quad (\text{B.4})$$

where an identity $0 = d(UU^\dagger)/dt = \dot{U}U^\dagger + U\dot{U}^\dagger$ is used. \mathcal{H} is an original Hamiltonian and the above equation indicates that the transformed Hamiltonian is given by

$$\mathcal{H}' = U \mathcal{H} U^\dagger - i\hbar U \dot{U}^\dagger. \quad (\text{B.5})$$

First example is a simple harmonic oscillator with $\mathcal{H} = \hbar\omega_c a^\dagger a$ transformed by $U(t) = \exp[i\omega a^\dagger a t]$ which is defined by the Taylor series of the operator. Since the operator in the exponent commutes with the Hamiltonian, so $U(t)$ does. This greatly simplifies the transformation of the Hamiltonian: $U \mathcal{H} U^\dagger = UU^\dagger \mathcal{H} = \mathcal{H}$ and thus

$$\mathcal{H}' = \mathcal{H} - i\hbar U \dot{U}^\dagger = \hbar\omega_c a^\dagger a - i\hbar U(-i\omega a^\dagger a)U^\dagger \quad (\text{B.6})$$

$$= \hbar(\omega_c - \omega)a^\dagger a \quad (\text{B.7})$$

$$= \hbar\Delta_c a^\dagger a. \quad (\text{B.8})$$

In a very similar way, we can transform $\mathcal{H} = \hbar\omega_a\sigma_z/2$ by $U(t) = \exp[i\omega(\sigma_z/2)t]$ to get the one in the rotating frame $\mathcal{H}' = \hbar\Delta_a\sigma_z/2$ with the detuning being defined by $\Delta_a = \omega_a - \omega$.

Now let us deal with a second example, the Jaynes–Cummings Hamiltonian

$$\mathcal{H}_{\text{JC}} = \frac{\hbar\omega_a}{2}\sigma_z + \hbar\omega_c a^\dagger a - i\hbar g(\sigma_+ a - a^\dagger \sigma_-). \quad (\text{B.9})$$

We can rotate the frame by the unitary transformation $U(t) = e^{i\omega\sigma_z t/2 + i\omega a^\dagger a t} = U_1(t)U_2(t)$, where $U_1(t) = \exp[i\omega\sigma_z t/2]$ and $U_2(t) = \exp[i\omega a^\dagger a t]$. Since a 's and σ 's commute, the first two terms in the Jaynes–Cummings Hamiltonian are transformed into $\hbar\Delta_a\sigma_z/2 + \hbar\Delta_c a^\dagger a$. However, the transformation of the interaction term is not as straightforward as these two terms. To execute the calculation, Baker–Campbell–Hausdorff formula

$$e^{-S} H e^S = H + [H, S] + \frac{1}{2!} [[H, S], S] + \frac{1}{3!} [[[H, S], S], S] + \dots \quad (\text{B.10})$$

is useful. Another useful tools are the commutation relations $[a^\dagger a, a] = -a$, $[a^\dagger a, a^\dagger] = a^\dagger$ and $[\sigma_z, \sigma_\pm] = \pm 2\sigma_\pm$. Aided by these, let us transform the interaction part with $U_2(t)$ first and proceed step by step.

$$U_2(t)(\sigma_+ a - a^\dagger \sigma_-)U_2^\dagger(t) \quad (\text{B.11})$$

$$= e^{i\omega a^\dagger a t}(\sigma_+ a - a^\dagger \sigma_-)e^{-i\omega a^\dagger a t} \quad (\text{B.12})$$

$$= (\sigma_+ a - a^\dagger \sigma_-) + [(\sigma_+ a - a^\dagger \sigma_-), -i\omega a^\dagger a t] \quad (\text{B.13})$$

$$+ \frac{1}{2!} [[(\sigma_+ a - a^\dagger \sigma_-), -i\omega a^\dagger a t], -i\omega a^\dagger a t] + \dots \quad (\text{B.14})$$

$$= (\sigma_+ a - a^\dagger \sigma_-) + (-i\omega t)(\sigma_+ a + a^\dagger \sigma_-) \quad (\text{B.15})$$

$$+ \frac{(-i\omega t)^2}{2!}(\sigma_+ a - a^\dagger \sigma_-) + \frac{(-i\omega t)^3}{3!}(\sigma_+ a + a^\dagger \sigma_-) + \dots \quad (\text{B.16})$$

$$= \left[1 + (-i\omega t) + \frac{(-i\omega t)^2}{2!} + \frac{(-i\omega t)^3}{3!} + \dots \right] \sigma_+ a \quad (\text{B.17})$$

$$- \left[1 - (-i\omega t) + \frac{(-i\omega t)^2}{2!} - \frac{(-i\omega t)^3}{3!} + \dots \right] a^\dagger \sigma_- \quad (\text{B.18})$$

$$= e^{-i\omega t}\sigma_+ a - e^{i\omega t}a^\dagger \sigma_-. \quad (\text{B.19})$$

Now these resultant terms are transformed by $U_1(t)$ as follows, and you will observe that everything will end up with a really nice (or boring) result!

$$U_1(t)(e^{-i\omega t}\sigma_+ a - e^{i\omega t}a^\dagger \sigma_-)U_1^\dagger(t) \quad (\text{B.20})$$

$$= e^{i\omega\sigma_z t/2}(e^{-i\omega t}\sigma_+ a - e^{i\omega t}a^\dagger \sigma_-)e^{-i\omega\sigma_z t/2} \quad (\text{B.21})$$

$$= e^{-i\omega t}a \left(e^{i\omega\sigma_z t/2}\sigma_+ e^{-i\omega\sigma_z t/2} \right) - e^{i\omega t}a^\dagger \left(e^{i\omega\sigma_z t/2}\sigma_- e^{-i\omega\sigma_z t/2} \right). \quad (\text{B.22})$$

Noting that

$$e^{i\omega\sigma_z t/2}\sigma_{\pm}e^{-i\omega\sigma_z t/2} = \sigma_{\pm} + \left[\sigma_{\pm}, -i\frac{\omega\sigma_z t}{2} \right] + \frac{1}{2!} \left[\left[\sigma_{\pm}, -i\frac{\omega\sigma_z t}{2} \right], -i\frac{\omega\sigma_z t}{2} \right] \quad (\text{B.23})$$

$$+ \frac{1}{3!} \left[\left[\left[\sigma_{\pm}, -i\frac{\omega\sigma_z t}{2} \right], -i\frac{\omega\sigma_z t}{2} \right], -i\frac{\omega\sigma_z t}{2} \right] + \dots \quad (\text{B.24})$$

$$= \sigma_{\pm} \mp (-i\omega t)\sigma_{\pm} + \frac{1}{2!}(-i\omega t)^2\sigma_{\pm} \mp \frac{1}{3!}(-i\omega t)^3\sigma_{\pm} + \dots \quad (\text{B.25})$$

$$= e^{\pm i\omega t}\sigma_{\pm}, \quad (\text{B.26})$$

we have the interaction part in the rotating frame as

$$U_1(t)U_2(t)(-i\hbar g)(\sigma_+a - a^\dagger\sigma_-)U_2^\dagger(t)U_1^\dagger(t) \quad (\text{B.27})$$

$$= U_1(t)(-i\hbar g)(e^{-i\omega t}\sigma_+a - e^{i\omega t}a^\dagger\sigma_-)U_1^\dagger(t) \quad (\text{B.28})$$

$$= -i\hbar g(\sigma_+a - a^\dagger\sigma_-) \quad (\text{B.29})$$

which is totally the same form as the one before the transformation. Therefore, the Jaynes–Cummings Hamiltonian in the rotating frame is finally represented as

$$\mathcal{H}'_{\text{JC}} = \frac{\hbar\Delta_a}{2}\sigma_z + \hbar\Delta_c a^\dagger a - i\hbar g(\sigma_+a - a^\dagger\sigma_-). \quad (\text{B.30})$$

Extraction of a Two-Level System from a Three-Level System



Let us start from a Hamiltonian of a three-level system $\{|g\rangle, |e\rangle, |r\rangle\}$ where the two transitions $|g\rangle \leftrightarrow |r\rangle$ and $|e\rangle \leftrightarrow |r\rangle$ are considered (Fig. C.1). The Hamiltonian reads

$$\mathcal{H} = \hbar\omega_g |g\rangle \langle g| + \hbar\omega_e |e\rangle \langle e| + \hbar\omega_r |r\rangle \langle r| \quad (\text{C.1})$$

$$+ \hbar g_1 (|r\rangle \langle g| a_1 + |g\rangle \langle r| a_1^\dagger) + \hbar g_2 (|r\rangle \langle e| a_2 + |e\rangle \langle r| a_2^\dagger) \quad (\text{C.2})$$

and by the coherent driving we justify the replacement $a_1 \rightarrow \alpha_1 e^{-i(\omega_r - \omega_g + \delta_1)t}$ and $a_2 \rightarrow \alpha_2 e^{-i(\omega_r - \omega_e + \delta_2)t}$.² On these rotating frames, that is, $|g\rangle \langle g|$ at $\omega_r - \omega_g + \delta_1$ and $|e\rangle \langle e|$ at $\omega_r - \omega_e + \delta_2$, we get, by denoting $g_i \alpha_i$ as Ω_i ($i = 1, 2$),

$$\mathcal{H}' = \hbar\delta_1 |g\rangle \langle g| + \hbar\delta_2 |e\rangle \langle e| + \hbar\Omega_1 (|r\rangle \langle g| + |g\rangle \langle r|) + \hbar\Omega_2 (|r\rangle \langle e| + |e\rangle \langle r|) \quad (\text{C.3})$$

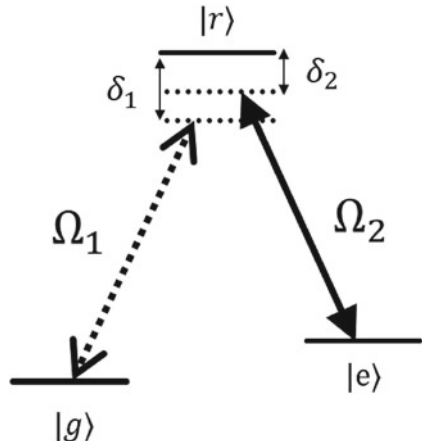
where results in Appendix B is used and the overall energy-shift $\hbar\omega_r I$ is ignored. What we want to do is to adiabatically eliminate the electronic excited state $|r\rangle$ and make a two-level system by the electronic ground states $|g\rangle$ and $|e\rangle$ whose lifetimes are long, usually infinitely, but the transition is dipole-forbidden. To do this, here the Schrieffer–Wolff transformation is executed with $S = -(\Omega_1/\delta_1)(|r\rangle \langle g| - |g\rangle \langle r|) - (\Omega_2/\delta_2)(|r\rangle \langle e| - |e\rangle \langle r|)$ (see Appendix F). This transformation partially diagonalizes the Hamiltonian and we have, up to first order in Ω_i/δ_i ,

$$\mathcal{H}'_{eff} = \hbar \left(\delta_1 + \frac{\Omega_1^2}{\delta_1} \right) |g\rangle \langle g| + \hbar \left(\delta_2 + \frac{\Omega_2^2}{\delta_2} \right) |e\rangle \langle e| \quad (\text{C.4})$$

$$+ \hbar \left(\frac{\Omega_1 \Omega_2}{2\delta_1} + \frac{\Omega_1 \Omega_2}{2\delta_2} \right) (|e\rangle \langle g| + |g\rangle \langle e|). \quad (\text{C.5})$$

² Rigorously the replacement should be accompanied with the quantum fluctuation, like $a_1 \rightarrow (\alpha_1 + \delta a_1)e^{-i(\omega_r - \omega_g + \delta_1)t}$, however, here we neglect the small δa .

Fig.C.1 A Λ -type three-level system



Note that this transformation is valid only when³ $\Omega_1/\delta_1, \Omega_2/\delta_2 \ll 1$ and the ac Stark shift of $|r\rangle$ by $-\hbar(\Omega_1^2/\delta_1 + \Omega_2^2/\delta_2)$ is present but $|r\rangle\langle r|$ -term itself is omitted since it does nothing⁴ to the manifold $\{|g\rangle, |e\rangle\}$ in this approximation. Redefining the parameters as

$$\delta'_1 = \delta_1 + \frac{\Omega_1^2}{\delta_1}, \quad \delta'_2 = \delta_2 + \frac{\Omega_2^2}{\delta_2}, \quad \Omega' = \frac{\Omega_1\Omega_2}{2\delta_1} + \frac{\Omega_1\Omega_2}{2\delta_2},$$

we find our three-level system reduces to the driven two-level system:

$$\mathcal{H}'_{eff} = \hbar\delta'_1 |g\rangle\langle g| + \hbar\delta'_2 |e\rangle\langle e| + \hbar\Omega'(|e\rangle\langle g| + |g\rangle\langle e|). \quad (\text{C.6})$$

Let us see what is going on in the three-level system by analyzing the eigenstates of the Hamiltonian in the presence of the third level. Its matrix form reads

$$\mathcal{H}' = \hbar \begin{pmatrix} \delta_1 & \Omega_1 & 0 \\ \Omega_1 & 0 & \Omega_2 \\ 0 & \Omega_2 & \delta_2 \end{pmatrix} \quad (\text{C.7})$$

and the eigenvalues λ are the solutions of $\lambda(\lambda - \delta_1)(\lambda - \delta_2) - \Omega_2^2(\lambda - \delta_1) - \Omega_1^2(\lambda - \delta_2) = 0$. Suppose the two-photon detuning is zero, namely $\delta_1 = \delta_2 = \delta$. Then the eigenvalues are $\lambda = \delta \equiv \lambda_0$ and $\lambda = (\delta/2) \pm \sqrt{(\delta/2)^2 + \Omega_1^2 + \Omega_2^2} \equiv \lambda_{\pm}$. The eigenvector $|\psi_0\rangle$ corresponding to λ_0 is a superposition of $|g\rangle$ and $|e\rangle$ only, while those corresponding to λ_{\pm} , $|\psi_{\pm}\rangle$, contain the auxiliary state $|r\rangle$ that might cause decay into the manifold $\{|g\rangle, |e\rangle\}$ accompanied with the emission of a photon. For such reasons, the former state $|\psi_0\rangle$ is often dubbed as the dark state and the latter the bright state.

³ Usually the detunings are taken to be large compared to the driving strengths.

⁴ If the loss or decoherence of $|r\rangle$ is non-negligible, it does something, e.g., let the quantum gate incomplete.

Since the astonishing experimental results by Rutherford, an atom is recognized to be an object consisting of electrons orbiting around an atomic nucleus. Nevertheless, the puzzle had still remained that the electrons in accelerated motion should have radiated electromagnetic fields and lost their velocities to fall into the nucleus, but they do not in reality. This puzzle had not been solved until the birth of quantum theory and quantum mechanics. In this Appendix, let us consider a hydrogen atom, the most simple atomic species, with the help of Bohr's model. Back-of-the-envelope calculations for the fine and hyperfine structures are also given here to make this appendix a quick introduction to quantum systems accompanied with optical transitions.

D.1 Bohr's Atom

Bohr's atomic model considers an electron orbiting around a proton as in the classical picture, except that the electron behaves as a matter wave. It assumes that the phase acquisition by the electron as a matter wave with one circulation around the nucleus equals to an integer-multiple of 2π . Then we reinterpret this argument as the discretization of the orbital angular momentum of the electron that is expressed by

$$mv r = \hbar n \quad (\text{D.1})$$

where m is the electron mass, v the velocity, and r the radius of the orbit. n is here a positive integer. In an inertial system that the electron is at rest, the Coulomb force and the centrifugal force should equilibrate:

$$m \frac{v^2}{r} = \frac{1}{4\pi\epsilon_0} \frac{e^2}{r^2}. \quad (\text{D.2})$$

By using the above two equations, we can eliminate v and get the radius of electron's orbit as

$$r = \frac{4\pi\epsilon_0\hbar^2}{me^2}n^2 \quad (\text{D.3})$$

which means that the radius of electron's orbit has to take discrete values. The energy E of the hydrogen atom can be calculated as follows:

$$E = \frac{1}{2}mv^2 - \frac{1}{4\pi\epsilon_0}\frac{e^2}{r} \quad (\text{D.4})$$

$$= -\frac{1}{4\pi\epsilon_0}\frac{e^2}{2r} \quad (\text{D.5})$$

$$= -\frac{me^4}{2(4\pi\epsilon_0)^2\hbar^2}\frac{1}{n^2}. \quad (\text{D.6})$$

As expected, the energy of Bohr's hydrogen atom can only take discrete values

$$E_n = -\frac{me^4}{2(4\pi\epsilon_0)^2\hbar^2}\frac{1}{n^2}. \quad (\text{D.7})$$

The energy difference between E_1 and E_∞ is evaluated to be 13.6 eV that explains the experimentally obtained ionization energy. Moreover, the above formula reproduces the empirical formula of the atomic spectra found by Rydberg. These facts made scientists believe in Bohr's atomic model.

Let us next summarize the quantum mechanical treatment very briefly. First, the energy of the hydrogen atom E_n calculated above coincides with the one derived from the non-relativistic quantum mechanics. The quantum states are labeled by three integers (n, l, m) with $n = 1, 2, 3, \dots$, $l = 0, 1, \dots, n-1$, and $m = -l, -(l-1), \dots, l$ are respectively called principal, azimuthal, and magnetic quantum numbers. One should note that the electronic ground state in Bohr's model describes an orbiting electron around the nucleus but it is not the case in quantum mechanics; the ground-state electron is not orbiting but rather have probability distribution with its peak at the nucleus.

The velocity of the electron in an atom is very large that the relativistic effect also has non-negligible modifications. Dirac equation, instead of Schrödinger equation, is to be used for taking into account spins, fine structure, and other effects. Here after we shall admit the electron and nuclear spin to overview the fine and hyperfine structures.

D.2 Fine Structure

Suppose again that an electron is orbiting around the nucleus. In the rest frame of the electron, in turn, the nucleus is orbiting around the electron. Given the electric

charge of the nucleus be $+e$, the orbiting nucleus forms a loop current $\mathbf{I} = ev/2\pi r$ that generates the magnetic field

$$B = \frac{\mu_0 I}{2r} = \frac{\mu_0 ev}{4\pi r^2} = \frac{\mu_0 eL}{4\pi mr^3} \quad (\text{D.8})$$

at the position of the electron, where $L = mvr$ denotes the orbital angular momentum. The Zeeman effect says that the energy shift of the spin states of the electron by this magnetic field reads

$$-\boldsymbol{\mu} \cdot \mathbf{B} = \frac{g\mu_B}{\hbar} \mathbf{S} \cdot \frac{\mu_0 e}{4\pi m^2 r^3} \mathbf{L} = -\frac{g\mu_B e^2}{8\pi m^2 r^3} \mathbf{S} \cdot \mathbf{L}. \quad (\text{D.9})$$

Here $g \simeq 2$ denotes the Landé g factor and $\mu_B = e\hbar/2m$ is called the Bohr magneton. Indeed, the above discussion neglects the relativistic effect of Thomas precession and correct expression is given by replacing g by $g - 1$. If we look at this phenomena from the original frame, above energy shift can be interpreted as an interaction energy between the electron spin and the magnetic field generated by the electron's orbital angular momentum. This interaction is called the spin-orbit interaction. In such a situation, \mathbf{L} or \mathbf{S} are not good quantum numbers alone, but the sum $\mathbf{J} = \mathbf{S} + \mathbf{L}$ is. For example, if the electron is in the S state, $L = 0$ so that the spin-orbit interaction energy is zero. In contrast, if in the P state, the energy level is split into two depending on whether the \mathbf{L} and \mathbf{S} are parallel or anti-parallel. This energy splitting is called the fine-structure splitting and the energy scale of the splitting is ranging from GHz to THz, depending on the atomic species.

D.3 Hyperfine Structure

The interaction between the spin and orbital degrees of freedom was discussed in the previous section, and we mentioned that the total angular momentum \mathbf{J} becomes a good quantum number. In this section, we further estimate the amount of interaction between the electron's angular momentum \mathbf{J} and nuclear spin \mathbf{I} .

Let us consider a simple case that the electron is in the S state, where the electron's wavefunction exhibits finite value $\psi(0)$ at the position of nucleus. The nucleus thus feels magnetic field generated by the electron spin that is proportional to $|\psi(0)|^2$. The magnetic field generated by the electron spin is here roughly estimated by substituting the magnetization $\mathbf{M} = -\mu_B g|\psi(0)|^2 \mathbf{J}$ into the magnetic flux of a uniformly magnetized sphere $\mathbf{B} = (2/3)\mu_0 \mathbf{M}$. The nuclear spin $\mu_N \mathbf{I}$ interacts With this magnetic field to yield the Zeeman shift of

$$-\boldsymbol{\mu}_N \cdot \mathbf{B} = \frac{2}{3} \mu_N \mu_0 \mu_B g |\psi(0)|^2 \mathbf{I} \cdot \mathbf{J} \equiv A \mathbf{I} \cdot \mathbf{J} \quad (\text{D.10})$$

that catches the basic concept of hyperfine interaction. Here μ_N denotes the nuclear magnetic moment. Like in the fine structure, a good quantum number is not \mathbf{J} or

I alone, but the sum $\mathbf{F} = \mathbf{J} + \mathbf{I} = \mathbf{S} + \mathbf{L} + \mathbf{I}$ acts as a good quantum number. The energy splitting by the values of $\mathbf{I} \cdot \mathbf{J}$ is called hyperfine splitting. The amount of the hyperfine splitting is small compared to the fine splitting, for the nuclear magnetic moment is about 1/1000 times smaller than that of the electron. The hyperfine splitting is on the order of GHz in most atomic species.⁵

⁵ The above discussion takes only the magnetic dipole interaction into account, however, it is known that the quadrupole interaction also have a sizable effect.

E.1 Density Matrix

In quantum mechanics, the physical system is described by operators and state vectors, which respectively represent the physical quantities and the probabilities that the system is in some state. Suppose that a Hamiltonian of our interest is given. How do we analyze the system, or in other words, what quantity do we keep track of? One way is to look at the operators that obey the Heisenberg equations of motion, which is useful for directly inspecting the evolution of the experimentally observable physical quantities. Another way is to focus on the state to see that with how much probability the system evolves into a certain state. For the latter purpose, density matrix nicely addresses the time evolution of the system including the transition of one state to another to allow us to analyze the rate equation, optical Bloch equation, Raman transition and electromagnetically induced transparency, and so forth.

When state vectors $\{|\psi_k\rangle\}$ of the system are given, the density matrix is constructed by

$$\rho = \sum_k w_k |\psi_k\rangle \langle \psi_k| \quad (\text{E.1})$$

where the coefficients satisfy $\sum_k w_k = 1$. If the density matrix can be written by a single state vector $|\psi\rangle$, i.e., $\rho = |\psi\rangle \langle \psi|$, the system is said to be in a pure state, otherwise in a mixed state. The pure and mixed states can be discriminated by the quantity $\text{Tr}[\rho^2]$ that exhibits a value of 1 for the pure state and less than 1 for the mixed state. Let us express the density matrix using some basis set $\{|i\rangle\}$. By inserting the completeness condition $\sum_i |i\rangle \langle i|$, we get

$$\rho = \sum_{i,j} |i\rangle \langle i| \rho |j\rangle \langle j| = \sum_{i,j} |i\rangle \rho_{ij} \langle j|. \quad (\text{E.2})$$

The ρ_{ij} in the above expression dictates the matrix element of the density matrix represented in the current basis. The expectation value of the operator A is written by the density matrix as

$$\sum_k w_k \langle \psi_k | A | \psi_k \rangle = \sum_k \sum_i w_k \langle \psi_k | A | i \rangle \langle i | \psi_k \rangle \quad (\text{E.3})$$

$$= \sum_k \sum_i w_k \langle i | \psi_k \rangle \langle \psi_k | A | i \rangle \quad (\text{E.4})$$

$$= \sum_i \langle i | \rho A | i \rangle \quad (\text{E.5})$$

$$= \text{Tr}[\rho A]. \quad (\text{E.6})$$

It is instructive to give an example of the density matrix with a two-level system where a state is represented by $|\psi\rangle = c_g|g\rangle + c_e|e\rangle = (c_e \ c_g)^t$. The density matrix constituted by this state vector is

$$\rho = |\psi\rangle \langle \psi| = \begin{pmatrix} c_e \\ c_g \end{pmatrix} \begin{pmatrix} c_e^* & c_g^* \end{pmatrix} = \begin{pmatrix} |c_e|^2 & c_e c_g^* \\ c_e^* c_g & |c_g|^2 \end{pmatrix}. \quad (\text{E.7})$$

One can immediately see that the diagonal elements of the density matrix express the populations in the basis states. The off-diagonal elements are called the coherences. At first sight these are mysterious, however, the off-diagonal elements connect the different basis states, hence one can guess that they have something to do with the interference or transition among the states. Actually, the coherence terms play an essential role in the optical Bloch equations as we describe later.

How about the dynamics of the density matrix? To address this, we depart from the state vector in the Schrödinger picture, where the time evolution of the state reads $|\psi_k(t)\rangle = e^{-i(H/\hbar)t} |\psi_k\rangle = U_t |\psi_k\rangle$ with the system Hamiltonian H . Let us differentiate the density matrix evolving with $\rho(t) = U_t \rho U_t^\dagger$:

$$\frac{d\rho(t)}{dt} = \frac{dU_t}{dt} \rho U_t^\dagger + U_t \rho \frac{dU_t^\dagger}{dt} = -\frac{i}{\hbar} H \rho(t) + \frac{i}{\hbar} \rho(t) H = \frac{1}{i\hbar} [H, \rho(t)] \quad (\text{E.8})$$

which leads us to the von Neumann equation

$$i\hbar \frac{d\rho}{dt} = [H, \rho]. \quad (\text{E.9})$$

Note the difference between the von Neumann equation for a *state* and the Heisenberg equation of motion for an *operator*: $i\hbar dA/dt = [A, H]$.

Basic properties of trace operation

Here for the later use we list the elementary algebraic properties of trace operation. Most of the following properties can be derived by straightforwardly calculating the trace of the matrices involved. First, the trace operation is linear:

$$\text{Tr}[A + B] = \text{Tr}[A] + \text{Tr}[B], \quad (\text{E.10})$$

$$\text{Tr}[cA] = c\text{Tr}[A]. \quad (\text{E.11})$$

The trace is invariant under cyclic permutations of the matrices:

$$\text{Tr}[AB] = \text{Tr}[BA], \quad (\text{E.12})$$

$$\text{Tr}[ABC] = \text{Tr}[CAB] = \text{Tr}[BCA], \quad (\text{E.13})$$

$$\dots \quad (\text{E.14})$$

The trace of the tensor product of matrices is the product of the traces of the matrices:

$$\text{Tr}[A \otimes B] = \text{Tr}[A]\text{Tr}[B]. \quad (\text{E.15})$$

E.2 System-Bath Interaction

Let us now take a look at how to deal with the system–bath interaction using the density matrix. The starting point is the same Hamiltonian as the input-output theory (see Sect. 8.3). The total Hamiltonian $H_{tot} = H_s + H_b + H_i$ is the sum of the ones of the system H_s , bath H_b and interaction between them H_i that have concrete forms of

$$H_s = \hbar\omega_c a^\dagger a, \quad (\text{E.16})$$

$$H_b = \int_{-\infty}^{\infty} \frac{d\omega}{2\pi} \hbar\omega c^\dagger(\omega)c(\omega), \quad (\text{E.17})$$

$$H_i = -i\hbar \int_{-\infty}^{\infty} \frac{d\omega}{2\pi} [f(\omega)a^\dagger c(\omega) - f^*(\omega)c^\dagger(\omega)a]. \quad (\text{E.18})$$

Note that the system-bath coupling here is now in the general form $f(\omega)$, which is to be replaced by $\sqrt{\kappa}$ in most of the situations. We shall define

$$R^- = \int_{-\infty}^{\infty} \frac{d\omega}{2\pi} f(\omega)c(\omega), \quad (\text{E.19})$$

$$R^+ = \int_{-\infty}^{\infty} \frac{d\omega}{2\pi} f^*(\omega)c^\dagger(\omega) \quad (\text{E.20})$$

to simplify the interaction Hamiltonian as

$$H_i = -i\hbar(a^\dagger R^- - aR^+). \quad (\text{E.21})$$

Let us shortly make a note on the time evolution of the state and operator in the interaction representation. We list the equations governing the time evolution of these quantities without proof:

$$i\hbar \frac{d|\psi(t)\rangle}{dt} = H_i |\psi(t)\rangle, \quad (\text{E.22})$$

$$i\hbar \frac{d\rho(t)}{dt} = [H_i, \rho(t)], \quad (\text{E.23})$$

$$i\hbar \frac{dA(t)}{dt} = [A(t), H_s + H_b]. \quad (\text{E.24})$$

The first, second, and third ones are respectively called the Tomonaga–Schwinger, Liouville–von Neumann, and Heisenberg equations. It can be immediately observed that in the interaction picture, the time evolution of the states is governed by the interaction Hamiltonian H_i , while that of the operators by the “unperturbed” Hamiltonian $H_s + H_b$. This formalism was first invented in the context of developing the perturbation expansion of the quantum electrodynamics.

In the following, we switch to the interaction picture from the Schrödinger picture. Transformation of the density matrix and the Hamiltonian reads

$$\tilde{\rho}(t) = e^{i\frac{H_s+H_b}{\hbar}t} \rho(t) e^{-i\frac{H_s+H_b}{\hbar}t}, \quad (\text{E.25})$$

$$\tilde{H}_i = e^{i\frac{H_s+H_b}{\hbar}t} H_i e^{-i\frac{H_s+H_b}{\hbar}t} \quad (\text{E.26})$$

$$= -i\hbar \left(a^\dagger e^{i\omega_c t} \tilde{R}^- - a e^{-i\omega_c t} \tilde{R}^+ \right) \quad (\text{E.27})$$

where we have defined

$$\tilde{R}^- = e^{i\frac{H_s+H_b}{\hbar}t} R^- e^{-i\frac{H_s+H_b}{\hbar}t} = \int_{-\infty}^{\infty} \frac{d\omega}{2\pi} f(\omega) c(\omega) e^{-i\omega t}, \quad (\text{E.28})$$

$$\tilde{R}^+ = e^{i\frac{H_s+H_b}{\hbar}t} R^+ e^{-i\frac{H_s+H_b}{\hbar}t} = \int_{-\infty}^{\infty} \frac{d\omega}{2\pi} f^*(\omega) c^\dagger(\omega) e^{i\omega t}. \quad (\text{E.29})$$

The Liouville–von Neumann equation in the interaction picture becomes

$$i\hbar \frac{d\tilde{\rho}(t)}{dt} = \left[\tilde{H}_i(t), \tilde{\rho}(t) \right]. \quad (\text{E.30})$$

In what follows, we will work on the interaction picture so that the tilde is suppressed.

In order to dive deeper into the dynamics of the density matrix in the presence of the system–bath interaction, we rewrite the Liouville–von Neumann equation by using infinitesimal time interval Δt as

$$\Delta\rho(t) = \rho(t + \Delta t) - \rho(t) = \frac{1}{i\hbar} \int_t^{t+\Delta t} dt' [H_i(t'), \rho(t')] \quad (\text{E.31})$$

$$= \frac{1}{i\hbar} \int_t^{t+\Delta t} dt' [H_i(t'), \rho(t)] \quad (\text{E.32})$$

$$+ \left(\frac{1}{i\hbar} \right)^2 \int_t^{t+\Delta t} dt' \int_t^{t'} dt'' [H_i(t'), [H_i(t''), \rho(t)]] \quad (\text{E.33})$$

where we truncate the infinite series up to the second order.

Since we are here interested in the dynamics only of the system part, we define the reduced density matrices of the system $\sigma(t) = \text{Tr}_b [\rho(t)]$ and complementarily the one of the bath $\sigma_b(t) = \text{Tr}_s [\rho(t)]$ by tracing out the bath- and system-degrees of freedom, respectively. At this point we make a crucial assumption that the density matrix of the whole system can be written as the tensor product of the two reduced matrices:

$$\rho(t) = \sigma(t) \otimes \sigma_b(t) \quad (\text{E.34})$$

which implies the absence of the temporal correlation between the system and bath. We further assume that the bath is always stationary, i.e. $\sigma_b(t) = \sigma_b(0) = \sigma_b$, hence the σ_b commutes with the bath Hamiltonian H_b . Now we are to trace out $\Delta\rho(t)$ with respect to the bath degree of freedom to get the dynamics of the system.

$$\text{Tr}_b [\Delta\rho(t)] = \frac{1}{i\hbar} \int_t^{t+\Delta t} dt' \text{Tr}_b [H_i(t'), \rho(t)] \quad (\text{E.35})$$

$$+ \left(\frac{1}{i\hbar} \right)^2 \int_t^{t+\Delta t} dt' \int_t^{t'} dt'' \text{Tr}_b [H_i(t'), H_i(t''), \rho(t)]. \quad (\text{E.36})$$

Here the first term on the right-hand side vanishes, since

$$\text{Tr}_b [H_i(t'), \rho(t)] = \text{Tr}_b [H_i(t'), \sigma(t) \otimes \sigma_b(t)] \quad (\text{E.37})$$

$$= -i\hbar \left\{ a^\dagger e^{i\omega_c t'} \text{Tr}_b [R^-(t') \sigma_b] - ae^{-i\omega_c t'} \text{Tr}_b [R^+(t') \sigma_b] \right\} \sigma(t) \quad (\text{E.38})$$

$$+ i\hbar \sigma(t) \left\{ a^\dagger e^{i\omega_c t'} \text{Tr}_b [R^-(t') \sigma_b] - ae^{-i\omega_c t'} \text{Tr}_b [R^+(t') \sigma_b] \right\} \quad (\text{E.39})$$

$$= -i\hbar \left\{ a^\dagger e^{i\omega_c t'} \langle R^-(t') \rangle_b - ae^{-i\omega_c t'} \langle R^+(t') \rangle_b \right\} \sigma(t) \quad (\text{E.40})$$

$$+ i\hbar \sigma(t) \left\{ a^\dagger e^{i\omega_c t'} \langle R^-(t') \rangle_b - ae^{-i\omega_c t'} \langle R^+(t') \rangle_b \right\} \quad (\text{E.41})$$

$$= 0, \quad (\text{E.42})$$

where we used the fact that $\langle c(\omega) \rangle_b = \langle c^\dagger(\omega) \rangle_b = 0$. $\langle \cdot \rangle_b$ stands for the expectation value evaluated over the bath degree of freedom, which we shall omit the subscript below.

Then the remaining second term matters. The commutator inside the trace is expanded to give messy appearance; however, they are traced out to give eight surviving terms

$$\frac{\text{Tr}_b [H_i(t'), H_i(t''), \rho(t)]}{(-i\hbar)^2} = \quad (\text{E.43})$$

$$-\langle R^-(t')R^+(t'') \rangle a^\dagger(t')a(t'')\sigma(t) - \langle R^+(t')R^-(t'') \rangle a(t')a^\dagger(t'')\sigma(t) \quad (\text{E.44})$$

$$+ \langle R^-(t'')R^+(t') \rangle a(t')\sigma(t)a^\dagger(t'') + \langle R^+(t'')R^-(t') \rangle a^\dagger(t')\sigma(t)a(t'') \quad (\text{E.45})$$

$$+ \langle R^-(t')R^+(t'') \rangle a(t'')\sigma(t)a^\dagger(t') + \langle R^+(t')R^-(t'') \rangle a^\dagger(t'')\sigma(t)a(t') \quad (\text{E.46})$$

$$- \langle R^-(t'')R^+(t') \rangle \sigma(t)a^\dagger(t') - \langle R^+(t'')R^-(t') \rangle \sigma(t)a(t'')a^\dagger(t'). \quad (\text{E.47})$$

In this expression, the exponential factor for the cavity operator is absorbed by the operator itself, namely $a(t) = ae^{-i\omega_c t}$ and $a^\dagger(t) = a^\dagger e^{i\omega_c t}$. The two-time correlation functions $\langle R^-(t')R^+(t'') \rangle$ and $\langle R^+(t'')R^-(t') \rangle$ should be evaluated to eliminate the bath operator from above expression. These read

$$\langle R^-(t')R^+(t'') \rangle = \int_{-\infty}^{\infty} \frac{d\omega}{2\pi} \int_{-\infty}^{\infty} \frac{d\omega'}{2\pi} f(\omega) f^*(\omega') \langle c(\omega)c^\dagger(\omega') \rangle e^{-i\omega t'} e^{i\omega' t''} \quad (\text{E.48})$$

$$= \int_{-\infty}^{\infty} \frac{d\omega}{2\pi} \int_{-\infty}^{\infty} \frac{d\omega'}{2\pi} f(\omega) f^*(\omega') [\langle n(\omega) \rangle + 1] 2\pi\delta(\omega - \omega') e^{-i\omega t'} e^{i\omega' t''} \quad (\text{E.49})$$

$$= \int_{-\infty}^{\infty} \frac{d\omega}{2\pi} |f(\omega)|^2 [\langle n(\omega) \rangle + 1] e^{-i\omega(t'-t'')}, \quad (\text{E.50})$$

$$\langle R^+(t'')R^-(t') \rangle = \dots = \int_{-\infty}^{\infty} \frac{d\omega}{2\pi} |f(\omega)|^2 \langle n(\omega) \rangle e^{-i\omega(t'-t'')}. \quad (\text{E.51})$$

In integrating with respect to time t' and t'' , we transform the domain of integration by putting $\tau = t' - t''$ as

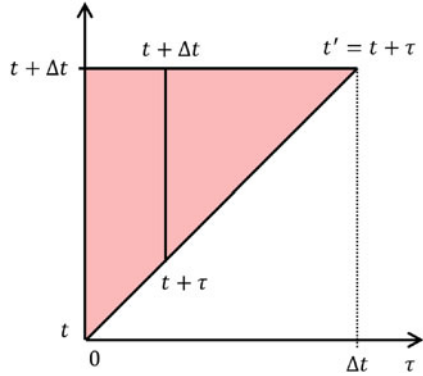
$$\int_t^{t+\Delta t} dt' \int_t^{t'} dt'' = \int_t^{t+\Delta t} dt' \int_0^{t'-t} d\tau = \int_0^{\Delta t} d\tau \int_{t+\tau}^{t+\Delta t} dt' \quad (\text{E.52})$$

and further assume that the quantities $\langle R^-(t')R^+(t'-\tau) \rangle$ and $\langle R^+(t'-\tau)R^-(t') \rangle$ have non-zero contribution only around $\tau \ll \Delta t$, which allows for the extension of the domain of integration:

$$\int_0^{\Delta t} d\tau \int_{t+\tau}^{t+\Delta t} dt' = \int_0^{\infty} d\tau \int_{t+\tau}^{t+\Delta t} dt' \simeq \int_0^{\infty} d\tau \int_t^{t+\Delta t} dt'. \quad (\text{E.53})$$

Note that since the limit $\Delta t \rightarrow +0$ is taken afterwards, this assumption is justified by the Markov approximation—the dynamics of the bath mode is memoryless. By

Fig. E.1 Transforming the domain of integration



executing these transformations, we arrive at the expressions

$$\int_t^{t+\Delta t} dt' \int_t^{t'} dt'' \left[\langle R^-(t') R^+(t'') \rangle e^{i\omega_c(t'-t'')} \right] = \Delta t \int_0^\infty d\tau \langle R^-(\tau) R^+(0) \rangle e^{i\omega_c \tau} \quad (\text{E.54})$$

$$= \Delta t \int_0^\infty d\tau \int_{-\infty}^\infty \frac{d\omega}{2\pi} |f(\omega)|^2 [\langle n(\omega) \rangle + 1] e^{-i(\omega - \omega_c)\tau} e^{-\epsilon\tau}, \quad (\text{E.55})$$

$$\int_t^{t+\Delta t} dt' \int_t^{t'} dt'' \left[\langle R^+(t'') R^-(t') \rangle e^{i\omega_c(t'-t'')} \right] = \Delta t \int_0^\infty d\tau \langle R^+(0) R^-(\tau) \rangle e^{i\omega_c \tau} \quad (\text{E.56})$$

$$= \Delta t \int_0^\infty d\tau \int_{-\infty}^\infty \frac{d\omega}{2\pi} |f(\omega)|^2 \langle n(\omega) \rangle e^{-i(\omega - \omega_c)\tau} e^{-\epsilon\tau}. \quad (\text{E.57})$$

Here the convergence factor $e^{-\epsilon\tau}$ has been introduced in above equations in order not to make these integrals diverge at $\omega = \omega_c$. These integrals are further calculated to yield

$$\Delta t \int_0^\infty d\tau \int_{-\infty}^\infty \frac{d\omega}{2\pi} |f(\omega)|^2 [\langle n(\omega) \rangle + 1] e^{-i(\omega - \omega_c)\tau} e^{-\epsilon\tau} \quad (\text{E.58})$$

$$= i \int_{-\infty}^\infty \frac{d\omega}{2\pi} |f(\omega)|^2 [\langle n(\omega) \rangle + 1] \left[-i \int_0^\infty d\tau e^{-i(\omega - \omega_c)\tau} e^{-\epsilon\tau} \right] \Delta t \quad (\text{E.59})$$

$$= i \int_{-\infty}^\infty \frac{d\omega}{2\pi} |f(\omega)|^2 [\langle n(\omega) \rangle + 1] \frac{\Delta t}{(\omega_c - \omega) + i\epsilon} \quad (\text{E.60})$$

$$\xrightarrow{\epsilon \rightarrow +0} i \mathcal{P} \int_{-\infty}^\infty \frac{d\omega}{2\pi} \frac{|f(\omega)|^2 [\langle n(\omega) \rangle + 1]}{\omega_c - \omega} \Delta t \quad (\text{E.61})$$

$$+ \frac{1}{2} \int_{-\infty}^\infty d\omega |f(\omega)|^2 [\langle n(\omega) \rangle + 1] \delta(\omega_c - \omega) \Delta t \quad (\text{E.62})$$

$$= i(\Delta + \Delta') \Delta t + \frac{\Gamma + \Gamma'}{2} \Delta t \quad (\text{E.63})$$

$$\Delta t \int_0^\infty d\tau \int_{-\infty}^\infty \frac{d\omega}{2\pi} |f(\omega)|^2 \langle n(\omega) \rangle e^{-i(\omega - \omega_c)\tau} e^{-\epsilon\tau} \quad (\text{E.64})$$

$$= i \int_{-\infty}^\infty \frac{d\omega}{2\pi} |f(\omega)|^2 \langle n(\omega) \rangle \left[-i \int_0^\infty d\tau e^{-i(\omega - \omega_c)\tau} e^{-\epsilon\tau} \right] \Delta t \quad (\text{E.65})$$

$$= i \int_{-\infty}^\infty \frac{d\omega}{2\pi} |f(\omega)|^2 \langle n(\omega) \rangle \frac{\Delta t}{(\omega_c - \omega) + i\epsilon} \quad (\text{E.66})$$

$$\xrightarrow{\epsilon \rightarrow +0} \left[i\mathcal{P} \int_{-\infty}^\infty \frac{d\omega}{2\pi} \frac{|f(\omega)|^2 \langle n(\omega) \rangle}{\omega_c - \omega} + \frac{1}{2} \int_{-\infty}^\infty d\omega |f(\omega)|^2 \langle n(\omega) \rangle \delta(\omega_c - \omega) \right] \Delta t \quad (\text{E.67})$$

$$= \left[i\Delta' + \frac{\Gamma'}{2} \right] \Delta t \quad (\text{E.68})$$

where we used the Dirac identity $\lim_{\epsilon \rightarrow +0} 1/[(\omega_c - \omega) + i\epsilon] = \mathcal{P}/(\omega_c - \omega) - i\pi\delta(\omega_c - \omega)$. The parameters Δ, Δ' are defined by

$$\Delta = \mathcal{P} \int_{-\infty}^\infty \frac{d\omega}{2\pi} \frac{|f(\omega)|^2}{\omega_c - \omega}, \quad (\text{E.69})$$

$$\Delta' = \mathcal{P} \int_{-\infty}^\infty \frac{d\omega}{2\pi} \frac{|f(\omega)|^2 \langle n(\omega) \rangle}{\omega_c - \omega} \quad (\text{E.70})$$

both representing the radiative shift. On the other hand, Γ and Γ' stand for

$$\Gamma = \int_{-\infty}^\infty d\omega |f(\omega)|^2 \delta(\omega_c - \omega) = |f(\omega_c)|^2, \quad (\text{E.71})$$

$$\Gamma' = \int_{-\infty}^\infty d\omega |f(\omega)|^2 \langle n(\omega) \rangle \delta(\omega_c - \omega) = \langle n(\omega_c) \rangle \Gamma \quad (\text{E.72})$$

which respectively represents the spontaneous and induced decay rates (Fig. E.1).

By using results obtained so far, the quantity $d\sigma(t)/dt = \lim_{\Delta t \rightarrow +0} \text{Tr}_b [\Delta\rho(t)] / \Delta t$ reads

$$\frac{\partial\sigma(t)}{\partial t} = -\frac{i}{\hbar} [\hbar\Delta a^\dagger a, \sigma(t)] + \frac{\Gamma + \Gamma'}{2} [2a\sigma(t)a^\dagger - a^\dagger a\sigma(t) - \sigma(t)a^\dagger a] \quad (\text{E.73})$$

$$+ \frac{\Gamma'}{2} [2a^\dagger \sigma(t)a - aa^\dagger \sigma(t) - \sigma(t)aa^\dagger] \quad (\text{E.74})$$

which looks in the Schrödinger picture like

$$\frac{d\sigma(t)}{dt} = -\frac{i}{\hbar} [\hbar(\omega_c + \Delta)a^\dagger a, \sigma(t)] + \frac{\Gamma + \Gamma'}{2} [2a\sigma(t)a^\dagger - a^\dagger a\sigma(t) - \sigma(t)a^\dagger a] \quad (\text{E.75})$$

$$+ \frac{\Gamma'}{2} [2a^\dagger \sigma(t)a - aa^\dagger \sigma(t) - \sigma(t)aa^\dagger] \quad (\text{E.76})$$

This is the celebrated master equation. The master equation is somewhat simplified by the Lindblad superoperator

$$\mathcal{L}[A]\sigma(t) = 2A\sigma(t)A^\dagger - A^\dagger A\sigma(t) - \sigma(t)A^\dagger A \quad (\text{E.77})$$

that lead to

$$\frac{d\sigma(t)}{dt} = -\frac{i}{\hbar} [\hbar(\omega_c + \Delta)a^\dagger a, \sigma(t)] + \frac{1}{2}\mathcal{L}[\sqrt{\Gamma + \Gamma'}a]\sigma(t) + \frac{1}{2}\mathcal{L}[\sqrt{\Gamma'}a^\dagger]\sigma(t). \quad (\text{E.78})$$

The first term describes the coherent dynamics of the system itself. Very roughly speaking, second and third terms have meanings of the decay into and excitation from the bath mode, respectively.

E.3 Rate Equation

The master equation

$$\frac{d\sigma(t)}{dt} = -\frac{i}{\hbar} [\hbar(\omega_c + \Delta)a^\dagger a, \sigma(t)] + \frac{\Gamma + \Gamma'}{2} [2a\sigma(t)a^\dagger - a^\dagger a\sigma(t) - \sigma(t)a^\dagger a] \quad (\text{E.79})$$

$$+ \frac{\Gamma'}{2} [2a^\dagger\sigma(t)a - aa^\dagger\sigma(t) - \sigma(t)aa^\dagger] \quad (\text{E.80})$$

describes the dynamical behavior of the system when sandwiched by various basis states. In this section, we evaluate the master equation with the Fock-state basis $\{|N\rangle\}$ to derive the rate equation. By sandwiching the master equation by $|N\rangle$, we get

$$\frac{dP(N)}{dt} = (\Gamma + \Gamma') [(N+1)P(N+1) - NP(N)] + \Gamma' [NP(N-1) - (N+1)P(N)] \quad (\text{E.81})$$

$$= \Gamma_\downarrow [(N+1)P(N+1) - NP(N)] + \Gamma_\uparrow [NP(N-1) - (N+1)P(N)] \quad (\text{E.82})$$

and hence the rate equation

$$\frac{d\langle N \rangle}{dt} = \frac{d}{dt} \sum_N NP(N) \quad (\text{E.83})$$

$$= \sum_N N [(N+1)P(N+1)\Gamma_\downarrow + NP(N-1)\Gamma_\uparrow - (N+1)P(N)\Gamma_\uparrow - NP(N)\Gamma_\downarrow] \quad (\text{E.84})$$

$$= \Gamma_\uparrow \sum_N (N+1)P(N) - \Gamma_\downarrow \sum_N NP(N) \quad (\text{E.85})$$

$$= \Gamma_\uparrow \langle N+1 \rangle - \Gamma_\downarrow \langle N \rangle \quad (\text{E.86})$$

$$= -\Gamma \langle N \rangle + \Gamma' \quad (\text{E.87})$$

$$= -\Gamma \langle N \rangle + \Gamma \langle n(\omega_c) \rangle. \quad (\text{E.88})$$

Note that we made use of the identities $\sum_{N=0}^{\infty} N^2 P(N) = \sum_{N=0}^{\infty} (N+1)^2 P(N+1)$ and $\sum_{N=0}^{\infty} N(N+1)P(N+1) = \sum_{N=0}^{\infty} (N-1)NP(N)$ in the third line.

E.4 Optical Bloch Equation

Next, let us consider the two-level system and sandwich the master equation for it with the basis states $|g\rangle$ and $|e\rangle$. The master equation for the atomic density matrix $\rho(t)$ is dictated by

$$\frac{d\rho(t)}{dt} = -\frac{i}{\hbar} [H_s, \rho(t)] + \frac{\Gamma + \Gamma'}{2} [2\sigma_{-}\rho(t)\sigma_{+} - \sigma_{+}\sigma_{-}\rho(t) - \rho(t)\sigma_{+}\sigma_{-}] \quad (\text{E.89})$$

$$+ \frac{\Gamma'}{2} [2\sigma_{+}\rho(t)\sigma_{-} - \sigma_{-}\sigma_{+}\rho(t) - \rho(t)\sigma_{-}\sigma_{+}]. \quad (\text{E.90})$$

The system Hamiltonian is set here to be $H_s = \hbar(\Delta_q/2)\sigma_z + \hbar(\Omega/2)(\sigma_{+} + \sigma_{-})$, a driven atom, for simplicity (see Appendix C). Evaluating the both sides of the master equation by multiplying $|g\rangle$'s and $|e\rangle$'s, one can obtain a set of equations

$$\frac{d\rho_{ee}}{dt} = -(\Gamma + \Gamma')\rho_{ee} + \Gamma'\rho_{gg} + i\frac{\Omega}{2}(\rho_{eg} - \rho_{ge}), \quad (\text{E.91})$$

$$\frac{d\rho_{gg}}{dt} = (\Gamma + \Gamma')\rho_{ee} - \Gamma'\rho_{gg} - i\frac{\Omega}{2}(\rho_{eg} - \rho_{ge}), \quad (\text{E.92})$$

$$\frac{d\rho_{eg}}{dt} = \left(-i\frac{\Delta_q}{2} - \frac{\Gamma + 2\Gamma'}{2}\right)\rho_{eg} - i\frac{\Omega}{2}(\rho_{gg} - \rho_{ee}), \quad (\text{E.93})$$

$$\frac{d\rho_{ge}}{dt} = \left(i\frac{\Delta_q}{2} - \frac{\Gamma + 2\Gamma'}{2}\right)\rho_{ge} + i\frac{\Omega}{2}(\rho_{gg} - \rho_{ee}) \quad (\text{E.94})$$

where $\rho_{ij} = \langle i | \rho | j \rangle$. We shall make a short note that the atomic decay rate Γ and the atomic dipole moment μ are related to each other by

$$\Gamma = \frac{\mu^2 \omega_a^3}{3\pi\hbar\epsilon_0 c^3} \iff \mu = \sqrt{\frac{3\pi\hbar\epsilon_0 c^3 \Gamma}{\omega_a^3}}. \quad (\text{E.95})$$

We are now close to the final form of the equation. We further consider the situation that the transition energy of the two-level atom is in the optical domain. With this assumption, almost no photon is found in the thermal bath, since the optical photon has the energy of $\hbar\omega_c \sim k_B \times 10\,000$ K,⁶ that is far larger than the bath temperature ~ 300 K and make $\langle n(\omega_c) \rangle = 1/(e^{\hbar\omega_c/k_B T} - 1) \simeq 0$. Therefore, the

⁶ Temperature of the surface of the sun is about 6000 K.

“bath-stimulated” decay $\Gamma' = \langle n(\omega_c) \rangle \Gamma$ can be safely ignored to make the above set of equations

$$\frac{d\rho_{ee}}{dt} = -\Gamma\rho_{ee} + i\frac{\Omega}{2}(\rho_{eg} - \rho_{ge}), \quad (\text{E.96})$$

$$\frac{d\rho_{gg}}{dt} = \Gamma\rho_{ee} - i\frac{\Omega}{2}(\rho_{eg} - \rho_{ge}), \quad (\text{E.97})$$

$$\frac{d\rho_{eg}}{dt} = \left(-i\Delta_q - \frac{\Gamma}{2}\right)\rho_{eg} - i\frac{\Omega}{2}(\rho_{gg} - \rho_{ee}), \quad (\text{E.98})$$

$$\frac{d\rho_{ge}}{dt} = \left(i\Delta_q - \frac{\Gamma}{2}\right)\rho_{ge} + i\frac{\Omega}{2}(\rho_{gg} - \rho_{ee}) \quad (\text{E.99})$$

which are called the optical Bloch equations. By putting $w = \rho_{gg} - \rho_{ee}$, the optical Bloch equations yield

$$\frac{dw}{dt} = -\Gamma w - i\Omega(\rho_{eg} - \rho_{eg}^*) + \Gamma, \quad (\text{E.100})$$

$$\frac{d\rho_{eg}}{dt} = \left(-i\Delta_q - \frac{\Gamma}{2}\right)\rho_{eg} - i\frac{\Omega}{2}w \quad (\text{E.101})$$

with the use of the relations $\rho_{gg} + \rho_{ee} = 1$ and therefore $2\Gamma\rho_{ee} = \Gamma\rho_{ee} + \Gamma(1 - \rho_{gg}) = -\Gamma w + \Gamma$. Inspecting the steady-state solution and combining these two, w and ρ_{ee} are found to be

$$w = \frac{1}{1+s}, \quad (\text{E.102})$$

$$\rho_{ee} = \frac{1-s}{2(1+s)} = \frac{(\Omega/2)^2}{(\Delta_q)^2 + (\tilde{\Gamma}/2)^2} \quad (\text{E.103})$$

with parameters defined by

$$s = \frac{s_0}{1 + (2\Delta_q/\Gamma)^2}, \quad (\text{E.104})$$

$$s_0 = \frac{2\Omega^2}{\Gamma^2}, \quad (\text{E.105})$$

$$\tilde{\Gamma} = \Gamma\sqrt{1+s_0}. \quad (\text{E.106})$$

There are two points to be noted: one is that as the driving strength becomes larger, the population in the ground and excited states approaches 1/2 as a result of the balance between the stimulated absorption and emission including spontaneous and stimulated ones. The other point is that the effective linewidth of the transition is given by $\tilde{\Gamma}$, which gets broader as the driving field increases. This phenomenon is called the power broadening.

F.1 General Prescription

In a system of nicely isolated multiple particles, the energy of the system is given by the sum of the energies of particles involved. For example, when an electromagnetic field and an atom are not interacting with each other, the energy of the whole system is written by the sum of the energies of the photon and the atom. However, we always consider a system of interacting particles which generally possesses eigenenergies different from the ones in the non-interacting case. If the interaction between particles is weak enough, perturbation theory allows for obtaining approximated energies and eigenstates. In such an attempt, Schrieffer–Wolff transformation describes how to arrive at the diagonalized effective Hamiltonian of the system of weakly interacting particles.

Here we present the general prescription of how we can derive perturbatively diagonalized Hamiltonian from the original Hamiltonian $H = H_0 + \lambda V$ consisting of the non-interacting part H_0 and the interaction part λV where the parameter λ is introduced so that the order of the perturbation becomes apparent. Without loss of generality, H_0 is set to be diagonal with the eigenbasis $|m\rangle$ of itself, and λV to be off-diagonal, that is, $\langle m | \lambda V | m \rangle = 0$ for all eigenstates $|m\rangle$. Let us consider the unitary transformation of this Hamiltonian by $e^{\lambda S}$, which reads

$$e^{\lambda S} H e^{-\lambda S} = H_0 + \lambda V + \lambda [S, H_0] + \lambda^2 [S, V] + \frac{\lambda^2}{2!} [S, [S, H_0]] + \frac{\lambda^3}{2!} [S, [S, V]] + \dots \quad (\text{F.1})$$

Note that since e^S is unitary, S should be anti-Hermitian $S^\dagger = -S$. In order for the first-order terms in λ vanishes, one should have

$$[H_0, S] = V \quad (\text{F.2})$$

and the Hamiltonian is perturbatively diagonalized up to the first order as

$$H_{eff} = e^{\lambda S} H e^{-\lambda S} = H_0 + \frac{\lambda^2}{2!} [S, V] + \mathcal{O}(\lambda^3). \quad (\text{F.3})$$

How to find an appropriate S for such a diagonalization greatly relies on the “educated guess”, therefore it should be helpful to list some examples below to get the flavor.

F.2 Examples

F.2.1 Driven Spin

First example is a driven spin expressed by a Hamiltonian

$$H = \omega s_z + g(s_+ + s_-) \quad (\text{F.4})$$

where the spin operators s_z , s_+ and s_- satisfy $[s_z, s_\pm] = \pm s_\pm$ and $[s_+, s_-] = 2s_z$. We are working with the unit where $\hbar = 1$. The specific transformation for the Schrieffer–Wolff transformation is $U = \exp [\alpha (s_+ - s_-)]$, with which we can exactly diagonalize H by correct choice of the parameter α . To find this “correct” value, we shall transform the Hamiltonian in practice.

$$\begin{aligned} UHU^\dagger &= \omega s_z + g(s_+ + s_-) + [\alpha (s_+ - s_-), \omega s_z] + [\alpha (s_+ - s_-), g(s_+ + s_-)] \\ &\quad + \frac{1}{2!} [\alpha (s_+ - s_-), [\alpha (s_+ - s_-), \omega s_z]] \\ &\quad + \frac{1}{2!} [\alpha (s_+ - s_-), [\alpha (s_+ - s_-), g(s_+ + s_-)]] + \dots \\ &= \omega s_z + g(s_+ + s_-) - \alpha [\omega (s_+ + s_-) - 4gs_z] - \frac{1}{2!} \alpha^2 [4\omega s_z + 4g(s_+ + s_-)] \\ &\quad + \frac{1}{3!} \alpha^3 [4\omega (s_+ + s_-) - 16gs_z] + \dots \\ &= s_z \left[\omega \left(1 - \frac{(2\alpha)^2}{2!} + \dots \right) + 2g \left(2\alpha - \frac{(2\alpha)^3}{3!} + \dots \right) \right] \\ &\quad + (s_+ + s_-) \left[g \left(1 - \frac{(2\alpha)^2}{2!} + \dots \right) - \frac{\omega}{2} \left(2\alpha - \frac{(2\alpha)^3}{3!} + \dots \right) \right] \\ &= [\omega \cos 2\alpha + 2g \sin 2\alpha] s_z + \left[g \cos 2\alpha - \frac{\omega}{2} \sin 2\alpha \right] (s_+ + s_-) \end{aligned}$$

Now remember the motivation of this calculation—to eliminate the off-diagonal terms. We can accomplish this to arbitrary order in the present case, by setting

$$\tan 2\alpha = \frac{2g}{\omega} \quad (\text{F.5})$$

so that

$$\cos 2\alpha = \frac{1}{\sqrt{1 + \frac{4g^2}{\omega^2}}}, \quad \sin 2\alpha = \frac{\frac{2g}{\omega}}{\sqrt{1 + \frac{4g^2}{\omega^2}}}. \quad (\text{F.6})$$

This leads to the effective Hamiltonian transformed into a diagonal form

$$H_{eff} = \omega s_z \sqrt{1 + \frac{4g^2}{\omega^2}} \quad (\text{F.7})$$

This form of the effective Hamiltonian says that the energy difference between the ground and excited state of the spin system is blue-shifted as the driving strength increases, which can be regarded as the resonant version of the ac Stark shift.

F.2.2 Generalized “Spin” Subject to the “Driving Field”

Let us consider more general situation that more generalized “spin” is driven;

$$H = \Delta X_z + g(X_+ + X_-) \quad (\text{F.8})$$

where operators are defined to support $[X_z, X_\pm] = \pm X_\pm$ and $[X_+, X_-] = P(X_z)$. $P(X_z)$ in the second commutation relation is defined as a polynomial function of X_z . Here for the second term to be treated as the perturbation, $g/\Delta \ll 1$ should hold. Given these, the unitary transformation is guessed to be $U = \exp [-(g/\Delta)(X_+ - X_-)]$ and this leads straightforwardly to the effective Hamiltonian of the form

$$H_{eff} = \Delta X_z + \frac{g^2}{\Delta} P(X_z). \quad (\text{F.9})$$

which is clearly a diagonal one.

Derivation of the SWAP Gate from the Heisenberg Hamiltonian

G

The starting point is the Heisenberg interaction

$$\mathcal{H}_{\text{int}} = \hbar g \frac{\sigma_x \sigma_x + \sigma_y \sigma_y + \sigma_z \sigma_z}{2}. \quad (\text{G.1})$$

Before we exponentiate this, let us calculate $D = \sigma_x \sigma_x + \sigma_y \sigma_y + \sigma_z \sigma_z$ and its polynomials D^n . First the concrete form of D reads

$$D = \sigma_x \sigma_x + \sigma_y \sigma_y + \sigma_z \sigma_z \quad (\text{G.2})$$

$$= \begin{pmatrix} 0 & 0 & 1 \\ 0 & 1 & 0 \\ 0 & 1 & 0 \end{pmatrix} + \begin{pmatrix} 0 & 0 & -1 \\ 0 & 1 & 0 \\ 0 & 1 & 0 \end{pmatrix} + \begin{pmatrix} 1 & 0 & 0 & 0 \\ 0 & -1 & 0 & 0 \\ 0 & 0 & -1 & 0 \\ 0 & 0 & 0 & 1 \end{pmatrix} \quad (\text{G.3})$$

$$= \begin{pmatrix} 1 & 0 & 0 & 0 \\ 0 & -1 & 2 & 0 \\ 0 & 2 & -1 & 0 \\ 0 & 0 & 0 & 1 \end{pmatrix} \quad (\text{G.4})$$

Since D is block-diagonal, we have only to diagonalize the two-by-two matrix in the middle. Then we have

$$\begin{pmatrix} -1 & 2 \\ 2 & -1 \end{pmatrix}^n = \left[\frac{1}{\sqrt{2}} \begin{pmatrix} 1 & 1 \\ 1 & -1 \end{pmatrix} \begin{pmatrix} 1 & 0 \\ 0 & -3 \end{pmatrix} \frac{1}{\sqrt{2}} \begin{pmatrix} 1 & 1 \\ 1 & -1 \end{pmatrix} \right]^n \quad (\text{G.5})$$

$$= \frac{1}{\sqrt{2}} \begin{pmatrix} 1 & 1 \\ 1 & -1 \end{pmatrix} \begin{pmatrix} 1 & 0 \\ 0 & (-3)^n \end{pmatrix} \frac{1}{\sqrt{2}} \begin{pmatrix} 1 & 1 \\ 1 & -1 \end{pmatrix} \quad (\text{G.6})$$

$$= \begin{pmatrix} \frac{1+(-3)^n}{2} & \frac{1-(-3)^n}{2} \\ \frac{1-(-3)^n}{2} & \frac{1+(-3)^n}{2} \end{pmatrix}. \quad (\text{G.7})$$

Next we calculate the exponential of $e^{-iD\alpha}$. It is expanded as $\sum_{n=0}^{\infty} (-iD\alpha)^n / n!$ and

$$e^{-iD\alpha} = \sum_{n=0}^{\infty} \frac{(-i)^n \alpha^n}{n!} D^n \quad (\text{G.8})$$

$$= \sum_{n=0}^{\infty} \frac{(-i)^n \alpha^n}{n!} \left[\text{diag}(1, 0, 0, 1) + \begin{pmatrix} 0 & 0 & 0 & 0 \\ 0 & \frac{1+(-3)^n}{2} & \frac{1-(-3)^n}{2} & 0 \\ 0 & \frac{1-(-3)^n}{2} & \frac{1+(-3)^n}{2} & 0 \\ 0 & 0 & 0 & 0 \end{pmatrix} \right] \quad (\text{G.9})$$

$$= \text{diag}(e^{-i\alpha}, 0, 0, e^{-i\alpha}) + \begin{pmatrix} 0 & 0 & 0 & 0 \\ 0 & \frac{e^{-i\alpha}+e^{3i\alpha}}{2} & \frac{e^{-i\alpha}-e^{3i\alpha}}{2} & 0 \\ 0 & \frac{e^{-i\alpha}-e^{3i\alpha}}{2} & \frac{e^{-i\alpha}+e^{3i\alpha}}{2} & 0 \\ 0 & 0 & 0 & 0 \end{pmatrix} \quad (\text{G.10})$$

$$= \begin{pmatrix} e^{-i\alpha} & 0 & 0 & 0 \\ 0 & \frac{e^{-i\alpha}+e^{3i\alpha}}{2} & \frac{e^{-i\alpha}-e^{3i\alpha}}{2} & 0 \\ 0 & \frac{e^{-i\alpha}-e^{3i\alpha}}{2} & \frac{e^{-i\alpha}+e^{3i\alpha}}{2} & 0 \\ 0 & 0 & 0 & e^{-i\alpha} \end{pmatrix} \quad (\text{G.11})$$

Thus, finally we have

$$e^{-ig\frac{\sigma_x\sigma_x+\sigma_y\sigma_y+\sigma_z\sigma_z}{2}t} = \begin{pmatrix} e^{-i\frac{g}{2}t} & 0 & 0 & 0 \\ 0 & \frac{e^{-i\frac{g}{2}t}+e^{3i\frac{g}{2}t}}{2} & \frac{e^{-i\frac{g}{2}t}-e^{3i\frac{g}{2}t}}{2} & 0 \\ 0 & \frac{e^{-i\frac{g}{2}t}-e^{3i\frac{g}{2}t}}{2} & \frac{e^{-i\frac{g}{2}t}+e^{3i\frac{g}{2}t}}{2} & 0 \\ 0 & 0 & 0 & e^{-i\frac{g}{2}t} \end{pmatrix}. \quad (\text{G.12})$$

H.1 Quantum Noise Spectrum and Rate Equation

One fascinating feature of the cavity optomechanical system is the ability to cool down, i.e., reduce the number of phonons in the mechanical mode under concern. This is done by employing the beam-splitter-type interaction described above, since the phonon-annihilating anti-Stokes scattering overwhelms the reverse process with the help of the cavity. This is often called the “laser cooling” or “sideband cooling” of mechanical mode in close similarity with those that have been familiar techniques to cool down the motions of trapped atoms or ions.

To illustrate how it works and how cold the modes can be laser-cooled, we follow the quantum noise approach. The noise spectrum with a quantum-mechanical quantity is defined as

$$S_{cc}(\omega) = \int_{-\infty}^{\infty} d\tau e^{i\omega\tau} \langle c(\tau)c(0) \rangle \quad (\text{H.1})$$

mimicking the one with a classical quantity. The angled braces stand for the expectation value. With $c(t)$ being defined by the difference between operator itself and its expectation value, S_{cc} is actually the noise spectrum. We are here interested in the optical noise generated by the presence of mechanical motion through the optomechanical interaction, and how these noises can be utilized in the cavity cooling.

Our starting point is the photon noise in the interaction part

$$\mathcal{H}_{int} = \hbar g_0 (a^\dagger a - \langle a^\dagger a \rangle) (b + b^\dagger) = \hbar g_0 \nu(t) (b + b^\dagger) \quad (\text{H.2})$$

of the Hamiltonian $\mathcal{H} = \mathcal{H}_0 + \mathcal{H}_{int}$, where the overall phase of the interaction is changed so that the minus sign vanishes. Since the optomechanical interaction acts as a perturbation, things are going to be handy in the interaction picture. Let the phonon

number state in the Schrödinger picture be $|N\rangle$ that satisfies $b^\dagger b|N\rangle = N|N\rangle$. This is represented in the interaction picture as $|N, t\rangle = U_I(t)|N\rangle$ with the unitary operator satisfying the equation

$$i\hbar \frac{\partial U_I(t)}{\partial t} = \mathcal{H}_{int}^I(t)U_I(t) \quad (\text{H.3})$$

where

$$\mathcal{H}_{int}^I(t) = e^{i\frac{\mathcal{H}_0}{\hbar}t}\mathcal{H}_{int}e^{-i\frac{\mathcal{H}_0}{\hbar}t} \quad (\text{H.4})$$

$$= \hbar g_0\nu(t)(be^{-i\omega_m t} + b^\dagger e^{i\omega_m t}). \quad (\text{H.5})$$

A formal solution of this differential equation is approximated as

$$U_I(t) = 1 - \frac{i}{\hbar} \int_0^t d\tau \mathcal{H}_{int}^I(\tau)U_I(\tau) \quad (\text{H.6})$$

$$= 1 - \frac{i}{\hbar} \int_0^t d\tau \mathcal{H}_{int}^I(\tau) \left[1 - \frac{i}{\hbar} \int_0^t d\tau' \mathcal{H}_{int}^I(\tau') \left(1 + \dots \right) \right] \quad (\text{H.7})$$

$$\simeq 1 - \frac{i}{\hbar} \int_0^t d\tau \mathcal{H}_{int}^I(\tau). \quad (\text{H.8})$$

We are to evaluate the probability amplitude $\alpha_{N \rightarrow N \pm 1}$ of the event that after a interaction time t , $|N, t\rangle$ evolves to the phonon number state $|N \pm 1\rangle$.

$$\alpha_{N \rightarrow N+1} = \langle N+1 | N, t \rangle \quad (\text{H.9})$$

$$= \langle N+1 | N \rangle - ig_0 \int_0^t d\tau \nu(\tau) \langle N+1 | be^{-i\omega_m \tau} + b^\dagger e^{i\omega_m \tau} | N \rangle \quad (\text{H.10})$$

$$= -ig_0 \int_0^t d\tau \nu(\tau) \left[\langle N+1 | b | N \rangle e^{-i\omega_m \tau} + \langle N+1 | b^\dagger | N \rangle e^{i\omega_m \tau} \right] \quad (\text{H.11})$$

$$= -ig\sqrt{N+1} \int_0^t d\tau \nu(\tau) e^{i\omega_m \tau}, \quad (\text{H.12})$$

$$\alpha_{N \rightarrow N-1} = \dots \quad (\text{H.13})$$

$$= -ig\sqrt{N} \int_0^t d\tau \nu(\tau) e^{-i\omega_m \tau}. \quad (\text{H.14})$$

We then obtain probabilities of finding the system in $|N \pm 1\rangle$ after the time evolution by taking square of α 's and its expectation value:

$$P_{N \rightarrow N+1} = \langle \alpha_{N \rightarrow N+1}^* \alpha_{N \rightarrow N+1} \rangle = g_0^2(N+1) \int_0^t d\tau \int_0^t d\tau' \langle \nu(\tau)\nu(\tau') \rangle e^{-i\omega_m(\tau-\tau')} \quad (\text{H.15})$$

$$= g_0^2(N+1) \int_0^t d\tau S_{\nu\nu}(-\omega_m) \quad (\text{H.16})$$

$$= g_0^2(N+1)t S_{\nu\nu}(-\omega_m), \quad (\text{H.17})$$

$$P_{N \rightarrow N-1} = \langle \alpha_{N \rightarrow N-1}^* \alpha_{N \rightarrow N-1} \rangle = \dots \quad (\text{H.18})$$

$$= g_0^2 N t S_{\nu\nu}(\omega_m). \quad (\text{H.19})$$

by using the Wiener–Khinchin theorem. Given these formulae, the transition rates of above two processes are

$$\Gamma_{N \rightarrow N+1} = \frac{dP_{N \rightarrow N+1}}{dt} = g_0^2(N+1)S_{\nu\nu}(-\omega_m) = (N+1)\Gamma_{\uparrow}, \quad (\text{H.20})$$

$$\Gamma_{N \rightarrow N-1} = \frac{dP_{N \rightarrow N-1}}{dt} = g_0^2 N S_{\nu\nu}(\omega_m) = N\Gamma_{\downarrow}. \quad (\text{H.21})$$

At this point we notice that the quantum noise spectrum is closely related to the transition rate and thus plays an essential role in the optomechanical interaction. Here the transition rates

$$\Gamma_{\uparrow} = g_0^2 S_{\nu\nu}(-\omega_m) \quad (\text{H.22})$$

$$\Gamma_{\downarrow} = g_0^2 S_{\nu\nu}(\omega_m) \quad (\text{H.23})$$

are the ones of increasing and decreasing phonon number by 1.

Before deriving the concrete form of $S_{\nu\nu}(\omega)$, let us step a bit more into the dynamics of the phonon number. What we want to do is to see the temporal variation of the average number of phonons $\langle N \rangle = \sum_N N P(N)$. The rate of change of the average number of phonon reads

$$\frac{d\langle N \rangle}{dt} = \frac{d}{dt} \sum_N N P(N) \quad (\text{H.24})$$

$$= \sum_N N [(N+1)P(N+1)\Gamma_{\downarrow} + NP(N-1)\Gamma_{\uparrow} - (N+1)P(N)\Gamma_{\uparrow} - NP(N)\Gamma_{\downarrow}] \quad (\text{H.25})$$

$$= \Gamma_{\uparrow} \sum_N (N+1)P(N) - \sum_N \Gamma_{\downarrow} N P(N) \quad (\text{H.26})$$

$$= \Gamma_{\uparrow} \langle N+1 \rangle - \Gamma_{\downarrow} \langle N \rangle \quad (\text{H.27})$$

$$= -(\Gamma_{\downarrow} - \Gamma_{\uparrow}) \langle N \rangle + \Gamma_{\uparrow} \quad (\text{H.28})$$

$$= -\Gamma_{opt} \langle N \rangle + \Gamma_{\uparrow}. \quad (\text{H.29})$$

Note that we made use of the identities $\sum_{N=0}^{\infty} N^2 P(N) = \sum_{N=0}^{\infty} (N+1)^2 P(N+1)$ and $\sum_{N=0}^{\infty} N(N+1)P(N+1) = \sum_{N=0}^{\infty} (N-1)NP(N)$ in the third line. This is the rate equation for mechanical phonon without any intrinsic loss. $\Gamma_{opt} = \Gamma_{\downarrow} - \Gamma_{\uparrow}$ denotes the optical damping, which is essential for the cavity cooling. If we incorporate the intrinsic loss of the mechanical mode Γ_m and the effect

of thermal phonons with the average phonon number being n_{th} , the rate equation is modified as

$$\frac{d\langle N \rangle}{dt} = \Gamma_\uparrow \langle N + 1 \rangle - \Gamma_\downarrow \langle N \rangle + \langle N + 1 \rangle \Gamma_\uparrow^{th} - \langle N \rangle \Gamma_\downarrow^{th} \quad (\text{H.30})$$

$$= -(\Gamma_{opt} + \Gamma_m) \langle N \rangle + \Gamma_\uparrow + n_{th} \Gamma_m \quad (\text{H.31})$$

where use has been made of $\Gamma_\uparrow^{th} = n_{th} \Gamma_m$ and $\Gamma_\downarrow^{th} = (n_{th} + 1) \Gamma_m$. The final number of phonons reached after the cavity cooling is thus estimated to be

$$\langle N \rangle_{t \rightarrow \infty} = \frac{\Gamma_\uparrow + n_{th} \Gamma_m}{\Gamma_{opt} + \Gamma_m}. \quad (\text{H.32})$$

H.2 Limits on the Cavity Cooling

In order to know how cold you can get the mechanical mode with the cavity cooling, remaining thing is to evaluate the quantum noise spectrum

$$S_{\nu\nu}(\omega) = \int_{-\infty}^{\infty} d\tau e^{i\omega\tau} \langle \nu(\tau)\nu(0) \rangle \quad (\text{H.33})$$

with $\nu(t) = a^\dagger a - \langle a^\dagger a \rangle$. Plugging this into $\langle \nu(\tau)\nu(0) \rangle$, we have

$$\langle \nu(\tau)\nu(0) \rangle = \langle (a^\dagger(\tau)a(\tau) - \langle a^\dagger(\tau)a(\tau) \rangle)(a^\dagger(0)a(0) - \langle a^\dagger(0)a(0) \rangle) \rangle \quad (\text{H.34})$$

$$= \langle a^\dagger(\tau)a(\tau)a^\dagger(0)a(0) - a^\dagger(\tau)a(\tau)\langle a^\dagger(0)a(0) \rangle \rangle \quad (\text{H.35})$$

$$- \langle a^\dagger(0)a(0)\langle a^\dagger(\tau)a(\tau) \rangle + \langle a^\dagger(\tau)a(\tau) \rangle\langle a^\dagger(0)a(0) \rangle \rangle \quad (\text{H.36})$$

$$= \langle a^\dagger(\tau)a(\tau)a^\dagger(0)a(0) \rangle - 2\langle a^\dagger(0)a(0) \rangle^2 + \langle a^\dagger(0)a(0) \rangle^2 \quad (\text{H.37})$$

$$= \langle a^\dagger(\tau)a(\tau)a^\dagger(0)a(0) \rangle - n_{cav}^2. \quad (\text{H.38})$$

Suppose that the photon operator a can be written in a form $a(t) = [\alpha + d(t)] e^{-i\omega_l t}$ where α denotes the amplitude of the coherent drive and $d(t)$ the fluctuation. By definition, when it acts on a state, $a(t)|\psi(t)\rangle = \alpha e^{-i\omega_l t}|\psi(t)\rangle$ and $d(t)|\psi(t)\rangle = \langle\psi(t)|d^\dagger(t) = 0$. In calculating $\langle a^\dagger(\tau)a(\tau)a^\dagger(0)a(0) \rangle$, the only surviving terms are the ones having d on the leftmost and d^\dagger on the rightmost and the one without any operators. Thus the above expression turns out to be

$$\langle \nu(\tau)\nu(0) \rangle = \langle a^\dagger(\tau)a(\tau)a^\dagger(0)a(0) \rangle - n_{cav}^2 \quad (\text{H.39})$$

$$= \alpha^* \alpha \alpha^* \alpha + \alpha^* \alpha \langle d(\tau)d^\dagger(0) \rangle - n_{cav}^2 \quad (\text{H.40})$$

$$= n_{cav} \langle d(\tau)d^\dagger(0) \rangle \quad (\text{H.41})$$

There appears the term $\langle d(\tau)d^\dagger(0) \rangle$ which seems to be difficult to approach. However, “quantum regression theorem” [31] allows us to write down the equation for this quantity by the same form as for $d(t)$, that is,

$$\frac{d\langle d(\tau)d^\dagger(0) \rangle}{dt} = -i\Delta_c \langle d(\tau)d^\dagger(0) \rangle - \frac{\kappa}{2} \langle d(\tau)d^\dagger(0) \rangle \quad \text{for } t \geq 0, \quad (\text{H.42})$$

therefore $\langle d(\tau)d^\dagger(0) \rangle = \exp[-i\Delta_c t - (\kappa/2)t]$, where $\Delta_c = \omega_c - \omega_l$ and κ the loss rate of the cavity. Then the quantum noise spectrum can be explicitly calculated:

$$S_{\nu\nu}(\omega) = \int_{-\infty}^{\infty} d\tau e^{i\omega\tau} \exp\left[-i\Delta_c t - \frac{\kappa}{2}t\right] \quad (\text{H.43})$$

$$= \frac{\kappa n_{cav}}{(\Delta_c - \omega)^2 + (\kappa/2)^2}. \quad (\text{H.44})$$

In the rate equation, noise spectra appear in the forms $S_{\nu\nu}(\pm\omega_m)$. These are the “noises” (or in another viewpoint, the “signals”) exposed to the optical mode by the mechanical mode, each of which has Lorentzian peak at $\pm\omega_m$.

We immediately get the full expression of the transition rates Γ_\uparrow and Γ_{opt} using this noise spectrum, leading to

$$\Gamma_\uparrow = g_0^2 S_{\nu\nu}(-\omega_m) \quad (\text{H.45})$$

$$= g_0^2 \frac{\kappa}{(\Delta_c + \omega_m)^2 + (\kappa/2)^2} n_{cav} \quad (\text{H.46})$$

$$\Gamma_{opt} = g_0^2 [S_{\nu\nu}(\omega_m) - S_{\nu\nu}(-\omega_m)] \quad (\text{H.47})$$

$$= g_0^2 \left[\frac{\kappa}{(\Delta_c - \omega_m)^2 + (\kappa/2)^2} - \frac{\kappa}{(\Delta_c + \omega_m)^2 + (\kappa/2)^2} \right] n_{cav} \quad (\text{H.48})$$

Now we revisit the lowest number of phonons achievable with the cavity cooling

$$\langle N \rangle_{t \rightarrow \infty} = \frac{\Gamma_\uparrow + n_{th}\Gamma_m}{\Gamma_{opt} + \Gamma_m}. \quad (\text{H.49})$$

We assume here that the frequency of the mechanical mode is much larger than the linewidth of the cavity mode, so that the noise spectrum originated in the mechanical mode is well separated from the signal of the cavity in the frequency domain. This regime is called the resolved sideband regime. When the cooling rate Γ_{opt} is much smaller than Γ_m , it holds trivially that $\langle N \rangle_{t \rightarrow \infty} = n_{th}$, where the system remains in the initial thermal state. When the spectrum of the mechanical mode is sufficiently narrow and $\Gamma_{opt} \gg \Gamma_m$ holds, we have

$$\langle N \rangle_{t \rightarrow \infty} = \frac{\Gamma_\uparrow}{\Gamma_{opt}} = \frac{(\Delta_c - \omega_m)^2 + (\kappa/2)^2}{4\omega_m \Delta_c} \quad (\text{H.50})$$

This is minimized when $\Delta_c = \omega_m$ and gives a minimum available number of phonons $\kappa^2/16\omega_m^2$, which is well below 1 since $\kappa \ll \omega_m$ in the resolved sideband regime. Another thing we should note is that the cooling rate Γ_{opt} is proportional to the number of photons in the cavity, therefore the cooling rate can relatively easily become larger than the decay rate of the high-Q mechanical mode. Given these estimations, the cavity optomechanical system has been a cutting-edge of the modern quantum physics as the one being capable of seeing the quantum behavior of macroscopic (\gg atomic scale) objects.

Entangled States and Quantum Teleportation

This appendix introduces the quantum entanglement and its celebrated applications.

I.1 Separable and Entangled States

Suppose there are two quantum systems labeled 1 and 2. A composite quantum system can be like $|\psi_1\rangle \otimes |\psi_2\rangle \stackrel{\text{def}}{=} |\psi_1\psi_2\rangle$ that is friendly to our intuition. This kind of composite quantum systems, which is decomposed into the product of the constituent individual quantum systems, are said to be separable states. In general, the separable state is written in terms of the density matrices of the subsystems ρ_1^i and ρ_2^i as $\rho = \sum_i p_i \rho_1^i \otimes \rho_2^i$ with probabilities p_i .

On the other hand, there are states that cannot be decomposed into such a product. The most famous ones are Bell states $|\Psi_{12}^\pm\rangle = (|e_1g_2\rangle \pm |g_1e_2\rangle)/\sqrt{2}$ and $|\Phi_{12}^\pm\rangle = (|e_1e_2\rangle \pm |g_1g_2\rangle)/\sqrt{2}$. Bell states cannot be written as a separable states in any basis transformation as one can immediately check by *reductio ad absurdum*. Other non-separable states are, e.g. a Schrödinger's cat ($|g\rangle |\alpha\rangle + |e\rangle |-\alpha\rangle$)/ $\sqrt{2}$ with coherent states $|\pm\alpha\rangle$ of a harmonic oscillator, Greenberger–Horne–Zeilinger (GHZ) state $(|g\cdots g\rangle + |e\cdots e\rangle)/\sqrt{2}$ of a many-qubit system, N00N ("Noon") state $(|N\rangle |0\rangle + |0\rangle |N\rangle)/\sqrt{2}$ of two harmonic oscillators. These family of non-separable states are named entangled states.

I.2 Measures of Entanglement

One might expect there is some measure of the degree or at least the existence of the entanglement. Actually there are several attempts to develop such a quantity, however, there is no satisfactory one that can be used to judge whether a quantum state is entangled or not. However, for a two-qubit system, there are good measures telling the existence and degree of entanglement.

I.2.1 Entanglement Entropy

We can see below what information can be extracted when we focus on one of the subsystems in the composite system, represented by a reduced density matrix. Moreover, we will try to calculate the von Neumann entropy of the reduced density matrix, a quantity called an entanglement entropy.

First, the reduced density matrix $\tilde{\rho}_1$ or $\tilde{\rho}_2$ is a density matrix of the composite system ρ_{12} traced out for one of the two constituent quantum systems: $\tilde{\rho}_1 = \text{Tr}_2 \rho_{12}$ or $\tilde{\rho}_2 = \text{Tr}_1 \rho_{12}$. Let us consider two cases, the separable state $|\Psi_0\rangle = |g_1\rangle(|g_2\rangle + |e_2\rangle)/\sqrt{2}$ and one of the Bell state $|\Phi^+\rangle = (|g_1, g_2\rangle + |e_1, e_2\rangle)/\sqrt{2}$. On one hand, reduced density matrices of $|\Psi_0\rangle$ is easily obtained as $\tilde{\rho}_1 = |g_1\rangle\langle g_1|$ and $\tilde{\rho}_2 = (|g_2\rangle + |e_2\rangle)(\langle g_2| + \langle e_2|)/2$, the density matrices that can be derived from the original individual states $|g_1\rangle$ and $(|g_2\rangle + |e_2\rangle)/\sqrt{2}$. On the other hand, for $|\Phi^+\rangle$ the reduced density matrices reads $\tilde{\rho}_1 = I/2$ and $\tilde{\rho}_2 = I/2$ as well, meaning that by taking a trace over one Hilbert space, the quantum state in the other Hilbert space is completely ruined, down to the completely mixed state.

Next, let us define one of the measures of the entanglement. The quantum von Neumann entropy is defined in analogy to the Shannon entropy as $-\text{tr}\{\rho \log \rho\}$. For a pure state $|\psi\rangle$, quantum von Neumann entropy can be calculated by using eigenvalues λ_k of the density matrix as $-\text{tr}\{\rho \log \rho\} = -\sum_k \lambda_k \log \lambda_k = 0$, since the eigenvalues are either 0 or 1. If the density matrix is a completely mixed state $\rho = I/2$, the von Neumann entropy reads $\log 2$. In a similar manner, the entanglement entropy S_1 or S_2 is defined by the von Neumann entropy of the reduced density matrix ρ_1 or ρ_2 , respectively:

$$S_1 = -\text{Tr}[\rho_1 \log \rho_1], \quad S_2 = -\text{Tr}[\rho_2 \log \rho_2]. \quad (\text{I.1})$$

For the quantum state $|\Psi_0\rangle$, $S_1 = S_2 = 0$. In contrast, the Bell state $|\Phi^+\rangle$ yields the entanglement entropy of $\log 2$. One might want to think that non-zero entanglement entropy signals the entanglement, however, the state $\rho_{12} = (|g, g\rangle + |g, e\rangle + |e, g\rangle + |e, e\rangle)/4$, the completely mixed state, also gives $\rho_1 = I/2$ and $\rho_2 = I/2$ to yield $S_1 = S_2 = \log 2$. The entanglement entropy is a good measure only when we consider pure states.

I.2.2 Negativity

Instead of considering the reduced density matrix, we shall take a look at the density matrix ρ of the composite quantum system comprised of qubit A and qubit B. ρ is of course Hermitian, that is, $\rho^\dagger = (\rho^T)^* = \rho$. Since its diagonal components represent the probability, its eigenvalues should be non-negative.

Let us then think about what happens with the partial transposition of ρ , which is denoted by ρ^{T_A} . We explicitly write the density matrix in general as

$$\rho = \sum_{\xi_A, \eta_A, \xi_B, \eta_B} p_{\xi_A \eta_A \xi_B \eta_B} |\xi_A\rangle \langle \eta_A| \otimes |\xi_B\rangle \langle \eta_B| \quad (\text{I.2})$$

with $|\xi_A\rangle, |\eta_A\rangle \in \{|g_A\rangle, |e_A\rangle\}$ and $|\xi_B\rangle, |\eta_B\rangle \in \{|g_B\rangle, |e_B\rangle\}$. According to this expression, the partial transposition reads

$$\rho^{T_A} = \sum_{\xi_A, \eta_A, \xi_B, \eta_B} p_{\xi_A \eta_A \xi_B \eta_B} |\eta_A\rangle \langle \xi_A| \otimes |\xi_B\rangle \langle \eta_B|. \quad (\text{I.3})$$

This is Hermitian again, meaning that the eigenvalues of ρ^{T_A} is still real. However, the eigenvalues are not necessarily non-negative. An exceptional situation is that ρ is separable. Peres–Horodecki criterion [32] states that if ρ is separable, then all the eigenvalues of ρ^{T_A} are non-negative. Therefore, an existence of negative eigenvalues in ρ^{T_A} heralds the existence of quantum entanglement in ρ . On top of that, the converse is true with the two-qubit system: the separability of ρ and non-negativity of the eigenvalues of ρ^{T_A} are equivalent in two-qubit systems.

Here we saw an essential idea of negativity, an alternative entanglement measure. Negativity $\mathcal{N}(\rho)$ is defined as a sum of absolute values of the negative eigenvalues of ρ^{T_A} :

$$\mathcal{N}(\rho) = \sum_{\lambda_n < 0} |\lambda_n| \quad (\text{I.4})$$

where λ_n are eigenvalues of ρ^{T_A} . Since ρ^{T_A} is just a partial transposition of ρ , the trace should be preserved, i.e. $\text{Tr}[\rho] = \text{Tr}[\rho^{T_A}] = 1$. Thence it holds that $1 = \sum_n \lambda_n = \sum_{\lambda_n > 0} \lambda_n - \sum_{\lambda_n < 0} |\lambda_n|$. We further define a trace norm $\|\rho^{T_A}\|_1 \stackrel{\text{def}}{=} \text{Tr}[\sqrt{(\rho^{T_A})^\dagger \rho^{T_A}}]$. Since this definition sums up the absolute values of the eigenvalues of ρ^{T_A} , $\|\rho^{T_A}\|_1 = \sum_n |\lambda_n| = 2 \sum_{\lambda_n < 0} |\lambda_n| + 1$. Here an alternative expression of the negativity is achieved:

$$\mathcal{N}(\rho) = \frac{\|\rho^{T_A}\|_1 - 1}{2} \quad (\text{I.5})$$

The Peres–Horodecki criterion for the negativity is valid for mixed state, providing a more general measure than the entanglement entropy that is only useful for pure states. In order for the entanglement measure to be additive when the two systems are synthesized, One might use logarithmic negativity $\mathbb{L}(\rho) \stackrel{\text{def}}{=} \log[2\mathcal{N}(\rho) + 1]$. With this quantity, we have a nice formula $\mathbb{L}(\rho_1 \otimes \rho_2) = \mathbb{L}(\rho_1) + \mathbb{L}(\rho_2)$.

As an example, let us take a glimpse of the Bell state $|\Phi^+\rangle$. The density matrix ρ_{Φ^+} reads

$$\rho_{\Phi^+} = \frac{1}{2} \begin{pmatrix} 1 & 0 & 0 & 1 \\ 0 & 0 & 0 & 0 \\ 0 & 0 & 0 & 0 \\ 1 & 0 & 0 & 1 \end{pmatrix} \quad (\text{I.6})$$

and its partial transposition does

$$\rho_{\Phi^+}^{T_A} = \frac{1}{2} \begin{pmatrix} 1 & 0 & 0 & 0 \\ 0 & 0 & 1 & 0 \\ 0 & 1 & 0 & 0 \\ 0 & 0 & 0 & 1 \end{pmatrix}. \quad (\text{I.7})$$

The eigenvalues of this partially transposed density matrix are three $1/2$ and one $-1/2$. Provided these, the negativity is $1/2$ and the logarithmic negativity is $\log 2$.

A more interesting example is Werner state

$$\rho_W = p |\Phi^+\rangle\langle\Phi^+| + (1-p) \frac{I \otimes I}{4} \quad (\text{I.8})$$

$$= \frac{p}{2} \begin{pmatrix} 1 & 0 & 0 & 1 \\ 0 & 0 & 0 & 0 \\ 0 & 0 & 0 & 0 \\ 1 & 0 & 0 & 1 \end{pmatrix} + \frac{1-p}{4} \begin{pmatrix} 1 & 0 & 0 & 0 \\ 0 & 1 & 0 & 0 \\ 0 & 0 & 1 & 0 \\ 0 & 0 & 0 & 1 \end{pmatrix} \quad (\text{I.9})$$

$$= \begin{pmatrix} \frac{1+p}{4} & 0 & 0 & \frac{p}{2} \\ 0 & \frac{1-p}{4} & 0 & 0 \\ 0 & 0 & \frac{1-p}{4} & 0 \\ \frac{p}{2} & 0 & 0 & \frac{1+p}{4} \end{pmatrix}. \quad (\text{I.10})$$

Whether this state is entangled or not depends on the value of p and we are to clarify the threshold. The partial transposition of this appears as

$$\rho_W^{T_A} = \begin{pmatrix} \frac{1+p}{4} & 0 & 0 & 0 \\ 0 & \frac{1-p}{4} & \frac{p}{2} & 0 \\ 0 & \frac{p}{2} & \frac{1-p}{4} & 0 \\ 0 & 0 & 0 & \frac{1+p}{4} \end{pmatrix}, \quad (\text{I.11})$$

which yields eigenvalues three $(1+p)/4$ and one $(1-3p)/4$. The latter takes a negative value when $1/3 < p \leq 1$, so that according to the Peres–Horodecki criterion, the Werner state is entangled only if $1/3 < p \leq 1$ and separable when $0 \leq p \leq 1/3$. Here the term “entangled” stands for another sense: the Werner state with $1/3 < p \leq 1$ cannot be generated through local operation and classical communication (LOCC, see the last section of this appendix) starting from the separable state, whereas the one with $0 \leq p \leq 1/3$ can be.

I.3 Quantum Teleportation

In this section, we introduce the concept of quantum teleportation as an application of the entangled state, as well as an interesting phenomena exhibited by the quantum world. All the thing wanted be done is transmitting an unknown state $|\psi\rangle = c_g|g_\psi\rangle + c_e|e_\psi\rangle$ from a transmitter Alice, to a receiver Bob. The subscript ψ is the reminder of the quantum states belonging to $|\psi\rangle$. Alice should keep $|\psi\rangle$ unknown in contrast to the classical communication because once Alice knows the quantum state by measurement, the measured state has no longer be the same state as $|\psi\rangle$. One might keep a copy of the transmitted information in the classical communication, however, no-cloning theorem inhibits that. Therefore, sending an unknown state requires special trick that fully utilizes the bizarre nature of entangled state.

First thing to do is to share an entangled pair, say $|\Psi_{ab}^-\rangle = (|e_a\rangle|g_b\rangle + |g_a\rangle|e_b\rangle)/\sqrt{2}$, between Alice and Bob. Here the subscripts a and b indicates the qubit systems of Alice and Bob. Combining together with $|\psi\rangle$, a whole quantum state reads $|\psi\rangle|\Psi_{ab}^-\rangle$. Let us rewrite this state in terms of Bell states involving Alice's qubit and the qubit system ψ . Using $|\Psi_{\psi a}^\pm\rangle(|\psi\rangle|\Psi_{ab}^-\rangle) = (\pm c_g|g_b\rangle - c_e|e_b\rangle)/2\sqrt{2}$ and $|\Phi_{\psi a}^\pm\rangle(|\psi\rangle|\Psi_{ab}^-\rangle) = (c_e|g_b\rangle \mp c_g|e_b\rangle)/2\sqrt{2}$, we have

$$|\psi\rangle|\Psi_{ab}^-\rangle = \frac{c_g|g_\psi\rangle + c_e|e_\psi\rangle}{\sqrt{2}} \frac{|e_a\rangle|g_b\rangle + |g_a\rangle|e_b\rangle}{\sqrt{2}} \quad (I.12)$$

$$= \frac{|\Psi_{\psi a}^+\rangle}{2}(c_g|g_b\rangle - c_e|e_b\rangle) - \frac{|\Psi_{\psi a}^-\rangle}{2}(c_g|g_b\rangle + c_e|e_b\rangle) \quad (I.13)$$

$$+ \frac{|\Phi_{\psi a}^+\rangle}{2}(c_e|g_b\rangle - c_g|e_b\rangle) + \frac{|\Phi_{\psi a}^-\rangle}{2}(c_e|g_b\rangle + c_g|e_b\rangle) \quad (I.14)$$

Alice then operates an X gate, X_a , on their qubit and successively the CNOT gate with Alice's qubit being the control qubit and ψ the target one. Then we have $|\Psi_{\psi a}^\pm\rangle \rightarrow \text{CNOT} \cdot X_a |\Psi_{\psi a}^\pm\rangle = |g_\psi\rangle(\pm|g_a\rangle + |e_a\rangle)/\sqrt{2}$ and $|\Phi_{\psi a}^\pm\rangle \rightarrow \text{CNOT} \cdot X_a |\Phi_{\psi a}^\pm\rangle = |e_\psi\rangle(|g_a\rangle \pm |e_a\rangle)/\sqrt{2}$ for the subsystem ψa . Finally Alice operates the Hadamard gate H_a for their qubit to obtain

$$|\Psi_{\psi a}^+\rangle(c_g|g_b\rangle - c_e|e_b\rangle) \rightarrow H_a \cdot \text{CNOT} \cdot X_a |\Psi_{\psi a}^+\rangle(c_g|g_b\rangle - c_e|e_b\rangle) \quad (I.15)$$

$$= |g_\psi\rangle|g_a\rangle(c_g|g_b\rangle - c_e|e_b\rangle), \quad (I.16)$$

$$|\Psi_{\psi a}^-\rangle(c_g|g_b\rangle + c_e|e_b\rangle) \rightarrow H_a \cdot \text{CNOT} \cdot X_a |\Psi_{\psi a}^-\rangle(c_g|g_b\rangle + c_e|e_b\rangle) \quad (I.17)$$

$$= |g_\psi\rangle|e_a\rangle(c_g|g_b\rangle + c_e|e_b\rangle), \quad (I.18)$$

$$|\Phi_{\psi a}^+\rangle(c_e|g_b\rangle - c_g|e_b\rangle) \rightarrow H_a \cdot \text{CNOT} \cdot X_a |\Phi_{\psi a}^+\rangle(c_e|g_b\rangle - c_g|e_b\rangle) \quad (I.19)$$

$$= |e_\psi\rangle|g_a\rangle(c_e|g_b\rangle - c_g|e_b\rangle), \quad (I.20)$$

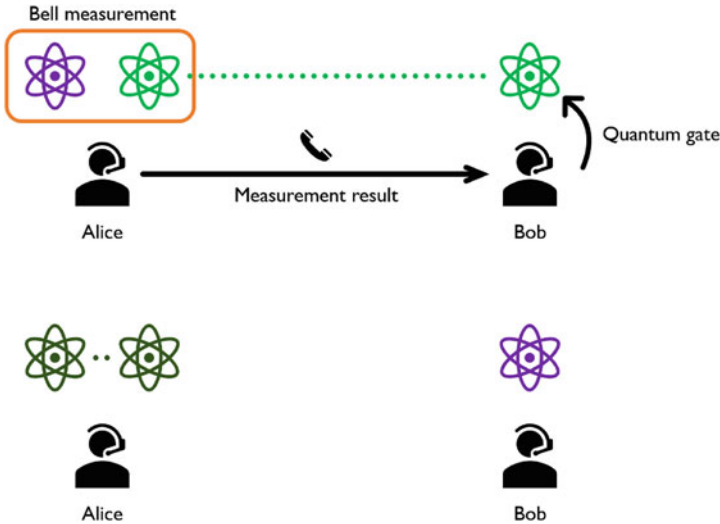


Fig. I.1 Schematics of quantum teleportation

$$\left| \Phi_{\psi a}^- \right\rangle (c_e |g_b\rangle + c_g |e_b\rangle) \rightarrow H_a \cdot \text{CNOT} \cdot X_a \left| \Phi_{\psi a}^- \right\rangle (c_e |g_b\rangle + c_g |e_b\rangle) \quad (\text{I.21})$$

$$= -|e_\psi\rangle |e_a\rangle (c_e |g_b\rangle + c_g |e_b\rangle), \quad (\text{I.22})$$

With this knowledge, Alice measures the system ψa in the bases $|g_\psi\rangle |g_a\rangle$, $|g_\psi\rangle |e_a\rangle$, $|e_\psi\rangle |g_a\rangle$ and $|e_\psi\rangle |e_a\rangle$, which is termed Bell measurement. Alice should tell Bob the measurement result in order to finish their work. If Alice's measurement says the system ψa is in $|g_\psi\rangle |g_a\rangle$, then Bob should operate Z gate Z_b on their qubit. When it says $|e_\psi\rangle |g_a\rangle$, Bob does Z_b gate and then X_b gate. For $|e_\psi\rangle |e_a\rangle$, X_b gate is fine, and nothing is to be done for the measurement result $|g_\psi\rangle |e_a\rangle$. All the way here, Bob has a quantum state $|\psi\rangle = c_g |g_b\rangle + c_e |e_b\rangle$, the very state that Alice wanted to transmit. At the time when Alice made measurement, the quantum state $|\psi\rangle$ had been destroyed, so that the quantum state is not copied (Fig. I.1).

I.4 Entanglement Swapping

As a close relative of the quantum teleportation, we here introduce entanglement swapping which is of frequent use in the quantum communication. The problem is as follows. Alice and Bob have pairs of known entangled states, say $|\Phi_A^+\rangle = (|g_1g_2\rangle + |e_1e_2\rangle)/\sqrt{2}$ for Alice and $|\Phi_B^+\rangle = (|g_3g_4\rangle + |e_3e_4\rangle)/\sqrt{2}$ for Bob. Then Alice and Bob want to somehow generate an entangled state shared between them. This can be accomplished by the Bell measurement of the two-qubit system consisting of one Alice's qubit and one Bob's, and successively applying local quantum operations. Let us briefly see how this works.

The total system $|\Psi\rangle$ including Alice's and Bob's entangled states is written as

$$|\Psi\rangle = |\Phi_A^+\rangle \otimes |\Phi_B^+\rangle \quad (\text{I.23})$$

$$= \frac{|g_1g_2g_3g_4\rangle + |g_1g_2e_3e_4\rangle + |e_1e_2g_3g_4\rangle + |e_1e_2e_3e_4\rangle}{2}. \quad (\text{I.24})$$

By defining the Bell states of the subsystem involving the first and the fourth (the second and the third) qubits as $|\Psi_{14}^\pm\rangle$ and $|\Phi_{14}^\pm\rangle$ ($|\Psi_{23}^\pm\rangle$ and $|\Phi_{23}^\pm\rangle$) as in the previous section, we can rewrite $|\Psi\rangle$ as

$$|\Psi\rangle = \frac{|\Phi_{14}^+\rangle|\Phi_{23}^+\rangle + |\Phi_{14}^-\rangle|\Phi_{23}^-\rangle + |\Psi_{14}^+\rangle|\Psi_{23}^+\rangle + |\Psi_{14}^-\rangle|\Psi_{23}^-\rangle}{2}. \quad (\text{I.25})$$

Then let us make a Bell measurement for the second and the third qubits, with which the subsystem involving the first and the fourth qubits can be turned into the desired entangled state, say $|\Phi_{14}^+\rangle$. If the Bell measurement says the measured system is in the state $|\Phi_{23}^+\rangle$, the remaining system is projected onto the state $|\Phi_{14}^+\rangle$ and there is nothing we have to do. If in the state $|\Phi_{23}^-\rangle$, Z_1 gate, a Z gate on the first qubit, transforms $|\Phi_{14}^-\rangle$ into $|\Phi_{14}^+\rangle$ and we get the desired state. With the measured state being $|\Psi_{23}^+\rangle$, X_1 gate, an X gate on the first qubit, allows us to get $X_1|\Psi_{14}^+\rangle = |\Phi_{14}^+\rangle$. Finally, when the state $|\Psi_{23}^-\rangle$ is obtained, we apply Z_1X_1 on the remaining system $|\Psi_{14}^-\rangle$, resulting in $|\Phi_{14}^+\rangle$. In this manner, by passing ones of Alice's and Bob's entangled pairs and measuring those qubits in the Bell basis, Alice and Bob acquire an entangled pair between them after the proper local operation (Fig. I.2).

I.5 Local Operation and Classical Communication (LOCC)

In quantum teleportation and entanglement swapping, procedures are summarized as follows: (i) measurement of qubit(s) of one party, represented by a Kraus operator M_A (ii) classical communication to tell the measurement result and (iii) quantum operation U_B on qubit of another party. These are termed as local operation and classical communication (LOCC). If we naively neglect the communication time, the density matrix evolution after above LOCC can be written as $\sum_r U_B(r)M_A(r)\rho M_A^\dagger(r)U_B^\dagger(r)$.

We do not intend to introduce every theoretical detail but list some important properties of LOCC.

- LOCC cannot increase the entanglement measures with unit probability.
- LOCC cannot entangle the separable state.
- LOCC can probabilistically increase the entanglement measure, which is dubbed as the entanglement distillation.

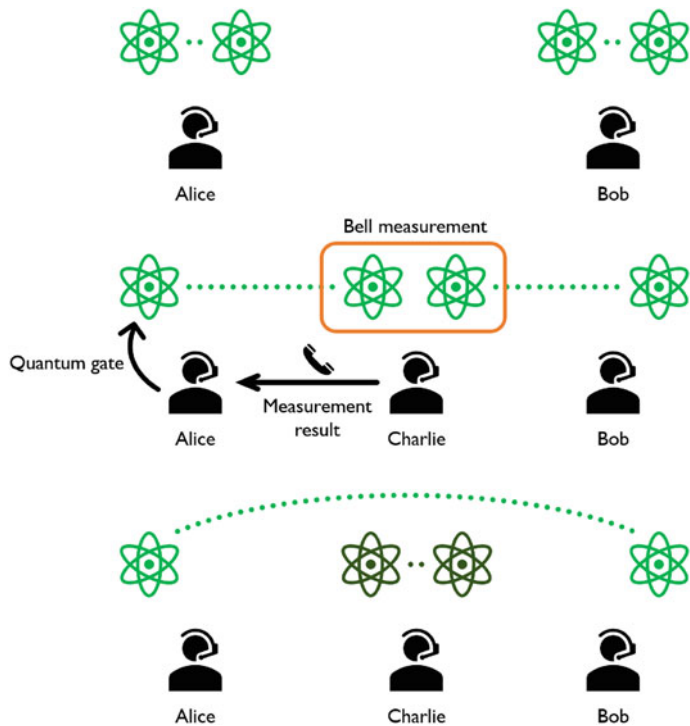


Fig. I.2 Schematics of entanglement swapping

An important operation that is allowed in classical information and not possible in quantum information is copying the state. For example, if a value x is given and we would like to $y = x^2 + x$, then one can first copy x and add 1 to the original x and multiply by the copied x to perform,

$$y = x^2 + x = x(x + 1). \quad (\text{J.1})$$

In quantum information, however, Quantum No-Cloning Theorem prohibits the copying of a quantum state and therefore the calculation cannot be performed in the same way. This first seems to be a huge disadvantage for the quantum computation, but there are number of tricks known so that the quantum computation can actually perform numerous calculations. So please do not worry. Here we show a simple proof of the no-cloning theorem.

Suppose there is an arbitrary quantum state $|\psi\rangle = a|0\rangle + b|1\rangle$ and copy it to another quantum state $|i\rangle$, so that $|i\rangle \rightarrow |\psi\rangle$, using a unitary transformation \hat{U} . Another words, there exist a two-qubit gate,

$$\hat{U}|\psi\rangle|i\rangle = |\psi\rangle|\psi\rangle. \quad (\text{J.2})$$

Similarly, using the same operation \hat{U} , different quantum state $|\phi\rangle$ can also be copied, thus

$$\hat{U}|\phi\rangle|i\rangle = |\phi\rangle|\phi\rangle. \quad (\text{J.3})$$

Using above results,

$$\begin{aligned} \langle\phi|\langle i|U^\dagger U|\psi\rangle|i\rangle &= \langle\phi|\psi\rangle\langle i|i\rangle \\ &= \langle\phi|\psi\rangle, \end{aligned} \quad (\text{J.4})$$

is calculated and likewise,

$$\begin{aligned}\langle \phi | \langle i | U^\dagger U |\psi\rangle |i\rangle &= \langle \phi | \langle \phi | \psi \rangle |\psi\rangle \\ &= \langle \phi | \psi \rangle^2.\end{aligned}\quad (\text{J.5})$$

These results demand $\langle \phi | \psi \rangle = \langle \phi | \psi \rangle^2$, however, it can be only fulfilled with either $\langle \phi | \psi \rangle = 0$ or $\langle \phi | \psi \rangle = 1$. The later is a trivial case, $|\phi\rangle = |\psi\rangle$, and be ignored. Then, the first case tells us that two states can be duplicated only when they are orthogonal, and not for an arbitrary quantum state.

Let us take a look at an actual example. Suppose, operation \hat{U} is capable of duplicating both $|0\rangle$ and $|1\rangle$ as,

$$\hat{U} |0\rangle |i\rangle = |0\rangle |0\rangle \quad (\text{J.6})$$

$$\hat{U} |1\rangle |i\rangle = |1\rangle |1\rangle. \quad (\text{J.7})$$

Now, let's try to copy $|\psi\rangle = a|0\rangle + b|1\rangle$. In quantum information, a measurement will destroy the quantum state, so we need some method of copying an arbitrary quantum state without knowing the state itself.

Performing the same operation to $|\psi\rangle$,

$$\begin{aligned}\hat{U} |\psi\rangle |i\rangle &= \hat{U}(a|0\rangle + b|1\rangle) |i\rangle = a\hat{U}|0\rangle |i\rangle + b\hat{U}|1\rangle |i\rangle \\ &= a|0\rangle |0\rangle + b|1\rangle |1\rangle,\end{aligned}\quad (\text{J.8})$$

is obtained. It may seem like the copying worked, but the state to be copied is $|\psi\rangle = a|0\rangle + b|1\rangle$, so if the actual copying worked, we should have obtained

$$\begin{aligned}|\psi\rangle |\psi\rangle &= (a|0\rangle + b|1\rangle)(a|0\rangle + b|1\rangle) \\ &= a^2|00\rangle + b^2|11\rangle + ab(|01\rangle + |10\rangle).\end{aligned}\quad (\text{J.9})$$

So we were not duplicating the state. It is possible to find an operation \hat{U} , which copies a known state and another state which is orthogonal to the state, however, the same operation cannot be used to duplicate an arbitrary quantum state.

References

1. Shor, P.W.: Algorithms for quantum computation: discrete logarithms and factoring. In: Proceedings 35th Annual Symposium on Foundations of Computer Science, pp. 124–134. IEEE Computer Society Press (1994)
2. Shor, P.W.: Scheme for reducing decoherence in quantum computer memory. Phys. Rev. A **52**, R2493 (1995)
3. Einstein, A., Podolsky, B., Rosen, N.: Phys. Rev. **47**, 777 (1935)
4. Bennett, C.H., Brassard, G., Crépeau, C., Jozsa, R., Peres, A., Wootters, W.K.: Phys. Rev. Lett. **70**, 1895 (1993)
5. Bouwmeester, D., Pan, J.-W., Mattle, K., Eibl, M., Weinfurter, H., Zeilinger, A.: Nature **390**, 575 (1997)
6. Boschi, D., Branca, S., De Martini, F., Hardy, L., Popescu, S.: Phys. Rev. Lett. **80**, 1121 (1998)
7. Bennett, C.H., Brassard, G.: Proceedings of IEEE International Conference on Computers Systems and Signal Processing, p. 175 (1984)
8. Loudon, R.: The Quantum Theory of Light, 3rd edn. Oxford University Press (2000)
9. DeMill, D.: Atomic Physics, 3rd edn. Oxford University Press (2000)
10. Jaynes, R., Cummings, A.: J. Phys. B: Mol. Opt. Phys. **38**(9), S551 (2005)
11. Molmer, K., Sørensen, A.: Multiparticle entanglement of hot trapped ions. Phys. Rev. Lett. **82**, 1835 (1999)
12. Gaebler, J.P., Tan, T.R., Lin, Y., Wan, Y., Bowler, R., Keith, A.C., Glancy, S., Coakley, K., Knill, E., Leibfried, D., Wineland, D.J.: High-fidelity universal gate set for ${}^9\text{Be}^+$ ion qubits. Phys. Rev. Lett. **117**, 060505 (2016)
13. Johansson, J.R., Nation, P.D., Nori, F.: QuTiP 2: a Python framework for the dynamics of open quantum systems. Comp. Phys. Comm. **184**, 1234–1240 (2013)
14. Yariv, A.: Quantum Electronics. Wiley, New York (1989)
15. Feynmann, R.P., Leighton, R.B., Sands, M.: The Feynman Lectures on Physics, vol. 3, Chapter 21 (Basic Books); https://www.feynmanlectures.caltech.edu/III_21.html
16. Schuster, D.I., Houck, A.A., Schreier, J.A., Wallraff, A., Gambetta, J.M., Blais, A., Frunzio, L., Johnson, B., Devoret, M.H., Girvin, S.M., Schoelkopf, R.J.: Resolving photon number states in a superconducting circuit. Nature **445**, S15 (2007)
17. Auffeves-Garnier, A., Simon, C., Gerard, J.-M., Poizat, J.-P.: Giant optical nonlinearity induced by a single two-level system interacting with a cavity in the Purcell regime. Phys. Rev. A **75**, 053823 (2007)

18. Nielsen, M., Chuang, I.: Quantum Computation and Quantum Information, 10th anniversary ed. Cambridge University Press (2010)
19. Emerson, J., Alicki, R., Zyczkowski, K.: Scalable noise estimation with random unitary operators. *J. Opt. B: Quantum Semiclass. Opt.* **7**, S347 (2005)
20. Fujii, K.: Quantum Computation with Topological Codes. Springer (2015)
21. Fukui, K., Tomita, A., Okamoto, A., Fujii, K.: High-threshold fault-tolerant quantum computation with analog quantum error correction. *Phys. Rev. X* **8**, 021054 (2018)
22. Gottesman, D., Kitaev, A., Preskill, J.: Encoding a qubit in an oscillator. *Phys. Rev. A* **64**, 012310 (2001)
23. Fluhmann, C., Nguyen, T.L., Marinelli, M., Negnevitsky, V., Mehta, K., Home, J.P.: Encoding a qubit in a trapped-ion mechanical oscillator. *Nature* **566**, 513 (2019)
24. Campagne-Ibarcq, P., Eickbusch, A., Touzard, S., Zalys-Geller, E., Frattini, N.E., Sivak, V.V., Reinhold, P., Puri, S., Shankar, S., Schoelkopf, R.J., Frunzio, L., Mirrahimi, M., Devoret, M.H.: Quantum error correction of a qubit encoded in grid states of an oscillator. *Nature* **584**, 368 (2020)
25. Schuster, D.I., Houck, A.A., Schreier, J.A., Wallraff, A., Gambetta, J.M., Blais, A., Frunzio, L., Johnson, B., Devoret, M.H., Girvin, S.M., Schoelkopf, R.J.: Resolving photon number states in a superconducting circuit. *Nature* **445**, S15 (2007)
26. http://www.qc.rcast.u-tokyo.ac.jp/lecture_en.html
27. Igi, K., Kawai, H.: Quantum Mechanics II. Kodansha (1994)
28. Auffeves-Garnier, A., Simon, C., Gerard, J.-M., Poizat, J.-P.: *Phys. Rev. A* **75**, 053823 (2007)
29. DiVincenzo, D.P.: *Fortschr. Phys.* **48**, 771 (2000)
30. Aspelmeyer, M., Kippenberg, T.J., Marquardt, F.: *Rev. Mod. Phys.* **86**, 1391 (2014)
31. Clerk, A.A., Devoret, M.H., Girvin, S.M., Marquardt, F., Schoelkopf, R.J.: *Rev. Mod. Phys.* **82**, 1155 (2010)
32. Peres, A.: Separability criterion for density matrices. *Phys. Rev. Lett.* **77**, 1413 (1996); Horodecki, M., Horodecki, P., Horodecki, R.: Separability of mixed states: necessary and sufficient conditions. *Phys. Lett. A* **223**, 1–8 (1996)
33. Kadowaki, T., Nishimori, H.: Quantum annealing in the transverse Ising model. *Phys. Rev. E* **58**, 5355 (1998)
34. Preskill, J.: Quantum computing in the NISQ era and beyond. *Quantum* **2**, 79 (2018)
35. Scarani, V., Bechmann-Pasquinucci, H., Cerf, N.J., Dušek, M., Lütkenhaus, N., Peev, M.: The security of practical quantum key distribution. *Rev. Mod. Phys.* **81**, 1301 (2009)
36. Degen, C.L., Reinhard, F., Cappellaro, P.: Quantum sensing. *Rev. Mod. Phys.* **89**, 035002 (2017)
37. Rondin, L., Tetienne, J.-P., Hingant, T., Roch, J.-F., Maletinsky, P., Jacques, V.: Magnetometry with nitrogen-vacancy defects in diamond. *Rep. Prog. Phys.* **77**, 056503 (2014)
38. Schirhagl, R., Chang, K., Loretz, M., Degen, C.L.: Nitrogen-vacancy centers in diamond: nanoscale sensors for physics and biology. *Annu. Rev. Phys. Chem.* **65**, 83 (2014)
39. Jaklevic, R.C., Lambe, J., Mercereau, J.E., Silver, A.H.: Macroscopic quantum interference in superconductors. *Phy. Rev.* **140**(5A), A1628 (1965)
40. Fagaly, R.L.: Superconducting quantum interference device instruments and applications. *Rev. Sci. Instrum.* **77**, 101101 (2006)
41. Hatridge, M., Vijay, R., Slichter, D.H., Clarke, J., Siddiqi, I.: Dispersive magnetometry with a quantum-limited SQUID parametric amplifier. *Phys. Rev. B* **83**, 134501 (2011)
42. Kominis, K., Kornack, T.W., Allred, J.C., Romalis, M.V.: A subfemtotesla multichannel atomic magnetometer. *Nature* **422**, 596 (2003)
43. Shah, V., Knappe, S., Schwindt, P.D.D., Kitching, J.: Subpicotesla atomic magnetometry with a microfabricated vapour cell. *Nat. Photonics* **1**(11), 649 (2007)
44. Jensen, K., Budvytyte, R., Thomas, R.A., Wang, T., Fuchs, A.M., Balabas, M.V., Vasilakis, G., Mosgaard, L.D., Stærkind, H.C., Mueller, J.H., Heimborg, T., Olesen, S.-P., Polzik, E.S.: Non-invasive detection of animal nerve impulses with anatomic magnetometer operating near quantum limited sensitivity. *Sci. Rep.* **6**, 29638 (2016)

45. Aspelmeyer, M., Kippenberg, T.J., Marquardt, F.: Cavity optomechanics. *Rev. Mod. Phys.* **86**, 1391 (2014)
46. Rugar, D., Budakian, R., Mamin, H.J., Chui, B.W.: Single spin detection by magnetic resonance force microscopy. *Nature* **430**, 329 (2004)
47. Trabesinger, A.: Quantum simulation. *Nat. Phys.* **8**, 263 (2012)
48. Georgescu, I.M., Ashhab, S., Nori, F.: Quantum simulation. *Rev. Mod. Phys.* **86**, 153 (2014)
49. Awschalom, D., et al.: *Phys. Rev. X* **2**, 017002 (2021)
50. Safavi-Naini, A.H., van Thourhout, D., Baets, R., van Laer, R.: *Optica* **6**, 213 (2019)
51. Lambert, N.J., Rueda, A., Sedlmeir, F., Schwefel, H.G.L.: *Adv. Quantum Technol.* **3**, 1900077 (2020)
52. Kimble, H.J.: The quantum internet. *Nature* **453**, 1023 (2008)
53. Buhrman, H., Röhrig, H.: Distributed quantum computing. In: *Mathematical Foundations of Computer Science*, Lecture Notes 2747 (2003)
54. Gottesman, D., Jennewein, T., Croke, S.: Longer-baseline telescopes using quantum repeaters. *Phys. Rev. Lett.* **109**, 070503 (2012)
55. Kómár, P., Kessler, E.M., Bishof, M., Jiang, L., Sørensen, A.S., Ye, J., Lukin, M.D.: A quantum network of clocks. *Nat. Phys.* **10**, 582–587 (2014)
56. Bennett, C., Wiesner, S.: Communication via one- and two-particle operators on Einstein-Podolsky-Rosen states. *Phys. Rev. Lett.* **69**, 2881 (1992)
57. Pan, J.W., Bouwmeester, D., Weinfurter, H., Zeilinger, A.: Experimental entanglement swapping: entangling photons that never interacted. *Phys. Rev. Lett.* **80**, 3891 (1998)
58. Feynman, R.: Simulating physics with computers. In: *International Journal of Theoretical Physics* (1981)
59. Greiner, M., Mandel, O., Esslinger, T., Hänsch, T.W., Bloch, I.: Quantum phase transition from a superfluid to a Mott insulator in a gas of ultracold atoms. *Nature* **415**, 39 (2002)
60. Kim, K., Chang, M.-S., Korenblit, S., Islam, R., Edwards, E.E., Freericks, J.K., Lin, G.-D., Duan, L.-M., Monroe, C.: Quantum simulation of frustrated Ising spins with trapped ions. *Nature* **465**, 590 (2010)
61. Broadbent, A., Fitzsimons, J., Kashefi, E.: Universal blind quantum computation. In: *2009 50th Annual IEEE Symposium on Foundations of Computer Science*. IEEE (2009)
62. Mattle, K., Weinfurter, H., Kwiat, P.G., Zeilinger, A.: Dense coding in experimental quantum communication. *Phys. Rev. Lett.* **76**, 4656 (1996)
63. Galindo, A., Martín-Delgado, M.A.: Information and computation: classical and quantum aspects. *Rev. Mod. Phys.* **74**, 347 (2002)

Index

A

Ac Stark shift, 96
Amplitude correlation, 133
Amplitude damping, 224
Anharmonic oscillator, 144, 196, 198
Annihilation operator, 123
Anti-crossing, 96
Anti-Jaynes-Cummings interaction, 145, 186
Atomic gas, 147
Atomic ion, 189
Avoided crossing, 96

B

Baker-Campbell-Hausdorff formula, 127, 130, 139, 248
BB84 protocol, 239
Beam-splitter interaction, 187, 203
Bell measurement, 286
Bell state, 47, 281
Bit-flip error, 223
Bit-phase-flip error, 224
Bloch equation, 151, 266
Bloch sphere, 43, 143
Blue-sideband transition, 193
Bohr magneton, 255
Bohr's model, 253
Boundary condition, 166
Bra vector, 31
Bright state, 252

C

Carrier transition, 193
Cavity, 159
Cavity cooling, 275
Cavity mode, 124
© The Editor(s) (if applicable) and The Author(s), under exclusive license
to Springer Nature Singapore Pte Ltd. 2022
A. Osada et al., *Introduction to Quantum Technologies*, Lecture Notes in Physics 1004,
<https://doi.org/10.1007/978-981-19-4641-7>

Cavity optomechanics, 201, 275
Cavity Quantum Electrodynamics (QED), cavity, 172
Charge energy, 198
Clifford group, 218
Code concatenation, 231
Coherence, 258
Coherent, 134
Coherent state, 126
Commutation relation, 66
Completely mixed state, 63
Composite system, 36
Controlled gate, 213
Controlled-NOT (CNOT) gate, 211, 214, 219
Controlled-Z gate, 214
Cooperativity, 177, 204, 206
Cooper-pair box, 199
Coulomb interaction, 192
Coupling capacitor, 200
Coupling strength, 145, 177, 185
Creation operator, 123
Cross-Kerr effect, 189

D

Dark state, 252
Density matrix, 63, 257
Density of states, 114
Density operator, 61, 63
Dephasing, 152
Depolarizing error, 224
Dirac notation, 30
Dirac picture, 78, 86
Direct product, 36
Dispersive Hamiltonian, 178
Displacement operator, 126
Dissipator, 152

DiVincenzo criteria, 232
Dual-port measurement, 171

E

Electric dipole interaction, 189
Entangled state, 47, 281
Entanglement entropy, 282
Entanglement swapping, 243, 286
Error threshold, 228, 231
Even cat state, 129
External coupling, 168

F

Fabry-Perót cavity, 190
Fano lineshape, 181
Fault-tolerant, 231
Fermi's golden rule, 111, 166
Fidelity, 222
Finesse, 160, 161
Fine structure, 254
First-order coherence, 133
Flux quantum, 196
Fock state, 123
Four-wave mixing, 189

G

Gate fidelity, 225
Generalized Rabi frequency, 95, 154
Global phase, 42
Gottesman-Kitaev-Preskill (GKP) code, 231
Gottesman-Knill theorem, 218
Greenberger-Horne-Zeilinger (GHZ) state, 49, 281
Ground-state cooling, 201
Grover's algorithm, 236

H

Hadamard gate, 213
Harmonic oscillator, 123
Heisenberg equation of motion, 88, 150
Heisenberg picture, 78, 81
Heisenberg uncertainty principle, 67
Hermitian operator, 54
Hybrid quantum system, 204
Hyperfine structure, 147, 255

I

Incoherent, 134
Input-output relation, 167
Input-output theory, 166
Intensity correlation, 134
Intrinsic loss, 168
Ion trap, 189, 192

Ising coupling gate, 215

J

Jaynes-Cummings Hamiltonian, 172, 248
Jaynes-Cummings interaction, 145, 186, 190
Jaynes-Cummings ladder, 173
Jaynes-Cummings model, 172
Josephson effect, 196, 197
Josephson energy, 198
Josephson junction, 149, 195

K

Ket vector, 31
Kraus operator, 220, 223

L

Ladder operator, 125
Lamb-Dicke parameter, 192
Landé g factor, 255
Laser cooling, 275
Light shift, 96
Lindblad superoperator, 152
Local Operation and Classical Communication (LOCC), 284, 287
Logarithmic negativity, 283
Logical qubit, 229
Longitudinal relaxation, 146, 152

M

Magic state, 218
Magnetic flux, 196
Marginal distributions, 135
Master equation, 150, 152, 257
Measurement with errors, 221
Minimum-uncertainty state, 127
Mixed state, 62
Mode volume, 160, 191
Momentum representation, 245

N

Negativity, 282
No-cloning theorem, 228
Noise superoperator, 223
Noisy Intermediate-Scale Quantum (NISQ) device, 236, 242
Non-classicality, 135
Non-Clifford gate, 218
Nonlinear interaction, 188
N00N ("Noon") state, 281
Nuclear magnetic resonance, 146
Number distribution, 128
Number operator, 125, 126
Number state, 123

O

Odd cat state, 129
Operator function, 53
Optical Bloch equation, 266
Optical damping, 277
Optical spring effect, 202
Optomechanical interaction, 201

P

Parity measurement, 229
Partially coherent, 134
Partial trace, 65
Partial transposition, 283
Pauli group, 218
Pauli operator, 59, 142
Paul trap, 192
Peres-Horodecki criterion, 283
Perturbation theory, 101
Phase estimation algorithm, 237
Phase-flip error, 223
Phonon, 192, 201
Phonon-phonon coupling, 195
Photon flux, 167
Poissonian distribution, 128
Population, 258
Position representation, 245
Positive Operator-Valued Measure (POVM),
 221

Power broadening, 157, 267
p-representation, 245
Projection operator, 56, 220
Projective measurement, 220
Propagating mode, 166
Purcell factor, 177
Pure state, 62

Q

q-representation, 245
Quality factor, Q factor, 160, 161
Quantum bit, 141
Quantum circuit, 219
Quantum computation, 235
Quantum computer, 235
Quantum conversion efficiency, 206
Quantum defects, 148
Quantum dot, 148
Quantum error correction, 227
Quantum error-correction code, 229
Quantum Fourier transform, 238
Quantum gates, 211
Quantum internet, 242
Quantum Key Distribution (QKD), 239
Quantum measurement, 219, 220
Quantum noise, 275, 278

Quantum Non-Demolition (QND) measurement, 221

Quantum number, 254
Quantum Phase Estimation (QPE), 237
Quantum process tomography, 224
Quantum regression theorem, 279
Quantum repeater, 242
Quantum sensing, 240
Quantum simulation, 242
Quantum state tomography, 221
Quantum teleportation, 243, 285
Qubit, 141

R

Rabi frequency, 95, 153
Rabi oscillation, 110, 153
Radiation pressure, 202
Raising and lowering operators, 144
Ramsey interference, 155
Randomized benchmarking, 226
Rate equation, 265, 277
Red-sideband transition, 193
Reflection measurement, 163
Relaxation, 149
Resolved-sideband regime, 201, 279
Resonator, 159
Rotating frame, 91, 247
Rotating-wave approximation, 145

S

Schrieffer-Wolff transformation, 178, 251, 269
Schrödinger equation, 26, 73
Schrödinger picture, 78, 81
Schrödinger's cat state, 129, 137, 281
Second-order coherence, 134
Self-Kerr effect, 189
Separable state, 281
S gate, 213
Shor code, 230
Shor's algorithm, 238
Sideband cooling, 275
Sideband transition, 192
Single-port measurement, 168
Single-qubit gate, 219
Solovay-Kitaev theorem, 218
SPAM error, 225, 226
Spin echo, 155
Spontaneous emission, 145
Spontaneous decay, 152
Squeezed state, 130
Squeezed vacuum, 131
Squeezing Hamiltonian, 130
Squeezing interaction, 187
Squeezing operator, 130

Stabilizer generator, 228
 Stabilizer group, 228
 Stabilizer subspace, 228
 Stimulated emission, 145
 Strong coupling regime, 177
 Strong dispersive regime, 149, 179
 Superconducting quantum bit, 197
 Superconducting qubit, 149
 Surface code, 231
 SWAP gate, 214
 Syndrome measurement, 230
 System-bath interaction, 259

T

Tavis-Cummings Hamiltonian, 174
 Tavis-Cummings model, 173
T gate, 213, 218
 Thermal distribution, 132
 Thermal state, 63, 132
 Three level system, 251
 Three-qubit repetition code, 229
 Three-wave mixing, 188
 Threshold theorem, 231
 Time-dependent perturbation theory, 107
 Time-independent Schrödinger equation, 74
 Trace operation, 259
 Transition dipole moment, 190
 Transition frequency, 142
 Transmission measurement, 163
 Transmon, 196, 199
 Transverse relaxation, 146, 152
 Trapped ion, 147
 Traveling photon, 166
 Twirling, 227
 Two-level system, 141

Two-mode-squeezing interactions, 187, 203
 Two-qubit gate, 213, 219

U

Unitary operator, 58
 Universal set of quantum gate, 211
V
 Vacuum amplitude, 125
 Vacuum fluctuation, 185
 Vacuum Rabi splitting, 173
 Von Neumann entropy, 282
 Von Neumann equation, 89, 150, 258

W

Wavefunction, 26
 Waveguide-coupled cavity QED, 179
 Weak coupling regime, 176
 Werner state, 284
 Wigner function, 135
 W state, 49

X

X gate, 212
 XX gate, 215
 χ -matrix, 224
 $\chi^{(2)}$ interaction, 188
 $\chi^{(3)}$ interaction, 188
 $\chi^{(2)}$ nonlinearity, 130

Z

Zeeman effect, 104
 Zero-point fluctuation, 125
 Z gate, 212
 ZZ gate, 215